ELECTROSPUN BIO POLYMERIC DRESSING FOR ADVANCED WOUND CARE APPLICATION

Thesis Submitted for the Award of the Degree of

DOCTOR OF PHILOSOPHY

in

Clinical Biochemistry

By

Kalpana Rathore

Registration Number: 42000082

Supervised By	Co-Supervised by
Prof. Sandeep Sharma (23995)	**Prof. Vivek Verma**
Medical Laboratory Sciences	**Materials Science and Engineering**
(Professor of Clinical Microbiology)	**(Professor of Material Sciences)**
Lovely Professional University	**Indian Institute of Technology**
Punjab	**Kanpur**

Transforming Education Transforming India

LOVELY PROFESSIONAL UNIVERSITY, PUNJAB
2025

DECLARATION

I, hereby declared that the presented work in the thesis entitled **"*Electrospun Bio-Polymeric Dressing for Advanced Wound Care Application*"** in fulfilment of degree of **Doctor of Philosophy (Ph. D.)** is outcome of research work carried out by me under the supervision of ***Professor Sandeep Sharma***, working as *Professor of Clinical Microbiology*, in the ***Department of Medical Laboratory Sciences, School of Allied Medical Sciences*** of ***Lovely Professional University***, Punjab, India and my co-supervisor, ***Professor Vivek Verma***, working as Professor of ***Department of Materials Science and Engineering*** of ***Indian Institute of technology Kanpur***, Kanpur, India. In keeping with general practice of reporting scientific observations, due acknowledgements have been made whenever work described here has been based on findings of another investigator. This work has not been submitted in part or full to any other University or Institute for the award of any degree.
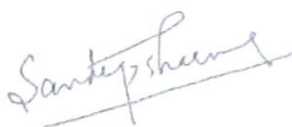
(Signature of Scholar)

Name of the scholar: **Kalpana Rathore**

Registration No.:   **42000082**

Department/school: **Department of Medical Laboratory Sciences**

School of Allied Medical Sciences

Lovely Professional University,

Punjab, India

CERTIFICATE

This is to certify that the work reported in the Ph. D. thesis entitled *"Electrospun Bio-Polymeric Dressing for Advanced Wound Care Application"* submitted in fulfillment of the requirement for the award of degree of **Doctor of Philosophy (Ph.D.)** in the *Department of Medical Laboratory Sciences, School of Allied Medical Sciences*, is a research work carried out by Kalpana Rathore, 42000082, is bonafide record of her original work carried out under my supervision and that no part of thesis has been submitted for any other degree, diploma or equivalent course.

(Signature of Supervisor)

(Signature of Co-Supervisor)

Name of supervisor: **Prof. Sandeep Sharma**

Designation: Professor

Department/school: Department of Medical Laboratory Sciences

University: Lovely Professional University

Name of Co-Supervisor: **Prof. Vivek Verma**

Designation: Professor

Department/school: Department of Materials Science and Engineering

University: Indian Institute of Technology Kanpur

ii

SYNOPSIS

Name of student: **Kalpana Rathore**   Registration No: **42000082**

Degree for which submitted: **PhD**

Department: **Clinical Biochemistry**

Thesis Title: **Electrospun Bio-Polymeric Dressing for Advanced Wound Care Application**

Name of the Supervisor: **Dr. Sandeep Sharma (LPU)**

Name of the Co-supervisor: **Dr. Vivek Verma (IIT Kanpur)**

Month and year of thesis submission:

Several wound dressings are widely available in the market (semi-permeable, foam, hydrogel, hydrocolloids, and bioactive dressings) that offer both functional support and protection against external damage. Apart from their exhibited properties, complete healing of wound still requires time and attention. Although, in the process of healing, functionality of wound area gets affected and ended with scar formation. Therefore, an optimum property for wound healing must be present in a wound dressing that require following properties. An ideal wound dressing must possess the certain characteristics, including the ability to protect the wound site, the capacity to absorb wound exudates, the potential to alleviate associated pain, permeability to facilitate air and moisture exchange, and the ability to control wound infection. All the mentioned attributes are mostly targeted to develop a wound dressing. However, the conventional wound dressings are unable to address each of the mentioned attributes and often demands frequent change of dressings from the wound site. Modern dressings like hydrocolloids

and hydrogels, effectively retain moisture but fall short in facilitating adequate gases exchange. Similarly, foam and semi-permeable dressings provide balanced gases and moisture exchange at the injury site; however, they absorb too much moisture leading to dehydration that renders them to relate with normal healing. Most advanced dressings have animal-derived polymer matrix, such as collagen, chitosan, gelatin, hyaluronic acid, etc. However, these materials can trigger immune responses in the body after application. Alternatively, synthetic materials like polymethacrylates, polyvinyl pyrrolidine, polyurethane, etc., employed to develop dressings, but have limitations such as being hydrophobic and not efficiently absorbing wound exudates. These limitations can further increase the risk of infection and delay in wound healing. Hence, it is essential to develop a wound healing material that is derived from non-animal sources and possesses the properties of being hydrophilic, superabsorbent, and biocompatible.

A continuous requirement exists for advanced wound dressing material capable of mimicking the extracellular matrix of the skin epidermis. A dressing that can be loaded with required amounts of drugs or bioactive agents with modulated permeability. Nanofibrous dressings, also known as electrospun dressing, have a surface morphology comparable to that of skin while regulating air and moisture permeability. However single layer electrospun dressing exhibits a rapid drug release owing to burst release and therefore for multiple layered structure could control the drug release dynamics. Moreover, the enhanced water holding properties and increased absorption capacity are a consequence of its nanofibrous structure. Apart from the surface morphology, polymer matrix also significantly contributes in enhancing the properties of the dressings. Therefore, we selected agar, derived from seaweed, as a substrate for the wound dressing material. Furthermore, the attributes of the material may be readily adjusted to meet specific needs by using different fillers, additives, and co-polymers. Moreover, only limited research has investigated the agar-based nanofibers for biomedical sector and there could be a significant opportunity for untapped applications that require further investigation.

In the present research, electrospinning of agar and polycaprolactone (PCL) blend nanofibers is demonstrated for the first-time using agar blend that can be used to deliver

hydrophobic and hydrophilic drugs. The optimization of electrospinning process parameters like choice of solvents, ratio of agar and PCL polymer concentration, flow rate, applied potential, distance from nozzle to collector, and collector drum speed were studied to produce continuous fibres with fewer beads. This includes binary solvents for the dissolution of the polymers. Agar and PCL were dissolved in formic acid and acetic acid, respectively. 20% polymer concentrations were used to blend in different ratios of agar:PCL from 4:5 to 7:5. The flow rate was varied from 10 and 15 µL/min. The applied potential was varied from 10, 15 and 20 kV and the different nozzle to collector distance was used from 5 cm, 7 cm, and 10 cm.

Apart from electrospinning parameters, different strategies were used to develop bilayer advanced wound dressing. The first generation of symmetric bilayer structure was developed using electrospinning and, in second generation, asymmetric bilayers were fabricated using two different methods including electrospinning and solvent casting method. To control drug delivery kinetics in symmetric bilayer dressing, uniaxial and coaxial nanofibres were generated, where coaxial nanofibers contain polyvinyl alcohol (PVA) with cephalexin hydrate, an antibacterial drug, as core and agar-PCL as sheath material. Bilayer structure was fabricated by electrospinning agar-PCL layer over the layer of coaxial PVA and agar-PCL fibres.

In the second-generation asymmetric bilayer dressing, agar-based wound dressing consisting of support and electrospun layer with antibacterial and anti-oxidant properties respectively was presented. The support layer containing agar and silver nitrate was fabricated using solvent casting. Silver nitrate was reduced into silver nanoparticles using agar as reducing agent in a one-pot synthesis step to induce antibacterial properties. A mixture of agar and poly caprolactone infused with gallic acid was electrospun over the support layer to impart anti-oxidant properties.

Scanning electron microscope (SEM) was used to analyse the morphology of the developed bilayer dressing. Transmission electron microscopy (TEM) demonstrated incorporation of nanoparticles/drug into the PVA core of coaxial fibres. The developed samples with drug exhibited antimicrobial activity against gram positive and gram-negative bacterial strains while maintaining cyto- and hemocompatibility. Employing

coaxial fibres and bilayer structure proved effective in controlling drug delivery kinetics. In addition, the fluid holding properties like absorption, moisture permeability, and dehydration were suitable for wound dressing applications. The presence of impregnated silver nanoparticles was confirmed through UV-vis spectroscopy and transmission electron microscopy. The release kinetics of silver nanoparticles were evaluated with ICPMS. The chemical was characterized using Fourier transform infrared spectroscopy. The developed bilayer structure exhibited excellent fluid-handling properties, with a moisture permeability of 1200 $g/m^2/day$ and water absorption of ~250%. The developed dressings provided excellent mechanical support and exhibited anti-oxidant properties with over 90% scavenging efficacy. The biocompatibility of bilayer dressing was evaluated to assess their hemocompatible and cytocompatible properties. In the wound scratch assay, more than 79% wound closure confirmed the efficacy of the developed dressing for wound care application. Moreover, the bacteriostatic effect was also evaluated using time kill assay against gram-positive and gram-negative bacteria.

Most importantly, in vivo studies demonstrated the efficacy of the developed bilayer dressing, promoting over 97% healing within 12 days of injury. Overall, the *in vitro* and *in vivo* assessment of the developed bilayer dressing confirmed its potential to function as a versatile and effective material for chronic wound dressings. Hence, the developed bilayer dressing has significant potential to serve as an effective material for chronic wound dressings.

ACKNOWLEDGMENT

My doctoral research is the most anticipated journey of my life, giving its share of unforgettable moments of joy, excitement, and everlasting memories. During this journey, several individuals contributed significantly by offering encouragement, support, guidance, and vision while simultaneously inspiring and boosting my willpower through constructive criticism and direction in places where I certainly required the most.

*My deepest appreciation goes to my co-supervisor, mentor **Prof. Vivek Verma**, for having faith in me and providing me with consistent encouragement, support, guidance, and constructive criticism throughout the duration of my research. The longest professional association realigned my career in the best possible way and transformed the tenor of my life. It was he who first introduced me to the concept of research and how, by enjoying diligence, dedication, and vigilance, I could uncover untapped possibilities. I heartily thank him for giving me the opportunity to pursue a PhD under his guidance and providing me with all the required facilities and research resources to conduct my research.*

*Further, I wish to extend my deepest gratitude to my PhD thesis supervisor, **Prof. Sandeep Sharma.** Sandeep sir motivated and enabled me to pursue my research objectives by providing constant encouragement throughout the journey of this thesis, with a positive attitude that helped me to overcome every obstacle. Despite my initial scepticism about working with two supervisors, I consider myself extremely fortunate to have the expertise of two mentors, especially Sandeep sir who provided me with the same energetic advice, consistent encouragement, and enthusiastic guidance, bringing a positive and valuable influence to my experience.*

TABLE OF CONTENTS

LIST OF TABLES

LIST OF FIGURES

LIST OF ABBREVIATIONS

°	Degree
%	Percent
μL	Microliter
AgNO3	Silver nitrate
AgNPs	Silver nanoparticles
AP	Agar: PCL
ASTM	American Society for Testing and Materials
BL	Bilayer
BLC	Bilayer with drug cephalexin hydrate
bNRL	Biomedical natural rubber latex
LbL	Layer by layer
CA	Citric acid
CEX	Cephalexin hydrate
CFU	Colony forming Unit
CMC	Carboxymethyl cellulose
CTRL	Control
DCM	Dichloromethane
DI	Deionized
DMA	Dimethylacetamide
DMEM	Dulbecco's modified eagle medium
DMF	Dimethylformamide
DMSO	Dimethyl sulfoxide
DNA	Deoxyribonucleic acid
DPPH	2, 2-diphenyl-1- picrylhydrazyl
ECM	Extracellular matrix
EDS	Energy Dispersive X-ray spectrometry
EDTA	Ethylenediaminetetraacetic acid
ES	Electrospun
FBS	Fetal bovine serum
FESEM	Field emission scanning electron microscope
FGF	Fibroblast growth factor
FP	Filter paper
FTIR	Fourier transform infrared spectroscopy
GA	Gallic acid
H_2O_2	Hydrogen peroxide
HFIP	Hexafluoro-2-propanol
KBr	Potassium bromide
kV	Kilovolt
LiCl	Lithium chloride
MBC	Minimum bactericidal concentration
MHA	Mueller Hinton agar
MHB	Mueller Hinton broth
MIC	Minimum inhibitory concentration

mM	Mili molar
mm	Mili meter
MMPs	Matrix metalloproteinases
MPa	Mega pascal
MTT	3-(4,5 dimethylthiazol-2-yl)-2,5 -diphenyl tetrazolium bromide
NCC	Cellulose nanocrystal
nm	Nanometer
PAN	Polyacrylonitrile
PBS	Phosphate buffered saline
PCL	Polycaprolactone
PDGF	Platelet derived growth factor
PDMS	Polydimethylsiloxane
PE	Polyester
PEI	Polyethyleneimine
PEO	Polyethylene oxide
PLA	Polylactic acid
PLGA	Lactic-co-glycolic acid
PPP	Platelet-poor plasma
PRP	Platelet-rich plasma
PS	Polystyrene
PVA	Polyvinyl alcohol
PVAC	PVA with cephalexin hydrate
PVC	Poly vinyl chloride
PVDF	Polyvinylidene fluoride
PVP	Polyvinylpyrrolidone
RBC	Red blood cells
RH	Relative humidity
ROS	Reactive oxygen species
rpm	Rotation per minute
SEM	Scanning electron microscope
SERS	Surface Enhanced Raman Spectroscopy
SLC	Single layer with cephalexin hydrate
TCP	Tissue culture plastic
TEM	Transmission electron microscopy
TFA	Trifluoroacetic acid
TGF-β	Transforming growth factor-beta
THF	Tetrahydrofuran
UTM	Universal testing machine
UV	Ultraviolet
WVTR	Water vapor transmission rate
ZOI	Zone of inhibition

CHAPTER 1
INTRODUCTION

This chapter aims to provide a comprehensive overview of the study, enhancing understanding of the terminology, methodologies, materials, and procedures used. This chapter provides a brief overview of the fundamentals of wound care management, focusing mainly on various forms of wound dressing. A simplified outline of the fabrication procedure for nanofibrous wound dressings utilizing the electrospinning technique is also described. Additionally, we addressed the potential use of agar biopolymers as an alternative for wound dressing applications.

1.1. Wound Care Management

Wound care management is a comprehensive field that involves the analysis of different types of wounds and their effective healing strategies, with appropriate measures for each stage of healing (Flanagan et al., 2000). It also aids in the efficient utilization of different wound dressings for efficient healing. Several factors of wound management contribute to wound healing by regulating infection, inflammation, maintaining wound moisture without macerating or dehydrating, ensuring proper wound closure, and many more (O'Dwyer, 2005). Hence, for efficient wound healing, it is important to have a comprehensive grasp of the specific wound type requirements. This involves the restoration of cellular and tissue function and assisting in the recovery process (Vig et al., 2017).

1.2. Wound

All interior organs are protected from external harm by the greatest vital organ, the skin. It consists of three distinct layers, namely the epidermis, dermis, and subcutaneous tissue. The epidermis rejuvenates in 15-20 days. In addition, it provides a waterproof barrier using dead skin cells. The dermal layer is the skin's most vascularized living layer. The fibrous connective tissue of the dermis imparts the strongest elasticity to the skin. The subcutaneous layer, located beneath the dermal layer, stores fats and water.

Any injuries that lead to disintegration or damage to parts of the skin surface or underlying tissues are termed wounds. These wounds follow a normal healing pathway

to recover, displaying their usual healing signs. They can be classified according to the healing time and are known as acute and chronic wounds (discussed later). Wounds caused by cuts, bruises, burns, punctures, or surgery are in the category of acute wounds. Chronic wounds, such as diabetic foot ulcers or pressure ulcers (bedsores), take longer for self-healing, and often the reconstruction and regeneration of damaged tissue fail to regain its functioning(Greer et al., 2013). The normal healing mechanism in chronic wounds is impaired and requires special care for proper healing.

1.2.1. Types of wounds

Wounds can be categorized according to four distinct criteria: the depth of the incision, the mechanism of injury, the healing time, and the infection. Acute and chronic lesions are classified according to their recovery time. Acute wounds, including those resulting from incisions, cuts, abrasions, or traumatic injuries, typically recover rapidly through a standard healing process. Chronic wounds such as diabetic foot ulcers, infected burn wounds, and bedsores require a prolonged healing time and are often associated with conditions like diabetes(Alven & Aderibigbe, 2020). Furthermore, the injury mechanism can classify wounds as either intentional or unintentional. Surgical wounds, for example, are planned wounds, while unintentional wounds include accidental injuries like bruises, cuts, and punctures. These can be further categorized as either open or closed wounds. Open wounds, such as a cut from a kitchen knife, reveal the underlying tissues, whereas closed wounds, such as a burn from a sterilizer, cause harm to tissues without exposing them. Another classification of wounds is the infection-based classification, which depends on the degree of contamination. Sterile surgical incisions that are free of microbial infection are referred to as clean wounds. Clean wounds are the outcome of regulated surgical techniques that do not compromise the sterile method. Infected wounds are the result of delayed treatment of traumatic wounds, which lead to bacterial infection. Depending on their depth, we can classify wounds as superficial, partial-thickness, or full-thickness. The epidermis is the only area affected by superficial wounds, whereas partial-thickness wounds affect the dermis and epidermis(Paul & Sharma, 2004a). Gunshots and certain surgical wounds are examples of full-thickness wounds, which extend through the epidermis and dermis into deeper tissues, occasionally impacting muscles.

1.2.2. Wound healing and its challenges

Usually, the human body functions as a highly effective defence mechanism against several infections and illnesses, apart from instances involving open wounds and other medical disorders. Wound healing is a natural pathway that involves numerous cellular events and biological cascades at the cellular and molecular level that help in recovering from the injury by regaining normal cellular functioning and reconstructing and regenerating the damaged tissue (Flanagan et al., 2000; Memic et al., 2019a). Skin wound healing is a network of numerous physiological processes that involve multiple cell types. The process of wound healing comprises four physiological stages, including hemostasis, inflammation, granulation tissue development, re-epithelialization, and remodeling(Takayama & Aoki, 2012) and is displayed below **Figure 1.1** (Liang et al., 2021):

Hemostasis- Hemostasis triggers the formation of a fibrin clot near the wound, followed by the migration of inflammatory cells to the site of injury to eliminate foreign substances.

Inflammation- This stage of wound healing is commonly referred to as the inflammatory phase. Following an injury, fibroblast cells promptly start migrating towards the wound site, initiating the process of extracellular matrix production through the replacement of the fibrin clot.

Proliferation- This phase of wound healing is often characterized by a high concentration of collagen produced by fibroblast cells. This natural procedure is typically referred to as granulation tissue formation.

Re-epithelialization and remodeling- Similar to previous phase, keratinocytes undergo migration towards the location of the wound, facilitating the process of re-epithelialization, which is subsequently followed by the remodeling of the skin surface. During the process of remodeling, the maturation of collagen fibres occurs in the presence of several growth factors, such as platelet-derived growth factor (PDGF), transforming growth factor-β (TGF-β), and fibroblast growth factor (FGF). Ultimately, wound healing concludes with the development of scar tissue.

Figure 1.1. The four stages of normal wound healing comprise hemostasis (a), inflammation (b), proliferation (c), and remodeling (d).(Liang et al., 2021)
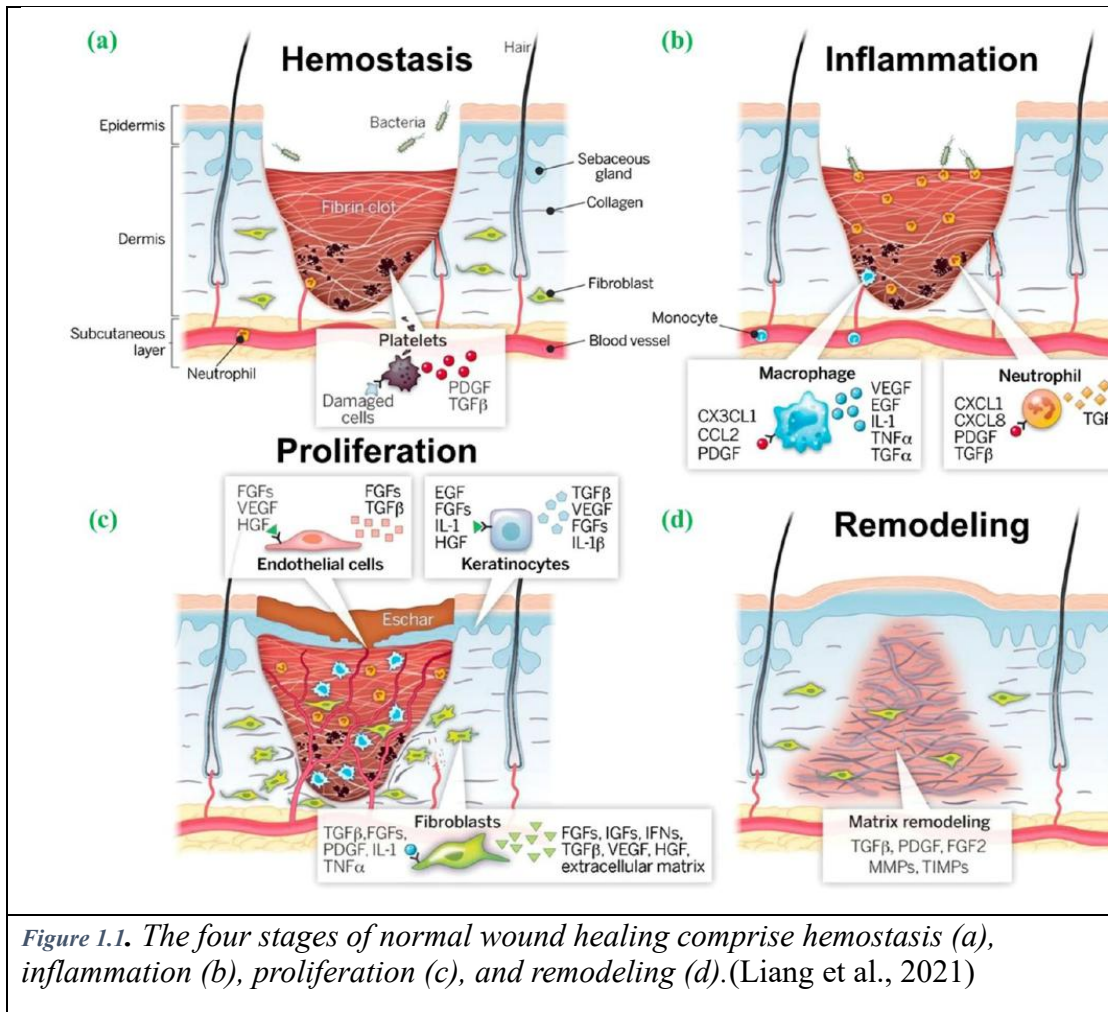
The healing phase of normal wounds proceeds along the mentioned pathway; however, chronic wounds experience a prolonged healing period due to the impaired healing pathway. Chronic injuries, which are hard-to-heal wounds, have a malfunctioning array of healing pathways. Increased expression of matrix metalloproteinase (MMPs), the presence of reactive oxygen species (ROS), a higher pH that turns the wound site into an alkaline micro-environment, and an increased susceptibility to microbial infection are all signs of a compromised state during chronic wound healing. These factors adversely affect wound healing by downregulating the essential growth factors (**Figure 1.2**) (Tronci, 2019) and, hence, taking a longer time to heal completely. The objectives that an advanced wound dressing should achieve include promoting accelerated wound healing, facilitating wound closure, managing wound infection, and alleviating wound

4

pain("Guidance for Industry: Chronic Cutaneous Ulcer and Burn Wounds-Developing Products for Treatment," 2001).

Figure 1.2. *Healing phases in normal and chronic wounds.* (Tronci, 2019)
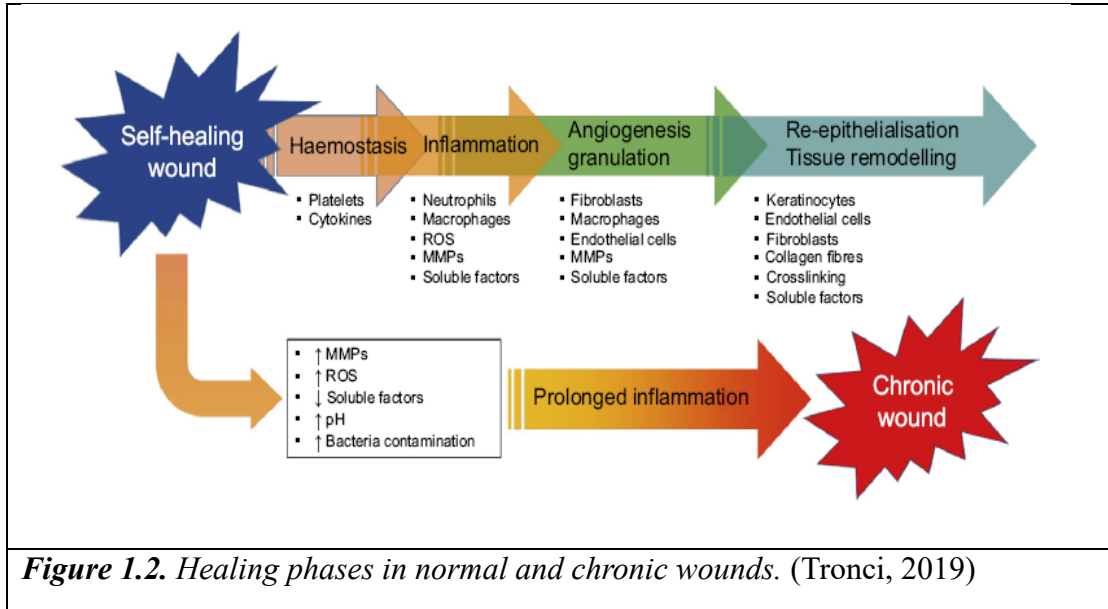
1.2.3. Wound dressings

Throughout history, wound dressings have progressed from simple methods such as bandaging and wound cleansing to plastering that incorporates advanced features to promote faster healing(Farahani & Shafiee, 2021). Various generations have implemented distinct approaches and strategies to treat wounds (**Figure 1.3**). Traditional wound dressings have been substituted with advanced dressings that provide several beneficial features. These dressings effectively promote wound healing by addressing limitations related to various stages of the healing process(R. Dong & Guo, 2021a).

Figure 1.3. *Historical evolution of wound dressings with timeline.* *(Farahani & Shafiee, 2021).*
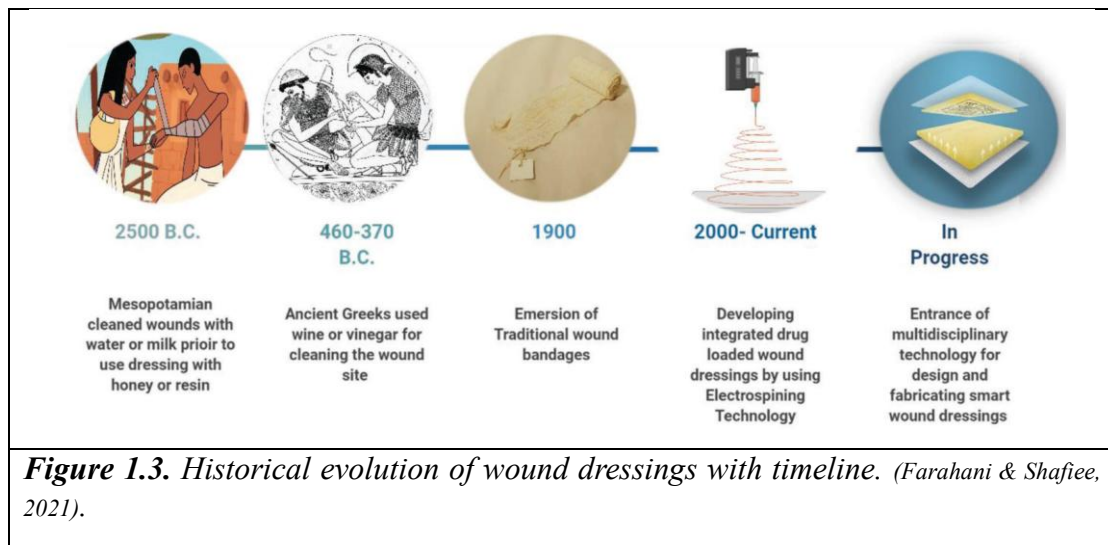
Although several wound dressings are available on the market, not a single dressing has wholly severed the purpose of wound care for all the stages of wound healing. The desired characteristics(Mohy Eldin et al., 2008) of an ideal wound dressing should include the following:

- *Absorption*- The dressing should absorb a large volume of wound exudates without any leakage into surrounding tissues. Barros et.al., in a bNRL-based dressing, demonstrated that the absorption of wound exudates can be increased with the addition of alginate(Barros et al., 2021). Studies performed by Cutting et. al. to compare the absorption capacity of six different dressings confirmed the influence of external compression on swelling properties(Cutting & Westgate, 2012).

- *Moist environment*- The wound dressings should maintain a moist environment at the wound site, which helps with accelerated wound healing and wound closure. Several studies were performed to develop moist wound dressings that result in better wound healing(Kim et al., 2019; Maneerung et al., 2008).

- *Antimicrobial-* Dressings should be sterile and protects from microbial infections. Several studies were performed, and antimicrobial dressings developed that control microbial growth(Bal-öztürk et al., 2021; Cui et al., 2021; Y. Dong et al., 2010; Ong et al., 2008; Sankarganesh et al., 2022; Tkachenko & Karas, 2012). Research performed by Zhang et.al. demonstrated

the efficacy of electrospun nanofibrous dressings against antibiotic-resistant wound infection(Y. Zhang et al., 2022).

- *Permeability-* Wound dressings should have ideal barrier and exchange properties with respect to air and moisture that could allow proper exchange of air and fluids through the dressing. The dressing's optimum permeability for air and moisture would prevent the wound from dehydration or maceration. Zhang et. al. demonstrated WVTR of fibroin dressing in a controlled clinical trial(W. Zhang et al., 2017).

- *Mechanical support-* The wound should be protected from further trauma by providing mechanical support to the wound area. Figueira et. al. developed a bilayer dressing that provides mechanical support by enhancing the physical barrier to the wound(Figueira et al., 2016).

- *Non-adherent-* Dressings should be non-sticky and easily removed from the wound site without damaging the integrity of the cells. In early studies, Diaz et. al. developed a wound dressing with reduced cell adhesion to alleviate the dressing removal pain(Díaz et al., 2022).

- *Biocompatible-* Dressings must be hypoallergenic, safe, and biocompatible. It should not generate an immune response while encountering the damaged tissues(Locilento et al., 2019).

- *Biodegradable-* It should be biodegradable because it can be easily degraded in the presence of body fluids(Stojko et al., 2020). Furthermore, it does not create any additional environmental pollution after usage.

- *Bioresorbable-* Internal wounds need additional surgery to remove the dressing materials if they are not bioresorbable. Bioresorbable dressings have advantages by slowly vanishing inside the body without any side effects or harm to other body parts(X. Huang et al., 2015).

- *Shelf life-* It should have a longer shelf life to avoid frequent dressing changes and production costs.

- *Cost-effective-* Dressing should be cheaper than treatment and easily accessible to locals.

However, no single wound dressing can fulfil all the required functions to heal all types of wounds. Therefore, it is possible that multiple dressings would be used for different healing phases of wound assisting in the healing process for a single injury. Wound care products are now available that take account of these factors and are now available on the market to treat chronic wounds (Cockbill et al., n.d.; Czemplik et al., 2013; Paul & Sharma, 2004b; Stashak et al., 2004).

1.3. Limitations of conventional wound dressings

Only a few wound dressings for various types of wounds have advanced to clinical trials, and even fewer have achieved successful commercialization. Most wound dressings have inherent restrictions that prevent them from offering broad solutions to wound-related issues. As previously observed, wound healing is an intricate and adaptive process that encompasses several components at different phases to ensure full recovery from the wound. Conventional dressings are insufficient for meeting all the requirements at various phases of wound healing. The dressing's insufficient absorption of wound exudates can cause maceration in the tissues around the wound, while excessive transmission of moisture via the dressing can result in dehydration. Furthermore, any disruption in the typical healing process may lead to a serious and persistent infection in a wound (R. Dong & Guo, 2021b).

1.4. Advanced wound dressings

Different types of dressing materials were employed according to the types of wounds and their severity. This includes wound dressings for acute and chronic injuries, whether they are conventional or advanced dressings. Most advanced wound dressings can be classified as mentioned in **Table 1.1**, whereas traditional dressings include moist saline compresses with or without zinc oxide, standard therapy, impregnated gauze dressings, and placebo(Heyer et al., 2013). The percent in **Table 1.1** signifies the usage percentage of dressing for wound care.

Table 1.1. Advanced wound care dressings percentage in terms of usage.

	Type of dressing	Percent
1.	Hydrocolloid dressing with/without silver	35.4
2.	Active dressings	18.5
3.	Mixed dressings	10.8
4.	Hydrogel with/without polyhexanide	7.7
5.	Polyurethane foam dressings	7.7
6.	Antiseptic dressings	6.2
7.	Semipermeable transparent film dressings	4.6
8.	Alginate dressings	3.1
9.	Hydro active impregnated dressings	3.1
10.	Coal dressings	1.5
11.	Hydrophobic dressings	1.5
List of advanced wound care dressings (Heyer et al., 2013)		

Although different wound dressings accelerate the healing process and wound closure process in different wound types, each dressing has its limitations as well. A comprehensive review was previously reported(Weller et al., 2020) for a range of dressings. **Table 1.2** summarizes the results of various types of dressings with their pros and cons, including semi-permeable film and foam-based dressings, hydrocolloid, hydrogel, alginate, chitosan, bioactive dressings, tissue-engineered scaffolds, polysaccharide-based dressings, nanofibrous dressings, and more.

Table 1.2. List of different types of wound dressing and their dressing material.

Dressing type	Dressing material	Advantages	Disadvantages	Ref.
Semi-permeable film dressings	Polyurethane film	Excellent strength, oxygen permeability and barrier properties	Hydrophobic, lack cell affinity, slower degradation	(Barrioni et al., 2015; Eskandarinia et al., 2020a; Unnithan et al., 2012)

Semi-permeable foam dressings	Polyurethane foam	Low cytotoxic, quick water absorption, non-adherent	Lower tensile strain%	(X. Liu et al., 2017; Weller et al., 2020)
Hydrocolloid dressings	Carboxymethyl cellulose	Excellent absorption capacity, good barrier properties	Low strength, limited fluid handling properties and induce hypoxic conditions	(N. Roy et al., 2010a; Weller et al., 2020)
	Gelatin	Excellent swelling, cell adhesion, biocompatibility, decrease dead volume of wound	Dissolve in wound exudates, animal origin	(Republic, n.d.; Taylor, 2013; Weller et al., 2020)
	Pectin	Excellent swelling, biocompatibility, decrease dead volume of wound	Soluble in exudates, non-spinnable	(Alipour et al., 2019; Weller et al., 2020)
Hydrogel dressings	Polyvinylpyrrolidone	Biocompatible, biodegradable	Low swelling properties	(Alipour et al., 2019; N. Roy et al., 2010a)
Nanofibrous dressings	Alginate	Excellent absorption capacity, permeability	Allergic, adherent, animal source	(K et al., 2021; Weller et al., 2020)
Polysaccharide-based dressings	Agarose	Excellent water affinity, thermosensitive	No inherent bioactivity, long degradation	(Chu et al., 2020; Piva et al., 2018; Ying et al., 2022; Zeng et al., 2015)
	Chitosan	Bioactivity, antimicrobial properties, biocompatible	Animal source	(H. Liu et al., 2018; Shojaee Kang Sofla et al., 2020; Trinca et al., 2017)
Medicated dressings	Growth factor Antibiotics Supplements	Enhanced biocompatibility, bioactivity	Require drug delivery optimization	(Bie et al., 2020; Locilento et al., 2019; Reesi et al., 2018; Thet et al., 2016)

Tissue engineered skin substitute	Polyglycolic acid	Biocompatible, biodegradable, water resistance	Water insoluble, hydrophobic	(Asadi et al., 2021; X. Liu et al., 2018; Soscia et al., 2010)
	Poly lactic acid	Biocompatible, biodegradable, bioresorbable	Water insoluble, hydrophobic	(Ahmadian et al., 2020; X. Liu et al., 2018)
	Collagen	Biocompatible, bioresorbable, biodegradable	Animal source, immunogenic	(Akturk et al., 2011; Armeda, 2018; Ooi et al., 2020)
	Polycaprolactone	Biocompatible, bioresorbable, biodegradable	Hydrophobic, water insoluble	(Armeda, 2018; Raina et al., 2022; Safdari et al., 2022; Shie Karizmeh et al., 2022)

1.5.   Electrospun fibers in wound dressing application

The fibrous dressing has demonstrated potential for wound healing(K et al., 2021) due to its ability to mimic compositional, structural, mechanical, and cellular responses, as well as the incorporation of bioactive agents and their release(S. Chen et al., 2017). Apart from the mentioned properties, the interconnected porous morphology assists in the proper permeability of moisture and oxygen, and the absorption and exchange of wound exudates and fluids, without dehydrating or macerating the surrounding wound tissues(Memic et al., 2019b). The nanofiber's large surface area-to-volume ratio helps in incorporating desired bioactive agents into more uniformly dispersed agents. The pictorial representation of ideal properties is mentioned in **Figure 1.4**.
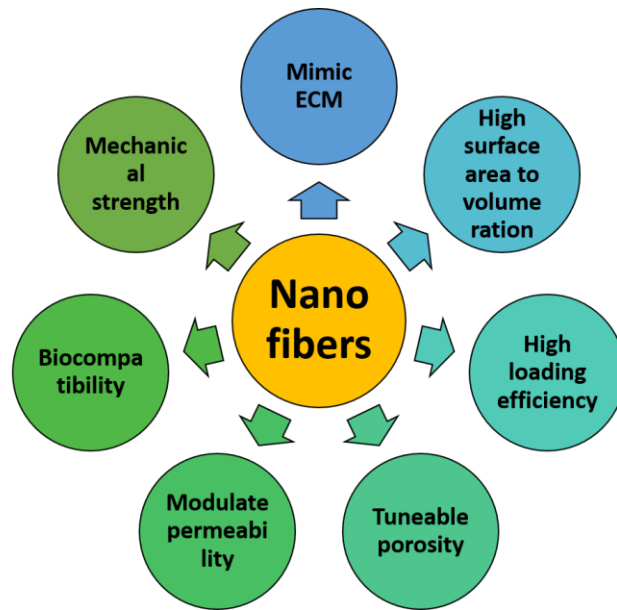
Figure 1.4. *Ideal attributes of nanofibrous wound dressing.*

1.5.1. Electrospinning

In the fields of biomedicine(Memic et al., 2019a), nanotechnology, and material science(Inagaki et al., 2012), electrospinning is one of the innovative technologies to develop nanofibers. The developed nanofibers possess enhanced physical, chemical, and biological properties(Islam et al., 2019a). The surface area-to-volume ratio of the nanostructures is responsible for these improved properties. Despite having various sorts of procedures for the fabrication of nanofibers, including wet spinning, phase separation, drawing, self-assembly, and others, the electrospinning method is more cost-effective for producing continuous nanofibers(Schiffman & Schauer, 2008). Using the electrospinning process, numerous synthetic and biopolymer-based nanofibers were being fabricated(Xue et al., 2019). In a typical electrospinning setup (**Figure 1.5a**), a syringe is connected to an automated pump, facilitating the deliver polymer solutions. The syringe needle tip was connected to a high voltage that helps in the formation of Tailor cone which eventually form nanofibers due to electrostatic charges that overcome the surface tension of the polymer droplet. The charged nanofibers spin toward the grounded collector.

1.5.2. Principle of electrospinning

In the electrospinning process, several forces play a role in drawing fine fibres from the polymers. The nanofibrous morphology is influenced by the viscosity of the solution, electrostatic force, surface tension of the solution, gravity, columbic forces, voltage difference, etc.(Khalf & Madihally, 2017). In simple terms, the polymer solution has some surface tension that is dependent on the viscosity of the solution. The solution's viscosity depends on the polymer-solvent interaction that defines the electrospinnability of the polymer solutions. The surface tension of the polymer solution maintains the drawing droplet formation at the tip of the syringe. After applying electrical potential, the accumulated electric charge overcomes the surface tension of the droplet, leading to the creation of a Taylor cone (**Figure 1.5b**), followed by the formation of nanofibers. The whole setup can be positioned in a vertical or horizontal position, depending on the ease of operation. Usually, low voltage is required for vertical setups as gravity influences fibre formation. Nanofiber formation requires applying high voltage to the spinneret while grounding the collection unit. Different parameters associated with the electrospinning techniques, discussed in the coming section, influence the formation of nanofibers.

Figure 1.5. *Schematic of electrospinning machine (a) and (inset b) formation of Tailor cone under the influence of various forces.*
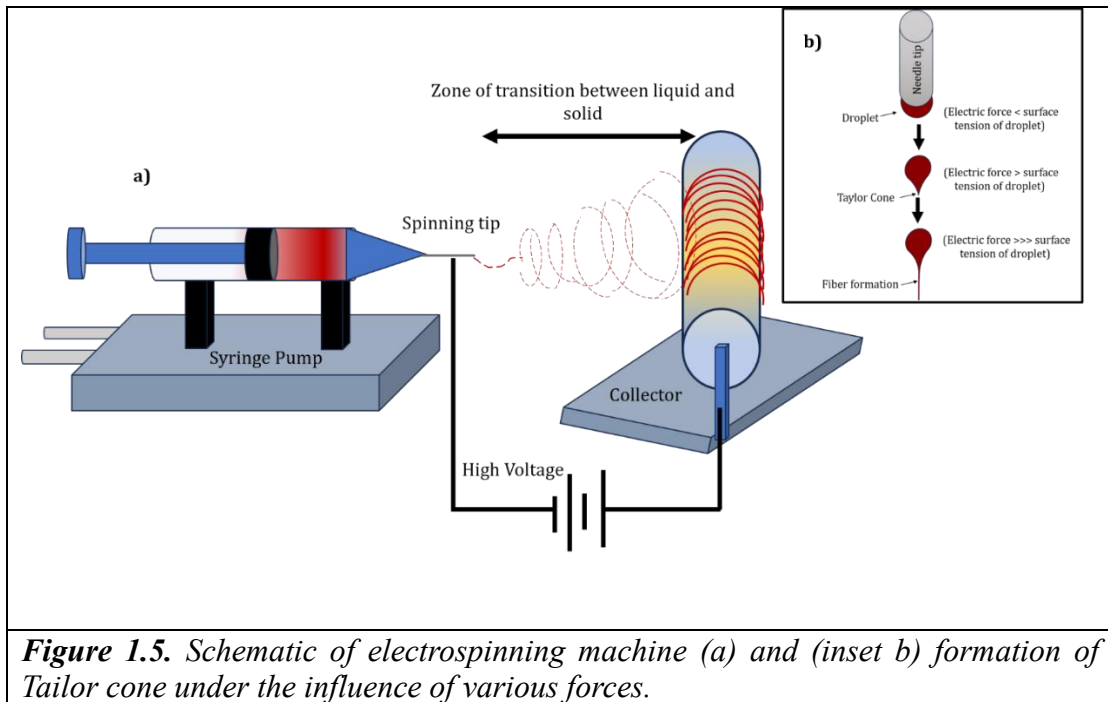
1.5.3. Parameters influencing electrospinning

Generally, there are three parameters that affect the formation of nanofibers, which are solution parameters, processing parameters, and ambient parameters. The solution parameters include properties like polymer concentration, type of solvent, viscosity, and conductivity of the solution. The electrospinning processing parameters influence the beaded or non-beaded morphologies of nanofibers, including the flowrate of polymer solution, spinneret needle inner diameter, applied potential, distance between spinneret and collector, rotational speed of the rotating collector, and alignment of the electrospinning setup. Lastly, the ambient or environmental conditions also influence the fibre morphology, which includes the temperature of the chamber, the humidity of the chamber, and the air flow in the electrospinning chamber. The properties(Angel et al., 2022a) influenced by the mentioned parameters are listed in **Table 1.3** with their effects on the formation of nanofibers.

Table 1.3. *Role of electrospinning parameters in the formation of nanofibers.*

Types	Effects on electrospinnability and fibre morphology

Solution parameter	
Polymer concentration	• Influence viscosity • High concentration results in high viscosity which increases fibre diameter • Lower concentration leads to less viscous solution, resulting in beaded fibrous morphology • Optimum polymer concentration results in nanofibrous structure
Solvent type	• Volatility of solvent influences fibre formation • Effect dissolution due to solvent-polymer interaction • High volatile solvents clog the spinneret • Low volatile solvents result in beaded morphology or thin films on the collector
Viscosity	• Low viscosity of the polymer solution results in beaded morphology • High viscosity requires high pressure for flowrate, mostly non-spinnable • Viscosity influences fibre formation, with or without beads • With an increase in viscosity, bead morphology changes from round to elongated to nanofiber(Haider et al., 2018).
Surface tension	• High surface tension of the solution results in beaded morphology • Electro-spraying • Low surface tension results in flattening of fibres
Conductivity	• Influence stretching and drawing of fibre • Poorly conducting solutions require high potential for fibre or bead formation • Highly conducting polymer solution draw fibres easily
Polymer chains	• High molecular weights take longer to dissolve in solvent • Influence solvent-polymer interaction

Processing parameter	
Flow(feed) rate	• High feed rates result in thicker fibre or fibre diameter increases • High feed rates form beaded structures • Low feed rates form thin fibres or fibre diameter decreases
Inner diameter of spinneret	• Smaller inner diameter of the needle results in a low feed rate, decreasing fibre diameter • Smaller diameter reduces clogging • Higher inner diameter results in thicker fibres or beaded morphology
Applied voltage	• High voltage accelerates fibre formation by drawing more volume from needle • High voltage results in decreased fibre diameter • Low voltage increases the fibre diameter • Low voltage face difficulty in forming a Taylor cone
Distance between needle and collector	• Smaller distance increases fibre diameter • Smaller distance also leads to merged fibres due to insufficient time for solvent evaporation • Increased strength of the fibre due to merging at the junction, forming inter- and intra- layer bonding • Larger distance decreases the fibre diameter
Collector type	• Conducting collectors have more packing density as compared to non-conducting collectors • Non-conducting collectors have fewer accumulated fibres • Non-conducting collectors result in honeycomb morphology due to the repulsive forces of fibres • Static collector collects non-aligned fibres forming uneven thickness • Rotating collector is used to collect aligned fibres
Ambient parameter	

Temperature	• Higher temperatures increase the solvent evaporation rate, forming thin fibres • Higher temperatures influence the solutions' viscosity
Humidity	• Low humidity influences the evaporation rate of solvent • High humidity increases fibre diameter
Air flow	• Airflow influences solvent evaporation, forming thinner fibres

1.5.4. Types of electrospinning process

The general electrospinning setup is almost the same for different kinds of electrospinning processes. All basic models include a high-potential difference, a spinneret, and a collecting unit. The modifications are usually made in the spinneret or collector units of the electrospinning setup. Depending upon the modifications in the setup, there are mainly four types of electrospinning methods, including dry electrospinning, wet electrospinning, coaxial electrospinning, and bubble electrospinning (Angel et al., 2022a). The detailed model is explained below:

Dry electrospinning- In dry electrospinning, the basic setup remains a high-voltage supply, spinneret, and collector. Potential is applied to the spinneret for the creation of nanofibers, while the collector is grounded. The setup can be aligned in vertical or horizontal positions. Meanwhile, the type of collector can also be varied, from static to dynamic or a rotating collector covered with conducting foil. The rotational speed of the rotating drum can be varied, and the distance between the nozzle and the collector can also be changed. To develop nanofibers, several combinations are required, including the distance between the needle and collector, the rotational speed of the drum, conducting and non-conducting collectors, the feed rate of the solution, and the viscosity of the solution. A schematic representation was provided in **Figure 1.5**.

Horizontal electrospinning set-up:

The syringe is positioned horizontally with the collector on the syringe pump in the electrospinning machine. The syringe pump's set flow rate enables the piston to dispense the required amount of volume from the needle at the required rate. The metallic needle of the needle is secured with the alligator clip for voltage supply. The

collector's distance from the needle tip can be varied and different substrates can be used, including aluminium foil or parchment paper. Either a static plate or a rotating drum, with variable speed, can be served as collector unit. (**Figure 1.6**)
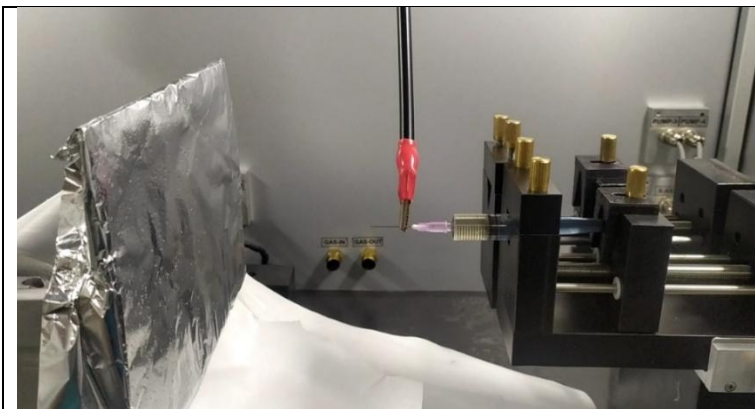
Figure 1.6. *Horizontal electrospinning set-up for the development of nanofibers.*

Vertical electrospinning set-up:

A soft silicon tube connected both the needle and the syringe, facilitating the pumping of the solution from the syringe to the needle, where the syringe was placed on the syringe pump, and the needle was placed on a Teflon vertical rod for holding the needle. The distance and flowrate were like a horizontal set-up. In vertical electrospinning, different collection unit can be used to collect the electrospun material. (**Figure 1.7**)

Figure 1.7. *Vertical electrospinning set-up for the development of nanofibers.*

Co-axial electrospinning

To develop core-shell nanofibers, a co-axial electrospinning unit was used where the inner and outer diameters of the nozzles were different. The co-axial unit and its arrangement in the electrospinning machine are displayed in **Figure 1.8 (a &b)**. In the set-up, two solutions were loaded into two different syringes and connected to the co-axial nozzles. The solution was moved towards the co-axial nozzle with the help of varied flow rates applied by the piston.

(a)	(b)

Figure 1.8. Co-axial electrospinning set up(a) Co-axial needle attached to syringe and (b) nanofiber formation using co-axial electrospinning.
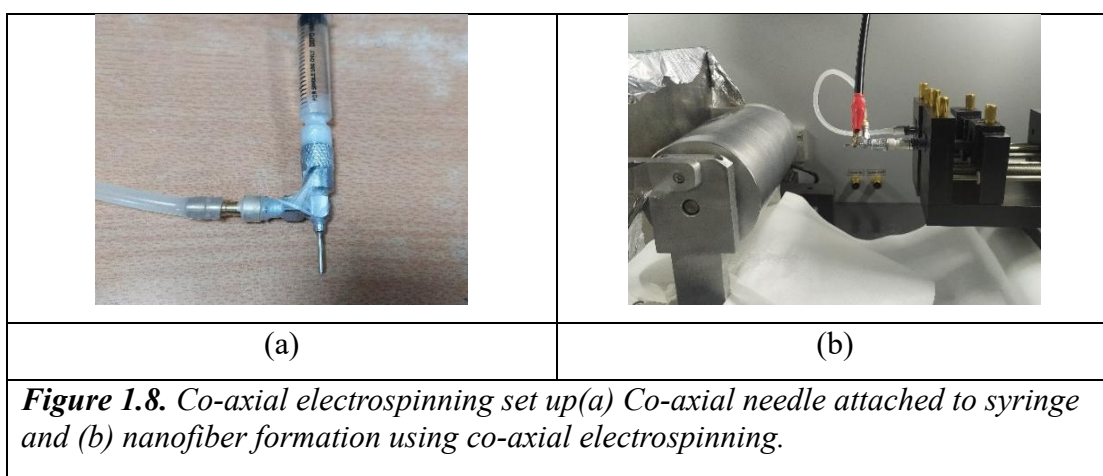
Wet electrospinning

The overall setup of wet electrospinning is like that of dry electrospinning, except for the collector unit. In wet electrospinning, the developed fibres are collected in a liquid bath that can be cured and washed depending upon the polymer-solvent interactions. Therefore, wet electrospinning is also known as wet spinning. The schematic of wet electrospinning is displayed in **Figure 1.9b**.

Needleless electrospinning

Polymer solutions were ejected from different sources, such as a ball, spiral coil, rotatory cone, or bubbles, which then formed nanofibers on the collector. As the spinneret forms numerous spinning jets of polymers, this approach has a higher production rate. (**Figure 1.9d**)

Figure 1.9. *Schematic of different types of electrospinning* (Angel et al., 2022a). *(a) Dry electrospinning, (b) Wet electrospinning, (c) Co-axial electrospinning, & (d) Bubble electrospinning*
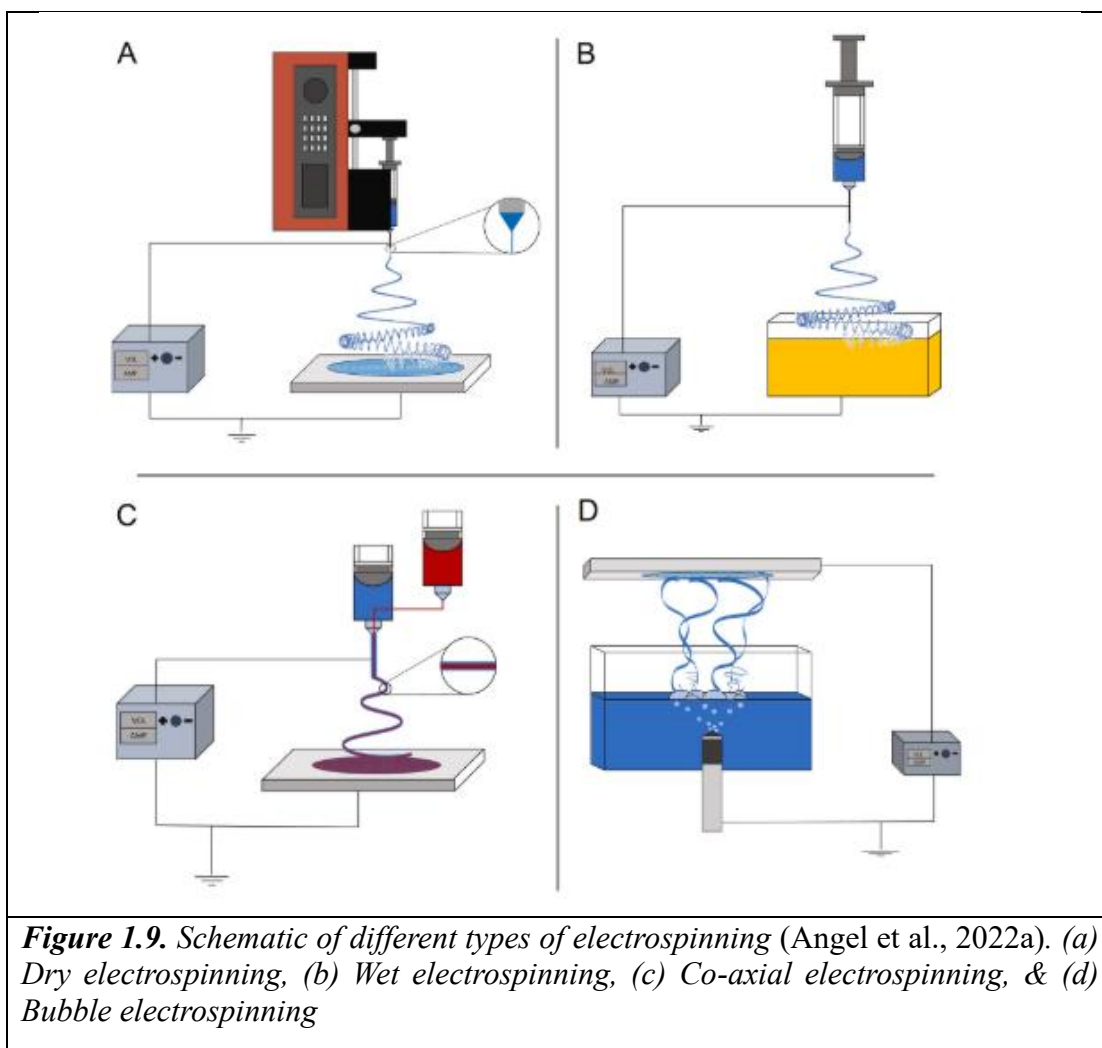
1.5.5. Incorporation of drug in nanofibers

In biomedical applications, the incorporation of drugs into the matrix often enhances the efficiency of the product. To incorporate drugs or bioactive agents for efficient loading, nanofiber morphology provides high loading efficiency due to the high surface-to-volume ratio. However, the selection of bioactive agents or drugs for the electrospinning process influenced by their molecular weight, hydrophobicity, hydrophilicity, and release mechanism (slow or fast release) according to the requirement(Jang et al., 2023a). Similar affinity between hydrophilic or hydrophobic agents and polymer matrices facilitates uniform blending. The molecular weight of the drug would also influence the release rate, as drugs with a high molecular weight would release slowly as compared to drugs with a lower molecular weight. Therefore, to

achieve efficient loading and release of drugs or bioactive agents' different electrospinning strategies can be used. Bioactive agents or drugs can be incorporated in nanofibers using different methods, including blend electrospinning, co-axial electrospinning, emulsion electrospinning, and surface modification of nanofibers with the desired drug for successful drug loading. The details of the various strategies are explained below:

a) **Blend electrospinning-** In the blend electrospinning process, drugs are blended directly into the polymer solution during the preparation of the polymer solution. Drug-infused polymer solutions can be used to develop drug-loaded nanofibers.

b) **Co-axial electrospinning-** Co-axial electrospinning helps in loading drug molecules in the inner or outer layer of the coaxial fibres, depending on the release rate requirement. Drugs loaded into the core would have a longer release rate than drugs loaded in the outer sheath. Apart from co-axial nanofibers, multiaxial nanofibers can be developed by incorporating different bioactive agents in different layers (Khalf & Madihally, 2017).

c) **Emulsion electrospinning-** Using emulsion electrospinning, drugs are often entrapped in water-to-oil or oil-to-water emulsions to boost the efficacy of the drug. The emulsion electrospinning prolongs the release rate without interrupting the drug's efficacy.

d) **Surface modification-** For efficient drug loading, the surface of the nanofibers can be modified with functional groups, enhancing the entrapment of the drug and further modulating the release of drug molecules depending upon the affinities of the polymer matrices.

e) **Multilayer-** To facilitate the release of different drugs, multilayer dressings were also fabricated using the electrospinning method, depending on the wound type(Song et al., 2023). Several strategies were used using blends or coaxials to incorporate drugs in different layers(S. Chen et al., 2017).

1.6. Electrospinnable polymers

Several synthetic and natural polymers can be electrospun using an electrospinning machine. To increase the efficacy of the developed mats, different bioactive and drugs can be incorporated, including proteins, enzymes, genes, drugs, antibiotics, and more. Some of the electrospinnable polymers are mentioned in **Table 1.4**.

1.6.1. Types of polymers

Synthetic polymers: Several thermoplastic and thermoset polymers were used to develop nanofibers using electrospinning. The use of organic and inorganic solvents to dissolve the polymer limits its use in biomedical applications. However, using mild acids and water increased the potential. A few synthetic polymers are polyacrylonitrile (PAN), polyvinyl alcohol (PVA), polycaprolactone (PCL), polyethyl oxide (PEO), polylactic acid (PLA), and more.

PAN can easily be blended with bio-based polymers using DMSO, DMF, DMA, etc. as solvents. Being a synthetic polymer, PAN exhibits exceptional mechanical properties and thermal resistance, providing synergistic effects after nanofiber formation for different applications, including wound dressing, gel electrolytes, etc. PVA, a hydrophilic polymer with excellent solubility in water, employed in biomedical applications owing to its biocompatibility and biodegradability. Electrospun PVA has shown its potential in several applications, including wastewater treatment, filtration, wound dressings, tissue regeneration, etc. Unlikely, polycaprolactone is a hydrophobic polymer, but owing to its bioresorbability, biodegradability, and biocompatibility, it is used in numerous applications like wound healing(Raina et al., 2022), tissue regeneration(Nazeer et al., 2019), implants, and more. Apart from biocompatibility, polyethylene oxide (PEO) has shown its potential in reducing cell adhesion owing to its antiadhesive properties and is hence used in wound dressings to reduce cell stickiness(Agarwal et al., 2013). Similarly, PLA(C. Dong et al., 2006) and PLGA(L. Zhang et al., 2018) with good mechanical properties and excellent biocompatibility, are used for biomedical applications. To deliver pharmaceutical drugs without compromising their efficacy, polyvinylpyrrolidone (PVP) was electrospun using ethanol as a solvent. The release rate was optimised by fabricating coaxial and triaxial

nanofibers(M. Wang, Li, et al., 2020a). Other synthetic polymers like polystyrene, polydimethylsiloxane, polyvinylchloride, and more were dissolved in inorganic solvents and used for different applications, including filtration(Lackowski et al., 2013), membrane(Lalia et al., 2014), energy storage(P. Lu et al., 2017), etc.

Although there are certain limitations associated with the synthetic electrospinnable polymers. Biodegradable polymers like PLA and PCL lack cellular binding sites, leading to poor cell adhesion and proliferation, which can delay wound healing. In some cases, where non-biodegradable polymers may remain at the wound site, requiring surgical measures. Therefore, blending synthetic polymers with natural polymers and introducing functional modifications may increase their potential for effective wound healing applications(Islam et al., 2019b; Jang et al., 2023b).

Natural polymers: Natural polymers have found applications in biomedical field due to their biocompatibility and biodegradability. It is mostly dissolved in water, which increases its applicability in biomedical applications. Despite their advantages, their electrospinnability sometimes requires the use of copolymers for successful nanofiber formation. Although the electrospinning of polymers helps modulate the fibre diameter, salignment, porosity, etc. A few natural polymers are listed in **Table 1.4**.

Table 1.4. List of synthetic and natural polymers used for biomedical applications.

a. Synthetic Polymer	Co-polymer	Solvent	Application
PAN	Agar	DMF, DMSO	Wound dressing(Alvandi et al., 2022), SERS measurement(T. Yang et al., 2015)
PVA	Sericin, PVP, CMC, agar	water	Air filtration(Purwar et al., 2016), drug delivery(El-Newehy et al., 2016), wound healing(Alipour et al., 2019)
PCL	Silk fibroin, Gelatin	Methanol: chloroform, acetone,	Tissue engineering(Nazeer et al., 2019), drug delivery

		acetic acid, formic acid	(Karuppuswamy & Reddy, 2015; Vittoria et al., 2009), wound dressing(Raina et al., 2022)
PEO	PVA, CMC, chitosan,	DI water	Wound dressings(Agarwal et al., 2013)
PLA	PVA, PEI	DMF, water	Tissue engineering(C. Dong et al., 2006)
PLGA	PEG,	DMF, chloroform	Wound healing(Soscia et al., 2010), drug delivery(L. Zhang et al., 2018)
PVP	Shellac	Ethanol, DMF	Drug delivery(Chinatangkul et al., 2019; M. Wang, Li, et al., 2020a)
PVC	PVDF	DMF, THF	Smoke filter(Lackowski et al., 2013)
PS		DMF	Thermal energy storage(P. Lu et al., 2017)
PDMS	PVP	DMF	Artificial skin, sensor, filtration(Niu et al., 2014)
PVDF	HFP, PVC, NCC	DMF, acetone, THF	Smoke filter(Lackowski et al., 2013), distillation membrane(Lalia et al., 2014)
b. Natural Polymer			
Alginate	PVA, PEO	Water, 2-propanol	Wound healing, drug delivery(Stone et al., 2013; Taemeh et al., 2020)
Chitosan	PCL	Acetic acid/formic acid, chloroform/methanol	Tissue engineering(Van Der Schueren et al., 2012), wound healing(Bayat et al., 2019), wound dressing(Trinca et al., 2017)
Gelatin	PCL	Acetic acid/water, ethanol/formic acid	Drug delivery(Laha et al., 2016), tissue engineering(C. Huang et al., 2015)

Silk	PVA	HFIP, water, acetone	Wound dressing(Kheradvar et al., 2018), O$_2$ generating patches(Aleemardani et al., 2020), drug delivery(Meng et al., 2021)
Collagen	PCL, PLA	Chloroform/formic acid, chloroform/ethanol	Wound dressing(Ahmadian et al., 2020; Armeda, 2018)
Cellulose	PCL, PVA	Formic acid/acetic acid, LiCl/DMAc	Cell proliferation(Unal et al., 2020), wound dressing(Firouzabadi et al., 2020)
Agar	PVA, PEO, chitosan, acrylamide, PAN	Water, TFA/DCM, DMF	Tissue engineering(Teng et al., 2009), biomedical(Cho et al., 2016a), SERS substrate(T. Yang et al., 2015)

1.6.2. Seaweed derived polysaccharide- Agar

Agar, a polysaccharide extracted from red seaweed, is an algal family of *Gelidiaceae* and *Gracilariaceae*. It is composed of repeating units of D-galactose and 3,6-anhydro-L-galactopyranose, forming agarose and agaropectin as components (Capillo et al., 2017). The alternate disaccharide units of agarobiose and neoagarobiose form the backbone of the agar(Alba & Kontogiorgos, 2020). Agarose, an agar-derived polysaccharide, has a high gelling fraction, is uncharged, and has a low sulphate content, whereas agaropectin contains a high sulphate content and has a low gelling capacity(Rhein-knudsen et al., 2015). Agar is utilized in the food industry as a gelling agent and thickener owing to its gelling properties. Additionally, its excellent biocompatibility and biodegradability have led to its adoption in the biomedical and microbiological applications, establishing it as a promising biopolymer.

1.6.3. Application of agar in medical field

Various components, including healing agents, systemic mediators, and others, work together to naturally repair injured tissues throughout the process of wound healing. The right concentration of these components is crucial for effective healing. In other

therapeutic circumstances, such as burns and chronic wounds, typically prolong the healing process and heightens the risk of microbial infection. Additional factors that impact the healing process include the nature of the wound, the extent of the injury, the presence of other medical conditions, and the presence of microbial infection. Consequently, these factors lead to a delay in the healing process, bacterial infection, and impaired growth and movement of cells. Therefore, an immediate requirement exists for a wound dressing that effectively manages the clinical complications linked to chronic and burn wounds(Bal-öztürk et al., 2021). Such a dressing should possess the following characteristics: sustained moisturization, resistance to bacterial invasion, promotion of collagen synthesis and cell proliferation, alleviation of pain, cost-effectiveness, biocompatibility, and biodegradability(Gruppuso et al., 2021).

Biopolymers are well-suited for wound dressings due to their biocompatibility, bio-activity, biodegradability, and non-toxic attributes. Moreover, it facilitates the transport of gene material, tissue, and medications(Ward & Georgiou, 2011). Polysaccharide-based biopolymers provide excellent features such as high-water absorption, non-immunogenicity, adjustable mechanical properties, and barrier properties that aid in wound healing. Additionally, it hinders the drying out of wounds by creating a moist environment, maintaining an appropriate level of water transfer, and regulating the release of medication.

Agar and its composites are currently being used for different biological applications. Controlled drug administration via agarose composite, biphasic scaffolds for bone production, microporous scaffolds for tissue engineering(Zarrintaj, Manouchehri, Ahmadi, Saeb, et al., 2018a), modular microbeads for cell-based therapies, and numerous others are among the suggested applications of agar-based materials(Annamalai et al., 2016; Wu et al., 2018; Zarrintaj, Manouchehri, Ahmadi, Saeb, et al., 2018b). Moreover, agar was also used as a reducing agent to develop metal nanoparticles(Rhim & Kanmani, 2015; Shukla et al., 2012). Apart from this, agar was also used for food packaging applications owing to its biodegradability(Arham et al., 2016; Madera-Santana et al., 2014a; Martínez-Sanz et al., 2019). Furthermore, its biocompatibility, bioactivity, non-immunogenicity, and biodegradability make it appropriate for wound healing purposes. An inexpensive and readily available agar

polymer can be processed for multiple supplementary applications, including wound healing. The polymer properties of this advanced wound care material show outstanding promise.

1.6.4. Electrospinning of agar biopolymer

As discussed earlier, the electrospinning technique assists in the development of polymeric scaffolds for tissue regeneration applications. It is a reliable and simpler technique to prepare an ECM-like structure. However, expensive instrumentation and limited biopolymers (Memic et al., 2019a) restrict its potential for biological applications. Several natural polymers have blended with polycaprolactone to enhance its mechanical properties and hydrophilicity (Armeda, 2018; C. Huang et al., 2015; Ji et al., 2010).

Fewer pieces of literature are present for the electrospinning of agar (Akshay Kumar et al., 2021), especially for biomedical applications, and therefore need further exploration. Previously, Teng et. al. reported the formation of agarose-chitosan electrospun fibers using trichloroacetic acid and dichloromethane as solvents (Teng et al., 2009). Agarose-based scaffolds were developed for tissue engineering as a potential wound healing material (Zarrintaj, Manouchehri, Ahmadi, & Saeb, 2018). Blends with other polymers, including PVA and agar, resulted in a smooth and homogenous nanofibrous structure (Sousa et al., 2015a). However, the concentration of agar was relatively lower than the copolymer for successful fiber formation for the differentiation of stem cells (Ziloochi Kashani et al., 2020). Using PAN as a copolymer, agar-based nanofibers were developed for different applications for controlled antibiotic release(Sadrearhami et al., 2015; H. Yang et al., 2014a) and SERS substrate formation(T. Yang et al., 2015). Forget et. al. developed carboxylated agar nanofibers as antibacterial films, demonstrated effectiveness against *S. aureus* and *P. aeruginosa*(Forget et al., 2016).

1.7. Research Gap

The natural wound healing process comprises four interconnected phases that require a multitude of internal and external factors to promote collagen formation, tissue

regeneration, and repression of free radical activities. In initial phase of wound healing, hemostasis ensures blood clot formation, followed by the formation of exudates, that require removal to prevent maceration due to excess fluids. Subsequently, during the inflammatory phase, it becomes essential to employ reactive oxygen species (ROS) scavengers to mitigate the negative effects they may cause. Throughout the proliferation phases of healing, antimicrobial measures are required until the wound completely heals. Furthermore, ideal moisture transfer rates are also necessary to promote optimum exudate evaporation at the wound site without dehydrating or macerating and to promote effective healing during the remodelling phase. Furthermore, various factors, including pH, temperature, moisture, infection, etc., can disrupt the natural healing phases, leading to delayed or impaired wound healing.

Depending on the wound care requirements, different functionality in the wound dressings is required. For instance, dressings with high swelling properties suit exudating wounds(Varshney et al., 2023), while antibacterial dressings aid in chronic wound healing(Eskandarinia et al., 2020a; Ranjbar-mohammadi et al., 2016), and hydrogel dressings accelerate healing in burn wounds(Alvandi et al., 2022). Natural polysaccharides-based dressings developed from hydrophilic matrices like agar, a natural polysaccharide extracted from seaweed, have gained attention in wound dressing applications(Tyeb et al., 2023) due to hydration and dehydration properties similar to skin(N. Roy et al., 2010b). Moreover, agar hydrogels have a high absorption capacity for fluids without transforming into free-flowing gels, which addresses the major concerns of exudate absorption and stickiness.

Aside from hydrogels, morphologies such as nanofibers are preferable for biomedical dressing(Yadav et al., 2024) attributed to their high surface area to volume ratio and structural resemblance to the extracellular matrix (ECM). The morphological asymmetries in the forms and attributes of nanofibers, films, and hydrogels, could potentially be used and enhanced by integrating different layers to enhance the efficacy of the wound dressings(Eskandarinia et al., 2020b). The limited literature(Cho et al., 2016b; Kashani et al., 2020) on agar-based nanofibers incorporated with bioactive agents for wound healing, underscores our rationale to pioneer the development of a bilayer agar-based dressing. Our approach involves the fabrication of asymmetric layers

comprising electrospun agar-based nanofibers of agar-PCL blend atop solvent-cast agar films. Polycaprolactone (PCL), known for its electrospinnability and hydrophobicity, would enhance the spinnability of agar nanofibers. Despite lacking inherent functional properties, agar is commonly modified with bioactive agents to impart antimicrobial and antioxidant properties(S. Roy & Rhim, 2019)

Nanomaterials, such as nanofibers and nanoparticles, exhibit extraordinary efficacy, bioavailability, and versatile capabilities due to their high surface area-to-volume ratio and dimensions of less than 1000 nm. Owing to their properties, nanomaterials have broad spectrum uses in multiple fields, including biological, pharmaceutical, and textile sectors. Particularly, nanofibers have demonstrated a successful approach for drug delivery, wound healing, and tissue engineering(Priya et al., 2022). Several nanoparticles, including silver, gold, and copper nanoparticles, have been incorporated into a polymer matrix(Abdollahi et al., 2021; Jeong & Park, 2014; L. Li et al., 2022) to impart antimicrobial properties. Among these, silver nanoparticles (AgNPs) are the highly tested nanoparticles owing to their strong antimicrobial activity(Agnihotri et al., 2013; Bruna et al., 2021; Sathiyaseelan et al., 2022) against a broad spectrum of microbes, including bacteria(Sawada et al., 2012), fungi, and viruses(Rai et al., 2009). New synthesis methods(Dawadi et al., 2021) have been evolved to form AgNPs by biological, chemical, and thermal reduction with one-pot synthesis(Emam et al., 2015; Rhim et al., 2013; Show et al., 2017) are also reported earlier(Pryshchepa et al., 2020). However, the emergence of reducing agent-free, one-pot green synthesis of nanoparticles has drawn attention for biocomposite films, considering the dose-dependent toxicity of the nanoparticles.

Furthermore, numerous bioactive agents, such as polyphenols, were integrated into polymers to impart biological functionalities, including anti-oxidant(Comino-Sanz et al., 2021), anti-inflammatory(Ninan et al., 2016), antiallergic(Mlcek et al., 2016), and antibacterial(El-Samad et al., 2022) properties. Gallic acid, a basic polyphenol(Das et al., 2021), has shown potency in neutralizing oxidative species, which is crucial for the early stage of healing, which involves scavenging reactive oxygen species (ROS). Dressings laden with antioxidant compounds could be designed, particularly electrospun nanofibrous dressings to release efficiently at the wound site to meet early

healing requirements. For drug delivery and wound healing properties, the application of nanofibers enhanced the loading and encapsulation efficiency of bioactive agents, site-specific delivery, controlled drug release, reduced drug side effects(Rasouli et al., 2019) and effective absorption of exudates(Ambekar & Kandasubramanian, 2019). Although fibre dimensions, drug loading concentration, and polymer properties(Ambekar & Kandasubramanian, 2019), all affect the release rate from the nanofibers. Most of the time, the initial burst drug release from the uniaxial nanofibers is a significant challenge that restricts its applications. However, this can be modulated with different fabrication methods, including co-axial fibresHasan & Shahid, 2023) that would control the release rate of the bioactive agents by reducing burst release and promoting sustained release(Sultanova et al., 2016) from the matrix. Additionally, the compatibility of the polymer matrix plays a critical role in initial burst release and low drug loading efficiency in the drug delivery system(H. Yang et al., 2014b). Therefore, we can develop new strategies to effectively release and deliver drugs during the wound healing process. Addressing this gap has the potential to significantly enhance the efficacy and efficiency of wound-healing treatments.

Advancements in fabrication techniques, including the electrospinning process have, facilitated the creation of nanofibers for advanced structures and functional applications(Duan et al., 2024; X. Huang et al., 2022; J. Li et al., 2024; Shlapakova et al., 2023; B. Singh et al., 2023; M. Wang, Hou, et al., 2020; D. G. Yu & Huang, 2023). This technique has evolved into more sophisticated techniques serving multiple loadings, such as uniaxial, coaxial, tri-axial, and side-by-side(Kumar Sen et al., 2024; Y. ; Wang et al., 2022; D.-G. Yu & Zhou, 2024). These advancements resulted in the development of various nanostructures, such as core-shell, Janus, and their combos(Angel et al., 2022b; Diep & Schiffman, 2023; Jain et al., 2020a; Jang et al., 2023b; J. Liu et al., 2021; H. H. Lu et al., 2023; Syed et al., 2023; M. Wang, Li, et al., 2020b; Y. ; Wang et al., 2023; Zhou et al., 2023).

Despite agar's high potential in wound healing applications, its properties remain underutilized in the form of nanofibers. Even at lower concentrations, forming agar nanofibers through electrospinning proved challenging, primarily due to its inherent gelling and film-forming capabilities, rendering it a non-spinnable polymer. Moreover,

additional studies are necessary to progress in this area due to the limited research available on the fabrication of agar nanofibers. Only a few researchers have examined its spinnability using copolymers such as polyvinyl alcohol (PVA)(Sousa et al., 2015a), polyacrylonitrile (PAN)(Wehlage et al., 2018), and polyethylene oxide (PEO)(Fuchs et al., 2017). Although the agar concentration used for the electrospinning process was comparatively lower, between 30% and 10%, the concentration of the co-polymers, which was more than 90%, predominantly resulted in nanofibers primarily composed of the copolymer rather than the agar. Furthermore, utilizing deep eutectic solvents and adding a co-polymer to the matrix polymer can result in the electrospinning of polysaccharides(Sousa et al., 2015b). Different co-polymers, like polycaprolactone (PCL), have been used to assist in the electrospinning of several biopolymers(Armeda, 2018; Ma et al., 2018; Raina et al., 2022; H. Yang et al., 2014b). The FDA-approved PCL, a hydrophobic polymer, is employed in biomedical applications due to its cost-effectiveness, biocompatibility, and excellent mechanical properties. However, its hydrophobic nature and lack of functional moieties severely restrict its applications (Aguirre-Chagala et al., 2017).

Introducing PCL into an agar matrix could increase both polymer's potential and utility for biomedical applications. Agar has higher swelling ratios as compared to polycaprolactone. Notably, by blending agar and PCL for nanofiber formation, we can increase the potential by imparting hydrophilic and hydrophobic phases to the dressing. This dual-phase characteristic of nanofibers would not only enhance the dressings versatility but also broaden the horizons for the incorporation of several hydrophilic and hydrophobic bioactive agents. As a result, the blend not only modifies the wettability of agar, but also provides synergistic mechanical characteristics with PCL. Additionally, the presence of hydrophilic and hydrophobic polymers in the same matrix allows for the integration of diverse pharmacological substances, such as hydrophilic and hydrophobic drugs, nanoparticles, and bioactive agents, which improves the bioactivity of the dressing. Blending of polymers with different water affinities results in phase separation, as in the case of agar and PCL, which may hinder the electrospinning process. To overcome such issues, the use of binary solvents was employed. Previously, researchers reported fabrication of agar nanofibers using a

variety of solvents, spinnable co-polymers, and other additives (Budurova et al., 2021; Gounani et al., 2020; Kanawung et al., 2007).

1.8. Organization of Thesis

The thesis is composed of five chapters and briefed as follows:

Chapter 1 begins by introducing the fundamental concepts of wound care management. The chapter provides the background information on the research and current state-of-the-art of bilayer electrospun dressing. While the notion of electrospinning polymers for different biomedical applications is well known, our current research focuses on exploring agar-based electrospun scaffolds.

Chapter 2 is dedicated to the scope and objectives of the current research. The research involves the fabrication of a bilayer advanced dressing for chronic wounds with efficient healing. The first objective outlines the fabrication process using the electrospinning technique for nanofibrous advanced wound dressing. The second objective is to evaluate the drug delivery from the dressing for efficient healing. The third objective was to assess the anti-bacterial properties of the developed dressing to minimize infection at the wound site. The fourth objective is to assess the biocompatibility and bioactivity of the dressing for accelerated healing. And lastly, in the fifth objective, degradation of the dressing in the presence of different enzymes and conditions will be studied.

Chapter 3 describes the materials and methods used to develop advanced wound dressings. This includes the fabrication of agar-PCL nanofibers via electrospinning. The fabrication process included controlled selection of parameter optimization for electrospinning. Coaxial nanofibers were fabricated to control the drug release and were examined using transmission electron microscopy. An electrospun layer was fabricated using the electrospinning method employing an agar/PCL blend. The supporting layer was fabricated using the solvent casted method and impregnated with silver nanoparticles (AgNPs). The AgNPs were synthesized by a green reduction method using agar in combination with a hydrothermal method. The physicochemical properties and antibacterial activity of the developed bilayer dressing were assessed. The biocompatibility was also evaluated using *in vitro* and *in vivo* experiments.

Chapter 4 presents the results and discussion of the advanced wound dressings developed for chronic wounds. The various attempts with the tandem approach performed in the electrospinning process were discussed. Furthermore, this chapter will present the results and discussion of the characterization methods, offering a detailed account of all the conducted studies, including antibacterial, antioxidant, *in vitro* and *in vivo* studies, will be described in this section.

Chapter 5 outlines the conclusive results of the performed study and proposes future research for the advancement of the fabricated bilayer dressing.

CHAPTER 2
HYPOTHESIS AND OBJECTIVES

2.1. Hypothesis

Nanofibrous dressing facilitates the efficient infusion of bioactive agents owing to its high surface area-to-volume ratio. Its excellent fibrous morphology mimics the extracellular matrix, enhancing permeability for air and moisture. The fabrication process of nanofibrous structural mats is performed with the help of electrospinning, which develops consistent and uniform nano- and microfibres. The uniform nanofibrous morphology facilitates gradual drug release from the fibres, enabling efficient release kinetics. However, several factors, including the diameter of the fibres, the loaded drug amount, polymer properties, and the morphology of the nanofiber construction, influence the release mechanism of drugs.

Depending on the polymer properties, certain biopolymers and synthetic polymers are electrospinnable. However, electrospinning of biopolymers is restricted owing to their high molecular weight, low surface tension, and limited solubility. Adding co-polymers improves the electrospinnability of the blend polymers, providing synergistic properties to the polymer blend.

In biopolymers, agar has shown promise in wound healing because of its impressive water-absorption capabilities and minimal cell adhesion. These properties effectively address the primary challenges of wound exudate absorption and dressing's stickiness. Nevertheless, when using electrospinning, the gelation of agar hinders the nanofibrous morphology. The addition of synthetic polymers as copolymers aids in the formation of nanofibers. The synergistic approach of combining biopolymers with an electrospinnable synthetic polymer facilitates the formation of nanofibers with enhanced properties. The resulting blend can be loaded with hydrophobic and hydrophilic drugs, owing to the complimentary properties of the polymers.

In the present research, agar-based nanofibers were developed using polycaprolactone (PCL) as a copolymer. The addition of polycaprolactone to an agar matrix enhances the versatility and applicability of both polymers in biomedical applications. The blend of

these polymers influences their properties, such as wettability, strength, and permeability. Furthermore, incorporating hydrophilic and hydrophobic polymer in a single matrix allows for integrating various drugs, such as cephalexin hydrate and other bioactive agents like gallic acid. This integration results in enhanced bioactivity of the dressing without compromising biocompatibility, as both polymers are known to be biocompatible.

However, utilizing two different polymers with varying water affinities requires common solvents to blend them without phase separation. Therefore, binary solvents with excellent miscibility were used in this study. The blend was created using formic acid and acetic acid, as both solvents dissolve agar and polycaprolactone without causing phase separation.

The current study aimed to electrospinning agar-based nanofibers by incorporating PCL as a copolymer. The research examined the outcome of utilizing two polymers with different water affinity. The investigation focused on assessing the influence of electrospinning factors, including voltage, spinneret to collector distance, collecting drum speed, flowrate, etc. on the morphology of the fibres. The developed nanofibrous dressing was then evaluated for its physicochemical properties, biocompatibility, biodegradation, and antibacterial efficacy.

2.2. Scope and Objectives

Nanofibrous dressings have emerged as advanced solutions to address the healing requirements of chronic wounds, providing a moist environment, adequate oxygen permeability, sustained drug release, mimicking cellular morphology, and improved cell proliferation and differentiation. Electrospinning offers a promising approach for developing advanced nanofibrous dressings and promoting effective wound healing. A primary challenge involves forming nanofibers from biopolymers that require optimization of electrospinning parameters and the incorporation of cosolvents and copolymers. The primary objective of the research is to develop agar nanofibers using different solvents and incorporating polycaprolactone as a copolymer. Another aim was to create a symmetric nanofibrous bilayer dressing capable of incorporating different

drugs and bioactive agents to address different stages of healing, including antibacterial and antioxidant properties. Additionally, an asymmetric bilayer dressing was fabricated using electrospinning and solvent casting to sustain the release of antibacterial agents. To achieve these aims, the following objectives have been configured for the present study:

2.1.1. Nanofibrous dressing mats

To fabricate a highly absorbent, nanofibrous bilayer dressing using different fabrication methods. For the electrospinning process, agar with a copolymer was used to develop an agar-based nanofibrous membrane.

2.1.2. Drug delivery

Due to the high surface area-to-volume ratio of electrospun mats, various bioactive agents and drugs were loaded, and their release in the wound microenvironment was studied. Silver nanoparticles and cephalexin hydrate were used as antibacterial agents, while gallic acid was used as an antioxidant agent.

2.1.3. Antibacterial properties

Since the proposed study focuses on wound healing and materials for advanced wounds, the study incorporated antibacterial properties to minimize infections at the wound site. This objective was assessed through antibacterial testing, including disk diffusion and time-kill assays of the antibacterial agents incorporated into the electrospun dressing.

2.1.4. Bio-compatibility

The fourth objective of the research, includes evaluating the biocompatibility of the developed dressing made from biopolymers and bio-compatible reagents, including bioactive agents. The study will also assess the hemocompatibility and cytocompatibility of the wound healing dressing material through wound scratch assays. Additionally, it includes a biochemical analysis of the free radical scavenging activity, known as the antioxidant activity, of the developed dressing. This includes in vitro and in vivo assessments of the developed dressing.

2.1.5. Biodegradability

Analysis of biodegradability is the fifth objectives of the proposed research. As a biopolymer-based dressing, it should degrade quickly without imposing any additional burden on the human body or the environment.

CHAPTER 3
EXPERIMENTAL METHODS

3.1. Materials

Agar, dulbecco's modified eagle medium (DMEM), fetal bovine serum (origin-Brazil) (FBS), penicillin-streptomycin-neomycin solution, and trypsin EDTA solution were procured from Himedia Laboratories Pvt. Ltd., India. Polycaprolactone (PCL), ethanol, gallic acid, bovine albumin, cephalexin hydrate, and piperine were procured from Sigma Aldrich Pvt. Ltd., India. Formic acid (85%), dimethyl sulfoxide (DMSO), polyvinyl alcohol (PVA), and glacial acetic acid were bought from Loba Chemie Pvt. Ltd., India. Phosphate buffered saline (PBS) formulation constituents including sodium chloride, sodium hydrogen phosphate, potassium chloride, potassium dihydrogen phosphate, sodium hydroxide, hydrochloric acid, calcium chloride dihydrate, and thiazolyl blue tetrazolium bromide (98%) were purchased from Thermo Fisher scientific India Pvt. Ltd., India. Silver nitrate was obtained from RFCL Limited, India. Potassium bromide (KBr), and 2, 2-diphenyl-1- picrylhydrazyl (DPPH) were procured from Sisco Research Laboratories (SRL) Pvt. Ltd., India. Thiazolyl blue tetrazolium bromide (98%) was procured from Thermo Fisher Scientific India Pvt. Ltd., India.

3.2. Method

3.2.1. Solution preparation

For the electrospinning process, a polymer solution was prepared using different solvents. Agar was initially dissolved in DMSO at different concentrations (5%, 7%, and 10%). The polymer was stirred in the solvent for 18 h at 90°C and then degassed for 24 h in a vacuum desiccator. Additionally, a 20% agar solution was prepared by dissolving in formic acid to blend with synthetic polymers. This agar solution in formic acid was stirred at room temperature and stored at 4°C.

Similarly, PCL solution was prepared by adding 4 g (w/v) in 20 mL of acetic acid followed by stirring at 60 °C for 4 h. A magnetic stirrer was used to blend the polymer solution in different ratios until a clear solution was achieved. The prepared agar: PCL solution was prepared freshly at room temperature just before the electrospinning process.

3.2.2. Fabrication of silver nanoparticles infused agar films

A stock solution of silver nitrate (50 mg/mL) was prepared and stored in the dark. The solvent casting method was employed to fabricate silver nanoparticles embedded agar films. In brief, 2 g of agar was mixed with 100 mL of deionized water containing 10% glycerol as a plasticizer. Different concentrations of silver nitrate (0.1 mM, 0.2 mM, 0.3 mM, 0.4 mM, and 0.5 mM) were added to the agar solution. To prevent degradation of silver nitrate by light, the flask containing the solutions was wrapped in aluminium foil before autoclaving at 121°C for 15 minutes to convert $AgNO_3$ into silver nanoparticles. After autoclaving, the lukewarm solutions were transferred onto 140 mm polystyrene petri dishes, dried overnight at 45 °C in the dark, and covered with aluminium foil for later use. The resulting agar-silver nanoparticles (agar/AgNPs) served as the substrate or base layer for the electrospun AP nanofibrous layer, creating a bilayer structure.

3.2.3. Fabrication of uniaxial electrospun films

The electrospinning parameter optimization was conducted using the E-Spin Super ES-3 electrospinning machine. The distance between the nozzle and the collector ranged from 5 cm to 15 cm. Various combinations were experimented with the agar solution, involving the distance between the nozzel and the collector, applied potential, collector drum speed, the feed rate of the solution and the concentration of the solution. The applied voltage was varied from 10 kV to 25 kV, and the feed rate was varied from 10 µL/min to 50 µL/mL.

For the electrospinning of agar: PCL blend solution, different ratios of the two polymers were blended at room temperature. Agar and PCL were combined in ratios of 4:5, 5:5. 6:5. And 7:5. For instance, a 3:5 ratio indicates 3 parts agar and 5 parts PCL. The solutions were mixed at ambient conditions for 30 min prior to electrospinning.

During electrospinning, the prepared agar: PCL solution was loaded into a 2 mL syringe, which was then connected to a programmed injection pump. The distance between the needle tip and the collecting drum was adjusted to 5 cm, 7 cm, and 10 cm. The applied potential varied between 10 kV, 15 kV, and 20 kV. The flow rate was adjusted between 10 µL/min to 15 µL/min. The spinning drum speed was adjusted at intervals of 200 rpm, ranging from 200 rpm to 1100 rpm. The electrospinning parameters were selected based on a tandem approach. The process was conducted at an ambient temperature of 30 °C and a relative humidity (RH) of approximately 37%.

3.2.4. Fabrication of coaxial electrospun films

For coaxial electrospinning, PVA was used as a core polymer incorporated with drug, and agar: PCL as a sheath polymer. Polyvinyl solution (8%, 10%, and 12%) was prepared by heating at 120 °C in DI water, stirring for overnight on a hot plate magnetic stirrer followed by storing at room temperature. PVA solution was subjected to electrospinning at 15 kV with flowrate 10 µL/min maintaining the distance of 10 cm between nozzle tip to the collector drum (500 rpm). Cephalexin hydrate (CEX) at a concentration of 20 mg/mL was incorporated into the core of co-axial agar: PCL electrospun films and was stored at 4 °C in dark. The outer layer of coaxial was formed using an agar: PCL solution. The flowrate was sustained at 10 µL/min by employing 2 mL syringe with an internal diameter of 9.12 mm. 15 kV potential difference was applied with 7 cm distance between the needle tip and collector sheet. The drum's rotating speed was consistently maintained at 500 revolutions per minute (rpm). Single layer films were produced using co-axial agar: PCL films with a PVA core. In contrast, bilayer films had an extra layer of agar: PCL electrospun material on top of the single layer films.

3.2.5. Fabrication of symmetric and asymmetric bilayer dressings

The agar:PCL electrospun layer was fabricated in two different types of bilayer dressings, including symmetric and asymmetric bilayer dressing. In symmetric bilayer dressing, both the layers were fabricated using electrospun nanofibers as transdermal patches, where upper layer was coaxial nanofibrous mat containing core of PVA on top of agar: PCL uniaxial nanofibrous layer. The schematic of the symmetric bilayer dressing is demonstrated in **Figure 3.1**. It was anticipated that the extra layer of agar:

PCL fibres would function as a barrier layer, slowing the release rate of the bioactive chemicals from the coaxial layer. **Figure 3.1**Error! Reference source not found. displayed the diagram of the produced uniaxial and coaxial bilayer film.
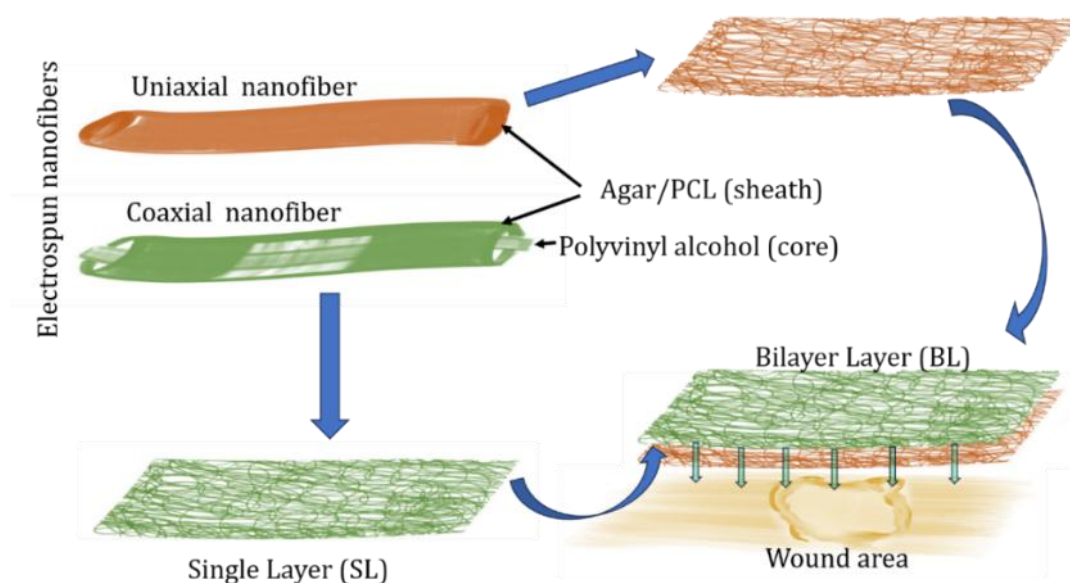
Figure 3.1. Schematic diagram for the development of single and bilayer dressing from uniaxial agar: PCL nanofibers and coaxial nanofibers where agar: PCL as sheath polymer and PVA as core.

In asymmetric bilayer dressing, primary layer was prepared using agar:PCL electrospun nanofibrous mat while the upper layer was fabricated using solvent casting of agar solution incorporated with silver nanoparticles. Both the layers had different morphology enhancing the wound healing properties. To avoid the delamination of both the fabricated layers, glutaraldehyde was used as a crosslinker. The electrospun AP-gallic acid and agar/AgNPs base layer were crosslinked by exposing them to vapours of glutaraldehyde (25%) aiming to form a prepared bilayer structure. Briefly the films that developed were enclosed in a vacuum desiccator made of polypropylene with a diameter of 210 mm. The desiccator contained 20 mL of glutaraldehyde solution. The bilayer dressings were crosslinked for five hours in the presence of glutaraldehyde vapours while the desiccator was vacuum sealed. The crosslinked bilayer structure was dried for 48 hours at 30°C in a hot air oven in the dark to eliminate glutaraldehyde, and then for another 24 hours at 50°C in a vacuum oven. The developed asymmetric

bilayer dressings were stored in aluminium foil for later use. The schematic of the fabrication of asymmetric bilayer dressing was shown in **Figure 3.2**.

Figure 3.2. Schematic of fabrication of agar-based bilayer dressing. Step 1 involves the fabrication of single layer of agar incorporated with silver nanoparticles as an antibacterial agent using the solvent casting method. In step 2, bilayer structure was developed using electrospinning of agar: PCL infused with gallic acid as an antioxidant. Step 3 details the sustained release of antioxidant and antibacterial agents at the wound site.

3.3. Characterization

3.3.1. Optical properties

Using a UV-vis spectrophotometer (Evolution 201, Thermo Fisher), the reduction of $AgNO_3$ to silver nanoparticles was validated. The AgNPs-containing agar films (1 cm × 1 cm) were adhered to the cuvette window using double-sided tape, and absorbance spectra from 300 nm to 600 nm were recorded.

3.3.2. Morphological properties

For the morphological analysis, samples were mounted on the aluminium stub with the help of double-sided carbon tape. The samples were coated with gold sputter for 180 seconds using the EMITECH SC 7620 sputter coater. Using FESEM microscopy (FEI

NOVA NANO SEM 450 FESEM) with a 10 kV voltage and a 5 mm working distance, micrographs of gold sputter-coated materials were captured. The resulting SEM micrographs were then analysed with ImageJ software to determine the average diameter of about 100 fibres per sample based on the obtained SEM micrographs. The micrographs were taken at 30000 × magnification.

3.3.3. Nanostructure analysis

To demonstrate the co-axial structural integrity, transmission electron microscopy was used to examine nanostructural features. We have incorporated silver nitrate (2 mg/mL) into the PVA core to image coaxial morphology. The uniaxial and coaxial fibres were dissected to less than 1 mm in length and dispersed in methanol. For effective dispersion, the fibres in methanol were sonicated for 20 min at room temperature. A 2 µL droplet was cast on a carbon-coated grid (PELCO GRIDS 200 CU), followed by vacuum drying. Following the imaging of silver nanoparticles, incorporated samples were performed using an electron transmission microscope (FEI-Tecnai G2 12 Twin 120 KV).

3.3.4. Chemical properties

Fourier transform infrared spectroscopy (FTIR) model Perkin Elmer spectrum version 10.03.06 in the range of 400-4000 cm^{-1}, was used to analyze the functional groups on the samples. For analysis, the samples were ground with KBr at a ratio of 1:10, followed by 24 h of conditioning at 45°C to remove any traces of moisture. The acquired spectrograms were examined for any peak shift, peak absence, or peak formation.

3.3.5. Mechanical properties

Universal Testing Machine (UTM) INSTRON 3345 was used to assess the tensile properties of the prepared samples according to the ASTM D882-12 standard. Using a gauze length of 40 mm for the experiment, samples were cut to 70 mm×10 mm, leaving 15 mm on both edges as gripping areas. The materials were stressed using a 5 kN load cell with a 10 mm/min crosshead speed. Prior to testing, samples were conditioned for 24 hours at 50% RH and 25°C. The tensile strength and elongation at break were determined by testing five strips from each sample and then calculating the mean value.

3.3.6. Fluid handling properties

Wettability

Using a Data Physics goniometer (Model OCA EC15), the contact angle was determined by dropping a 5 μL droplet of DI water on the surface of the nanofibers dressing surface, which would be in direct contact with the wound. The angle between the surface and the water droplet was measured, and the average of three drops was used for analysis.

Swelling properties

To assess the swelling percentage of the samples, 1 cm × 1 cm squares were cut from the electrospun sample and conditioned at 45 °C in a hot air oven until consistent weight was achieved. The samples were then immersed in deionized (DI) water for the specified time intervals, followed by the weighing of swollen samples after removing excess surface water with low-linting (Kimwipes®) tissues. The swelling percentage was calculated by using

$$Swelling\ percentage = \frac{Final\ wet\ weight - initial\ dry\ weight}{Initial\ dry\ weight} \times 100$$

After defined time interval, samples were again dehydrated for 24 h at 45 °C in a hot air oven, followed by measuring the weight difference of the dehydrated samples to evaluate the degree of dissolution.

Dissolution study

For the study, samples were cut in to dimensions of 1 cm×1 cm. The samples were soaked in the appropriate solution for a predetermined amount of time. After which, the samples were washed with deionized water and wiped with tissue and dehydrated at 45 °C in a hot air oven until a steady weight was obtained. The weight loss of the samples after washing represented the degree of weight loss (in percent %). Dissolution (%) was calculated using

$$Dissolution\ percentage = \frac{initial\ dry\ weight - Final\ dry\ weight}{Initial\ dry\ weight} \times 100$$

Where initial dry weight was the weight before dissolution and final dry weight was the final dried weight of the samples after dissolution.

Absorbency

The fluid handling properties were evaluated based on previously published literature (Kim et al., 2019; Uzun et al., 2013). The SMTL test standard BS EN 13726-1:2002 section 3.2 – free swell absorptive capacity was applied to determine the absorption capacity of electrospun dressing mats. The test was conducted in a solution prepared with sodium chloride (2.298 g/L) and calcium chloride dihydrate (0.368 g/L) dissolved in deionized water. The samples were hydrated with 40 times their own weight for 30 minutes at 37 °C. The wet weight of the samples was calculated after they were held in forceps for 30 seconds to drain off any excess solution on the surface of the sample. To calculate the absorption capacity of the samples, the mean of triplicate samples was determined. Absorbency refers to the capacity of fluid uptake followed by retention, which differs from swelling, wherein the material absorbs fluid and subsequently increases in dimensions. Unlike absorbency, the evaluation of swelling properties involves wiping the surface moisture of the samples to remove excess water.

$$Absorbency = \frac{wet\ weight\ (g) - dry\ weight(g)}{dry\ weight\ (g)}$$

Rate of Absorption

The rate of water droplet absorption on the surface of the sample was determined by placing 20 µL of test solution onto the surface. The dispersion time of the fluid was recorded using a digital stopwatch and the average absorption time from 10 droplets were recorded in seconds (s).

Dehydration

With the use of dehydration measurements, the rate of moisture loss from samples was calculated. Before submerging the samples were submerged for 30 minutes in an excess volume of sodium chloride and calcium chloride solution. After suspending samples with forceps to extract excess solution, their moisture content was determined. The samples were subsequently placed in an open petri dish and dehydrated at 37 °C for a specified period of time. The dehydration rate (g/min) was calculated using

$$Dehydration = \frac{wet\ weight\ (g) - dry\ weight(g)}{time\ duration\ (min)}$$

Where, wet weight (in g) was the weight of the mats after immersion in the fluid solution, and dried weight (in g) was the weight of the dehydrated sample after the specified time interval (in min).

Water Vapor Transmission Rate

A modified version of the ASTM E96 standard technique was used to calculate the water vapor transmission rate of the developed electrospun membranes(Sonker et al., 2017). For the water vapor transmission tests, 15 mL of culture bottles were filled with 10 mL of DI water. To place the sample discs on the mouths of the glass containers, 18 mm diameter discs were cut from the samples. Parafilm was utilized to secure the electrospun membrane discs to the openings of the glass bottles, preventing any moisture loss. After mounting the samples, each bottle was carefully weighed every 24 hours for seven days at a relative humidity difference between (inner and outer space of bottle) of 60% RH at 30°C. The WVTR of the permeation area (m^2) of the electrospun membranes was determined from the slopes of the linear curves depicting the weight loss (g) with time (24 h) using

$$WVTR = \frac{\Delta weight}{\Delta Time \times Area}$$

3.3.7. In vitro degradation study

Biodegradation of the bilayer dressing was performed using *in vitro* degradation study, as previously described (Ahtzaz et al., 2017a). 1 cm × 1 cm samples were incubated in 5 mL phosphate buffered saline (PBS), pH 7.4, containing lysozyme (1 mg/mL) and H_2O_2 (2.58 µM) at 37 °C for defined time intervals (1, 3, and 7 days). The degradation percentage of the samples was calculated as follows

$$Degradation\ \% = \frac{W0 - Wt}{W0} \times 100$$

where W_0 was the initial weight before degradation and W_t was the dried weight of the sample at time t.

3.3.8. Antioxidant properties

To quantify free-radical scavenging properties of gallic acid incorporated electrospun top layer on silver AgNPs containing agar-based bilayer dressing, 2,2- diphenyl-1-picrylhydrazyl (DPPH) spectroscopic method was employed. Dressings of 1 cm (diameter) were taken off from the bilayer dressing using a 1 cm (diameter) biopsy cutter. After 15 minutes of soaking in 200 µL of DI water, 500 µL of DPPH methanolic solution (500 µM) was added to the circular discs and were incubated at 37°C for varying amounts of time. The absorption of reduced DPPH radicals from hydrogen donor gallic acid was measured using a microplate reader at 517 nm after a predetermined time interval. As a control, DPPH solution was taken. The test was conducted in triplicate, with the mean value and standard error reported.

$$Inhibition \% = \frac{(Absorbance\ of\ control - Absorbance\ of\ sample)}{Absorbance\ of\ control} \times 100$$

3.3.9. Antibacterial properties

Disk Diffusion assay

Cephalexin hydrate was evaluated against gram negative (*E. coli, P. vulgaris, & P. aeruginosa*) and gram-positive bacteria (*S. aureus*) to determine its minimum inhibition concentration (MIC) and minimum bactericidal concentration (MBC). The microorganisms were cultured in Muller-Hinton (MH) broth, which was prepared by dissolving 21 g of MH powder in DI water, followed by autoclaving for 15 minutes at 121 °C. Similar to the MH broth preparation, additional 1.5% agar was added to prepare Muller-Hinton agar (MHA) plates. Following autoclaving, the entire MHA plate preparation procedure was carried out under a laminar airflow. To prepare the plates, the autoclaved MHA was cooled slightly. In a laminar hood, 20 mL of the MHA solution was then poured into sterile 90 mm polystyrene plates, and the plates were allowed to cool at room temperature until completely solidified. The prepared MHA plates and MHB were sealed with parafilm and stored at 4 °C for further use. MIC was calculated using broth microdilution method according to previous literature (Balouiri et al., 2015; Sharma et al., 2009) in a 96 well plate. The MIC of cephalexin hydrate was calculated in a 96-well plate using the broth microdilution procedure. MIC was quantified against

mentioned bacteria after half-fold serial dilution starting from 2.5 mg. The wells showing no turbidity were considered as minimum inhibitory concentration. For MBC, the lowest concentration of drug with bactericidal activity was determined by sub-culturing bacterial cultures on MHA plate from MIC 96- wells and incubating them at 37 °C for 24 hours. Kanamycin and MHB without sample, served as positive and negative control in the experiment.

MHA plates were inoculated with mentioned bacteria using an L-shaped spreader. For zone of inhibition (ZOI), a 6 mm diameter sample disc and placed aseptically on the cultured MHA plates. The test sample were incubated at 37 °C for 24 h in an incubator shaker to determine the ZOI diameter for each sample.

Time-kill assay-log reduction

Time kill assay was performed to analyse the antibacterial properties of silver nanoparticles incorporated agar films in accordance with the procedure described by Sharma *et. al*. (Sharma et al., 2009). Briefly, over-night grown culture of *E. coli, S. aureus, P. aeruginosa,* and *P. vulgaris* were cultured starting with inoculating single colony of the respective bacteria in MH Broth (MHB). The overnight bacterial cultures were diluted to 0.1 OD (600 nm) for the log reduction assay using MHB. In a 48 well plate, samples incorporated with 0.1 mM, 0.2 mM, and 0.3 mM silver nitrate were incubated in the mentioned bacterial solution at 37 °C for varied duration. After every 2 h intervals, samples of the bacterial suspension were collected followed by serial dilution in sterile normal saline solution, plating on MHA plates, and incubation at 37°C for overnight. The bacterial colonies were enumerated from the overnight incubated plates and number of colonies forming units per unit volume (CFU/mL) was evaluated. The results were presented in log CFU count of bacterial growth.

3.3.10. Biocompatibility testing

Haemolysis

The haemolysis assay was performed according to the aforementioned literature (Sonker et al., 2019) to assess the hemocompatibility of the developed electrospun mat using RBC suspension. Briefly, fresh goat blood was collected from a butcher and chelated with 0.5 mM EDTA as an anticoagulant. The collected blood was centrifuged

at 700 g for 10 min. The supernatant was discarded, and the pellet was resuspended in the PBS buffer and was again washed thrice with cold PBS (pH 7.4). The RBC pellet was diluted 10 times in cold PBS to obtain erythrocytes or RBC suspension and was used within 24 hours of preparation. For the *in-vitro* haemolysis assay, samples were cut into 8 mm discs and rinsed with cold PBS to prevent erythrocytes from osmotic shock. The PBS-saturated samples were incubated in the prepared RBC suspension for 90 min at 37 °C. After incubation, the samples were centrifuged at 700 g for 10 minutes, and the supernatant was collected. At 540 nm, the absorbance of the collected supernatant was measured using a microplate reader (medispec BioTek cytation 5 imaging reader). As a positive control, 0.1% Triton-X was added to a suspension of erythrocytes to induce complete hemolysis, while RBC suspension was used as a negative control. The average result of triplicate samples was recorded, and the haemolysis % was calculated by

$$Haemolysis \% = \frac{Abs\ of\ sample}{Abs\ of\ positive\ control} \times 100$$

where Abs means recorded absorbance at 540 nm.

3.3.11. Platelet adhesion

With the help of a platelet aggregation assay (Quan et al., 2015), the hemocompatibility of bilayer dressing was determined. Platelet-rich plasma (PRP) was extracted from fresh goat blood by centrifuging at $700 \times g$ for 10 min. The supernatant PRP was again centrifuged at $2000 \times g$ for 20 minutes at 4 °C using a tabletop centrifuge (Thermo Scientific SORVALL ST 16R) to obtain platelet poor plasma (PPP). Platelets were enumerated with a haemocytometer and adjusted to 1×10^7 platelets with platelet-poor plasma (PPP). The bilayer dressing (1 cm in diameter) was rinsed twice with PBS, infused with 200 µL PRP, and incubated at 37°C for 1 hour. Followed the incubation period, samples were delicately rinsed three times with PBS and dehydrated using a gradient ethanol treatment (50%, 60%, 70%, 80%, 90%, & 100% ethanol) for 10 minutes in each concentration. The alcohol was removed from the dehydrated samples using freeze-drying, followed by gold coating for SEM visualization (as mentioned above).

3.3.12. *In-vitro* Assay

In-vitro cytocompatibility assay was performed using NIH 3T3 fibroblast cells, which were cultured in Dulbecco's DMEM (also known as complete DMEM) containing 10%, Fetal Bovine Serum (FBS) and 1% antibiotics (penicillin and streptomycin). Incomplete DMEM was deprived of serum and antibiotic. The cells were incubated at 37°C with 5% CO_2 until they reached 70% confluence, followed by trypsinizing them for a subsequent passage by the addition of trypsin. Meanwhile, the electrospun samples were cut into 1 cm diameter discs using a biopsy cutter and each side were UV-sterilized for 2 hours. The sterilized samples were pre-washed three times with PBS (pH 7.4) followed by saturating the samples in complete DMEM medium and testing.

Cytocompatibility -MTT assay

The cell viability was determined using direct and indirect contact assay. For direct assay, cells were grown in the presence of samples whereas, cell culture insert plates were used for indirect assay facing top layer of agar: PCL towards cells. The 3-(4,5 dimethylthiazol-2-yl)-2,5 -diphenyl tetrazolium bromide (MTT) assay was conducted to evaluate the cell proliferation and cytocompatibility of the samples. Fresh MTT solution was prepared in incomplete DMEM medium and kept at 37 °C until use. On the conditioned samples, 70% confluent fibroblast cells were trypsinized before being seeded at a density of 3×10^4 cells per well. After 2 hours of incubation, the samples were incubated for 24 h at 37 °C in a CO_2 incubator with the addition of complete medium. To determine the cell viability, the medium was replaced with 500 μL (0.5 mg/mL) MTT solution for an additional 4 h of incubation. The developed formazan crystals were dissolved by adding 400 μL of DMSO (100%) followed by 15 min of stirring. At 570 nm, the absorbance of the dissolved formazan crystals was measured using a microplate reader (Medispec BioTek Cytation 5 imaging reader). The wells seeded without any sample in the culture plate served as a positive control for the cytocompatibility assay, and the viability (%) of the cells was determined by calculating the number of viable cells using

$$cell\ viability\ \% = \frac{sample\ absorbance}{Positive\ control\ absorbance} \times 100$$

Cell adhesion assay

Trypsinized cells were seeded at a density of 3×10^4 cells per well onto conditioned DMEM samples in a 24 well plate. After incubating the samples for 4 h, 400 µL of complete DMEM medium was added to each well. After a specified incubation period, samples were fixed overnight at 4°C with 2.5% glutaraldehyde solution. The fixed cells on the samples were dehydrated using a gradient alcohol treatment for 10 minutes each in 50% ethanol, 70% ethanol, 90% ethanol, and finally with 100% ethanol. For the morphological studies, the dehydrated samples were freeze-dried and stored at room temperature until SEM examination.

3.3.13. Wound scratch assay

The wound scratch assay was conducted in accordance with previously cited literature (Vivcharenko, Wojcik, et al., 2020). In short, fibroblast cells were cultured in a 24-well plate with a cell density of 4×10^5 cells/well and incubated for 48 h at 37° C with 5% CO_2 in a humidified environment until 90% confluency was achieved. To simulate a wound scratch, a monolayer of fibroblast cells was scratched with a 10 µL pipette tip. The 5 mm × 5 mm samples were UV-sterilized for 2 hours, washed with PBS (pH 7.4), and then saturated with DMEM complete medium. The cells were then treated with saturated samples comprising bilayer agar films devoid of silver nanoparticles (A), 0.1 mM bilayer agar films (B), 0.2 mM bilayer agar films (C), and an electrospun primary layer with gallic acid (D) loaded in insert plates. As a positive control, cells cultured on tissue culture plates (TCP) without any sample were considered, whereas DMSO infused cultured cells were used as negative control. After 24 hours of cell culture, digital images were acquired using a Leica inverted DMi8 microscope at 20× magnification and the wound scratches was monitored for cell migration and proliferation by captured images. Wound closure area was measured with the help of ImageJ software (Suarez-Arnedo et al., 2020) by using the equation

$$Wound\ closure\ area\ (\%)$$
$$= \frac{(Initial\ scratched\ area - Final\ scratched\ area\ )}{Initial\ scratched\ area} \times 100$$

3.3.14. *In vitro* release of silver nanoparticles

Silver release from the developed bilayer dressing was assessed using an Inductive coupled Plasma Mass Spectrophotometer (ICP-MS) from Agilent Technologies (model no- 7900 ICP-MS). For the ICP-MS analysis, Milli-Q ultrapure deionized (DI) water was utilized for all dilutions and standard preparations. A high-purity ICP multi element calibration standard 2A solution from Agilent Technologies was employed for the standard calibration curve. The linearity of the samples in relation to the reference solution curve was considered acceptable with a standard deviation less than 5% (coefficient of linear correlation, >0.999).

For the release assay, 1 cm^2 circular discs (triplicates) of the developed dressing were incubated in milli-Q ultrapure water for the required time intervals. After defined incubation intervals, aliquots from each sample were collected and replaced with same volume of milli-Q ultrapure water. To evaluate total amount of silver content, samples discs were dissolved in the required milli-Q ultrapure water at 90 °C and diluted accordingly.

The release kinetics were evaluated with the assistance of different release models, including zero order, first order, Higuchi, and Korsmeyer-Peppas models. The models that best fitted with the data with an R^2 value of 0.99 was considered the best release model for the developed dressing. The model equations (Ahmed et al., 2019; Chalitangkoon et al., 2020) are mentioned below:

Zero-order model: $Q = kt + Qo$

First-order model: $Q = Qo(1 - e^{-kt})$

Higuchi model: $Q = kt^{1/2}$

Korsmeyer- Peppas model: $Q = kt^n$

Where Q represents silver release at any t time, Qo defines total drug concentration, the rate constant is specified as k, and n is a release exponent. The power law model("Mathematical Models of Drug Release," 2015) includes different mechanisms, including Fickian diffusion and release mechanism due to relaxation and swelling of the polymer matrix, depending upon the n value. Where, n= 0.5, it represents Fickian

diffusion, n=1 represents zero-order release, and n > 0.5 indicates non-Fickian release due to relaxation or swelling of the polymer matrix.

3.3.15. *In vitro* drug release study

The release study, used cephalexin hydrate (CEX) as a model drug to analyse the role of uniaxial and co-axial electrospun nanofibrous layer. To determine the total concentration of the drug, a 1 cm diameter disc was dispensed in 3 mL of pH 7.4 PBS. To ascertain the amount of the drug released, the solution was heated to 100 °C for 15 minutes before being cooled to room temperature. The total amount of cephalexin hydrate drug released in the PBS was determined using an Evolution 201 (Thermo Fisher) UV-VIS spectrophotometer at 260 nm. As a control, readings were recorded to quantify PVA, PCL, and agar in PBS to rule out any absorbance owing to the respective polymers. Even though agar exhibited absorbance at 260 nm, drug-free control samples were developed to negate the absorbance of the antibiotic CEX in composite agar at 260 nm. For the release study, circular samples with a diameter of 1 cm diameter were taken from electrospun films. These samples were then mounted on the openings of glass containers filled with 3 mL of PBS buffer (pH 7.4). To ensure that the buffer remained secure (leak-proof), the samples were carefully sealed using parafilm. The mounted samples were inverted for the specified time interval to permit the release of the drug from the desired surface of the mounted samples. The experiments were conducted at 37°C, to simulate the release of antibiotic in wound exudates. The mounted surface in contact with the PBS for drug release was regarded as the permeation area, and precautions were taken to mount the samples to prevent drug leakage from unintended sample surface during the test. After a pre-defined time interval, the released drug from the affixed surface of the electrospun films was quantified by measuring the absorbance of the buffer at 260 nm. The released amount of drug was evaluated using calibration curve at 260 nm. The average value of release% was determined from quadruplicate samples.

$$Release \ \% = \frac{Released \ amount \ of \ drug}{Total \ amount \ of \ loaded \ drug} \times 100$$

3.3.16. *In vivo* wound healing studies

The wound healing ability of the developed bilayer dressing was evaluated using in vivo studies with full thickness excisional wound healing on a rat model approved by the Institutional Animal Ethics Committee (approval number: IAEC/UIP/AUG.2023/029). The adult male SD rats weighing 200- 250 g were kept separately in plastic cages and acclimatized at 23 ± 2 °C and humidity 50-60 %. They were fed pelleted food and tap water ad libitum during an experimental period of 18 days. The animals were anesthetized with two inter-peritoneal injections of Ketamine and Diazepam with a dose of 50 mg/kg and 5 mg/kg of rat, respectively. The sedation was followed by the shaving of the surgical area on the dorsal skin of the rats using a manual razor. Prior to the experiment, the rats were divided into six groups (n=3 per group). Six excision wounds of 6 mm diameter were created on the dorsal skin, three on each side of the median line, using a punch-biopsy needle. Then the wounds were treated with a 1 cm^2 circular disk of developed dressings and other controls (groups II and IV). While groups I and V were treated with 200 µL AgNPs and povidone solution, respectively, followed by the measurement of the contractions area of each wound after every consecutive 3 days for each group of animals until completely healed. For the study, group I was a 0.2 mM silver nanoparticles solution (AgNPs), group II was treated with neat agar film, group III was an agar-based electrospun bilayer dressing, group IV was an antibacterial silver-based commercial dressing (Sterizone™), group V was treated with Povidone, and group VI was the untreated control group. After 9 days, 100 µL blood was collected from the rats to analyse the presence of silver nanoparticles using ICP-MS. The blood samples were lysed using 0.1% triton-X 100. The lysed blood was diluted with milli-Q water, followed by filtering with 0.22 µm syringe filters. The ICP-MS characterization of silver nanoparticles was similar to that described earlier. For the wound contraction, the healing was examined visually, and measured the wound area using ImageJ software.

$$Wound\ contraction\ \% = \frac{Wound\ area\ day\ 0 - Wound\ area\ (day\ 3,6,9,\&\ 12)}{Wound\ area\ day\ 0} \times 100$$

3.3.17. Statistics

The results were expressed as mean (n=3) ± standard error for all analysis. For the test groups, one-way analysis of variance (ANOVA) was performed, *p-value* ≤ 0.05 was considered significant. In the figures, p-value was represented as star "*", where one stars "*" equated to ≤ 0.05 significance level, two stars "**" equated to ≤ 0.01, and three stars "***" equated to ≤ 0.001.

CHAPTER 4
RESULTS AND DISCUSSION

4.1. Development of bilayer wound dressings

Different techniques were utilized to develop two types bilayer dressing, first include electrospun nanofibrous mat with uniaxial and coaxial nanofibers, and secondly, bilayer of electrospun and solvent casted layer for the release of bioactive agents. The two developed dressings will be presented in two different sections for ease of understanding.

AGAR-BASED NANOFIBROUS SYMMETRIC BILAYER DRESSING

4.1.1. Optimization of agar-based electrospun nanofibers

The current study focused on the fabrication of agar-based nanofibers using a methodology that involved dissolving agar in an acidic solution and subsequently integrating polymeric additives. During the initial phase, the concentrations of both polymers were systematically altered. Subsequently, a tandem methodology was utilized to ascertain the most favourable electrospinning parameters. After establishing the polymer ratio as 5:5, subsequent electrospinning parameters were selected using a tandem approach. All other electrospinning parameters, including applied potential, flow rate, distance between the nozzle tip and collector, and collector rotation speed, were studied.

Effect of solvent

Agar, a polysaccharide derived from seaweed, is mostly composed of alternating D-galactose and 3,6, -anhydropyranose saccharide units (L. Wang & Rhim, 2015a). When dissolved in water, agar formed a gel even at extremely low concentrations. Hence, a solvent was necessary to prevent agar from gelling at ambient temperature.

Initially, agar was dissolved using dimethyl sulfoxide (DMSO) to impede the gelling process. Yet, regardless of the concentration of the agar solution in DMSO (5%, 7%, or

10%), beads or a thin mat devoid of fibres were developing from electrospinning process. Increasing the concentration of agar could facilitate the formation of a constant tailor cone(Teng et al., 2009) if the agar solution was too dilute. Similar to previous research, starch dissolved in DMSO formed nanofibers at higher concentrations. Nevertheless, other electrospinning parameters also influenced fibre formation (Kong & Ziegler, 2013).

Furthermore, nanofibers can be generated with the inclusion of another polymer, which can be synthetic or natural. Polycaprolactone (PCL) was chosen as the electrospinnable polymer for the suggested application because of its biodegradability, bioresorbability, and cost-effectiveness. Thus, the hypothesis of the study was to develop a fibrous structure from agar polymer, wherein the addition of spinnable polymer would aid in the production of an electrospun fibrous mat. Moreover, electro-spinnability, biocompatibility, bio-absorbability, and biodegradability were achieved through the blending of polycaprolactone with the agar solution. The hydrophobic nature of PCL and hydrophilic nature of agar made their blending challenging due to inevitable phase separation as reported (Zhu et al., 2016). Since the polarity of both polymers was opposing, various solvents were utilized to create the polymer blend without phase separation. It was found that PCL could be dissolved in dimethyl sulfoxide (DMSO), acetone, acetic acid, and dimethylformamide (DMF), while agar could be dissolved in water, acetic acid, formic acid, DMSO, and DMF. DMF is a typical solvent to dissolve both the polymers, but because to its genotoxic properties, it was excluded from the study under consideration of using an eco-friendly solvent to develop the dressing mats. Although DMSO was safer compared to DMF, it was not used due to limited dissolvability of PCL. Despite the opposing hydrophilic nature of agar and hydrophobicity of PCL, they were combined in pre-electrospinning to avert phase separation by using binary solvents. Considering the miscibility of solvents that can be combined without causing phase separation in polymers, acetic acid and formic acid were chosen as green binary solvents. After dissolving PCL and agar in acetic acid and formic acid, respectively, both polymer solutions were blended for electrospinning process.

Formic acid can hydrolyse the agar chains at high temperature (Yun et al., 2016). Agar was dissolved overnight at room temperature to produce a pale, translucent solution. Yet, even at room temperature, acid hydrolysis cannot be ruled out, and the synthesis of oligosaccharides of agar was expected. Even if the agar oligosaccharides were formed, they would have increased the bioactivity (X. Chen, Fu, et al., 2021) of the dressing material, such as antioxidant, anti-inflammatory, and anti-tumour, among others.

Due to the compatibility with binary solvents, PCL was dissolved in acetic acid. Both formic acid and acetic acid have a high miscibility and are known to promote in the electrospinning of nanofibers (Van Der Schueren et al., 2012). As described by Haider *et. al.* (Haider et al., 2018), the use of acetic acid to dissolve PCL resulted in the creation of beads due to the rapid evaporation of the solvent. Thus, it was anticipated that the final mixture will produce beaded morphology that can be minimized through selection of processing parameter.

When adopting a binary solvent for agar: PCL electrospinning, nanofibrous structures were developed that required additional tuning of other electrospinning parameters like applied potential, feed rate, rotational speed of collector, distance between collector and nozzle tip, many others.

Effect of concentration
Higher concentrations of agar, greater than seven parts, caused solution to sputter from the needle tip during electrospinning and hence were not used. Electrospun mats with 7:5:: Agar: PCL exhibited large beads. Lower agar concentrations (4:5:: Agar: PCL), on the other hand, resulted in hydrophobic mats because of higher PCL content. As mentioned previously, low spinnability of agar and using acetic acid as solvent for PCL resulted in the formation of bead morphology. Hence, only a small window was available to develop a bead-less or low beaded nanofibrous structure form agar-PCL blend. In addition, by increasing the agar concentration, the fibre size was reduced and more beads were produced. Comparable morphological outcomes were reported earlier also (Teng et al., 2009). Similar morphology was observed for 6:5:: Agar: PCL concentration with thicker fibres and larger number of beads compared to 5:5:: Agar:

PCL. However, nanofibers developed from 5:5:: agar: PCL were thicker compared to those with ratios 4:5 and 6:5. Despite this, the 5:5:: agar: PCL nanofibers exhibited uniformity with fewer beads. Hence, the optimal nanofibrous microstructures were observed at 5:5 concentration with low bead formation **Figure 4.1b**). The obtained micrographs displayed beaded morphologies as other electrospinning parameters were further optimized to reduce bead formation in fibre. Hence, 5:5 concentration was chosen for further studies.

Distance between nozzle tip to collector

The distance between the nozzle tip and collector plays a critical role in defining fibre morphology, diameter, alignment, and uniformity(Haider et al., 2018). Notably, the beaded structure was present in each set of agar: PCL mats. Extremely short (< 5 cm) or very long distances (> 10 cm) between the nozzle tip and collector produced collapsed fibres or beaded morphology (**Figure 4.1 e-f**), respectively. For the distance between the nozzle tip and the collector ranging from 5 cm to 10 cm, the Taylor's cone formed most consistently. At lesser distances (5 cm), the fibres may not have significant time to solidify, resulting in the formation of non-uniform morphology with fibre diameter of 118 nm (**Figure 4.1e**). In contrast, when the distance between the tip-to-collector was increased, the thickness of the fibres was reduced to 92 nm, and the fibre was formed on the collector in a random orientation, resulting in non-aligned nanofibers with smaller beads. Therefore, optimum distance was needed for fibre formation with maximum solvent evaporation (Mitra et al., 2022). Hence, by considering the fibre formation and diameter distribution through histogram, 7 cm distance between the collector and the spinneret was found to be optimum for preparing nanofibrous and was finalized for further studies.
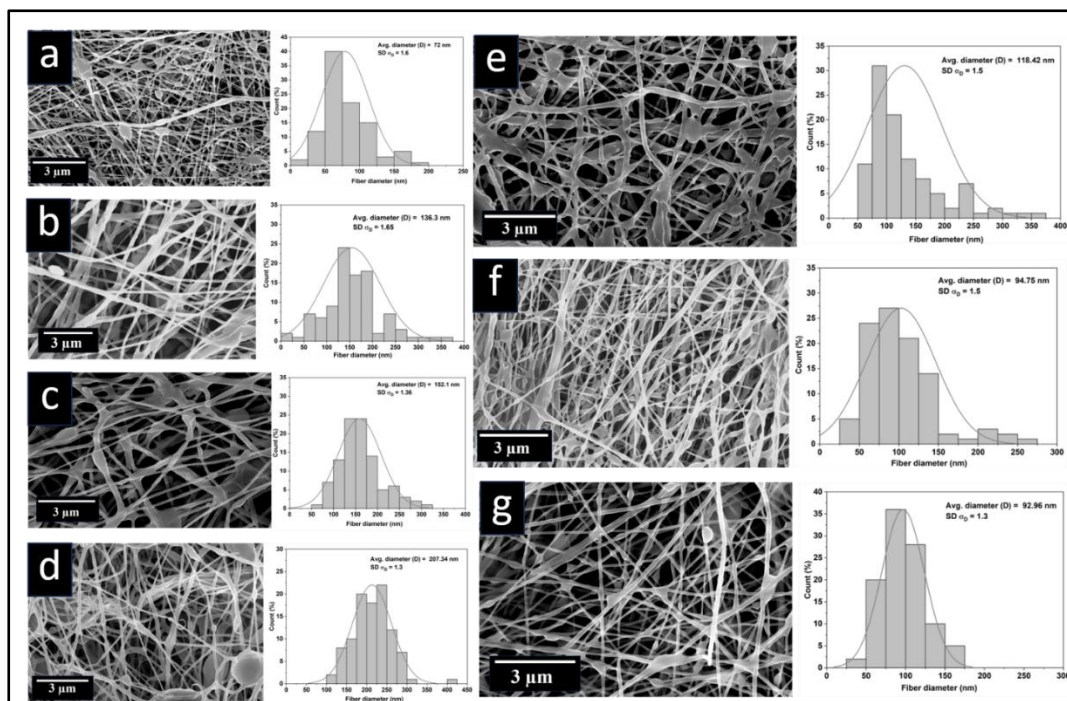
Figure 4.1. *Nanofibrous morphology of agar: PCL by varying agar: PCL ratios where agar: PCL ratios were 4:5 (a), 5:5 (b), 6:5 (c), 7:5 (d), electrospun from varied distance from 5 cm(e), 7 cm (f), and 10 cm (g).*

Effect of applied potential

Applied potential (kV) has an important function in the formation of Taylor's cone from polymer solution. To form Taylor's cone, potential difference between the spinneret and the collector plays its critical role. The formation of Taylor's cone includes increase in charges on the surface of liquid droplet due to applied potential resulting in minimizing surface tension which is followed by deformation of spherical droplet into Taylor's cone (Xue et al., 2019). For applied potential below 10 kV, the agar: PCL solution sputtered and was unable to produce a continuous Taylor's cone, which is necessary for the formation of continuous fibres. Taylor's cone stability was visually evaluated from 10 to 20 kV. However, within 10 to 20 kV of voltage, nanofibers with a beaded morphology were produced (**Figure 4.2 a, b, & c**). Even after increasing the voltage to 20 kV, the diameter of the nanofibers decreased to 95 (±1.4) nm but beads were still forming. However, at 15 kV, the nanofibers were more uniform with fewer beads with 85 nm diameter and was therefore considered for future parameter selection. The histogram (**Figure 4.2 a, b, & c**) displayed nanofibers diameter distribution which were mostly below range of ~200 nm.

Rotational speed of drum collector

Varying the drum speed results in change of fibre diameter and more aligned fibres. However, due to high rotational drum speed, the thickness of fibres would reduce from 108 nm to 89 nm, which was true in our case also (**Figure 4.2 f, g, h, & i**). Uniform less beaded nanofibers were obtained at 500 rpm and 700 rpm speed of the rotational drum and hence, 700 rpm was selected as best rotational speed.

Effect of feed rate

The solution feed rate has a significant effect in the formation of polymer nanofibers. While higher feed rates result in beaded and thicker fibres, thinner fibres are obtained with lower feed rates (Jain et al., 2020b). Collapsed fibrous structure and smaller fibre diameter were observed in agar: PCL blend at lower flow rates, whereas beaded morphology was produced at high flowrate. Sputtering of polymer solution without the formation of Taylor's cone was observed when feed rate was increased beyond 15 µL/min. However, at the flowrate of 10 µL/min, continuous and thin fibres formed (**Figure 4.2 d**).
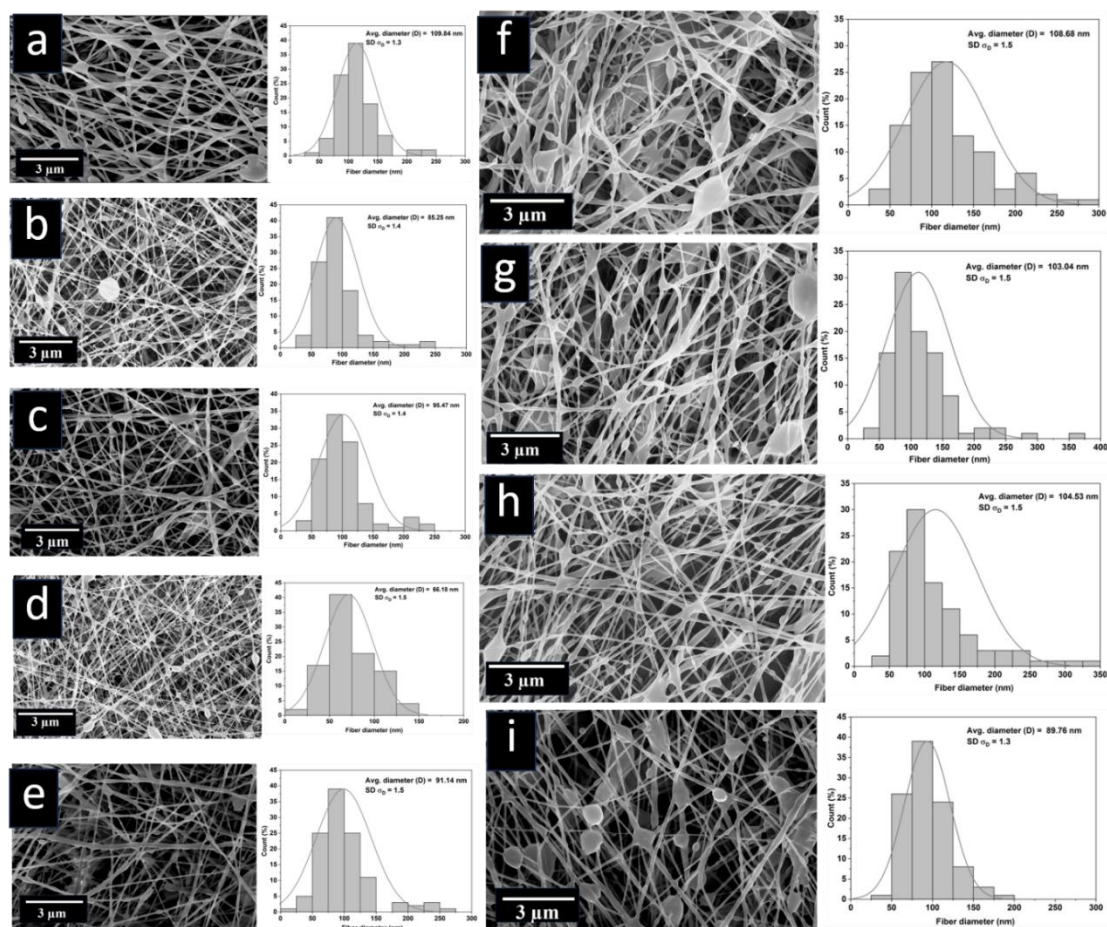
Figure 4.2. Agar: PCL (5:5) electrospun nanofibers after varying applied voltage of 10 kV(a), 15 kV(b), and 20 kV(c), at flowrate of 10 μL/min (d) and 15 μL /min (e) with fibre diameter distribution on right side. Agar: PCL (5:5) mats collected at varying rotational speeds of collector drum of 200 rpm (f), 500 rpm (g), 700 rpm (h), and 1100 rpm (i).

4.1.2. Fabrication of co-axial electrospun films with drug

Different concentrations of PVA solution (8%, 10% and 12%) were used for electrospinning (**Figure 4.3a**). In comparison to other concentrations, 10% PVA solution produced homogenous and beadless nanofibers; therefore, 10% PVA was decided for the co-axial core solution. Cephalexin hydrate, a water-soluble antibiotic that dissolves readily in PVA solution was used as a model drug that produced a homogeneous, and transparent solution. The formation of PVA nanofibers did not change significantly by the addition of the cephalexin hydrate antibiotic **Figure 4.3d**). As in coaxial electrospinning, several kinds of factors play a role in the development of

beadless, and continuous nanofibers. This includes polymer concentration, applied potential, distance between collector and spinneret, etc.
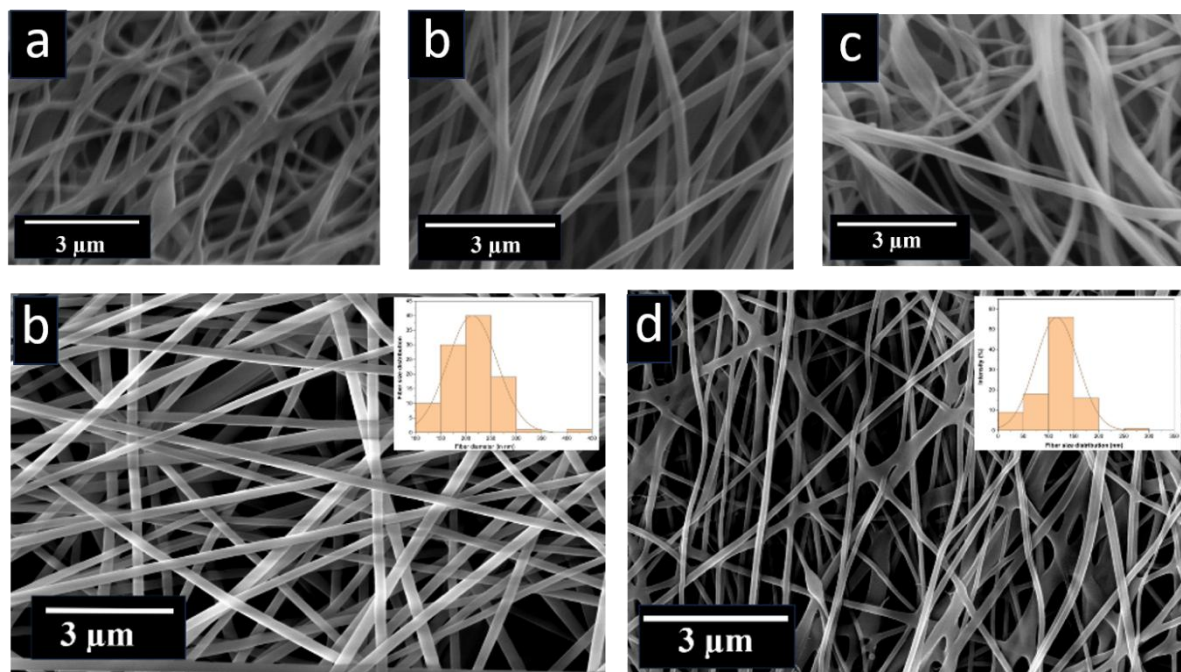
Figure 4.3. *Micrographs of nanofibers prepared from 8% PVA (a), 10% PVA (b), and 12% PVA (c) solution. 10% PVA nanofibers incorporated with cephalexin hydrate(d). The inset represents the size distribution histogram of the nanofibers, at 30000× magnification.*

4.1.3. Fabrication of uniaxial and coaxial agar: PCL electrospun mat

The final selected parameters were agar: PCL::5:5 with a feed rate of 10 µL/min, 15 kV applied potential, 7 cm between nozzle tip and collector, and rotation of drum collector at 700 rpm. Parchment paper was used as the substrate for the electrospinning process to make it simple to peel the samples off from the collector. Micrograph of the uniaxial agar: PCL mat was shown in **Figure 4.4a**.

The selected electrospinning parameters for agar: PCL were used to develop co-axial electrospun membranes for sustained release of drug. As coaxial nanofibers are divided into two parts i.e., sheath and core, agar: PCL (5:5) was used for sheath and PVA (10%) was used for core polymer. Concentration of PVA was selected based on nanofiber formation **(Figure 4.3)**. Electrospinning parameters used to generate coaxial nanofibers were same as those used for agar: PCL nanofibers. The electrospun mat developed from

coaxial agar: PCL with PVA core infused with cephalexin hydrate drug was labelled as single layer (SL). To further restrict the drug release, a secondary layer of uniaxial agar: PCL nanofibrous layer was applied on the single layer (SL) coaxial PVA- agar: PCL layer and the two layers were referred to as a bilayer (BL). **Figure 4.4b** depicts micrographs of the developed single layer of coaxial agar: PCL with PVA in core without cephalexin hydrate (CEX). Whereas **Figure 4.4c** displayed coaxial nanofibers after the incorporation of drug. Bilayer dressing was developed by layer-by-layer fabrication of coaxial layer followed by uniaxial layer, where uniaxial layer of agar: PCL would be in-contact with wound site as displayed in **Figure 3.1**Error! Reference s ource not found..

Uniaxial and coaxial nanofibers was further demonstrated with the help of TEM micrographs **(Figure 4.4 d & e)**. Silver nanoparticles were used to increase the contrast between the two polymer layers. The PVA core sheathed agar: PCL shell layer can be easily observed due to the presence of silver nanoparticles.
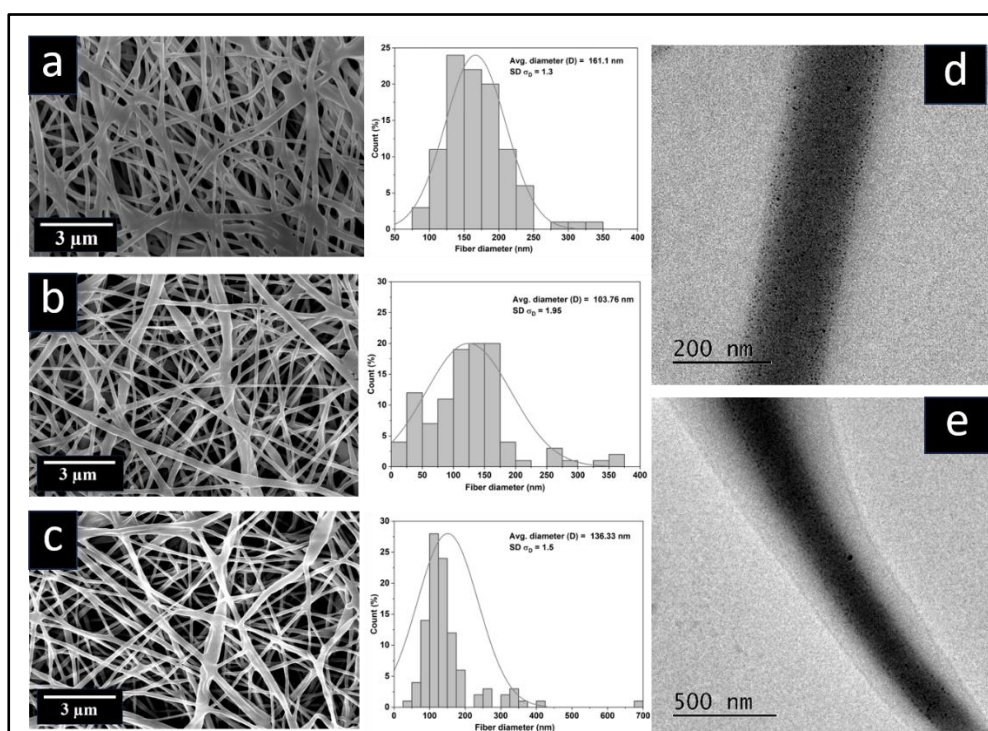
Figure 4.4. *Micrographs of uniaxial agar: PCL (a), coaxial agar: PCL with PVA as core (b), and coaxial agar: PCL with PVA-CEX (c) nanofibrous mat with their size distribution histograms on right. TEM micrographs of uniaxial nanofiber of PVA*

infused with silver nanoparticles (d) and coaxial nanofibers of agar: PCL layer encapsulating PVA layer incorporated with silver nanoparticles (e).

4.2. Fabrication of electrospun nanofibers mat with other additives

The goal of integrating various additives was to determine the compatibility of polymer fibres with various compounds, such as a hydrophobic medicament (piperine), a model protein (albumin), a bioactive agent (citric acid), etcetera. SEM micrographs illustrates that the formation of nanofibers after the addition of piperine, bovine albumin, or citric acid (**Figure 4.5**). Nevertheless, the quantity of nanometre-sized beads decreased with the addition of citric acid. With these fabrications in place, we have potential to explore numerous opportunities for different applications like drug delivery and wound healing in future. Current research demonstrated that several polar chemicals may be combined with the agar: PCL solution and have the potential for a variety of applications. Apart from this, the use of an indigenous polymer (agar-agar) along with synthetic polymer (PCL) can help reduce the cost of the developed nanofibers. However, limited commercialization of electrospinning may hinder its industrial applicability. Additionally, the cost of the developed dressing may increase with the incorporation of additives and drugs.
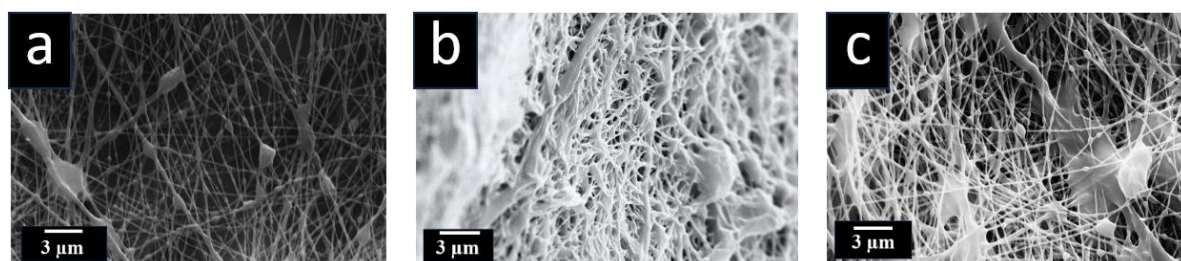
Figure 4.5. Citric acid (left), albumin (middle), and piperine (right) incorporated in 5:5 agar: PCL fibre, at 10000× magnification

4.3. Characterization of bilayer co-axial electrospun wound dressing
4.3.1. Chemical properties

FTIR spectra of agar, PCL and their blend is shown in **Figure 4.6**. The two polymers were blended in a variety of ratios, and the chemical compositions were confirmed using FTIR spectroscopic data. At 3500 cm^{-1}, the vibrational stretching of -OH bonds, which corresponds to the hydroxyl moiety, can be observed. At 2941 cm^{-1} and 2860 cm^{-}

[1], the asymmetrical and symmetrical stretching of -CH$_2$ and -CH$_3$, respectively, can be observed. For -CH bonds, these stretching were characteristic of synthetic polymers (PCL) and polysaccharide agar. Another distinctive peak of symmetrical and asymmetrical stretching vibrations of -COOH of carboxylate groups were being found in the spectrogram for polysaccharides (J. Liu et al., 2018) in agar matrix. In polycaprolactone, at 1732 cm^{-1}, the -C=O stretching vibration was present and as reported earlier (Salami et al., 2017). The peak of the PCL -C-O ester group was observed at around 1064 cm^{-1}. All of the aforementioned peaks were also observed in the blends of agar with PCL, demonstrating no chemical bond formation between the two polymers in the blend (**Figure 4.6a**). FTIR spectra of coaxial agar: PCL ::5:5 with PVA in the core incorporated with and without the drug (CEX) is shown the **Figure 4.6 b**. Due to the low concentration of CEX in the electrospun films, a small peak was detected at 1600 cm^{-1} corresponding to N-H bonds. The intensity of the peak was lower in bilayer as the concentration of the drug was decreased due to additional agar and PCL. Moreover, all other characteristic peaks of CEX were reduced in the single and bilayer dressing mat, which also corroborated with earlier studies (Montiel-Centeno et al., 2022).
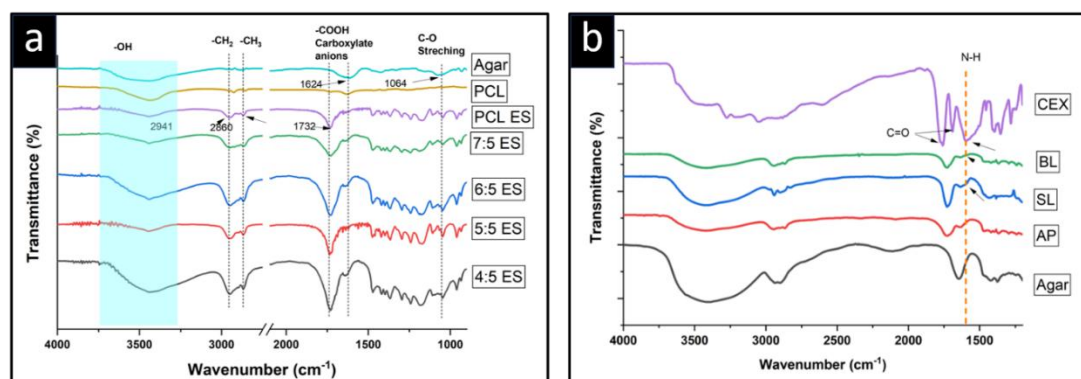
Figure 4.6. *FTIR spectrogram of all the compositions after blending both the polymers (a) (Top to bottom: Agar, PCL, PCL_ES, agar: PCL::7:5, 6:5, 5:5 (AP), & 4:5 electrospun mats) and (b) after the formation of coaxial single layer (SL) and coaxial bilayer with drug (CEX).*

4.3.2. Mechanical properties

Stress strain values and plot of agar: PCL::5:5, agar: PCL::5:5 with citric acid (CA), and agar: PCL::5:5 with albumin using uniaxial tensile testing is shown in **Figure 4.7.**

For mechanical testing, agar: PCL::5:5 with average thickness of around 85 μm was used for tensile testing. Agar: PCL samples demonstrated tensile strength of 7 MPa with 40% elongation at break compared to earlier reported 2 MPa strength of PCL and 300% elongation at break (Augustine et al., 2014). As both the polymers (agar and PCL) are incompatible in nature resulting in poor intermolecular interaction. Therefore, there could be chances that agar could be restricting the chain mobility of PCL and hence, decrease in elongation was observed. In a similar study (Prasad et al., 2015), the addition of chitosan to PCL caused a decline in the elongation at break value of PCL.

Furthermore, additives can be used to alter the material mechanical characteristics. In the case of citric acid, the elongation at break increased to 80% but the strength reduced to 5 MPa. Moreover, the addition of albumin reduced the elongation at break to 50 %, but improved the strength to 6 MPa. According to Trinca *et. al.* (Trinca et al., 2017), the mechanical strength of human skin ranges from 2 to 16 MPa, and its elongation at break is between 70 -77%. The electrospun dressings prepared from agar: PCL showed the optimum tensile properties, closely matching that of human skin.
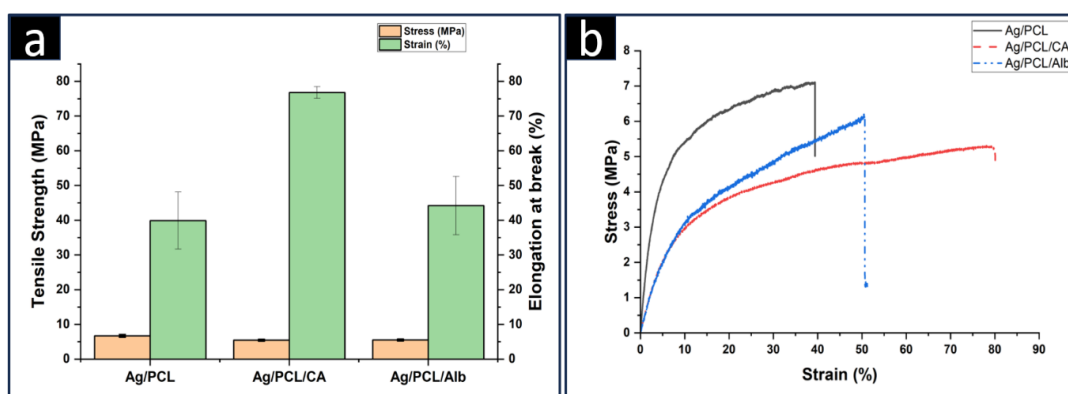
Figure 4.7. Tensile properties of electrospun mats prepared from agar: PCL solution (a) with stress-strain graph (b).

4.3.3. In-vitro fluid handling properties

Wettability

The wettability of the nanofibrous mat is critical for various activities, including cell attachment, protein adsorption, and cellular interaction (Unal et al., 2020). Considering PCL being a hydrophobic polymer with limited medical applications (Ranjbar-mohammadi et al., 2016; Safdari et al., 2022), adding certain hydrophilic polymers to

it can make it more biocompatible by decreasing its contact angle and therefore facilitating better cell proliferation. Furthermore, the hydrophilicity of agar reduces cell adhesion, facilitating the separation of the wound dressing from the wound site without disrupting the growing cells. Therefore, the agar: PCL::5:5 composition promote cell proliferation due to its optimum wettability but due to agar, the developed mat facilitates in lower cell attachment resulting in painless removal of dressing mat from the wounds. After blending both polymers, the contact angle of the resulting mat was around 60° (**Figure 4.8a**). Interestingly, the reported optimal contact angle range for cell adhesion is between 55° and 80° (Menzies & Jones, 2010).

Swelling properties

Agar has higher swelling ratios than polycaprolactone due to its hydrophilic moieties, it was anticipated that blending the polymers in varying proportions would modulate the swelling properties of agar and polycaprolactone. **Figure 4.8 b** demonstrates the swelling behaviour of the developed bilayer dressings. Due to the hydrophobic nature of PCL, the nanofibrous mat created from PCL alone exhibited less than 5% swelling. Following the combination of agar and PCL in a ratio of 4:5, the swelling percentage observed a significant eight-fold increase, equivalent to 40%. As the concentration of agar was further increased, for agar: PCL:: 5:5, there was a slight decrease in the swelling percentage, this can be attributed to the increased concentration of agar. As indicated in previous research (Madera-Santana et al., 2014b), the degree of swelling was found to decrease with an increase in polymer concentration per unit volume. This can be attributed to the limited mobility of polymer chains, which restricts the swelling process. This could be due hydrophilic nature of the protein. The dissolution study displayed that almost 15-20% of agar was getting dissolved from the developed mats.

Fluid handling capacity

Figure 4.8 c depicts the fluid absorption and holding capacity of the electrospun mats. Being hydrophobic in nature, the PCL demonstrated the lowest fluid retention capacity (1.3 g/g) and the maximum dehydration rate of moisture from the PCL (1 g/min) (**Figure 4.8 d**). Similarly, the fluid holding capacity of the uniaxial PVA was found to 3.5 g/g owing to its hydrophilicity. However, the fabrication of agar: PCL electrospun dressings with the blend of hydrophilic (agar) and hydrophobic (PCL) polymer resulted

in enhanced fluid-holding capacity (8.9 g/g), due to the highly hydrophilic nature of agar. Although, the single layer prepared from co-axial nanofibers containing PVA in core and agar: PCL as sheath showed lower fluid holding capacity. This could be due to lower agar: PCL content as compared to uniaxial agar: PCL. Nevertheless, the bilayer electrospun mats of uniaxial and coaxial displayed enhanced fluid holding capacity. This could be due to additional agar: PCL uniaxial mat, which was fabricated on single layer of coaxial nanofibrous mat resulted in an increased agar: PCL content.

In addition to the high absorption capacity of the agar: PCL electrospun mat, the fluid absorption rate was optimal at 134 seconds, which could be attributed to the unsteady dispersion of fluid but was comparable to work previously reported(Uzun et al., 2013). As seen in **Figure 4.8 d**, the addition of agar made the dispersion region clear, which would not have been the case with a hydrophobic PCL mat.

Water vapor transmission rate

In contrast to cytocompatibility, wettability, and bioactivity, the water vapor transmission rate of wound dressings plays an important role in wound healing. If the dressing has a high rate of moisture transfer from the wound, the wound will get dehydrated, resulting in the dressing sticking to the wound site and causing excruciating discomfort during removal while delaying the healing process. Nevertheless, if the rate of transmission is too low, the wound exudates can build and cause back pressure, which will cause the patient discomfort while promoting microbial colonization. Hence, a desired range of moisture permeability is essential for appropriate healing rate without increasing patient pain. Typically, 240 to 1920 $g/m^2/day$ of moisture loss from the intact skin surface was recorded in the previous studies (Yusof et al., 2003). The moisture transmission rate of the developed dressing mats could reduce the 4800 $g/m^2/day$ reported WVTR of exposed wounds (Yusof et al., 2003). As reported earlier WVTR of 2028 $g/m^2/day$ was found to be the most optimum for a bilayer wound dressing that assists in wound healing (Wojcik et al., 2021). Uniaxial agar: PCL and neat PVA electrospun samples showed much higher moisture transmission rate of 2585 $g/m^2/day$ and 2532 $g/m^2/day$, respectively, which could be due to lower thickness of the electrospun layers than bilayer structures. After bilayer formation, transmission rate of single coaxial layer was reduced from 2384 $g/m^2/day$ to 2174 $g/m^2/day$. The

transmission rate of the developed agar-based bilayer dressing mats was slightly higher than the necessary range of skin transpiration rate, about 2174 $g/m^2/day$ (**Figure 4.8e**) and hence, would be suitable for high exudating wounds. For effective wound healing without dehydration or macerating the wound site, wound dressings with this exhibit optimal moisture permeability via water vapour transpiration rate. Furthermore, it was previously reported that maceration can be occurred in a heavenly exudating wounds due to low WVTR of a bilayer dressing (H. E. Thu et al., 2012).

Dehydration rate

The dehydration rate of moisture from uniaxial agar: PCL and bilayer coaxial (BL) electrospun mats was found to be 0.4 g/min and 0.3 g/min, respectively (**Figure 4.8f**). The dehydration rates were higher than previous reported literature and indicated that the dehydration rate was inversely proportional to the dressing thickness (Uzun et al., 2013), which could be one of the main reasons of higher dehydration rate of the prepared dressings. It can therefore be used for heavily exudating wounds. Nevertheless, maintaining an optimal hydration balance in an injury is essential for promoting effective healing. As excessive wetness can cause maceration, and excessive dryness can cause desiccation, it is important to maintain a balance between the two. In both extremes, the wound recovery process would be hindered. Moreover, wounds generate varying quantities of exudates during the healing process. The prepared agar: PCL dressing mats can be used to treat highly exuding wounds that require a high dehydration rate to prevent maceration.

Dissolution study

Various wound dressings are intended to promote proper wound care by providing the optimal wound healing environment. Some dressings, for instance, produce a moist environment, whereas others absorb excessive wound exudate, resulting in effective healing. Due to exposure to body fluids, enzymes, and mechanical forces, wound dressings suffer incremental breakdown or degradation over time when applied directly to the wound surface. Frequent dressing changes may exacerbate the patient's discomfort and suffering if the dressing material degrades too rapidly, necessitating regular replacements without promoting wound healing. Further, if the dressing does not decompose over time, it will accrue as a pollutant and can burden the environment

69

by persisting in the environment and causing debris to accumulate in landfills. Therefore, biodegradable dressing materials are currently essential for promoting healing without harming the environment. Therefore, the test was performed to evaluate the stability, dissolvability, and degradability of the developed agar: PCL electrospun mat. Lysozyme and H_2O_2 are abundant in human bodily fluids, especially serum. In addition, an increase in local H_2O_2 concentration promotes proper healing (Ahtzaz et al., 2017b). In PBS solution, lysozyme and H_2O_2 degradation aid in simulating an infected wound, whereas collagenase degradation aids in simulating the remodelling phase of skin regeneration and repair of chronic wounds. The collagenase degradation was performed in a manner analogous to that described previously (Vivcharenko, Benko, et al., 2020).

The degradation percentage of the developed electrospun dressings is shown in **Figure 4.8 g**. There was no significant mass loss was observed after 9 days and the mats remained intact, which was confirmed by visual inspection. Initial dissolution was triggered by agar dissolution from the matrix. As the composition used for the dissolution study was agar: PCL :: 5:5 for agar and PCL, it was anticipated that the resultant residue in the majority of dissolved samples would be around 50% due to the dissolution of agar.
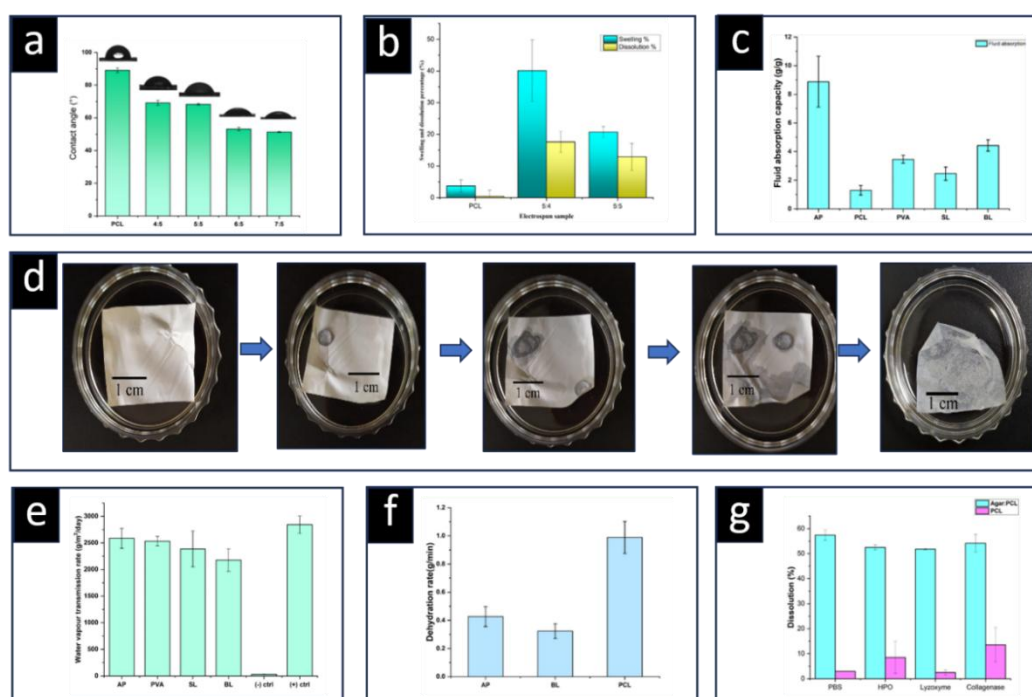
Figure 4.8. *Fluid handling properties of agar: PCL mats included water contact angle (a), swelling degree (b), fluid absorption capacity (c), fluid absorption behaviour (d), WVTR (e), dehydration rates (f), and dissolution properties (g).*

4.3.4. Hemocompatibility assay

A hemocompatibility assay was used to confirm the blood compatibility of the developed samples for erythrocytes, or red blood cells, for biomedical applications. A biomaterial is categorized as haemolytic (non-hemocompatible) if red blood cells (RBC) get disrupted upon interaction with the biomaterial. If the haemolysis range exceeds more than 10%, then it is non-hemocompatible. Materials are considered highly hemocompatible if the proportion of total hemolysis is less than 5% whereas if the range varies between 5 to 10%, then material comes in hemocompatible range (Tripathi et al., 2021). **Figure 4.9a** illustrates the images of the blood compatibility test. All the observations in our analysis exhibited hemolysis% values less than 5%, indicating that the developed nanofibrous mats were highly hemocompatible and ideal for the use in biomedical applications.

4.3.5. Cytocompatibility

The MTT test was used to assess the cytocompatibility of agar: PCL nanofiber mats produced by electrospinning. As observed (**Figure 4.9 b & c**), the viability percentage on tissue culture plates was greater than 90%. Considering both polymers are cytocompatible by nature, it was anticipated that the polymer matrix mix would be compatible with cells, which was validated by the MTT assay. Only the viable cells' active mitochondria can reduce the tetrazolium salt with the help of dehydrogenase into a purple formazan crystal that exhibits a maximum absorbance at 570 nm. Considerable cell attachment with adherent morphology was observed on the agar: PCL electrospun dressing mats, after 24 h of incubation. Furthermore, following a period of incubation on the dressing mats, a fewer number of cells were observed to adhere and exhibit cell spreading (**Figure 4.9 d**). This observation suggested that cell adherence and the initiation of cell spreading occurred on the mats. Thus, the fabricated agar: PCL dressing mats demonstrated cytocompatibility, which is essential for the healing of wounds since it encourages cell adhesion and proliferation. Furthermore, it was observed that cells had a low affinity towards PCL due to limited cell recognition (Zhu et al., 2016), while agar exhibited high hydrophilicity (Chu et al., 2020). Nevertheless,

the achievement of the most optimum hydrophilicity for cell proliferation was observed when agar and PCL were combined. However, due to the absence of cell recognition sites in the electropsun mat, it was expected to exhibit reduced cell adherence and therefore, fewer cells were adhered. This characteristic would be beneficial for facilitating the removal of dressings after the recovery phase. As adhesion of dressings to the wound bed can make dressing changes more excruciating and potentially disrupt the cells that has formed during wound healing, it is important to prevent dressings from adhering to the wound bed.

4.3.6. In-vitro drug release

Using hydrophilic (agar) and hydrophobic (PCL) polymers in the sheath layer was anticipated to assist in the sustained release of any (hydrophilic and hydrophobic) drugs from the core matrix. **Figure 4.9e** displays the percentage of drugs released overtime from the developed coaxial electrospun films. The uniaxial agar: PCL electrospun mats released 100 percent within 2 hours, whereas the uniaxial PVA nanofibrous mat released the drug slowly. After developing co-axial nanofibrous mats with PVA and agar: PCL as the membrane, a single coaxial mat discharged 77% of the drug within four hours. However, as anticipated, the addition of a secondary uniaxial layer of agar: PCL over the coaxial layer reduced the released rate to 29% from 71% compared to a single coaxial layer. The controlled release of the drug within the defined time interval from the developed electrospun nanofibrous dressing showed potential as a wound dressing material for highly exuding wounds. Certain medical conditions necessitate the sustained release of drugs from the dressing, which can be beneficial for the healing process. Initial burst release of drugs or bioactive agents may induce cellular toxicity instead of healing. Therefore, the incorporation of medicines or antibiotics with sustained release could prevent toxic shock to the cells while controlling microbial infection at wound site, thereby enhancing the healing outcomes of wound management. Due to the various incorporation methods for introducing drugs, nanofibers develop distinct morphologies that influence drug delivery. (J. Wang & Windbergs, 2019). Nevertheless, controlled release kinetics may follow a variety of mechanisms, such as a shift in environmental ionic conditions or the degradation or dissolution of a polymer containing a drug. (Young et al., 2005).

Cephalexin hydrate (CEX) is an effective antibiotic against both gram-positive and gram-negative microorganisms. Previous research (El-Newehy et al., 2016) was consulted to determine the percentage of antibiotics released in vitro from the nanofibrous PVA core of the coaxial films of agar: PCL. For the release study, 10 mm disc was cut from co-axial and uniaxial electrospun films developed using PVA as the antibiotic matrix in the core and agar: PCL as the exterior polymer mix. Multiple control samples were prepared with and without the incorporation of CEX.

4.3.7. Antibacterial properties

Incorporating cephalexin hydrate into the PVA core of the developed coaxial films delayed the drug release compared to uniaxial dressings. As revealed by the release study, this was decreased further by the fabrication of bilayer structures. The minimum inhibitory concentration (MIC) of cephalexin hydrate against *E. coli, S. aureus, P. vulgaris*, and *P. aeruginosa* was found to be 312.5 μg, 625 μg, 156 μg, and 78 μg, respectively, in 200 μL of bacterial culture (0.1 OD at 600 nm). The MBC values required to kill the respective bacteria were 625 μg, 1250 μg, 625 μg, and 312.5 μg, respectively. As the release rate of the antibiotic was affected by the addition of the uniaxial agar: PCL layer, a smaller inhibition zone was observed in bilayer dressings (sample no. 2) (**Figure 4.9 f, g, h & i**). This ensured the sustained release of the antibiotic, that will monitor bacterial growth at the wound site for an extended period unlike burst release of the drug. The trend for the zone of inhibition (ZOI) was observed as uniaxial PVA-CEX (PVAC) > coaxial single layer agar: PCL with PVA-CEX core (SLC) > bilayer uniaxial agar: PCL onto single layer coaxial agar: PCL with PVA-CEX as a core (BLC) shown in **Figure 4.9 j**. This was anticipated due to the antibiotic swift release from the uniaxial mat, followed by the coaxial single and bilayer dressing.
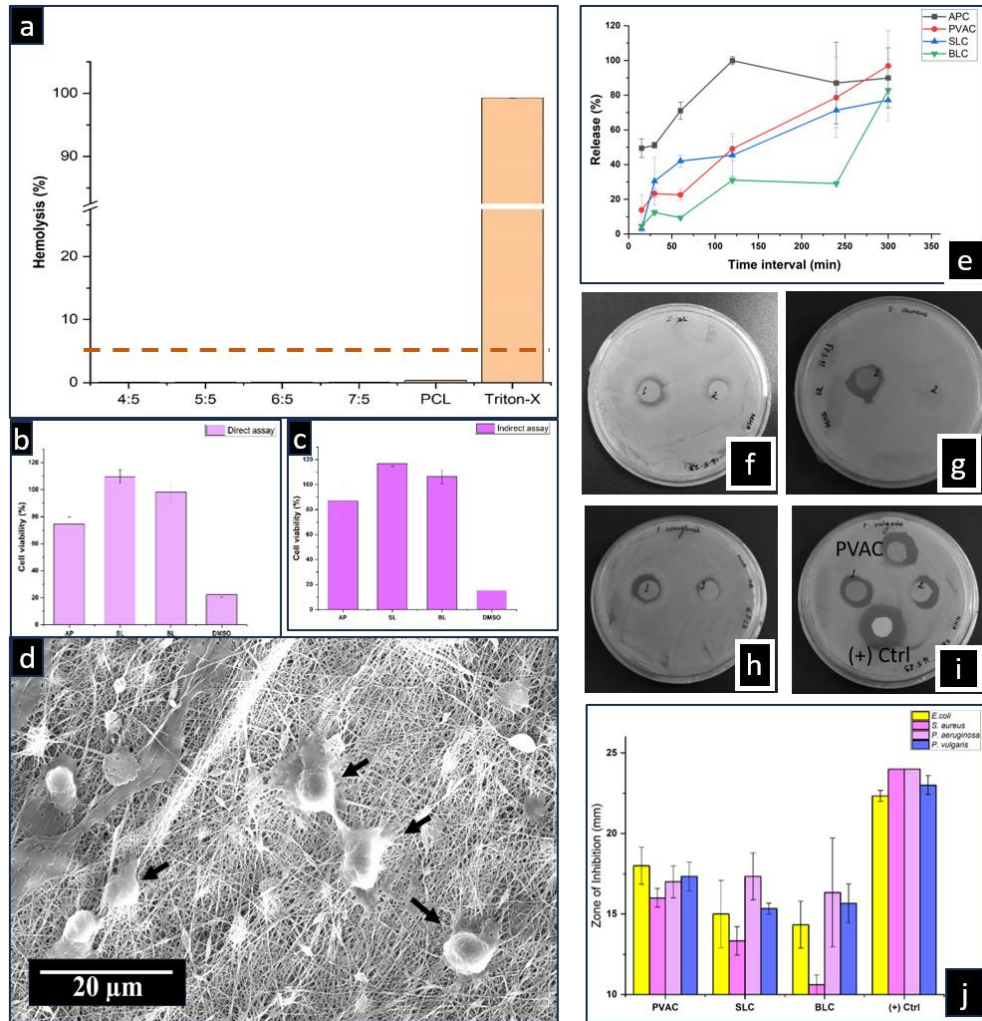
Figure 4.9. *Hemocompatibility (a) and cytocompatibility of agar: PCL:: 5:5 (AP), single coaxial electrospun (SL) and bilayer of uniaxial and coaxial electrospun mat (BL) via MTT direct (b) and indirect (c) assay and cell adhesion (d) on dressing mat. Release rate (e) of cephalexin hydrate antibiotic (C) from uniaxial electrospun mats of agar: PCL (APC) & PVA (PVAC), single layer of coaxial nanofibers of agar: PCL coated PVA mats (SLC), and bilayer of uniaxial over coaxial agar: PCL coated PVA (BLC). Antibacterial activity of cephalexin hydrate (C) in uniaxial (1) PVA mat (PVAC), coaxial (2) agar: PCL coated PVA single layer (SLC), and bilayer (BLC) dressing against E. coli(f), S. aureus(g), P. aeruginosa(h), and P. vulgaris(i) with ZOI (j) with kanamycin as (+) ctrl.*

AGAR-BASED ASYMMETRIC BILAYER WOUND DRESSING

4.4. Preparation of silver incorporated agar film

In the present study, one-pot in-situ reduction of silver nanoparticles was performed using a hydrothermal method in the presence of agar, which includes a standard autoclave procedure. To the best of our knowledge, this process has not been previously reported with agar. Earlier, similar studies were performed in the presence of starch and gum ghatti (Kora et al., 2012). After standard autoclaving, the agar solution containing the resultant silver nanoparticle solution changed from transparent to light yellow, suggesting the formation of Ag^0 from Ag^+ ions. The reduction of silver ions to silver atoms could occur by reducing groups, mainly aldehydes and alcoholic groups of saccharides (Emam et al., 2015; Shukla et al., 2012; H. Wang et al., 2005) and further catalysed by thermal activity using autoclaving. The developed nanoparticles were characterized using multiple techniques, including UV-vis spectroscopy and transmission electron microscopy.

4.5. Fabrication of bilayer dressing mats

With the development of bilayer wound dressings, it was anticipated that the primary layer, in contact with the wound, would release bioactive agents rapidly, while the secondary layer would exhibit sustained release of antibacterial agents over an extended period. By using bilayer or multilayer dressings laden with multiple bioactive agents, chronic wound management could be enhanced throughout various stages of the healing process. The nanofibrous layer in contact with a lesion would display high loading efficacy due to a high surface area to volume ratio and enhance vapour permeability. Furthermore, the second layer of agar would form hydrogel after absorbing the requisite volume of wound exudates, that would further assist in the release of infused silver nanoparticles. Moreover, exhibiting the antibacterial efficacy would enhance wound care management.

4.6. Characterization of advanced bilayer wound dressing

4.6.1. Optical properties

Due to autoclaving, the silver nitrate was reduced to silver nanoparticles (AgNPs) that exhibited a characteristic absorption peak at 417 nm (**Figure 4.10 a**) due to surface plasmon resonance (Ananth et al., 2011; Show et al., 2012). Furthermore, the solution changed from transparent to light pale, suggesting the formation of silver nanoparticles (AgNPs), during autoclaving process. After solvent casting of the autoclaved agar solution, the resultant dried films also exhibited same pale colour.

Figure 4.10 b&c shows the transmission electron micrographs of AgNPs with wide size distribution ranging from 10 nm to 100 nm. Electron diffraction patterns (**Figure 4.10 c-inset image**) of AgNPs are consistent with the family of the reflection of (111), (200), (220), (311), (222) planes that are reported in the literature (Guzmán et al., 2008; Tankhiwale & Bajpai, 2009).
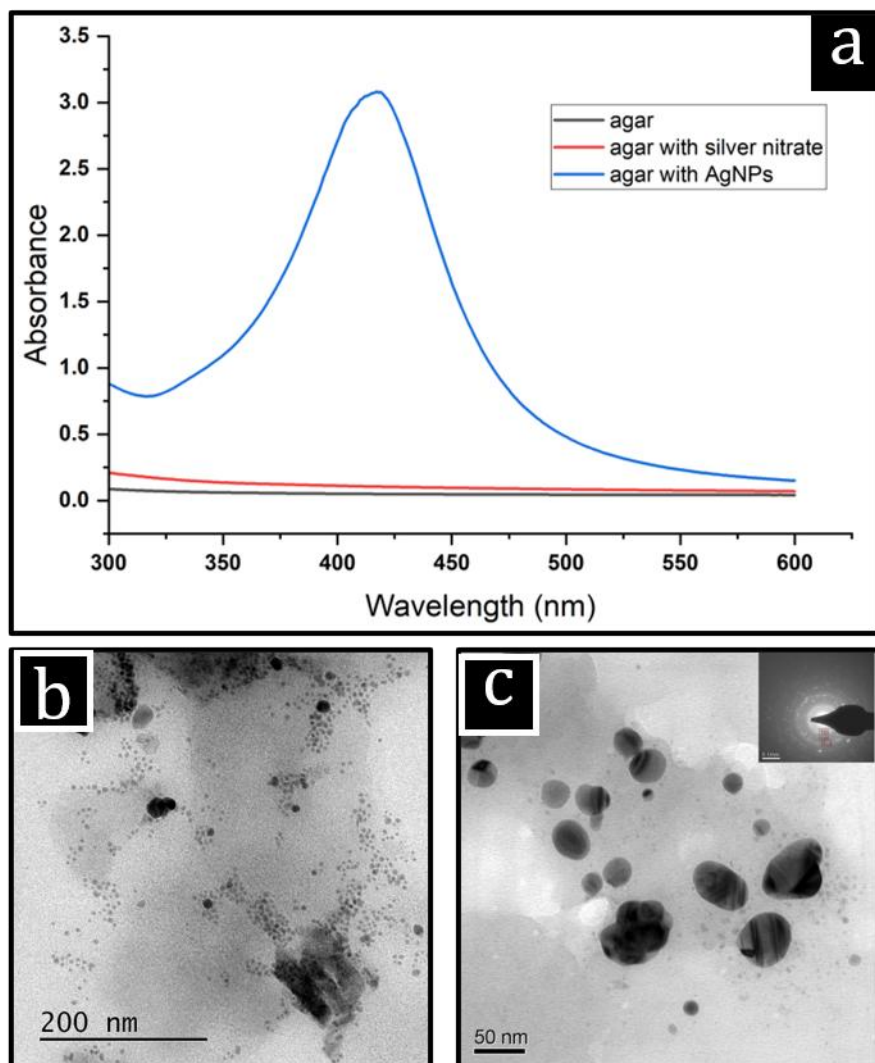
Figure 4.10. *(a)Absorption spectra of agar solution, agar with silver nitrate solution (before autoclaving), and agar with silver nanoparticles (after autoclaving). TEM micrograph (b & c) of AgNPs synthesized using autoclave with ED patterns in the inset view (c).*

4.6.2. Morphological analysis

Using SEM imaging, the surface and cross-sectional morphology of the electrospun nanofibrous dressings were evaluated (**Figure 4.11 a & b**). The developed nanofibrous mats exhibited a studded structure. As solvents such as glacial acetic acid evaporate rapidly, beaded structures form in the electrospun membranes(Haider et al., 2018).

The micrographs of cross-sections of the developed bilayer dressing revealed   both electrospun (~20 μm) and solvent casted (~90 μm) layers (**Figure 4.11c**). The cross-sectional image of the electrospun layer revealed a porous structure that would allow

for the consistent release of antibacterial silver nanoparticles to the wound. Albeit, the primary layer enhancing the free radical scavenging behaviour with the release of the gallic acid. Moreover, the porous structure will allow absorption of wound exudates thereby preventing maceration, in addition to protecting against external injury and infection (Han et al., 2010; Ooi et al., 2020; H. Thu et al., 2012).
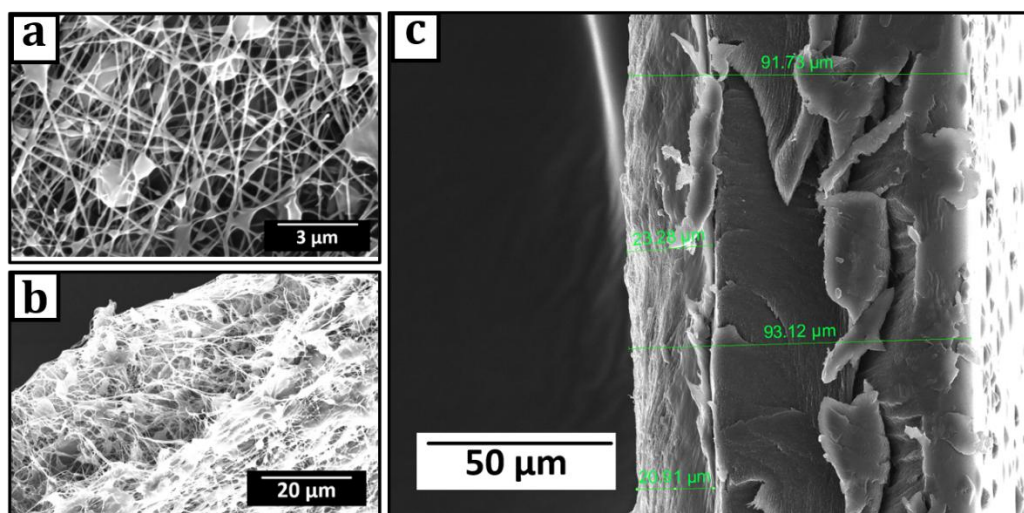
Figure 4.11. Micrograph of surface (a) and cross-sectional morphology (b) of agar/PCL-gallic acid electrospun mat, and bilayer morphology (c) of the developed agar-based dressing where electrospun layer (left side) was coated on solvent casted agar layer (right side)

4.6.3. Compositional analysis

Figure 4.12 a & b depict the FTIR spectrograms of the electrospun and solvent-cast films chemical compositions. Except for peak intensity, the chemical compositional peaks of agar with and without $AgNO_3$ were exactly same (**Figure 4.12 a**). The absorption band between 3600 cm^{-1} and 3100 cm^{-1} was allocated for O-H stretching, which accounted for the hydrophilic properties of the polymer. Carbonyl group (C=O) was associated with the distinct band at 1639 cm^{-1}. At 1364 cm^{-1}, an extra intense peak of ester sulfate was observed. In addition, the C-O-C vibration bands of anhydro-galactose and galactose of agar at 934 cm^{-1} and 890 cm^{-1}, respectively were observed. The spectrograms of agar with $AgNO_3$ are like the earlier reported literature (Belay et al., 2020; Madera-Santana et al., 2014a).

After combining the two polymers (agar and PCL) in equal proportions, FTIR spectroscopy was used to verify the chemical compositions of the electrospun layers.

The vibrational elongation of -OH bonds, which corresponds to the hydroxy group, can be observed between 3600 cm^{-1} and 3200 cm^{-1}. At 2931 cm^{-1} and 2868 cm^{-1}, the asymmetrical and symmetrical elongation of -CH$_2$ and -CH$_3$, respectively, can be observed. At approximately 1068 cm^{-1}, the synthetic polymer polycaprolactone -C-O stretch of ester group has attained its maximum. These stretching are typical of -CH bonds in polycaprolactone and agar. In polymer agar, another characteristic peak of symmetrical and asymmetrical stretching vibrations of -COOH of carboxylate ions can be identified in the spectrogram for polysaccharides (J. Liu et al., 2018). For synthetic polymers, the -C=O stretching vibration of the carbonyl functional group can be observed at 1727 cm^{-1} (Salami et al., 2017). All the previously mentioned peaks were also observed in the composites of polymers with synthetic polymers, indicating that the addition of polymer or silver nitrate had no effect on the chemical composition of the polymer matrix. The outcomes are depicted in **Figure 4.12 b**.
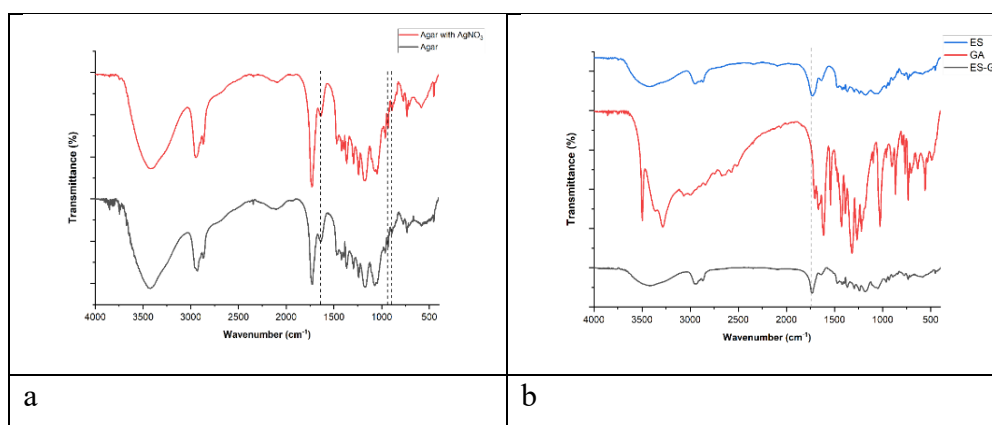
Figure 4.12. *FTIR spectrogram of both the layers after blending agents with the polymers a) agar film with and without silver nitrate and b) agar/PCL electrospun (ES) layer without gallic acid and with gallic acid (ES-GA), where GA indicates gallic acid.*

4.6.4. Mechanical properties

Agar demonstrated strength of 70 MPa, which increased up to 90 MPa for samples with addition of 0.5 mM silver nitrate **(Figure 4.13)**. Reduction of silver nitrate resulted in silver nanoparticles that were well distributed in the matrix and had served as hard phase resulting in higher strength. Since the material was developed for wound dressing application and very high amount of silver was not required for such applications, role of even higher silver content on the mechanical properties was not studied. Due to the inclusion of glycerol, the films exhibited moderate strain values.
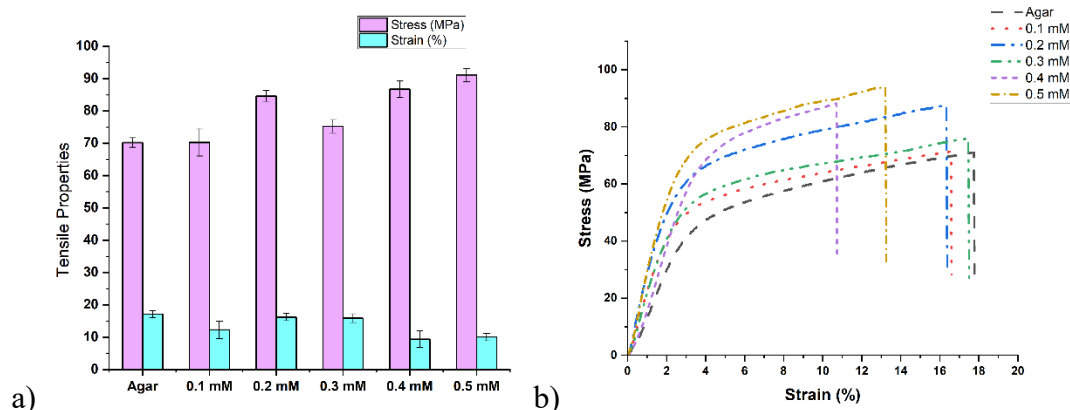
Figure 4.13. *Tensile properties (a) of the developed agar-based silver nanoparticles films with their characteristic stress-strain graphs (b).*

4.6.5. Fluid handling properties

The test measured fluid absorption capacity, dehydration rate, and absorption rate to evaluate the fluid-handling capabilities of the bilayer films. Fluid handling properties plays a crucial role in wound management and healing processes. Wound exudates comprise of numerous solutes, nutrients, growth factors, cellular agents (inflammatory agents and enzymes), etc. (Kim et al., 2019). Presence of wound exudates promotes wound healing but in optimum range to avoid both maceration and desiccation of wounds. The fluid handling properties of a dressing are demonstrated by their surface wetting behaviour, moisture absorption capacity, moisture permeability, and rate of dehydration from the dressing surface.

4.6.6. Wettability of electrospun agar films

Since the electrospun layer would serve as the interface between the wound dressing and the wound, its hydrophilicity was evaluated. Apart from fluid handling properties, surface hydrophilicity of a wound dressing is also a crucial property. In several processes, including cell adhesion, protein adsorption, cellular contact, and others, the wettability of the nanofibrous mat is crucial (Unal et al., 2020). The wettability was increased after mixing agar with PCL, and the resultant electrospun agar/PCL dressings contact angle was found to be 61.2°±2.4 (**Figure 4.14 a**). Given that synthetic polymer PCL is a hydrophobic polymer with a few biomedical applications (Ranjbar-Mohammadi & Bahrami, 2016; Safdari et al., 2022), some hydrophilic polymers can improve PCL biocompatibility, as PCL (**Figure 4.14 b**) contact angle (115.7°±1.4) was

too high to be effective for cell adhesion. Moreover, the surface wettability of agar films was found to be 42.1° ±1.5 (**Figure 4.14 c**), which falls within the hydrophilic range, could also limit the cell adhesion. Additionally, the ideal contact angle range for cell attachment should be between 55° and 80° (Menzies & Jones, 2010).

4.6.7. Swelling behaviour

The adsorption of wound exudates is an important requirement for a dressing, especially when employed on chronic wounds. Fluid absorption capacity of the wound dressing, depend upon composition of matrix polymer, the pH of the media (Hua et al., 2010; Vaghani et al., 2012), and the temperature (Awadhiya et al., 2016). The swelling percentage of neat PCL electrospun mat was observed 6%. After the blend of agar and PCL for the fabrication of agar/PCL electrospun mat, the swelling percentage was increased to 20%. Whereas the swelling percentage of solvent-cast agar was higher due to hydrophilic nature of agar matrix. Nevertheless, because of the distinct swelling properties of the two layers (electrospun and solvent-cast), the fabricated layers became detachable over time in a wet environment, a problem that was resolved by glutaraldehyde crosslinking. After crosslinking both layers with glutaraldehyde vapors, the developed bilayer of electrospun and solvent cast dressing, swelling percentage dropped from 400% to 250% (**Figure 4.14 d**).

The fluid handling capacity of the bilayer agar film (2.11 g/g ±0.1) was slightly lower than 0.2 mM agar films (2.15 g/g ±0.05), which could be due to the presence of silver in the modified films. Moreover, the dehydration rate of the developed bilayer agar films (0.0015 g/min) was also like the 0.2 mM agar films (0.002 g/min) as base layer was same, which was agar. Moreover, as displayed earlier in swelling percentage after crosslinking, the developed films were getting slowly saturated with the surrounding fluid within 10 min of absorption. Hence, the dressing would absorb the excess wound exudate efficiently impeding leakage of exudate in the surrounding tissue.

4.6.8. Water vapour transmission rate

The permeability of the dressing materials is highly crucial to the healing process. Low wound dressing permeability causes maceration, whereas high permeability promotes desiccation. To stay moist without retaining exudates, the wound dressing must have

optimal water vapour permeability ($\sim$2000 g/m^2/day)(Barros et al., 2021). Our electrospun and bilayer dressings transferred 1200 g/m^2/day of water (**Figure 4.14 e**), a comparable amount of intact skin transpiration rate (Yusof et al., 2003). Therefore, these bilayer dressing could be used for low to moderate exudating wounds (Akturk et al., 2011).

4.6.9. In vitro biodegradation study

The **Figure 4.14 f** depicts an analysis of *in vitro* biodegradation, wherein the agar-based bilayer dressing was subjected to various physiological environments. PBS solution enriched with lysozyme and hydrogen peroxide assisted in breaking down polymer chains within the matrix via hydrolytic and enzymatic degradation. Maximum degradation, approximately 37%, was observed in H_2O_2 PBS solution, attributed to hydrogen abstraction (X. Chen, Sun-Waterhouse, et al., 2021) resulting in the digestion of glycosidic bonds (Ahtzaz et al., 2017a).
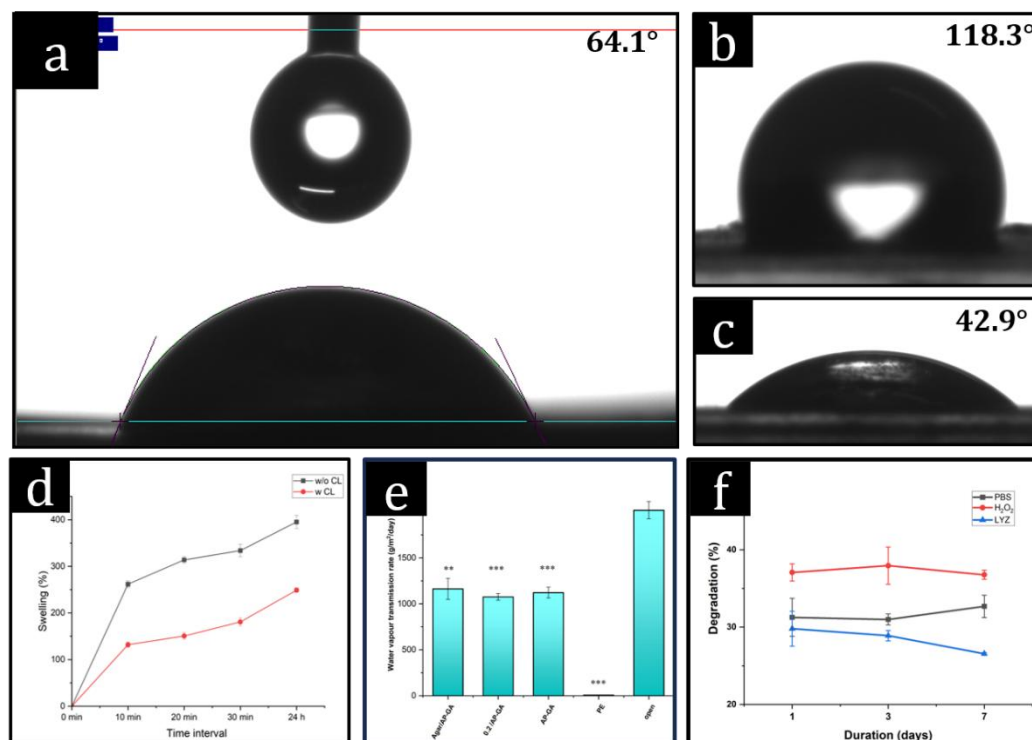
Figure 4.14. *Contact angle of electrospun agar/PCL with gallic acid (a) dressings as antioxidant agent (AP-GA). Contact angle of control films PCL (b) and agar (c) was also displayed their wettability. (d) Swelling behaviour of the developed bilayer*

dressings before and after glutaraldehyde crosslinking. (e) Water vapour transmission rate of the developed bilayer dressings agar/AP-GA, 0.2 agar/AP-GA, AP-GA, and polyester (PE) film.

4.6.9. Antioxidant properties

The antioxidant properties of a wound dressing are crucial for proper healing because they significantly reduce oxidative stress caused by reactive oxygen species (ROS) creation. Although ROS is required for signalling and tissue repair, excessive ROS in the lesion area may result in protein, DNA, and tissue damage. Incorporating antioxidant agents in the dressings to scavenge free radicals can help reduce ROS at the wound site. Additionally, this decreases inflammatory responses attributed to free radicals and promotes tissue regeneration and appropriate healing.

In the DPPH assay, the percent reduction of free radicals was quantified by measuring absorption drop from dark purple colour to pale-yellow colour. The developed bilayer dressing displayed free radical scavenging properties within minutes of sample interaction with the DPPH methanolic solution. In fifteen minutes, the material attained 90% of antioxidant properties (**Figure 4.15**). Even after 360 minutes, the scavenging capabilities were at their peak due to the incorporation of gallic acid. Gallic acid possesses anti-inflammatory, antibacterial, antioxidant, anti-lipid peroxidation, and tissue regeneration properties, among others (Lang et al., 2021a; Sanandiya et al., 2019).
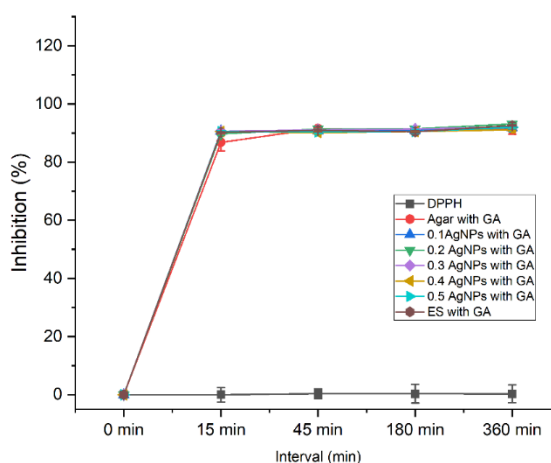
Figure 4.15. *Antioxidant properties of the developed bilayer dressing*

4.6.10. Antibacterial testing

Antibacterial mechanism of silver (Ag^0 or Ag^+) for a potent bactericidal effect is investigated in earlier studies (Bie et al., 2020; M. Singh et al., 2008; L. Wang & Rhim, 2015b; T. Yang et al., 2015). Multiple factors such as nanoparticles (NPs) size, NPs shape, and their uniform dispersion, may influence the antibacterial properties. It could also be affected by the type of bacteria, the thickness of its lipopolysaccharide layer, the structural distinctions between the outer and inner membrane, and the efflux pump (Hajipour, 2012).

Zone of inhibition (ZOI) test was performed on the samples with AgNPs to evaluate their antibacterial properties. In *E. coli,* the zone of inhibition was increased by 36%, 44.4%, and 22% for 0.1 mM, 0.2 mM, and 0.3 mM bilayer samples, respectively. For 0.2 test samples, the 44.4% and 39% increased inhibition zone was observed for *S. aureus* and *P. aeruginosa*, respectively. Compared to *S. aureus* and *P. aeruginosa*, the ZOI value of *E. coli* plates were significantly higher, indicating greater antibacterial activity of NPs against gram-negative bacteria than gram-positive bacteria. Similar antibacterial properties of silver have been observed in previous studies (Ghosh et al., 2010). Agar-AgNPs films (0.2 mM) demonstrated good antibacterial activity (**Figure 4.16 a)** without sacrificing their biocompatibility (discussed later) **(Figure 4.17 b)**, as higher concentrations of these particles result in cytotoxicity. In addition, increased silver nanoparticle concentrations result in agglomeration, which delays the nanoparticle dissolution from solvent-cast films.

Time kill assay

Using the time kill assay, antibacterial properties against gram-positive and gram-negative microorganisms were evaluated as log reduction in CFU count **(Figure 4.16 c- f)**. The growth curve of control cells increased with time, whereas the growth curve of cells in contact with silver NPs agar bilayer films remained stationary, indicating bacteriostatic behaviour of the bilayer structure. In addition, 0.2 mM AgNPs agar bilayer films exhibited the most potent antibacterial effect against gram-negative bacteria such as *P. aeruginosa and P. vulgaris*, reducing bacterial growth by 92% and 81%, respectively. Reduced antimicrobial properties were observed for 0.1 mM and 0.3 mM samples, which could be due to low concentration and nanoparticle agglomeration

respectively. The antibacterial effectiveness of silver nanoparticles was in order of *P. aeruginosa > P. vulgaris > E. coli > S. aureus.*
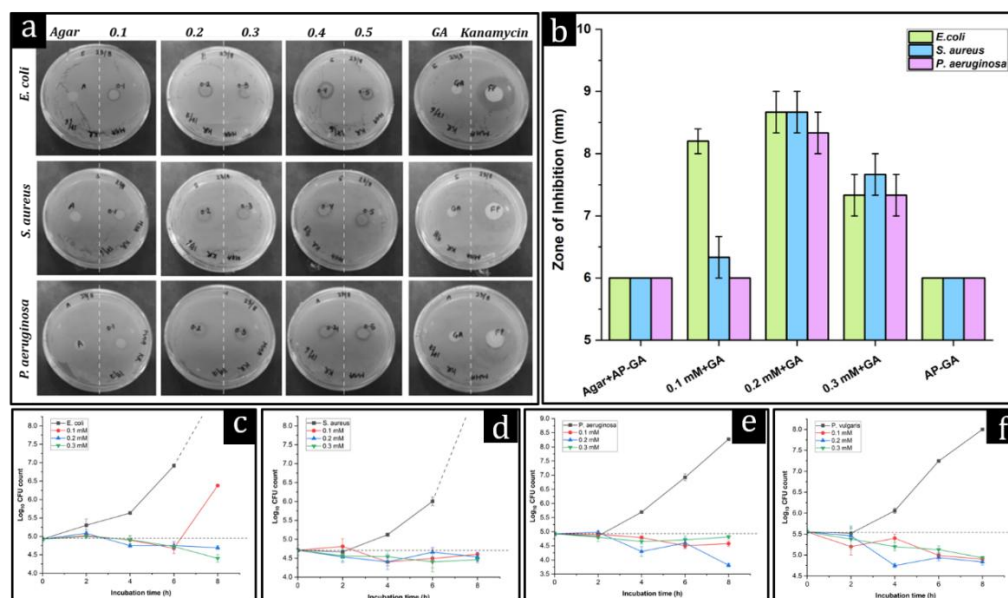
Figure 4.16. *(a) Zone of inhibition of silver nanoparticles impregnated in agar/AP-GA bilayer dressings (left to right- Ag, 0.1 mM, 0.2 mM, 0.3 mM, 0.4 mM, 0.5 mM, GA and filter paper with kanamycin (FP)) and (top to bottom- E. coli. S. aureus and P. aeruginosa). (b) Zone of inhibition of silver nanoparticles impregnated in solvent-cast agar with agar/PCL containing gallic acid as bilayer dressings (Left to right- Ag, 0.1 mM, 0.2 mM, 0.3 mM, and AP-GA mat). Antibacterial activity of 0.1 mM, 0.2 mM, and 0.3 mM agar-based bilayer films against E. coli(c), S. aureus(d), P. aeruginosa(e), and P. vulgaris(f). Dotted line indicates the growth was more than >log 9*

4.6.11. Haemocompatibility assay

The functionality of the developed samples for erythrocytes, or red blood cells, was examined using a haemocompatibility assay to validate their blood compatibility for wound dressing application. Haemolysis or non-haemocompatibility is demonstrated if the developed material disrupts RBC within the allotted period when interacting with the biomaterial. Haemolysis of all samples was less than 5% (**Figure 4.17 a**) depicting highly haemocompatible nature of the developed material (Tripathi et al., 2021).

4.6.12. Platelet adhesion

Additionally, the samples were incubated with platelet-rich plasma (PRP) to further explore the effect on platelets. As illustrated in **Figure 4.17 b**, the agar/PCL bilayer dressing exhibited platelet adhesion and aggregation, as indicated by the presence of

spiny pseudopodia, thus confirming platelet activation. The activation of platelets observed in this study can be attributed to the inclusion of gallic acid, which resulted in increased platelet aggregation and activation, which was absent in PCL nanofibrous mat **(Figure 4.17 c)**. Previous studies have demonstrated that gallic acid exhibits a comparable impact on platelet adhesion (Sanandiya et al., 2019).

The results indicate that the developed agar/PCL bilayer dressing, with its incorporation of gallic acid, plays a significant role in promoting platelet adhesion and activation, making it a promising option for improving wound healing and related applications.

4.6.13. *In-vitro* cytocompatibility test

Direct and indirect contact, using inset plates, cytocompatibility of the prepared dressing material was evaluated using MTT assay. Cellular attachment and proliferation were found to be more prominent in PCL electrospun mat (**Figure 4.17 d**), as compared to agar/PCL nanofibrous dressings (**Figure 4.17 e**). The cellular attachment and proliferation on the electrospun mats could be attributed to the surface morphologies, providing molecular physical cues for proliferation and attachment (Bharadwaz & Jayasuriya, 2020). Therefore, the beaded structure of the electrospun layer could influence the reduced cell adherence. After incubating in presence of cells, the electrospun mats exhibited the characteristic cell attachment. Since silver nanoparticles are toxic at high concentrations, cytocompatibility testing was used to determine the optimal concentration. The percentage of viable fibroblast cells decreased as the concentration of silver nanoparticles in the direct contact assay increased (**Figure 4.17 g**). Up to a concentration of 0.2 mM, more than 60% of cells were viable in silver nitrate incorporated agar films with agar/PCL-GA bilayer dressings, but as the concentration was increased, the mats began to exhibit cytotoxicity. Therefore. 0.2 mM of silver nitrate was the optimal concentration of silver nanoparticles for the mats. In the indirect contact experiment, all the produced films exhibited greater than 95% cell viability (**Figure 4.17 f**).
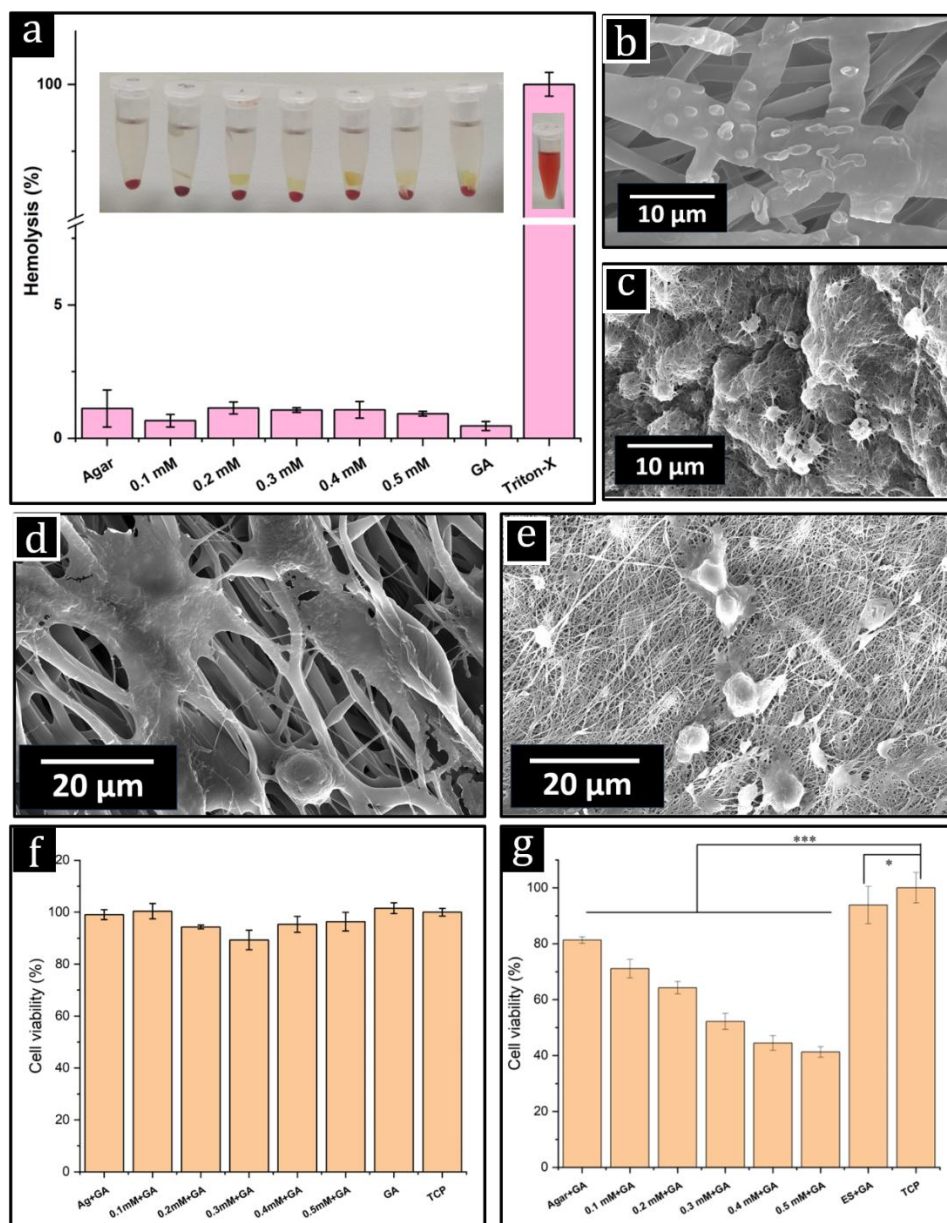
Figure 4.17. *(a) Digital images(a) of haemolysis assay of the developed bilayer dressing were presented in inset image. Hemolysis percentage of the developed bilayer dressing where GA was electrospun layer of agar/PCL with gallic acid, and triton-X treated RBC solution as (+) control. Micrographs of the platelet adhesion on the developed PCL nanofibrous mat (b) and agar/PCL-GA mats (c). Cellular attachment and proliferation on the PCL electrospun mat (d) and agar/PCL (e) electrospun layer. Indirect (f) and direct (g) contact assay of the developed bilayer dressings containing AgNPs at varied concentration from 0 mM to 0.5 mM.*

4.6.14. Wound scratch assay

After 24 hours of incubation in the presence of samples, the cells migrated and multiplied in the scratched area **(Figure 4.18 a-f)**. Although films containing silver

nanoparticles exhibited a small amount of cytotoxicity, the base material agar had a positive effect on cell migration and proliferation. Consequently, the developed dressing materials exhibited optimal cytocompatibility and cell proliferation.

Scratch analysis depicts the percentage of wound closure that signifies the scratch healing (**Figure 4.18 g**). The healing of the scratch in presence of samples was compared with the control samples. Bilayer agar films displayed good cell migration, which could be due to agar. Wound closure of 0.2 agar/AP-GA film (79.2%) was lower than that observed in 0.1 agar/AP-GA film (86.8%), which could be due to release of silver NPs. Although there was a slight decrease in cell migration within the scratched area compared to the control cells, the developed dressings demonstrated a promotion of cell proliferation and growth, albeit at a slower rate in the cell migration process. Nonetheless, as the developed bilayer dressing exhibited cell proliferation and growth, making it a viable candidate for biomedical application.

0 h	After 24 h
a)	
b)	

c)

d)

e)

f)

Figure 4.18. *Wound scratch assay, Micrographs of agar/AP-GA(a), 0.1mM agar/AP-GA(b), 0.2 mM agar/AP-GA(c), AP-GA(d), positive control(e), and negative control with DMSO(f) where left panel were before sample incubation and right panel displayed after 24 h sample incubation. Graphical representation illustrating the percent wound closure, in 24 h(g).*
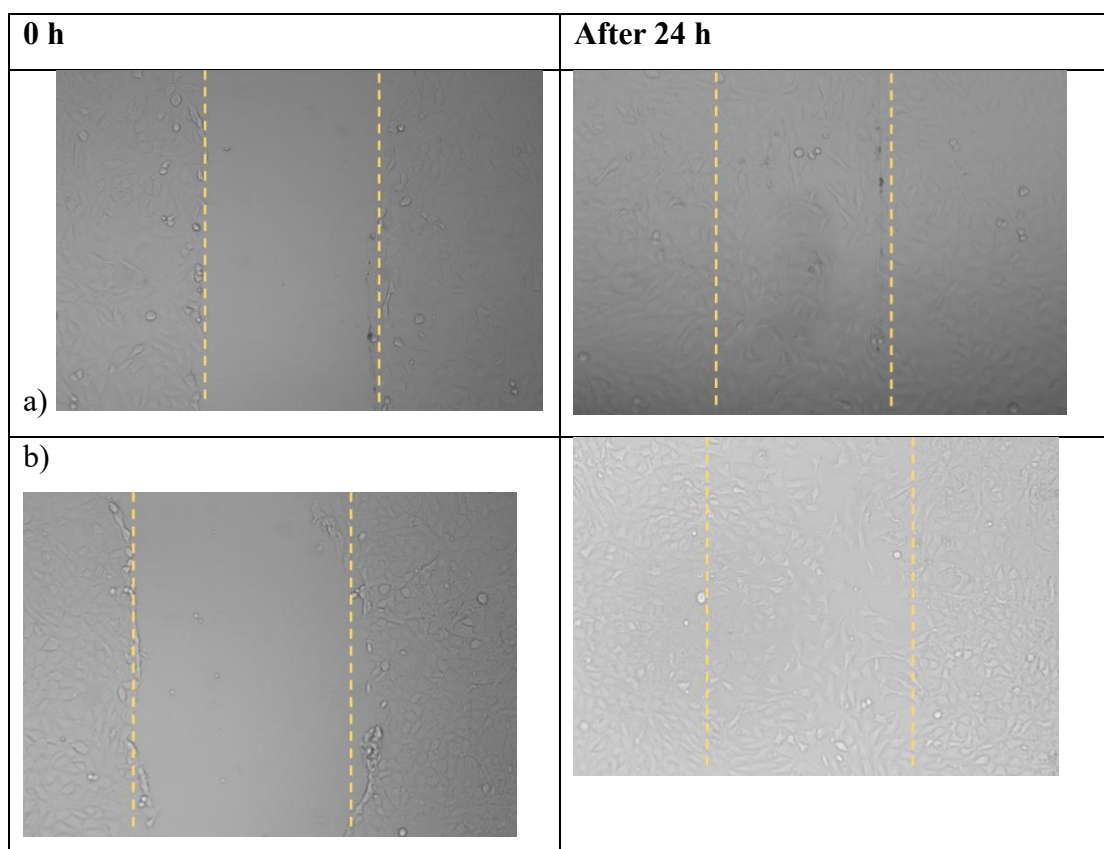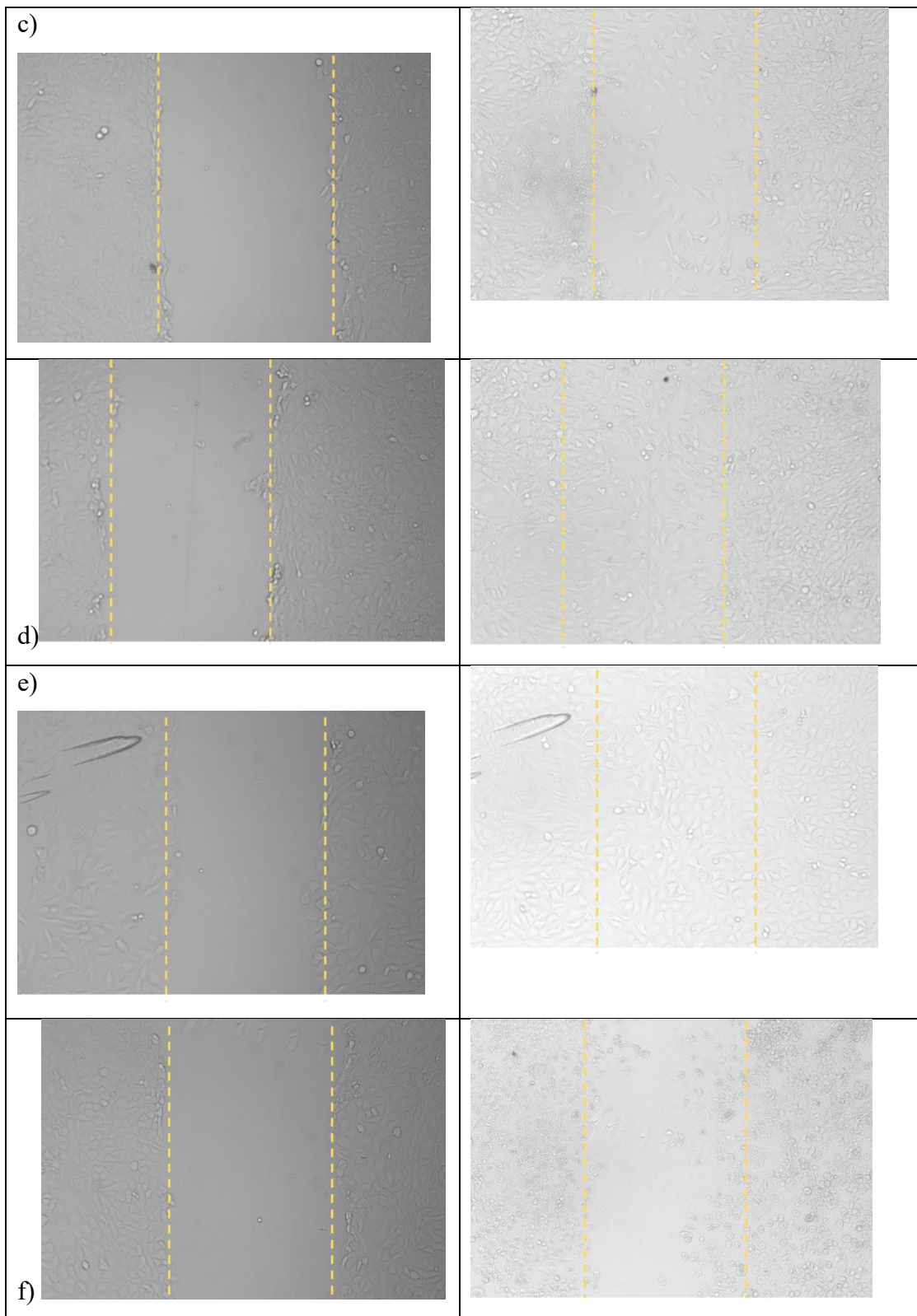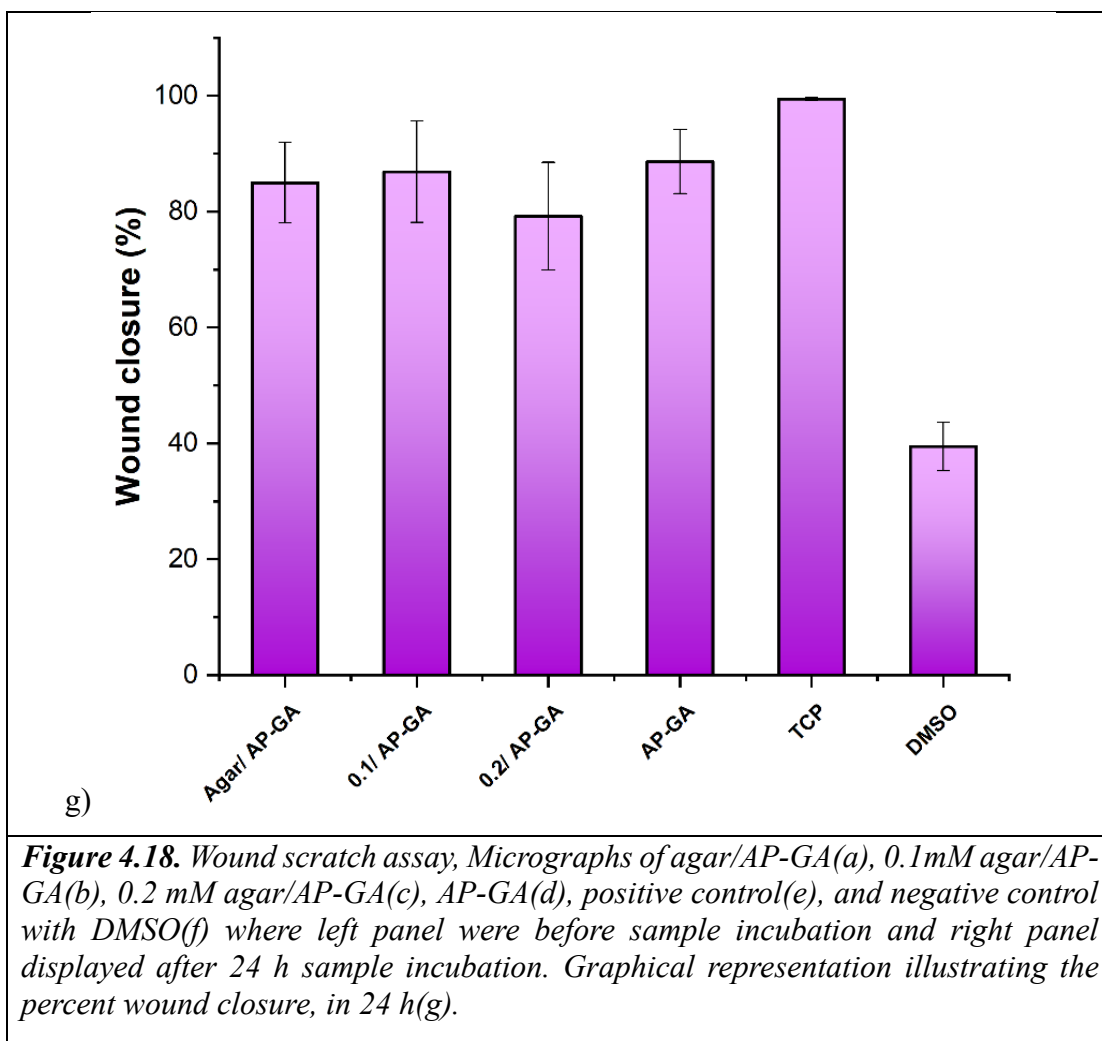
4.6.15. Release kinetics of silver nanoparticles

The efficacy of the developed antibacterial dressing incorporated with nanoparticles relies on the release kinetics of the nanoparticles. An instantaneous burst release could lead to cytotoxicity, highlighting the requirement for a controlled release to ensure efficient antibacterial properties throughout the healing phase. The release of silver nanoparticles from 0.2 agar/AP-GA was quantified using ICP-MS. A release of silver nanoparticles (8%) was observed within 24 h, gradually increasing to a release percentage of 73% over 14 days from the samples (**Figure 4.19**). The release kinetics were elucidated using different release kinetics models, including zero-order, first-order, Higuchi, and Korsmeyer-Peppas model. The initial 60% of the release curve were used for the model fitting (Elmas et al., 2020) and analysis was based on statistically higher R^2 value. After fitting Zero-order model, the R^2 value indicates high level of correlation suggesting a consistent release rate of silver nanoparticles over time,

independent of the concentration of the silver. However, Korsmeyer-Peppas was found strong fits based on statistically higher R^2 (**Table 4.1**). Since these models involve release kinetics from polymeric entities, typically exhibiting non-Fickian diffusional characteristics, where both diffusion and polymer relaxation contributes to the release, the release mechanism indicated that the release of silver nanoparticles is more dependent on the relaxational release of the polymeric chains. This release behaviour would mitigate the dose-dependent cytotoxicity associated with instant release and demonstrated antibacterial efficacy throughout the wound healing.

Figure 4.19. Silver nanoparticles cumulative release calculated through ICP-MS.
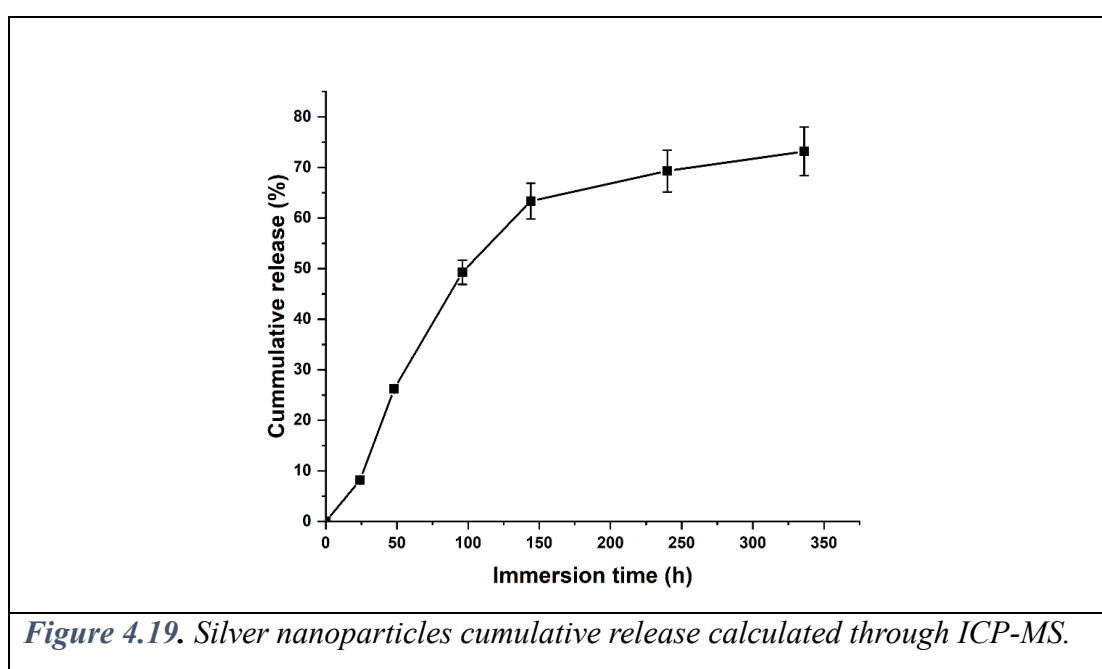
Table 4.1. *Release kinetics parameters obtained after applying different kinetic models for the release of silver from the dressing.*

Kinetic Models	Sample	
Zero order	R^2	0.98995
	k	0.4663
First order	R^2	0.90835
	k	0.015612
Higuchi model	R^2	0.963142

	k	4.368571
Korsmeyer-Peppas model	R^2	**0.99216**
	n	0.898786
	k	0.753433

4.6.16. *In vivo* wound healing studies

For the in vivo study, 0.2 agar/AgNPs samples were used as they demonstrated the best results in the in vitro studies. **Figure 4.20** summarizes the healing progress of the wound for all the groups at varying time intervals. The bioactivity of the bilayer wound dressing displayed the best healing action according to the wound area measurement (group III). Moreover, on the 3rd day, all the wounds showed inflammation and redness around the wound, except for the test sample, which had the least inflammation and redness. The anti-oxidant, anti-inflammatory, and antibacterial properties of agar: PCL incorporated with gallic acid and silver nanoparticles, could account for this. The incorporation of anti-oxidant agents can scavenge free radicals, resulting in accelerating wound healing (Lang et al., 2021b). Furthermore, due to the superior swelling properties of the bilayer dressing, the wound area has shown enhanced healing compared to other treated wound areas. The visual inspections were performed during dressing changes until the wounds were completely healed.

The wound contraction was highest for group III bilayer dressing, around 77.4% on the 3rd day, followed by 87% by 6th day. Group IV (treated with commercially available Sterizone dressing) also demonstrated 81% healing on the 6th day. However, group III (treated with bilayer dressing) and group IV (treated with Sterizone™ dressing) healed by day 12, the scar formation in the wound treated with bilayer dressing was significantly less compared to the other groups. Group V wounds treated with povidone healed in 15 days, whereas group VI untreated wounds took 18 days for natural healing. Additionally, the bilayer dressing samples showed the highest rate of wound contraction. By the end of day 12, group II, III, and IV were completely healed. This demonstrates that agar itself has healing capabilities, enhancing antioxidant and

antibacterial properties in the agar matrix, thereby broadening the spectrum for advanced solutions. This confirms that the developed bilayer agar-based wound dressing promotes healing by more than 97.5% within 12 days of injury.

(a)

(b)
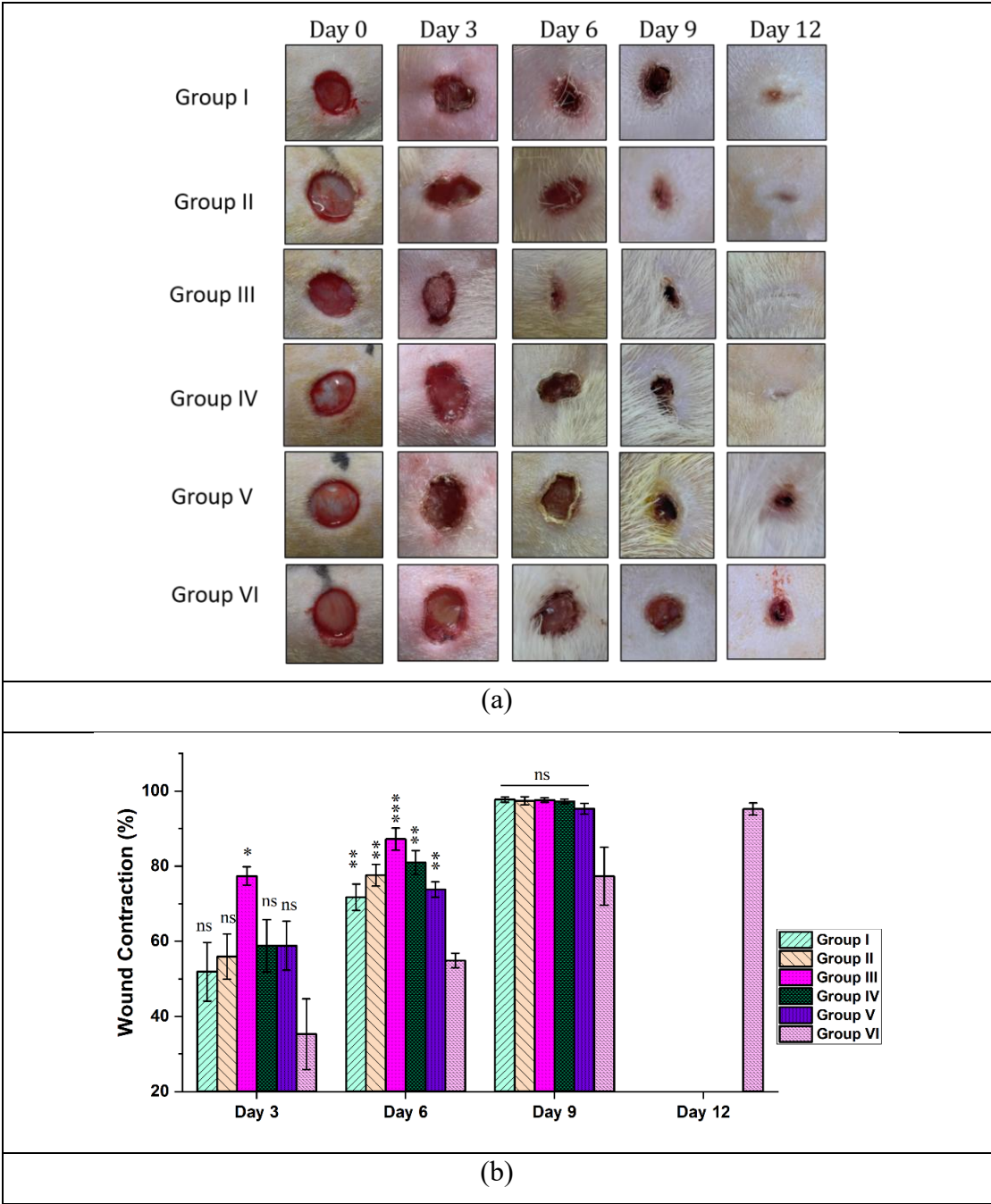
Figure 4.20. *In vivo wound healing. (a) Digital photographs of the wound for various treated group of different time intervals. (b) Wound contraction rate of different groups on 3rd, 6th, 9th, and 12th day of the study.*

CHAPTER 5
CONCLUSION

5.1. Conclusion

In conclusion, we have successfully developed a bilayer agar-based wound dressing with both symmetric and asymmetric morphologies. For the symmetric morphology, uniaxial and coaxial nanofibrous mats were fabricated, while the asymmetric morphology featured a solvent-cast support layer and a primary electrospun layer with antibacterial and antioxidant properties. The developed symmetric and asymmetric bilayer dressing promote healing by scavenging free radicals at the wound site, a crucial requirement of early wound healing, and provide antibacterial properties throughout the various phases of wound healing. This is achieved through the sustained release of antibacterial silver nanoparticles.

Previously performed research on bilayer dressings by Zhang *et.al.* (T. Zhang et al., 2022) and Eskanddarinia *et.al.* (Eskandarinia et al., 2020b) overlooked the significance of moisture transmission rate and biodegradation in the developed bilayer wound dressing, respectively. Our study demonstrated a sustained release of nanoparticles due to diffusion and relaxation of polymeric chains, which aids in creating a barrier to microbial infection and protects the wound during the healing process without affecting cell migration and proliferation.

The electrospinning technique shows significant possibilities in the development of agar: PCL nano/micro fibres for potential wound dressing applications. Investigations into the morphology, strength, wettability, and permeability of the mats have provided broad evidence supporting their efficacy in wound treatment. The use of binary solvents has facilitated the advancement of mats that exhibit enhanced wettability, fluid retention capacity, and permeability, thus promoting wound healing. The introduction of additives, such as citric acid, albumin, and piperine, has allowed for modification of the mechanical strength of electrospun agar: PCL mats, broadening their potential applications. Furthermore, the synthesis of symmetric bilayer wound dressing using coaxial mats through the integration of polyvinyl alcohol (PVA) as the core material

and agar: PCL as the membrane material has led to the advancement of dressings for controlled drug release, characterized by sustained release properties. The release rate was further controlled by the incorporation of an additional uniaxial layer composed of agar: PCL onto the coaxial mat, resulting in sustained release and enhanced efficacy in wound healing. The agar: PCL mats possess slow biodegradability, which results in a slow degrading process, allowing for prolonged utilization and reducing the need for frequent dressing changes. These advancements highlight the potential of electrospun agar: PCL mats in advancing wound care methodologies.

Moreover, the electrospun layer of asymmetric bilayer dressing, which is in contact with the wound, promotes healing by scavenging free radicals at the wound site. Meanwhile, the support layer, containing silver nanoparticles as an antibacterial agent, helps create a barrier to microbial infection and protects the wound.

The characterization of AgNPs using TEM revealed a size ranging from 10-20 nm while UV-Vis confirmed nanoparticle formation through surface plasmon resonance. Mechanical testing of the developed bilayer dressing confirmed significant tensile strength (84 MPa) and flexibility, with 16% elongation at break, establishing its suitability for wound dressing. Analysis of the swelling degree demonstrated the dressing ability to absorb 250% of DI water while maintaining its integrity. Additionally, the dressing's water vapor transmission rate was found to be 1200 $g/m^2/day$, which falls within the transmission range of human skin.

Furthermore, an assessment of the antioxidant properties of gallic acid revealed a scavenging of more than 90% of free radicals. The recorded zone of inhibition and a decrease in colony-forming units (CFU) demonstrated dressing's bacteriostatic efficacy. Additionally, the *in-vitro* hemocompatibility of the dressing exhibited less than 5% haemolysis, confirming its excellent hemocompatibility.

Moreover, the dose-dependent cytotoxicity of the developed bilayer dressing was analysed using MTT assay for varied concentrations of AgNPs. Silver nanoparticles formed from 0.2 mM $AgNO_3$ agar solution served the best biocompatible composition, aiding in evaluating their compatibility and clinical safety. The wound scratch assay displayed excellent wound closure (>79%), indicating accelerated wound healing.

Additionally, the sustained release of silver nanoparticles and the dressing's biodegradability broadened its potential applications. Moreover, *in vivo* experiments demonstrated the efficacy of the developed bilayer dressing by efficiently combating bacterial invasion, scavenging free radicals, and promoting wound healing up to 54.4% compared to untreated wounds.

Finally, the formulation containing a 2% agar film with 0.2 mM silver nitrate as supporting layer and an electrospun layer of agar/PCL (1:1; 20% each) with 0.5% gallic acid demonstrated excellent characteristics as a potential asymmetric wound dressing for chronic wounds. The developed symmetric and asymmetric bilayer dressing efficiently managed both microbial infection and oxidative stress. In addition, its fluid handling, bioactivity, and biocompatibility demonstrated its efficacy in chronic wound healing.

5.2. Future Scope

The potential biomedical applications have been significantly broadened through the fabrication of nanofibers using agar and PCL. The blend of hydrophilic and hydrophobic polymers resulted in an amphiphilic matrix that can be applied across various uses. Agar, due to its hydrophilic properties, can serve as a matrix polymer for hydrophilic drugs. Its excellent swelling properties of agar, which are concentration-dependent, facilitate the controlled release of agents with bioactivities or pharmaceutical medications. The introduction of hydrophobic PCL can regulate the release of hydrophilic drugs, ensuring a sustained release despite their high hydrophilicity. This behaviour also supports the sustained release for hydrophobic drugs as well, thanks to the amphiphilic nature of the matrix.

In addition, nanofibrous morphology mimics the extracellular matrix structure found in the epidermis. The porosity of the scaffolds and the surface area of the nanofibers can be customized according to the specific needs. Moisture permeability can also be modulated by the surface properties, porosity, and thickness. The developed agar: PCL nanofibrous mats possess many potentials applications besides biomedical uses, including tissue engineering, biosensors, electronic devices, bioremediation, and filters.

The developed bilayer dressing exhibits antibacterial, antioxidant, and biocompatible properties that can be further enhanced. Additional work can be performed on multilayered dressings to provide the specific needs of different types of chronic wounds, including the incorporation of bioactive agents, biomolecules like enzymes and proteins, and more.

Given the excellent physical and chemical characteristics of electrospun dressings, it is important to consider their mechanical properties. Enhancing the mechanical properties of nanofibrous dressings can be achieved through various polymer blends or by designing multilayered asymmetric structures for the dressings. Moreover, it is crucial to regulate the replicability of electrospinning parameters to enhance the commercial applicability of these dressings.

REFERENCES

Abdollahi, Z., Zare, E. N., Salimi, F., Goudarzi, I., Tay, F. R., & Makvandi, P. (2021). Bioactive carboxymethyl starch-based hydrogels decorated with cuo nanoparticles: Antioxidant and antimicrobial properties and accelerated wound healing in vivo. *International Journal of Molecular Sciences*, *22*(5), 1–18. https://doi.org/10.3390/ijms22052531

Agarwal, R., Alam, M. S., & Gupta, B. (2013). Polyvinyl alcohol-polyethylene oxide-carboxymethyl cellulose membranes for drug delivery. *Journal of Applied Polymer Science*, *129*(6), 3728–3736. https://doi.org/10.1002/app.39144

Agnihotri, S., Mukherji, S., & Mukherji, S. (2013). Immobilized silver nanoparticles enhance contact killing and show highest efficacy: elucidation of the mechanism of bactericidal action of silver. *Nanoscale*, *5*(16), 7328–7340. https://doi.org/10.1039/c3nr00024a

Aguirre-Chagala, Y. E., Altuzar, V., León-Sarabia, E., Tinoco-Magaña, J. C., Yañez-Limón, J. M., & Mendoza-Barrera, C. (2017). Physicochemical properties of polycaprolactone/collagen/elastin nanofibers fabricated by electrospinning. *Materials Science and Engineering C*, *76*, 897–907. https://doi.org/10.1016/j.msec.2017.03.118

Ahmadian, S., Ghorbani, M., & Mahmoodzadeh, F. (2020). International Journal of Biological Macromolecules Silver sulfadiazine-loaded electrospun ethyl cellulose / polylactic acid / collagen nano fi brous mats with antibacterial properties for wound healing. *International Journal of Biological Macromolecules*, *162*, 1555–1565. https://doi.org/10.1016/j.ijbiomac.2020.08.059

Ahmed, L., Atif, R., Salah Eldeen, T., Yahya, I., Omara, A., & Eltayeb, M. (2019). Study the Using of Nanoparticles as Drug Delivery System Based on Mathematical Models for Controlled Release. *International Journal of Latest Technology in Engineering*, *VIII*. www.ijltemas.in

Ahtzaz, S., Nasir, M., Shahzadi, L., Iqbal, F., Chaudhry, A. A., Yar, M., Rehman, I. ur, Amir, W., Anjum, A., & Arshad, R. (2017a). A study on the effect of zinc oxide and zinc peroxide nanoparticles to enhance angiogenesis-pro-angiogenic grafts for tissue regeneration applications. *Materials and Design*, *132*, 409–418. https://doi.org/10.1016/j.matdes.2017.07.023

Ahtzaz, S., Nasir, M., Shahzadi, L., Iqbal, F., Chaudhry, A. A., Yar, M., Rehman, I. ur, Amir, W., Anjum, A., & Arshad, R. (2017b). A study on the effect of zinc oxide and zinc peroxide nanoparticles to enhance angiogenesis-pro-angiogenic grafts for tissue regeneration applications. *Materials and Design*, *132*, 409–418. https://doi.org/10.1016/j.matdes.2017.07.023

Akshay Kumar, K. P., Zare, E. N., Torres-Mendieta, R., Wacławek, S., Makvandi, P., Černík, M., Padil, V. V. T., & Varma, R. S. (2021). Electrospun fibers based on botanical, seaweed, microbial, and animal sourced biomacromolecules and their multidimensional applications. *International Journal of Biological Macromolecules*, *171*, 130–149. https://doi.org/10.1016/j.ijbiomac.2020.12.205

Akturk, O., Tezcaner, A., Bilgili, H., Deveci, M. S., Gecit, M. R., & Keskin, D. (2011). Evaluation of sericin/collagen membranes as prospective wound dressing biomaterial. *Journal of Bioscience and Bioengineering*, *112*(3), 279–288. https://doi.org/10.1016/j.jbiosc.2011.05.014

Alba, K., & Kontogiorgos, V. (2020). *Seaweed Polysaccharides (Agar , Alginate Carrageenan) Seaweed Polysaccharides (Agar , Alginate Carrageenan). January 2018*, 0–11. https://doi.org/10.1016/B978-0-08-100596-5.21587-4

Aleemardani, M., Solouk, A., Akbari, S., Dehghan, M. M., & Moeini, M. (2020). Silk-derived oxygen-generating electrospun patches for enhancing tissue regeneration: Investigation of calcium peroxide role and its effects on controlled oxygen delivery. *Materialia*, *14*(August), 100877. https://doi.org/10.1016/j.mtla.2020.100877

Alipour, R., Khorshidi, A., Fallah, A., & Mashayekhi, F. (2019). *Skin wound healing acceleration by Ag nanoparticles embedded in PVA / PVP / Pectin / Mafenide acetate composite nano fi bers*. *79*(August), 1–11.

Alvandi, H., Jaymand, M., Eskandari, M., Aghaz, F., Hosseinzadeh, L., Heydari, M., & Arkan, E. (2022). A sandwich electrospun nanofibers/Tragacanth hydrogel composite containing Aloe vera extract and silver sulfadiazine as a wound dressing. *Polymer Bulletin*, *0123456789*. https://doi.org/10.1007/s00289-022-04603-6

Alven, S., & Aderibigbe, B. A. (2020). Chitosan and cellulose-based hydrogels for wound management. *International Journal of Molecular Sciences*, *21*(24), 1–30. https://doi.org/10.3390/ijms21249656

Ambekar, R. S., & Kandasubramanian, B. (2019). Advancements in nanofibers for wound dressing: A review. *European Polymer Journal*, *117*(May), 304–336. https://doi.org/10.1016/j.eurpolymj.2019.05.020

Ananth, a. N., Daniel, S. C. G. K., Sironmani, T. A., & Umapathi, S. (2011). PVA and BSA stabilized silver nanoparticles based surface-enhanced plasmon resonance probes for protein detection. *Colloids and Surfaces B: Biointerfaces*, *85*(2), 138–144. https://doi.org/10.1016/j.colsurfb.2011.02.012

Angel, N., Li, S., Yan, F., & Kong, L. (2022a). Recent advances in electrospinning of nanofibers from bio-based carbohydrate polymers and their applications. *Trends in Food Science and Technology*, *120*(December 2021), 308–324. https://doi.org/10.1016/j.tifs.2022.01.003

Angel, N., Li, S., Yan, F., & Kong, L. (2022b). Recent advances in electrospinning of nanofibers from bio-based carbohydrate polymers and their applications. *Trends in Food Science and Technology*, *120*(December 2021), 308–324. https://doi.org/10.1016/j.tifs.2022.01.003

Annamalai, R. T., Mertz, D. R., Daley, E. L. H., & Stegemann, J. P. (2016). Collagen Type II enhances chondrogenic differentiation in agarose-based modular microtissues. *Cytotherapy*, *18*(2), 263–277. https://doi.org/10.1016/j.jcyt.2015.10.015

Arham, R., Mulyati, M. T., Metusalach, M., & Salengke, S. (2016). Physical and mechanical properties of agar based edible film with glycerol plasticizer. *International Food Research Journal*, *23*(4), 1669–1675.

Armeda, T. P. (2018). Fabrication of Pcl-Collagen Nanofiber Using Chloroform-Formic Acid Solution and Its Application As Wound Dressing Candidate. *Journal of Stem Cell Research and Tissue Engineering*, *1*(1). https://doi.org/10.20473/jscrte.v1i1.7567

Asadi, N., Pazoki-toroudi, H., Rahmani, A., Bakhshayesh, D., Akbarzadeh, A., Davaran, S., & Annabi, N. (2021). International Journal of Biological Macromolecules Multifunctional hydrogels for wound healing : Special focus on biomacromolecular based hydrogels. *International Journal of Biological Macromolecules*, *170*, 728–750. https://doi.org/10.1016/j.ijbiomac.2020.12.202

Augustine, R., Malik, H. N., Singhal, D. K., & Mukherjee, A. (2014). *Electrospun polycaprolactone / ZnO nanocomposite membranes as biomaterials with antibacterial and cell adhesion properties*. https://doi.org/10.1007/s10965-013-0347-6

Awadhiya, A., Kumar, D., Rathore, K., Fatma, B., & Verma, V. (2016). *Synthesis and characterization of agarose – bacterial cellulose biodegradable composites*. 1–23. https://doi.org/10.1007/s00289

Balouiri, M., Sadiki, M., & Ibnsouda, S. K. (2015). Methods for in vitro evaluating antimicrobial activity : A review Author ' s Accepted Manuscript. *Journal of Pharmaceutical Analysis*, *6*(January 2016), 71–79. https://doi.org/10.1016/j.jpha.2015.11.005

Bal-öztürk, A., Özkahraman, B., Tamahkar, E., & Alarçin, E. (2021). *Advancements and future directions in the antibacterial wound dressings – A review. September 2020*, 703–716. https://doi.org/10.1002/jbm.b.34736

Barrioni, B. R., De Carvalho, S. M., Oréfice, R. L., De Oliveira, A. A. R., & Pereira, M. D. M. (2015). Synthesis and characterization of biodegradable polyurethane films based on HDI with hydrolyzable crosslinked bonds and a homogeneous structure for biomedical applications. *Materials Science and Engineering C*, *52*, 22–30. https://doi.org/10.1016/j.msec.2015.03.027

Barros, N. R., Ahadian, S., Tebon, P., Rudge, M. V. C., Barbosa, A. M. P., & Herculano, R. D. (2021). Highly absorptive dressing composed of natural latex loaded with alginate for exudate control and healing of diabetic wounds. *Materials Science and Engineering C*, *119*(April 2020), 111589. https://doi.org/10.1016/j.msec.2020.111589

Bayat, S., Pishavar, E., Kalalinia, F., & Mova, J. (2019). *Bromelain-loaded chitosan nano fi bers prepared by electrospinning method for burn wound healing in animal models*. *229*(May), 57–66. https://doi.org/10.1016/j.lfs.2019.05.028

Belay, M., Tyeb, S., Rathore, K., Kumar, M., & Verma, V. (2020). International Journal of Biological Macromolecules Synergistic effect of bacterial cellulose reinforcement and succinic acid crosslinking on the properties of agar. *International Journal of Biological Macromolecules*, *165*, 3115–3122. https://doi.org/10.1016/j.ijbiomac.2020.10.144

Bharadwaz, A., & Jayasuriya, A. C. (2020). Recent trends in the application of widely used natural and synthetic polymer nanocomposites in bone tissue regeneration. *Materials Science and Engineering C*, *110*(May 2019), 110698. https://doi.org/10.1016/j.msec.2020.110698

Bie, X., Khan, M. Q., Ullah, A., Ullah, S., Kharaghani, D., Phan, D. N., Tamada, Y., & Kim, I. S. (2020). Fabrication and characterization of wound dressings containing gentamicin/silver for wounds in diabetes mellitus patients. *Materials Research Express*, *7*(4). https://doi.org/10.1088/2053-1591/ab8337

Bruna, T., Maldonado-Bravo, F., Jara, P., & Caro, N. (2021). Silver Nanoparticles and Their Antibacterial Applications. *International Journal of Molecular Sciences 2021, Vol. 22, Page 7202*, *22*(13), 7202. https://doi.org/10.3390/IJMS22137202

Budurova, D., Ublekov, F., & Penchev, H. (2021). The use of formic acid as a common solvent for electrospinning of hybrid PHB/Soy protein fibers. *Materials Letters*, *301*(March), 130313. https://doi.org/10.1016/j.matlet.2021.130313

Capillo, G., Sanfilippo, M., Zoologica, S., Dohrn, A., & Aliko, V. (2017). *Gracilaria gracilis, Source of Agar: A Short Review*. *January 2018*. https://doi.org/10.2174/1385272820666161017164

Chalitangkoon, J., Wongkittisin, M., & Monvisade, P. (2020). Silver loaded hydroxyethylacryl chitosan/sodium alginate hydrogel films for controlled drug release wound dressings. *International Journal of Biological Macromolecules*, *159*, 194–203. https://doi.org/10.1016/J.IJBIOMAC.2020.05.061

Chen, S., Liu, B., Carlson, M. A., Gombart, A. F., Reilly, D. A., & Xie, J. (2017). Recent advances in electrospun nanofibers for wound healing. *Nanomedicine*, *12*(11), 1335–1352. https://doi.org/10.2217/nnm-2017-0017

Chen, X., Fu, X., Huang, L., Xu, J., & Gao, X. (2021). Agar oligosaccharides : A review of preparation , structures , bioactivities and application. *Carbohydrate Polymers*, *265*(March), 118076. https://doi.org/10.1016/j.carbpol.2021.118076

Chen, X., Sun-Waterhouse, D., Yao, W., Li, X., Zhao, M., & You, L. (2021). Free radical-mediated degradation of polysaccharides: Mechanism of free radical formation and degradation, influence factors and product properties. *Food Chemistry*, *365*(June), 130524. https://doi.org/10.1016/j.foodchem.2021.130524

Chinatangkul, N., Tubtimsri, S., & Panchapornpon, D. (2019). Design and characterisation of electrospun shellac-polyvinylpyrrolidone blended micro / nano fi bres loaded with monolaurin for application in wound healing. *International Journal of Pharmaceutics*, *562*(March), 258–270. https://doi.org/10.1016/j.ijpharm.2019.03.048

Cho, M. K., Singu, B. S., Na, Y. H., & Yoon, K. R. (2016a). *Fabrication and characterization of double-network agarose / polyacrylamide nanofibers by electrospinning*. *42914*, 1–8. https://doi.org/10.1002/app.42914

Cho, M. K., Singu, B. S., Na, Y. H., & Yoon, K. R. (2016b). *Fabrication and characterization of double-network agarose / polyacrylamide nanofibers by electrospinning*. *42914*, 1–8. https://doi.org/10.1002/app.42914

Chu, B., Zhang, A., Huang, J., Peng, X., You, L., Wu, C., & Tang, S. (2020). Preparation and biological evaluation of a novel agarose-grafting-hyaluronan scaffold for accelerated wound regeneration. *Biomedical Materials (Bristol, England)*, *15*(4). https://doi.org/10.1088/1748-605X/AB7B3E

Cockbill, S. M. E., Pharm, B., Pharm, M., & Turner, T. D. (n.d.). *The Development of Wound Management Products*.

Comino-Sanz, I. M., López-Franco, M. D., Castro, B., & Pancorbo-Hidalgo, P. L. (2021). The role of antioxidants on wound healing: A review of the current evidence. *Journal of Clinical Medicine*, *10*(16). https://doi.org/10.3390/jcm10163558

Cui, H., Liu, M., Yu, W., Cao, Y., Zhou, H., Yin, J., Liu, H., Que, S., Wang, J., Huang, C., Gong, C., & Zhao, G. (2021). Copper Peroxide-Loaded Gelatin Sponges for Wound Dressings with Antimicrobial and Accelerating Healing Properties. *ACS Applied Materials and Interfaces*, *13*(23), 26800–26807. https://doi.org/10.1021/acsami.1c07409

Cutting, K. F., & Westgate, S. J. (2012). Super-absorbent dressings: How do they perform in vitro? *British Journal of Nursing*, *21*(20 SUPPL.). https://doi.org/10.12968/bjon.2012.21.sup20.s14

Czemplik, M., Kulma, A., & Szopa, J. (2013). *The local treatment and available dressings designed for chronic wounds*. https://doi.org/10.1016/j.jaad.2011.06.028

Das, A., Ahmad, P., & Kumar, A. (2021). A coaxially structured trilayered gallic acid-based antioxidant vascular graft for treating coronary artery disease. *European Polymer Journal*, *143*(September 2020), 110203. https://doi.org/10.1016/j.eurpolymj.2020.110203

Dawadi, S., Katuwal, S., Gupta, A., Lamichhane, U., Thapa, R., Jaisi, S., Lamichhane, G., Bhattarai, D. P., & Parajuli, N. (2021). Current Research on Silver Nanoparticles: Synthesis, Characterization, and Applications. *Journal of Nanomaterials*, *2021*. https://doi.org/10.1155/2021/6687290

Díaz, M., Hamm, E., & Urzúa, M. (2022). *Coaxial fibers of poly (styrene- co -maleic anhydride)@ poly (vinyl alcohol) for wound dressing applications : Dual and sustained delivery of bioactive agents promoting fibroblast proliferation with reduced cell adherence as Gonz a*. *611*(September 2021). https://doi.org/10.1016/j.ijpharm.2021.121292

Diep, E., & Schiffman, J. D. (2023). Electrospinning Living Bacteria: A Review of Applications from Agriculture to Health Care. *ACS Applied Bio Materials*, *6*(3), 951–964. https://doi.org/10.1021/ACSABM.2C01055

Dong, C., Yuan, X., He, M., & Yao, K. (2006). Preparation of PVA/PEI ultra-fine fibers and their composite membrane with PLA by electrospinning. *Journal of Biomaterials Science, Polymer Edition*, *17*(6), 631–643. https://doi.org/10.1163/156856206777346287

Dong, R., & Guo, B. (2021a). Smart wound dressings for wound healing. *Nano Today*, *41*, 101290. https://doi.org/10.1016/j.nantod.2021.101290

Dong, R., & Guo, B. (2021b). Smart wound dressings for wound healing. *Nano Today*, *41*, 101290. https://doi.org/10.1016/j.nantod.2021.101290

Dong, Y., Liu, H. Z., Xua, L., Li, G., Ma, Z. N., Han, F., Yao, H. M., Sun, Y. H., & Li, S. M. (2010). A novel CHS/ALG bi-layer composite membrane with sustained antimicrobial efficacy used as wound dressing. *Chinese Chemical Letters*, *21*(8), 1011–1014. https://doi.org/10.1016/j.cclet.2010.04.010

Duan, H., Chen, H., Qi, C., Lv, F., Wang, J., Liu, Y., Liu, Z., & Liu, Y. (2024). A novel electrospun nanofiber system with PEGylated paclitaxel nanocrystals enhancing the transmucus permeability and in situ retention for an efficient cervicovaginal cancer therapy. *International Journal of Pharmaceutics*, *650*, 123660. https://doi.org/10.1016/J.IJPHARM.2023.123660

Elmas, A., Akyüz, G., Bergal, A., Andaç, M., & Andaç, Ö. (2020). Mathematical modelling of drug release. *Research on Engineering Structures and Materials*, *6*(4), 327–350. https://doi.org/10.17515/resm2020.178na0122

El-Newehy, M. H., El-Naggar, M. E., Alotaiby, S., El-Hamshary, H., Moydeen, M., & Al-Deyab, S. (2016). Preparation of biocompatible system based on electrospun

CMC/PVA nanofibers as controlled release carrier of diclofenac sodium. *Journal of Macromolecular Science, Part A: Pure and Applied Chemistry*, *53*(9), 566–573. https://doi.org/10.1080/10601325.2016.1201752

El-Samad, L. M., Hassan, M. A., Basha, A. A., El-Ashram, S., Radwan, E. H., Abdul Aziz, K. K., Tamer, T. M., Augustyniak, M., & El Wakil, A. (2022). Carboxymethyl cellulose/sericin-based hydrogels with intrinsic antibacterial, antioxidant, and anti-inflammatory properties promote re-epithelization of diabetic wounds in rats. *International Journal of Pharmaceutics*, *629*(October), 122328. https://doi.org/10.1016/j.ijpharm.2022.122328

Emam, H. E., Saleh, N. H., Nagy, K. S., & Zahran, M. K. (2015). Functionalization of medical cotton by direct incorporation of silver nanoparticles. *International Journal of Biological Macromolecules*, *78*, 249–256. https://doi.org/10.1016/j.ijbiomac.2015.04.018

Eskandarinia, A., Kefayat, A., Agheb, M., Rafienia, M., Amini Baghbadorani, M., Navid, S., Ebrahimpour, K., Khodabakhshi, D., & Ghahremani, F. (2020a). A Novel Bilayer Wound Dressing Composed of a Dense Polyurethane/Propolis Membrane and a Biodegradable Polycaprolactone/Gelatin Nanofibrous Scaffold. *Scientific Reports*, *10*(1), 1–15. https://doi.org/10.1038/s41598-020-59931-2

Eskandarinia, A., Kefayat, A., Agheb, M., Rafienia, M., Amini Baghbadorani, M., Navid, S., Ebrahimpour, K., Khodabakhshi, D., & Ghahremani, F. (2020b). A Novel Bilayer Wound Dressing Composed of a Dense Polyurethane/Propolis Membrane and a Biodegradable Polycaprolactone/Gelatin Nanofibrous Scaffold. *Scientific Reports*, *10*(1), 1–15. https://doi.org/10.1038/s41598-020-59931-2

Farahani, M., & Shafiee, A. (2021). *Wound Healing : From Passive to Smart Dressings*. *2100477*, 1–32. https://doi.org/10.1002/adhm.202100477

Figueira, D. R., Miguel, S. P., de Sá, K. D., & Correia, I. J. (2016). Production and characterization of polycaprolactone- hyaluronic acid/chitosan- zein electrospun bilayer nanofibrous membrane for tissue regeneration. *International Journal of Biological Macromolecules*, *93*, 1100–1110. https://doi.org/10.1016/j.ijbiomac.2016.09.080

Firouzabadi, P. Z., Ghanbari, H., Mohammad, S., Haramshahi, A., & Javadpour, J. (2020). *Synthesis of Nanobentonite – Poly (vinyl alcohol) – Bacterial Cellulose Nanocomposite by Electrospinning for Wound Healing Applications*. *1900536*, 1–10. https://doi.org/10.1002/pssa.201900536

Flanagan, M., Ed, C., & Lecturer, P. (2000). *The physiology of wound healing*. *9*(6), 11–12.

Forget, A., Arya, N., Randriantsile, R., Miessmer, F., Buck, M., Ahmadi, V., Jonas, D., Blencowe, A., & Shastri, V. P. (2016). *Nonwoven Carboxylated Agarose-Based*

Fiber Meshes with Antimicrobial Properties. https://doi.org/10.1021/acs.biomac.6b01401

Fuchs, S., Hartmann, J., Mazur, P., Reschke, V., Siemens, H., Wehlage, D., & Ehrmann, A. (2017). Electrospinning of Biopolymers and Biopolymer Blends. *Journal of Chemical and Pharmaceutical Sciences*, *2017*(Special 10), 1–3.

Ghosh, S., Kaushik, R., Nagalakshmi, K., Hoti, S. L., Menezes, G. A., Harish, B. N., & Vasan, H. N. (2010). Antimicrobial activity of highly stable silver nanoparticles embedded in agar – agar matrix as a thin film. *Carbohydrate Research*, *345*(15), 2220–2227. https://doi.org/10.1016/j.carres.2010.08.001

Gounani, Z., Pourianejad, S., Asadollahi, M. A., Meyer, R. L., Rosenholm, J. M., & Arpanaei, A. (2020). Polycaprolactone-gelatin nanofibers incorporated with dual antibiotic-loaded carboxyl-modified silica nanoparticles. *Journal of Materials Science*, *55*(36), 17134–17150. https://doi.org/10.1007/s10853-020-05253-7

Greer, N., Foman, N. A., MacDonald, R., Dorrian, J., Fitzgerald, P., Rutks, I., & Wilt, T. J. (2013). Advanced wound care therapies for nonhealing diabetic, venous, and arterial ulcers: a systematic review. *Annals of Internal Medicine*, *159*(8), 532–542. https://doi.org/10.7326/0003-4819-159-8-201310150-00006

Gruppuso, M., Turco, G., Marsich, E., & Porrelli, D. (2021). Polymeric wound dressings, an insight into polysaccharide-based electrospun membranes. *Applied Materials Today*, *24*, 101148. https://doi.org/10.1016/j.apmt.2021.101148

Guidance for industry: chronic cutaneous ulcer and burn wounds-developing products for treatment. (2001). *Wound Repair and Regeneration : Official Publication of the Wound Healing Society [and] the European Tissue Repair Society*, *9*(4), 258–268. https://doi.org/10.1046/J.1524-475X.2001.00258.X

Guzmán, M. G. M., Dille, J., & Godet, S. (2008). Synthesis of silver nanoparticles by chemical reduction method and their antibacterial activity. *International Sholarly and Scientific Reserach & Innovation*, *2*(7), 91–98. https://doi.org/10.1007/s11814-010-0067-0

Haider, A., Haider, S., & Kang, I. (2018). REVIEW A comprehensive review summarizing the effect of electrospinning parameters and potential applications of nanofibers in biomedical and biotechnology. *Arabian Journal of Chemistry*, *11*(8), 1165–1188. https://doi.org/10.1016/j.arabjc.2015.11.015

Hajipour, M. J. et al. (2012). Antibacterial properties of nanoparticles. *Trends in Biotechnology*, *30*(10), 499–511. https://doi.org/10.1016/j.tibtech.2012.06.004

Han, J., Salmieri, S., Le Tien, C., & Lacroix, M. (2010). Improvement of water barrier property of paperboard by coating application with biodegradable polymers. *Journal of Agricultural and Food Chemistry*, *58*(5), 3125–3131. https://doi.org/10.1021/jf904443n

Hasan, M. M., & Shahid, M. A. (2023). PVA, licorice, and collagen (PLC) based hybrid bio-nano scaffold for wound healing application. *Journal of Biomaterials Science, Polymer Edition*, *34*(9), 1217–1236. https://doi.org/10.1080/09205063.2022.2163454

Heyer, K., Augustin, M., Protz, K., Herberger, K., Spehr, C., & Rustenbach, S. J. (2013). *Effectiveness of Advanced versus Conventional Wound Dressings on Healing of Chronic Wounds : Systematic Review and Meta-Analysis*. https://doi.org/10.1159/000348331

Hua, S., Ma, H., Li, X., Yang, H., & Wang, A. (2010). pH-sensitive sodium alginate/poly(vinyl alcohol) hydrogel beads prepared by combined $Ca2+$ crosslinking and freeze-thawing cycles for controlled release of diclofenac sodium. *International Journal of Biological Macromolecules*, *46*(5), 517–523. https://doi.org/10.1016/j.ijbiomac.2010.03.004

Huang, C., Hu, R., & Yin, M. (2015). *Electrospun gelatin / polycaprolactone nanofibrous membranes combined with a coculture of bone marrow stromal cells and chondrocytes for cartilage engineering*. 2089–2099.

Huang, X., Jiang, W., Zhou, J., Yu, D. G., & Liu, H. (2022). The Applications of Ferulic-Acid-Loaded Fibrous Films for Fruit Preservation. *Polymers 2022, Vol. 14, Page 4947*, *14*(22), 4947. https://doi.org/10.3390/POLYM14224947

Huang, X., Sun, Y., Nie, J., Lu, W., Yang, L., Zhang, Z., Yin, H., Wang, Z., & Hu, Q. (2015). Using absorbable chitosan hemostatic sponges as a promising surgical dressing. *International Journal of Biological Macromolecules*, *75*, 322–329. https://doi.org/10.1016/j.ijbiomac.2015.01.049

Inagaki, M., Yang, Y., & Kang, F. (2012). Carbon nanofibers prepared via electrospinning. *Advanced Materials*, *24*(19), 2547–2566. https://doi.org/10.1002/adma.201104940

Islam, M. S., Ang, B. C., Andriyana, A., & Afifi, A. M. (2019a). A review on fabrication of nanofibers via electrospinning and their applications. *SN Applied Sciences*, *1*(10), 1–16. https://doi.org/10.1007/s42452-019-1288-4

Islam, M. S., Ang, B. C., Andriyana, A., & Afifi, A. M. (2019b). A review on fabrication of nanofibers via electrospinning and their applications. *SN Applied Sciences*, *1*(10), 1–16. https://doi.org/10.1007/s42452-019-1288-4

Jain, R., Shetty, S., & Yadav, K. S. (2020a). *Journal of Drug Delivery Science and Technology Unfolding the electrospinning potential of biopolymers for preparation of nano fi bers*. *57*(February).

Jain, R., Shetty, S., & Yadav, K. S. (2020b). Journal of Drug Delivery Science and Technology Unfolding the electrospinning potential of biopolymers for

preparation of nano fi bers. *Journal of Drug Delivery Science and Technology*, *57*(February), 101604. https://doi.org/10.1016/j.jddst.2020.101604

Jang, E. J., Patel, R., & Patel, M. (2023a). Electrospinning Nanofibers as a Dressing to Treat Diabetic Wounds. *Pharmaceutics*, *15*(4). https://doi.org/10.3390/pharmaceutics15041144

Jang, E. J., Patel, R., & Patel, M. (2023b). Electrospinning Nanofibers as a Dressing to Treat Diabetic Wounds. *Pharmaceutics*, *15*(4). https://doi.org/10.3390/pharmaceutics15041144

Jeong, L., & Park, W. H. (2014). Preparation and characterization of gelatin nanofibers containing silver nanoparticles. *International Journal of Molecular Sciences*, *15*(4), 6857–6879. https://doi.org/10.3390/ijms15046857

Ji, W., Yang, F., Van Den Beucken, J. J. J. P., Bian, Z., Fan, M., Chen, Z., & Jansen, J. A. (2010). Fibrous scaffolds loaded with protein prepared by blend or coaxial electrospinning. *Acta Biomaterialia*, *6*(11), 4199–4207. https://doi.org/10.1016/j.actbio.2010.05.025

K, A., M, B., A, S., & P, A. (2021). Nanofiber Based Dressing Material Mechanism in Wound Healing Property. *International Journal of Zoological Investigations*, *7*(2), 949–954. https://doi.org/10.33745/ijzi.2021.v07i02.086

Kanawung, K., Panitchanapan, K., Puangmalee, S. O., Utok, W., Kreua-Ongarjnukool, N., Rangkupan, R., Meechaisue, C., & Supaphol, P. (2007). Preparation and characterization of polycaprolactone/ diclofenac sodium and poly(vinyl alcohol)/tetracycline hydrochloride fiber mats and their release of the model drugs. *Polymer Journal*, *39*(4), 369–378. https://doi.org/10.1295/polymj.PJ2006011

Karuppuswamy, P., & Reddy, J. (2015). Polycaprolactone nano fi bers for the controlled release of tetracycline hydrochloride. *Materials Letters*, *141*, 180–186. https://doi.org/10.1016/j.matlet.2014.11.044

Kashani, M. Z., Bagher, Z., Asgari, H. R., Koruji, M., & Mehraein, F. (2020). Systems Biology in Reproductive Medicine Differentiation of neonate mouse spermatogonial stem cells on three-dimensional agar / polyvinyl alcohol nanofiber scaffold. *Systems Biology in Reproductive Medicine*, *66*(3), 202–215. https://doi.org/10.1080/19396368.2020.1725927

Khalf, A., & Madihally, S. V. (2017). Recent advances in multiaxial electrospinning for drug delivery. *European Journal of Pharmaceutics and Biopharmaceutics*, *112*, 1–17. https://doi.org/10.1016/j.ejpb.2016.11.010

Kheradvar, S. A., Nourmohammadi, J., Tabesh, H., & Bagheri, B. (2018). Starch nanoparticle as a vitamin E-TPGS carrier loaded in silk fibroin-poly(vinyl alcohol)-Aloe vera nanofibrous dressing. *Colloids and Surfaces B: Biointerfaces*, *166*, 9–16. https://doi.org/10.1016/j.colsurfb.2018.03.004

Kim, Y., Doh, S. J., Lee, G. D., Kim, C., & Im, J. N. (2019). Composite Nonwovens Based on Carboxymethyl Cellulose for Wound Dressing Materials. *Fibers and Polymers*, *20*(10), 2048–2056. https://doi.org/10.1007/s12221-019-9261-9

Kong, L., & Ziegler, G. R. (2013). Quantitative relationship between electrospinning parameters and starch fiber diameter. *Carbohydrate Polymers*, *92*(2), 1416–1422. https://doi.org/10.1016/j.carbpol.2012.09.026

Kora, A., Beedu, S., & Jayaraman, A. (2012). Size-controlled green synthesis of silver nanoparticles mediated by gum ghatti (Anogeissus latifolia) and its biological activity. *Organic and Medicinal Chemistry Letters*, *2*(1), 17. https://doi.org/10.1186/2191-2858-2-17

Kumar Sen, R., Prabhakar, P., Verma, P., Vikram, A., Mishra, A., Dwivedi, A., Sorna Gowri, V., Prasad Chaurasia, J., Pada Mondal, D., Kumar Srivastava, A., Dwivedi, N., & Dhand, C. (2024). Smart Nanofibrous Hydrogel Wound Dressings for Dynamic Infection Diagnosis and Control: Soft but Functionally Rigid. *Cite This: ACS Appl. Bio Mater*, *7*, 999–1016. https://doi.org/10.1021/acsabm.3c01000

Lackowski, M., Krupa, A., & Jaworek, A. (2013). Nanofabric nonwoven mat for fi ltration smoke and nanoparticles. *Polish Journal of Chemical Technology*, *15*(2), 48–52. https://doi.org/10.2478/pjct-2013-0023

Laha, A., Yadav, S., Majumdar, S., & Sharma, C. S. (2016). In-vitro release study of hydrophobic drug using electrospun cross-linked gelatin nanofibers. *Biochemical Engineering Journal*, *105*, 481–488. https://doi.org/10.1016/j.bej.2015.11.001

Lalia, B. S., Guillen, E., Arafat, H. A., & Hashaikeh, R. (2014). *Nanocrystalline cellulose reinforced PVDF-HFP membranes for membrane distillation application*. *332*, 134–141.

Lang, S., Chen, C., Xiang, J., Liu, Y., Li, K., Hu, Q., & Liu, G. (2021a). Facile and Robust Antibacterial Functionalization of Medical Cotton Gauze with Gallic Acids to Accelerate Wound Healing. *Industrial and Engineering Chemistry Research*, *60*(28), 10225–10234. https://doi.org/10.1021/acs.iecr.1c01833

Lang, S., Chen, C., Xiang, J., Liu, Y., Li, K., Hu, Q., & Liu, G. (2021b). Facile and Robust Antibacterial Functionalization of Medical Cotton Gauze with Gallic Acids to Accelerate Wound Healing. *Industrial and Engineering Chemistry Research*, *60*(28), 10225–10234. https://doi.org/10.1021/acs.iecr.1c01833

Li, J., Du, Q., Wan, J., Yu, D.-G., Tan, F., & Yang, X. (2024). *Improved synergistic anticancer action of quercetin and tamoxifen citrate supported by an electrospun complex nanostructure*. https://doi.org/10.1016/j.matdes.2024.112657

Li, L., Wang, Y., Liu, K., Yang, L., Zhang, B., Luo, Q., Luo, R., & Wang, Y. (2022). Nanoparticles-stacked superhydrophilic coating supported synergistic

antimicrobial ability for enhanced wound healing. *Materials Science and Engineering: C*, *132*, 112535. https://doi.org/10.1016/J.MSEC.2021.112535

Liang, Y., He, J., & Guo, B. (2021). Functional Hydrogels as Wound Dressing to Enhance Wound Healing. *ACS Nano*, *15*(8), 12687–12722. https://doi.org/10.1021/acsnano.1c04206

Liu, H., Wang, C., Li, C., Qin, Y., Wang, Z., Yang, F., Li, Z., & Wang, J. (2018). A functional chitosan-based hydrogel as a wound dressing and drug delivery system in the treatment of wound healing. *RSC Advances*, *8*(14), 7533–7549. https://doi.org/10.1039/c7ra13510f

Liu, J., Xue, Z., Zhang, W., Yan, M., & Xia, Y. (2018). Preparation and properties of wet-spun agar fibers. *Carbohydrate Polymers*, *181*(March 2017), 760–767. https://doi.org/10.1016/j.carbpol.2017.11.081

Liu, J., Zou, Q., Wang, C., Lin, M., Li, Y., Zhang, R., & Li, Y. (2021). Electrospinning and 3D printed hybrid bi-layer scaffold for guided bone regeneration. *Materials and Design*, *210*, 110047. https://doi.org/10.1016/j.matdes.2021.110047

Liu, X., Hagner, L., Natalie, S., Mørck, H., & Qu, H. (2018). *European Journal of Pharmaceutics and Biopharmaceutics Cipro fl oxacin-loaded sodium alginate / poly (lactic-co-glycolic acid) electrospun fi brous mats for wound healing*. *123*(November 2017), 42–49. https://doi.org/10.1016/j.ejpb.2017.11.004

Liu, X., Niu, Y., Chen, K. C., & Chen, S. (2017). Rapid hemostatic and mild polyurethane-urea foam wound dressing for promoting wound healing. *Materials Science and Engineering C*, *71*, 289–297. https://doi.org/10.1016/j.msec.2016.10.019

Locilento, D. A., Mercante, L. A., Andre, R. S., Mattoso, L. H. C., Luna, G. L. F., Brassolatti, P., Anibal, F. de F., & Correa, D. S. (2019). Biocompatible and biodegradable electrospun nanofibrous membranes loaded with grape seed extract for wound dressing application. *Journal of Nanomaterials*, *2019*, 1–12. https://doi.org/10.1155/2019/2472964

Lu, H. H., Zheng, K., Boccaccini, A. R., & Liverani, L. (2023). Electrospinning of cotton-like fibers based on cerium-doped sol–gel bioactive glass. *Materials Letters*, *334*, 133712. https://doi.org/10.1016/J.MATLET.2022.133712

Lu, P., Chen, W., Zhu, M., & Murray, S. (2017). Embedding Lauric Acid into Polystyrene Nanofibers To Make High-Capacity Membranes for Efficient Thermal Energy Storage. *ACS Sustainable Chemistry and Engineering*, *5*(8), 7249–7259. https://doi.org/10.1021/acssuschemeng.7b01476

Ma, K., Qiu, Y., Fu, Y., & Ni, Q. Q. (2018). Electrospun sandwich configuration nanofibers as transparent membranes for skin care drug delivery systems. *Journal*

of Materials Science, *53*(15), 10617–10626. https://doi.org/10.1007/s10853-018-2241-4

Madera-Santana, T. J., Freile-Pelegrín, Y., & Azamar-Barrios, J. A. (2014a). Physicochemical and morphological properties of plasticized poly(vinyl alcohol)-agar biodegradable films. *International Journal of Biological Macromolecules*, *69*(May), 176–184. https://doi.org/10.1016/j.ijbiomac.2014.05.044

Madera-Santana, T. J., Freile-Pelegrín, Y., & Azamar-Barrios, J. a. (2014b). Physicochemical and morphological properties of plasticized poly(vinyl alcohol)–agar biodegradable films. *International Journal of Biological Macromolecules*, *69*, 176–184. https://doi.org/10.1016/j.ijbiomac.2014.05.044

Maneerung, T., Tokura, S., & Rujiravanit, R. (2008). Impregnation of silver nanoparticles into bacterial cellulose for antimicrobial wound dressing. *Carbohydrate Polymers*, *72*(1), 43–51. https://doi.org/10.1016/j.carbpol.2007.07.025

Martínez-Sanz, M., Martínez-Abad, A., & López-Rubio, A. (2019). Cost-efficient bio-based food packaging films from unpurified agar-based extracts. *Food Packaging and Shelf Life*, *21*(July), 100367. https://doi.org/10.1016/j.fpsl.2019.100367

Mathematical models of drug release. (2015). *Strategies to Modify the Drug Release from Pharmaceutical Systems*, 63–86. https://doi.org/10.1016/B978-0-08-100092-2.00005-9

Memic, A., Abudula, T., Mohammed, H. S., Joshi Navare, K., Colombani, T., & Bencherif, S. A. (2019a). Latest Progress in Electrospun Nanofibers for Wound Healing Applications. *ACS Applied Bio Materials*, *2*(3), 952–969. https://doi.org/10.1021/acsabm.8b00637

Memic, A., Abudula, T., Mohammed, H. S., Joshi Navare, K., Colombani, T., & Bencherif, S. A. (2019b). Latest Progress in Electrospun Nanofibers for Wound Healing Applications. *ACS Applied Bio Materials*, *2*(3), 952–969. https://doi.org/10.1021/acsabm.8b00637

Meng, Z., Liu, Y., Xu, K., Sun, X., Yu, Q., Wu, Z., & Zhao, Z. (2021). *Biomimetic Polydopamine-Modi fi ed Silk Fibroin / Curcumin Nano fi brous Sca ff olds for Chemo-photothermal Therapy of Bone Tumor*. https://doi.org/10.1021/acsomega.1c02903

Menzies, K. L., & Jones, L. (2010). The impact of contact angle on the biocompatibility of biomaterials. *Optometry and Vision Science*, *87*(6), 387–399. https://doi.org/10.1097/OPX.0b013e3181da863e

Mitra, S., Mateti, T., Ramakrishna, S., & Laha, A. (2022). A Review on Curcumin-Loaded Electrospun Nanofibers and their Application in Modern Medicine. *Jom*, *74*(9), 3392–3407. https://doi.org/10.1007/s11837-022-05180-9

Mlcek, J., Jurikova, T., Skrovankova, S., & Sochor, J. (2016). Quercetin and its anti-allergic immune response. *Molecules*, *21*(5), 1–15. https://doi.org/10.3390/molecules21050623

Mohy Eldin, M. S., Soliman, E. A., Hashem, A. I., & Tamer, T. M. (2008). Chitosan modified membranes for wound dressing applications: Preparations, characterization and Bio-evaluation. *Trends in Biomaterials and Artificial Organs*, *22*(3), 158–168.

Montiel-Centeno, K., Barrera, D., García-Villén, F., Sánchez-Espejo, R., Borrego-Sánchez, A., Rodríguez-Castellón, E., Sandri, G., Viseras, C., & Sapag, K. (2022). Cephalexin loading and controlled release studies on mesoporous silica functionalized with amino groups. *Journal of Drug Delivery Science and Technology*, *72*(November 2021). https://doi.org/10.1016/j.jddst.2022.103348

Nazeer, M. A., Yilgor, E., & Yilgor, I. (2019). Electrospun polycaprolactone/silk fibroin nanofibrous bioactive scaffolds for tissue engineering applications. *Polymer*, *168*(January), 86–94. https://doi.org/10.1016/j.polymer.2019.02.023

Ninan, N., Forget, A., Shastri, V. P., Voelcker, N. H., & Blencowe, A. (2016). Antibacterial and Anti-Inflammatory pH-Responsive Tannic Acid-Carboxylated Agarose Composite Hydrogels for Wound Healing. *ACS Applied Materials and Interfaces*, *8*(42), 28511–28521. https://doi.org/10.1021/acsami.6b10491

Niu, H., Wang, H., Zhou, H., & Lin, T. (2014). Ultrafine PDMS fibers: Preparation from in situ curing-electrospinning and mechanical characterization. *RSC Advances*, *4*(23), 11782–11787. https://doi.org/10.1039/c4ra00232f

O'Dwyer, L. (2005). Wound assessment and management. *Veterinary Nursing Journal*, *20*(8), 15–18. https://doi.org/10.1080/17415349.2005.11013385

Ong, S. Y., Wu, J., Moochhala, S. M., Tan, M. H., & Lu, J. (2008). Development of a chitosan-based wound dressing with improved hemostatic and antimicrobial properties. *Biomaterials*, *29*(32), 4323–4332. https://doi.org/10.1016/j.biomaterials.2008.07.034

Ooi, K. S., Haszman, S., Wong, Y. N., Soidin, E., Hesham, N., Mior, M. A. A., Tabata, Y., Ahmad, I., Fauzi, M. B., & Yunus, M. H. M. (2020). Physicochemical characterization of bilayer hybrid nanocellulose-collagen as a potential wound dressing. *Materials*, *13*(19), 1–17. https://doi.org/10.3390/ma13194352

Paul, W., & Sharma, C. P. (2004a). *Chitosan and Alginate Wound Dressings : A Short Review*. *18*(1), 18–23.

Paul, W., & Sharma, C. P. (2004b). *Chitosan and Alginate Wound Dressings : A Short Review*. *18*(1), 18–23.

Piva, H., Imasato, H., Piva, R. H., Rocha, M. C., & Rodrigues-filho, U. P. (2018). *Acidic Dressing Based on Agarose / Cs 2 . 5 H 0 . 5 PW 12 O 40 Nanocomposite for Infection Control in Wound Care*. 0–9. https://doi.org/10.1021/acsami.8b09066

Prasad, T., Shabeena, E. A., Vinod, D., Kumary, T. V, & Kumar, P. R. A. (2015). *Characterization and in vitro evaluation of electrospun chitosan / polycaprolactone blend fibrous mat for skin tissue engineering*. https://doi.org/10.1007/s10856-014-5352-8

Priya, S., Batra, U., Samshritha, R. N., Sharma, S., Chaurasiya, A., & Singhvi, G. (2022). Polysaccharide-based nanofibers for pharmaceutical and biomedical applications: A review. *International Journal of Biological Macromolecules*, *218*(July), 209–224. https://doi.org/10.1016/j.ijbiomac.2022.07.118

Pryshchepa, O., Pomastowski, P., & Buszewski, B. (2020). Silver nanoparticles: Synthesis, investigation techniques, and properties. *Advances in Colloid and Interface Science*, *284*, 102246. https://doi.org/10.1016/J.CIS.2020.102246

Purwar, R., Sai Goutham, K., & Srivastava, C. M. (2016). Electrospun Sericin/PVA/Clay nanofibrous mats for antimicrobial air filtration mask. *Fibers and Polymers*, *17*(8), 1206–1216. https://doi.org/10.1007/s12221-016-6345-7

Quan, K., Li, G., Luan, D., Yuan, Q., Tao, L., & Wang, X. (2015). *Colloids and Surfaces B : Biointerfaces Black hemostatic sponge based on facile prepared cross-linked graphene. 132*, 27–33.

Rai, M., Yadav, A., & Gade, A. (2009). Silver nanoparticles as a new generation of antimicrobials. *Biotechnology Advances*, *27*(1), 76–83. https://doi.org/10.1016/j.biotechadv.2008.09.002

Raina, N., Pahwa, R., Khosla, J. K., Gupta, P. N., & Gupta, M. (2022). Polycaprolactone-based materials in wound healing applications. *Polymer Bulletin*, *79*(9), 7041–7063. https://doi.org/10.1007/s00289-021-03865-w

Ranjbar-Mohammadi, M., & Bahrami, S. H. (2016). Electrospun curcumin loaded poly(ε-caprolactone)/gum tragacanth nanofibers for biomedical application. *International Journal of Biological Macromolecules*, *84*, 448–456. https://doi.org/10.1016/j.ijbiomac.2015.12.024

Ranjbar-mohammadi, M., Rabbani, S., Bahrami, S. H., Joghataei, M. T., & Moayer, F. (2016). Antibacterial performance and in vivo diabetic wound healing of curcumin loaded gum tragacanth / poly (ε -caprolactone) electrospun nano fi bers. *Materials Science & Engineering C*, *69*, 1183–1191. https://doi.org/10.1016/j.msec.2016.08.032

Rasouli, R., Barhoum, A., Bechelany, M., & Dufresne, A. (2019). Nanofibers for Biomedical and Healthcare Applications. *Macromolecular Bioscience*, *19*(2), 1–27. https://doi.org/10.1002/mabi.201800256

Reesi, F., Minaiyan, M., & Taheri, A. (2018). A novel lignin-based nanofibrous dressing containing arginine for wound-healing applications. *Drug Delivery and Translational Research*, *8*(1), 111–122. https://doi.org/10.1007/s13346-017-0441-0

Republic, C. (n.d.). *A Comparative Study of Crosslinked Sodium Alginate / Gelatin Hydrogels for Wound Dressing*. 384–389.

Rhein-knudsen, N., Ale, M. T., & Meyer, A. S. (2015). *Seaweed Hydrocolloid Production: An Update on Enzyme Assisted Extraction and Modification Technologies*. 3340–3359. https://doi.org/10.3390/md13063340

Rhim, J. W., & Kanmani, P. (2015). Synthesis and characterization of biopolymer agar mediated gold nanoparticles. *Materials Letters*, *141*(February), 114–117. https://doi.org/10.1016/j.matlet.2014.11.069

Rhim, J. W., Wang, L. F., & Hong, S. I. (2013). Food Hydrocolloids Preparation and characterization of agar / silver nanoparticles composite fi lms with antimicrobial activity. *Food Hydrocolloids*, *33*(2), 327–335. https://doi.org/10.1016/j.foodhyd.2013.04.002

Roy, N., Saha, N., Kitano, T., & Saha, P. (2010a). Development and characterization of novel medicated hydrogels for wound dressing. *Soft Materials*, *8*(2), 130–148. https://doi.org/10.1080/15394451003756282

Roy, N., Saha, N., Kitano, T., & Saha, P. (2010b). Development and characterization of novel medicated hydrogels for wound dressing. *Soft Materials*, *8*(2), 130–148. https://doi.org/10.1080/15394451003756282

Roy, S., & Rhim, J. (2019). Food Hydrocolloids Agar-based antioxidant composite fi lms incorporated with melanin nanoparticles. *Food Hydrocolloids*, *94*(March), 391–398. https://doi.org/10.1016/j.foodhyd.2019.03.038

Sadrearhami, Z., Morshed, M., & Varshosaz, J. (2015). Production and evaluation of polyblend of agar and polyacrylonitrile nanofibers for in vitro release of methotrexate in cancer therapy. *Fibers and Polymers*, *16*(2), 254–262. https://doi.org/10.1007/s12221-015-0254-z

Safdari, F., Gholipour, M. D., Ghadami, A., Saeed, M., & Zandi, M. (2022). Multi-antibacterial agent-based electrospun polycaprolactone for active wound dressing. *Progress in Biomaterials*, *11*(1), 27–41. https://doi.org/10.1007/s40204-021-00176-1

Salami, M. A., Kaveian, F., Rafienia, M., Saber-Samandari, S., Khandan, A., & Naeimi, M. (2017). Electrospun Polycaprolactone/lignin-based Nanocomposite as a Novel Tissue Scaffold for Biomedical Applications. *Journal of Medical Signals and Sensors*, *7*(4), 228–238. https://doi.org/10.4103/jmss.JMSS_11_17

Sanandiya, N. D., Lee, S., Rho, S., Lee, H., Kim, I. S., & Hwang, D. S. (2019). Tunichrome-inspired pyrogallol functionalized chitosan for tissue adhesion and hemostasis. *Carbohydrate Polymers*, *208*(September 2018), 77–85. https://doi.org/10.1016/j.carbpol.2018.12.017

Sankarganesh, P., Parthasarathy, V., Kumar, A. G., Saraniya, M., Udayakumari, N., & Ragu, S. (2022). Development of novel mannitol blended PVA hydrogel membrane and its anticancer and antimicrobial drug delivery potential for wound dressing applications. *Journal of Sol-Gel Science and Technology*, 447–456. https://doi.org/10.1007/s10971-022-05765-5

Sathiyaseelan, A., Saravanakumar, K., & Wang, M. H. (2022). Bimetallic silver-platinum (AgPt) nanoparticles and chitosan fabricated cotton gauze for enhanced antimicrobial and wound healing applications. *International Journal of Biological Macromolecules*, *220*, 1556–1569. https://doi.org/10.1016/J.IJBIOMAC.2022.09.045

Sawada, I., Fachrul, R., Ito, T., Ohmukai, Y., Maruyama, T., & Matsuyama, H. (2012). Development of a hydrophilic polymer membrane containing silver nanoparticles with both organic antifouling and antibacterial properties. *Journal of Membrane Science*, *387–388*(1), 1–6. https://doi.org/10.1016/j.memsci.2011.06.020

Schiffman, J. D., & Schauer, C. L. (2008). *A Review : Electrospinning of Biopolymer Nanofibers and their Applications A Review : Electrospinning of Biopolymer Nanofibers and their Applications*. *3724*(May). https://doi.org/10.1080/15583720802022182

Sharma, S., Khan, I. A., Ali, I., Ali, F., Kumar, M., Kumar, A., Johri, R. K., Abdullah, S. T., Bani, S., Pandey, A., Suri, K. A., Gupta, B. D., Satti, N. K., Dutt, P., & Qazi, G. N. (2009). Evaluation of the antimicrobial, antioxidant, and anti-inflammatory activities of hydroxychavicol for its potential use as an oral care agent. *Antimicrobial Agents and Chemotherapy*, *53*(1), 216–222. https://doi.org/10.1128/AAC.00045-08

Shie Karizmeh, M., Poursamar, S. A., Kefayat, A., Farahbakhsh, Z., & Rafienia, M. (2022). An in vitro and in vivo study of PCL/chitosan electrospun mat on polyurethane/propolis foam as a bilayer wound dressing. *Biomaterials Advances*, *135*(July 2021). https://doi.org/10.1016/j.msec.2022.112667

Shlapakova, L. E., Botvin, V. V., Mukhortova, Y. R., Zharkova, I. I., Alipkina, S. I., Zeltzer, A., Dudun, A. A., Makhina, T., Bonartseva, G. A., Voinova, V. V., Wagner, D. V., Pariy, I., Bonartsev, A. P., Surmenev, R. A., & Surmeneva, M. A. (2023). Magnetoactive Composite Conduits Based on Poly(3-hydroxybutyrate) and Magnetite Nanoparticles for Repair of Peripheral Nerve Injury. *ACS Applied Bio Materials*, *7*, 1095–1114. https://doi.org/10.1021/ACSABM.3C01032

Shojaee Kang Sofla, M., Mortazavi, S., & Seyfi, J. (2020). Preparation and characterization of polyvinyl alcohol/chitosan blends plasticized and compatibilized by glycerol/polyethylene glycol. *Carbohydrate Polymers*, *232*(December 2019). https://doi.org/10.1016/j.carbpol.2019.115784

Show, S., Ghosal, C., & Chattopadhyay, B. (2017). *Root Extracts (Gymnadenia orchidis Lindl) Facilitated Rapid Synthesis of Fluorescent Silver Nanoparticles (Ag-NPs) for Various Biological Applications*. 109–124. https://doi.org/10.4236/jbnb.2017.81008

Show, S., Ghosal, C., Chattopadhyay, B., Francis, S., Joseph, S., Koshy, E. P., Mathew, B., Azizi, S., Mohamad, R., Abdul, R., Mohammadinejad, R., Bin, A., Rhim, J. W., Wang, L. F., Hong, S. I., Datta, K. K. R., Srinivasan, B., Balaram, H., Eswaramoorthy, M., … Saha, B. (2012). In situ silver nanoparticles synthesis in agarose film supported on filter paper and its application as highly efficient SERS test stripes. *Forensic Science International*, *237*, e42–e46. https://doi.org/10.1016/j.forsciint.2014.01.019

Shukla, M. K., Singh, R. P., Reddy, C. R. K., & Jha, B. (2012). Bioresource Technology Synthesis and characterization of agar-based silver nanoparticles and nanocomposite film with antibacterial applications. *Bioresource Technology*, *107*, 295–300. https://doi.org/10.1016/j.biortech.2011.11.092

Singh, B., Kim, J., Shukla, N., Lee, J., Kim, K., & Park, M. H. (2023). Smart Delivery Platform Using Core-Shell Nanofibers for Sequential Drug Release in Wound Healing. *ACS Applied Bio Materials*, *6*(6), 2314–2324. https://doi.org/10.1021/ACSABM.3C00178/ASSET/IMAGES/LARGE/MT3C00178_0012.JPEG

Singh, M., Singh, S., Prasad, S., & Gambhir, I. S. (2008). Nanotechnology in Medicine and Antibacterial Effect of. *Digest Journal of Nanomaterials and Biostructure*, *3*(3), 115–122.

Song, Z., Wang, J., Tan, S., Gao, J., & Wang, L. (2023). Conductive biomimetic bilayer fibrous scaffold for skin regeneration. *Colloids and Surfaces A: Physicochemical and Engineering Aspects*, *656*(PA), 130211. https://doi.org/10.1016/j.colsurfa.2022.130211

Sonker, A. K., Rathore, K., Teotia, A. K., Kumar, A., & Verma, V. (2019). Rapid synthesis of high strength cellulose–poly(Vinyl alcohol) (PVA) biocompatible composite films via microwave crosslinking. *Journal of Applied Polymer Science*, *136*(17). https://doi.org/10.1002/app.47393

Sonker, A. K., Teotia, A. K., Kumar, A., Nagarale, R. K., & Verma, V. (2017). Development of Polyvinyl Alcohol Based High Strength Biocompatible Composite Films. *Macromolecular Chemistry and Physics*, *201700130*, 1–13. https://doi.org/10.1002/macp.201700130

Soscia, D. A., Raof, N. A., Xie, Y., Cady, N. C., & Gadre, A. P. (2010). Antibiotic-loaded PLGA nanofibers for wound healing applications. *Advanced Engineering Materials*, *12*(4), 83–88. https://doi.org/10.1002/adem.200980016

Sousa, A. M. M., Souza, H. K. S., Uknalis, J., Liu, S., & Gonc, M. P. (2015a). *Electrospinning of agar / PVA aqueous solutions and its relation with rheological properties*. *115*, 348–355. https://doi.org/10.1016/j.carbpol.2014.08.074

Sousa, A. M. M., Souza, H. K. S., Uknalis, J., Liu, S., & Gonc, M. P. (2015b). *International Journal of Biological Macromolecules Improving agar electrospinnability with choline-based deep eutectic solvents*. *80*, 139–148. https://doi.org/10.1016/j.ijbiomac.2015.06.034

Stashak, T. S., Acvs, D., Farstvedt, E., & Othic, A. (2004). *Update on Wound Dressings : Indications and Best Use*. *1*, 148–163. https://doi.org/10.1053/j.ctep.2004.08.006

Stojko, M., Włodarczyk, J., Sobota, M., Karpeta-Jarząbek, P., Pastusiak, M., Janeczek, H., Dobrzyński, P., Starczynowska, G., Orchel, A., Stojko, J., Batoryna, O., Olczyk, P., Komosińska-Vassev, K., Olczyk, K., & Kasperczyk, J. (2020). Biodegradable Electrospun Nonwovens Releasing Propolis as a Promising Dressing Material for Burn Wound Treatment. *Pharmaceutics 2020, Vol. 12, Page 883*, *12*(9), 883. https://doi.org/10.3390/PHARMACEUTICS12090883

Stone, S. A., Gosavi, P., Athauda, T. J., & Ozer, R. R. (2013). In situ citric acid crosslinking of alginate/polyvinyl alcohol electrospun nanofibers. *Materials Letters*, *112*, 32–35. https://doi.org/10.1016/j.matlet.2013.08.100

Suarez-Arnedo, A., Figueroa, F. T., Clavijo, C., Arbeláez, P., Cruz, J. C., & Muñoz-Camargo, C. (2020). An image J plugin for the high throughput image analysis of in vitro scratch wound healing assays. *PLoS ONE*, *15*(7 July), 1–14. https://doi.org/10.1371/journal.pone.0232565

Sultanova, Z., Kaleli, G., Kabay, G., & Mutlu, M. (2016). Controlled release of a hydrophilic drug from coaxially electrospun polycaprolactone nanofibers. *International Journal of Pharmaceutics*, *505*(1–2), 133–138. https://doi.org/10.1016/j.ijpharm.2016.03.032

Syed, M. H., Khan, M. M. R., Zahari, M. A. K. M., Beg, M. D. H., & Abdullah, N. (2023). Current issues and potential solutions for the electrospinning of major polysaccharides and proteins: A review. *International Journal of Biological Macromolecules*, *253*(P2), 126735. https://doi.org/10.1016/j.ijbiomac.2023.126735

Taemeh, M. A., Shiravandi, A., Korayem, M. A., & Daemi, H. (2020). Fabrication challenges and trends in biomedical applications of alginate electrospun nanofibers. *Carbohydrate Polymers*, *228*(October 2019), 115419. https://doi.org/10.1016/j.carbpol.2019.115419

Takayama, Y., & Aoki, R. (2012). *Roles of lactoferrin on skin wound healing 1. 503*(2011), 497–503. https://doi.org/10.1139/O11-054

Tankhiwale, R., & Bajpai, S. K. (2009). Graft copolymerization onto cellulose-based filter paper and its further development as silver nanoparticles loaded antibacterial food-packaging material. *Colloids and Surfaces B: Biointerfaces*, *69*(2), 164–168. https://doi.org/10.1016/j.colsurfb.2008.11.004

Taylor, P. (2013). *International Journal of Polymeric Materials and Porous Three-Dimensional PVA / Gelatin Sponge for Skin Tissue Engineering Porous Three-Dimensional PVA / Gelatin Sponge for Skin Tissue Engineering. July*, 37–41. https://doi.org/10.1080/00914037.2012.710862

Teng, S., Wang, P., & Kim, H. (2009). *Blend fi bers of chitosan – agarose by electrospinning. 63*, 2510–2512. https://doi.org/10.1016/j.matlet.2009.08.051

Thet, N. T., Alves, D. R., Bean, J. E., Booth, S., Nzakizwanayo, J., Young, A. E. R., Jones, B. V., & Jenkins, A. T. A. (2016). Prototype Development of the Intelligent Hydrogel Wound Dressing and Its Efficacy in the Detection of Model Pathogenic Wound Biofilms. *ACS Applied Materials and Interfaces*, *8*(24), 14909–14919. https://doi.org/10.1021/acsami.5b07372

Thu, H. E., Zulfakar, M. H., & Ng, S. F. (2012). Alginate based bilayer hydrocolloid films as potential slow-release modern wound dressing. *International Journal of Pharmaceutics*, *434*(1–2), 375–383. https://doi.org/10.1016/j.ijpharm.2012.05.044

Thu, H., Zulfakar, M. H., & Ng, S. (2012). *Alginate based bilayer hydrocolloid films as potential slow-release modern wound dressing. 434*, 375–383.

Tkachenko, O., & Karas, J. A. (2012). Standardizing an in vitro procedure for the evaluation of the antimicrobial activity of wound dressings and the assessment of three wound dressings. *Journal of Antimicrobial Chemotherapy*, *67*(7), 1697–1700. https://doi.org/10.1093/jac/dks110

Trinca, R. B., Westin, C. B., da Silva, J. A. F., & Moraes, Â. M. (2017). Electrospun multilayer chitosan scaffolds as potential wound dressings for skin lesions. *European Polymer Journal*, *88*, 161–170. https://doi.org/10.1016/j.eurpolymj.2017.01.021

Tripathi, S., Singh, B. N., Divakar, S., Kumar, G., Mallick, S. P., & Srivastava, P. (2021). Design and evaluation of ciprofloxacin loaded collagen chitosan oxygenating scaffold for skin tissue engineering. *Biomedical Materials (Bristol)*, *16*(2). https://doi.org/10.1088/1748-605X/abd1b8

Tronci, G. (2019). 13 - The application of collagen in advanced wound dressings. In *Advanced Textiles for Wound Care* (Second Edi). Elsevier Ltd. https://doi.org/10.1016/B978-0-08-102192-7.00013-8

Tyeb, S., Verma, V., & Kumar, N. (2023). Polysaccharide based transdermal patches for chronic wound healing: Recent advances and clinical perspective. *Carbohydrate Polymers*, *316*(May), 121038. https://doi.org/10.1016/j.carbpol.2023.121038

Unal, S., Arslan, S., Karademir Yilmaz, B., Kazan, D., Oktar, F. N., & Gunduz, O. (2020). Glioblastoma cell adhesion properties through bacterial cellulose nanocrystals in polycaprolactone/gelatin electrospun nanofibers. *Carbohydrate Polymers*, *233*(December 2019), 115820. https://doi.org/10.1016/j.carbpol.2019.115820

Unnithan, A. R., Barakat, N. A. M., Tirupathi Pichiah, P. B., Gnanasekaran, G., Nirmala, R., Cha, Y. S., Jung, C. H., El-Newehy, M., & Kim, H. Y. (2012). Wound-dressing materials with antibacterial activity from electrospun polyurethane-dextran nanofiber mats containing ciprofloxacin HCl. *Carbohydrate Polymers*, *90*(4), 1786–1793. https://doi.org/10.1016/j.carbpol.2012.07.071

Uzun, M., Anand, S. C., & Shah, T. (2013). *In Vitro* Characterisation and Evaluation of Different Types of Wound Dressing Materials. *Journal of Biomedical Engineering and Technology*, *1*(1), 1–7. https://doi.org/10.12691/jbet-1-1-1

Vaghani, S. S., Patel, M. M., & Satish, C. S. (2012). Synthesis and characterization of pH-sensitive hydrogel composed of carboxymethyl chitosan for colon targeted delivery of ornidazole. *Carbohydrate Research*, *347*(1), 76–82. https://doi.org/10.1016/j.carres.2011.04.048

Van Der Schueren, L., Steyaert, I., De Schoenmaker, B., & De Clerck, K. (2012). Polycaprolactone/chitosan blend nanofibres electrospun from an acetic acid/formic acid solvent system. *Carbohydrate Polymers*, *88*(4), 1221–1226. https://doi.org/10.1016/j.carbpol.2012.01.085

Varshney, N., Singh, P., Rai, R., Vishwakarma, N. K., & Mahto, S. K. (2023). Superporous soy protein isolate matrices as superabsorbent dressings for successful management of highly exuding wounds: In vitro and in vivo characterization. *International Journal of Biological Macromolecules*, *253*. https://doi.org/10.1016/J.IJBIOMAC.2023.127268

Vig, K., Chaudhari, A., Tripathi, S., Dixit, S., Sahu, R., Pillai, S., Dennis, V. A., & Singh, S. R. (2017). Advances in skin regeneration using tissue engineering. *International Journal of Molecular Sciences*, *18*(4). https://doi.org/10.3390/ijms18040789

Vittoria, V., Tammaro, L., & Russo, G. (2009). Encapsulation of diclofenac molecules into poly(-Caprolactone) electrospun fibers for delivery protection. *Journal of Nanomaterials*, *2009*. https://doi.org/10.1155/2009/238206

Vivcharenko, V., Benko, A., Palka, K., Wojcik, M., & Przekora, A. (2020). International Journal of Biological Macromolecules Elastic and biodegradable chitosan / agarose fi lm revealing slightly acidic pH for potential applications in regenerative

medicine as arti fi cial skin graft. *International Journal of Biological Macromolecules*, *164*, 172–183. https://doi.org/10.1016/j.ijbiomac.2020.07.099

Vivcharenko, V., Wojcik, M., & Przekora, A. (2020). Cellular Response to Vitamin C-Enriched Chitosan/Agarose Film with Potential Application as Artificial Skin Substitute for Chronic Wound Treatment. *Cells*, *9*(5). https://doi.org/10.3390/CELLS9051185

Wang, H., Qiao, X., Chen, J., & Ding, S. (2005). Preparation of silver nanoparticles by chemical reduction method. *Colloids and Surfaces A: Physicochemical and Engineering Aspects*, *256*(2–3), 111–115. https://doi.org/10.1016/j.colsurfa.2004.12.058

Wang, J., & Windbergs, M. (2019). Controlled dual drug release by coaxial electrospun fibers – Impact of the core fluid on drug encapsulation and release. *International Journal of Pharmaceutics*, *556*(December 2018), 363–371. https://doi.org/10.1016/j.ijpharm.2018.12.026

Wang, L., & Rhim, J. (2015a). International Journal of Biological Macromolecules Preparation and application of agar / alginate / collagen ternary blend functional food packaging films. *International Journal of Biological Macromolecules*, *80*, 460–468. https://doi.org/10.1016/j.ijbiomac.2015.07.007

Wang, L., & Rhim, J. (2015b). *International Journal of Biological Macromolecules Preparation and application of agar / alginate / collagen ternary blend functional food packaging films*. *80*, 460–468.

Wang, M., Hou, J., Yu, D. G., Li, S., Zhu, J., & Chen, Z. (2020). Electrospun tri-layer nanodepots for sustained release of acyclovir. *Journal of Alloys and Compounds*, *846*, 156471. https://doi.org/10.1016/J.JALLCOM.2020.156471

Wang, M., Li, D., Li, J., Li, S., Chen, Z., Yu, D., Liu, Z., & Zhanhu, J. (2020a). Electrospun Janus zein – PVP nano fi bers provide a two-stage controlled release of poorly water-soluble drugs. *Materials & Design*, *196*, 109075. https://doi.org/10.1016/j.matdes.2020.109075

Wang, M., Li, D., Li, J., Li, S., Chen, Z., Yu, D., Liu, Z., & Zhanhu, J. (2020b). Electrospun Janus zein – PVP nano fi bers provide a two-stage controlled release of poorly water-soluble drugs. *Materials & Design*, *196*, 109075. https://doi.org/10.1016/j.matdes.2020.109075

Wang, Y. ;, Liu, L. ;, Zhu, Y. ;, Wang, L. ;, Yu, D.-G. ;, Liu, L.-Y., Craig, D., Wang, Y., Liu, L., Zhu, Y., Wang, L., Yu, D.-G., & Liu, L.-Y. (2023). *Citation: Tri-Layer Core-Shell Fibers from Coaxial Electrospinning for a Modified Release of Metronidazole*. https://doi.org/10.3390/pharmaceutics15112561

Wang, Y. ;, Yu, D.-G. ;, Liu, Y. ;, Liu, Y.-N., Wang, Y., Yu, D.-G., Liu, Y., & Liu, Y.-N. (2022). Progress of Electrospun Nanofibrous Carriers for Modifications to Drug

Release Profiles. *Journal of Functional Biomaterials 2022, Vol. 13, Page 289*, *13*(4), 289. https://doi.org/10.3390/JFB13040289

Ward, M. A., & Georgiou, T. K. (2011). Thermoresponsive polymers for biomedical applications. *Polymers*, *3*(3), 1215–1242. https://doi.org/10.3390/polym3031215

Wehlage, D., Böttjer, R., Grothe, T., & Ehrmann, A. (2018). Electrospinning water-soluble/insoluble polymer blends. *AIMS Materials Science*, *5*(2), 190–200. https://doi.org/10.3934/matersci.2018.2.190

Weller, C. D., Team, V., & Sussman, G. (2020). *First-Line Interactive Wound Dressing Update : A Comprehensive Review of the Evidence*. *11*(February), 1–13. https://doi.org/10.3389/fphar.2020.00155

Wojcik, M., Kazimierczak, P., Benko, A., Palka, K., Vivcharenko, V., & Przekora, A. (2021). Superabsorbent curdlan-based foam dressings with typical hydrocolloids properties for highly exuding wound management. *Materials Science and Engineering C*, *124*(February), 112068. https://doi.org/10.1016/j.msec.2021.112068

Wu, C., Zhao, J., Hu, F., Zheng, Y., Yang, H., Pan, S., Shi, S., Chen, X., & Wang, S. (2018). Design of injectable agar-based composite hydrogel for multi-mode tumor therapy. *Carbohydrate Polymers*, *180*(October 2017), 112–121. https://doi.org/10.1016/j.carbpol.2017.10.024

Xue, J., Wu, T., Dai, Y., & Xia, Y. (2019). Electrospinning and electrospun nanofibers: Methods, materials, and applications. *Chemical Reviews*, *119*(8), 5298–5415. https://doi.org/10.1021/acs.chemrev.8b00593

Yadav, B. K., Solanki, N., & Patel, G. (2024). Electrospun nanofibers as advanced wound dressing materials: comparative analysis of single-layered and multilayered nanofibers containing polycaprolactone, methylcellulose, and polyvinyl alcohol. *Journal of Biomaterials Science, Polymer Edition*. https://doi.org/10.1080/09205063.2024.2311448

Yang, H., Gao, P. F., Wu, W. B., Yang, X. X., Zeng, Q. L., Li, C., & Huang, C. Z. (2014a). Antibacterials loaded electrospun composite nanofibers: Release profile and sustained antibacterial efficacy. *Polymer Chemistry*, *5*(6), 1965–1975. https://doi.org/10.1039/c3py01335a

Yang, H., Gao, P. F., Wu, W. B., Yang, X. X., Zeng, Q. L., Li, C., & Huang, C. Z. (2014b). Antibacterials loaded electrospun composite nanofibers: release profile and sustained antibacterial efficacy. *Polymer Chemistry*, *5*(6), 1965–1975. https://doi.org/10.1039/C3PY01335A

Yang, T., Yang, H., Zhen, S. J., & Huang, C. Z. (2015). Hydrogen-bond-mediated in situ fabrication of AgNPs/Agar/PAN electrospun nanofibers as reproducible SERS

substrates. *ACS Applied Materials and Interfaces*, *7*(3), 1586–1594. https://doi.org/10.1021/am507010q

Ying, R., Huang, W. C., & Mao, X. (2022). Synthesis of Agarose-Based Multistimuli-Responsive Hydrogel Dressing for Accelerated Wound Healing. *ACS Biomaterials Science and Engineering*, *8*(1), 293–302. https://doi.org/10.1021/acsbiomaterials.1c01215

Young, S., Wong, M., Tabata, Y., & Mikos, A. G. (2005). Gelatin as a delivery vehicle for the controlled release of bioactive molecules. *Journal of Controlled Release*, *109*(1–3), 256–274. https://doi.org/10.1016/j.jconrel.2005.09.023

Yu, D. G., & Huang, C. (2023). Electrospun Biomolecule-Based Drug Delivery Systems. *Biomolecules 2023, Vol. 13, Page 1152*, *13*(7), 1152. https://doi.org/10.3390/BIOM13071152

Yu, D.-G., & Zhou, J. (2024). Electrospun multi-chamber nanostructures for sustainable biobased chemical nanofibers. *Next Materials*, *2*, 100119. https://doi.org/10.1016/J.NXMATE.2024.100119

Yun, E. J., Kim, H. T., Cho, K. M., Yu, S., Kim, S., Choi, I. G., & Kim, K. H. (2016). Pretreatment and saccharification of red macroalgae to produce fermentable sugars. *Bioresource Technology*, *199*, 311–318. https://doi.org/10.1016/j.biortech.2015.08.001

Yusof, N. L. B. M., Wee, A., Lim, L. Y., & Khor, E. (2003). Flexible chitin films as potential wound-dressing materials: wound model studies. *Journal of Biomedical Materials Research. Part A*, *66*(2), 224–232. https://doi.org/10.1002/jbm.a.10545

Zarrintaj, P., Manouchehri, S., Ahmadi, Z., & Saeb, M. R. (2018). Agarose-based biomaterials for tissue engineering. *Carbohydrate Polymers*, *187*(October 2017), 66–84. https://doi.org/10.1016/j.carbpol.2018.01.060

Zarrintaj, P., Manouchehri, S., Ahmadi, Z., Saeb, M. R., Urbanska, A. M., Kaplan, D. L., & Mozafari, M. (2018a). Agarose-based biomaterials for tissue engineering. *Carbohydrate Polymers*, *187*(October 2017), 66–84. https://doi.org/10.1016/j.carbpol.2018.01.060

Zarrintaj, P., Manouchehri, S., Ahmadi, Z., Saeb, M. R., Urbanska, A. M., Kaplan, D. L., & Mozafari, M. (2018b). Agarose-based biomaterials for tissue engineering. *Carbohydrate Polymers*, *187*(December 2017), 66–84. https://doi.org/10.1016/j.carbpol.2018.01.060

Zeng, Q., Han, Y., Li, H., & Chang, J. (2015). Design of a thermosensitive bioglass/agarose-alginate composite hydrogel for chronic wound healing. *Journal of Materials Chemistry B*, *3*(45), 8856–8864. https://doi.org/10.1039/c5tb01758k

Zhang, L., Wang, Z., Xiao, Y., Liu, P., Wang, S., Zhao, Y., Shen, M., & Shi, X. (2018). Electrospun PEGylated PLGA nanofibers for drug encapsulation and release.

Materials Science and Engineering C, *91*(March), 255–262. https://doi.org/10.1016/j.msec.2018.05.045

Zhang, T., Xu, H., Zhang, Y., Zhang, S., Yang, X., Wei, Y., Huang, D., & Lian, X. (2022). Fabrication and characterization of double-layer asymmetric dressing through electrostatic spinning and 3D printing for skin wound repair. *Materials & Design*, *218*, 110711. https://doi.org/10.1016/J.MATDES.2022.110711

Zhang, W., Chen, L., Chen, J., Wang, L., Gui, X., Ran, J., Xu, G., Zhao, H., Zeng, M., Ji, J., Qian, L., Zhou, J., Ouyang, H., & Zou, X. (2017). Silk Fibroin Biomaterial Shows Safe and Effective Wound Healing in Animal Models and a Randomized Controlled Clinical Trial. *Advanced Healthcare Materials*, *6*(10), 1–16. https://doi.org/10.1002/adhm.201700121

Zhang, Y., Yu, J., Zhang, H., Li, Y., & Wang, L. (2022). Nanofibrous dressing: Potential alternative for fighting against antibiotic-resistance wound infections. *Journal of Applied Polymer Science*, *139*(20), 1–19. https://doi.org/10.1002/app.52178

Zhou, J., Yi, T., Zhang, Z., Yu, D.-G., Liu, P., Wang, L., & Zhu, Y. (2023). Electrospun Janus core (ethyl cellulose//polyethylene oxide) @ shell (hydroxypropyl methyl cellulose acetate succinate) hybrids for an enhanced colon-targeted prolonged drug absorbance. *Advanced Composites and Hybrid Materials 2023 6:6*, *6*(6), 1–16. https://doi.org/10.1007/S42114-023-00766-6

Zhu, J., Luo, J., Zhao, X., Gao, J., & Xiong, J. (2016). Electrospun homogeneous silk fibroin/poly (ϵ-caprolactone) nanofibrous scaffolds by addition of acetic acid for tissue engineering. *Journal of Biomaterials Applications*, *31*(3), 421–437. https://doi.org/10.1177/0885328216659775

Ziloochi Kashani, M., Bagher, Z., Asgari, H. R., Najafi, M., Koruji, M., & Mehraein, F. (2020). Differentiation of neonate mouse spermatogonial stem cells on three-dimensional agar/polyvinyl alcohol nanofiber scaffold. *Systems Biology in Reproductive Medicine*, *66*(3), 202–215. https://doi.org/10.1080/19396368.2020.1725927

LIST OF PUBLICATIONS

- **Kalpana Rathore**, Inderjeet Singh, Kantesh Balani, Sandeep Sharma, & Vivek Verma. *Fabrication and characterization of multi-layered coaxial polysaccharide-based electrospun nanocomposite mat, novel replacement for transdermal patches.* International Journal of Biological Macromolecules (IF-7.7), July 2024 (DOI: 10.1016/j.ijbiomac.2024.133712)

- **Kalpana Rathore**, Saravanan Matheshwaran, Sandeep Sharma, & Vivek Verma. *Bilayer agar-based wound dressing infused with enhanced antioxidant and antibacterial properties.* (Accepted, ACS Applied Bio Materials)

- Palwinder Kaur, Suraj Pal Verma, Sandeep Sharma, **Kalpana Rathore**, Vivek Verma, Manish Vyas. *Evaluation of Optimized flexi-liposomal dental gel on oral biofilms: A novel approach to prevent dental caries.* (Manuscript submitted)

LIST OF CONFERENCES

- Delivered an oral talk in the ***International Conference on Recent Trends in Biomedical Sciences* (RTBS-2023)** in association with **Science and Engineering Research Board (SERB)**, held in Phagwara, India from 6th Oct to 7Th Oct, 2023.

- Delivered an oral talk in the ***International Conference on Polymers for Advanced Technology* (APA 2023)**, held in Goa, India from 23rd to 25th of February, 2023.

- Presented an oral talk in the ***International Conference on Biomaterials, Regenerative Medicine and Devices* (BIO-Remedi-2022)**, held at IIT Guwahati, India from 14th to 18th of December, 2022.

- Delivered oral presentation at the ***International Conference on Emerging Trends in Bioscience and Chemical Technology* (ETBCT-2022)**, held in Katra, Jammu and Kashmir, India from 3rd to 5th of December, 2022.

International Conference on Recent Trends in Biomedical Sciences
(RTBS-2023)

Certificate of Achievement

This is to certify that Prof./Dr./Mr./Ms. *Kalpana Rathore* of *IIT Kanpur and Lovely Professional University* has presented Oral/Poster entitled *Polysaccharide based Electrospun Nanofibrous Mat for promising wound dressing applications* In International Conference on Recent Trends in Biomedical Sciences (RTBS-2023) organized by Department of Medical Laboratory Sciences from 6th-7th October 2023 at Lovely Professional University, Punjab, India.

Prof (Dr.) Sandeep Sharma
Covenor/Organizing Secretary
RTBS2023

Prof (Dr.) Monica Gulati
Chairperson
RTBS-2023

International Conference on Emerging Trends in Biosciences and Chemical Technology-2022

December 3-5, 2022
Organised by
School of Biotechnology, Shri Mata Vaishno Devi University, Katra

Certificate of Participation

This is to certify that Prof./Dr./Mr./Ms. *Kalpana Rathore*

has presented Poster / Oral Presentation entitled *Fabrication and Characterization of Electrospun Agar-based nanocomposites Mat for Wound Dressing Application.* at International Conference on Emerging Trends in Biosciences and Chemical Technology (ETBCT-2022) held at Shri Mata Vaishno Devi University, Katra, J&K in collaboration with CSIR-IIM Jammu and BRSI, India.

Dr. Indu Bhushan
Convener
ETBCT-2022

Dr. Asha Chaubey
Convener
ETBCT-2022

Prof. Ashok Pandey
Conference Chair
ETBCT-2022

Dr. Ratna Chandra
Organizing Secretary
ETBCT-2022

International Conference on
Polymers for Advanced Technology
February 23-25, 2023 | Goa, India

Certificate of Participation

This is to certify that

KALPANA RATHORE

Participated as a delegate & presented an Oral Talk

Titled

Agar-based bilayer structure with antioxidant electrospun layer on antibacterial film as a potential wound dressing

ID: 513

Bhuvanesh Gupta
APA President

APA 2023 Goa

Supported by

रसायन एवं पेट्रो-रसायन विभाग
DEPARTMENT OF
CHEMICALS & PETRO-CHEMICALS

Organised by

Asian Polymer Association
A.P.A.

BIO-Remedi 2022
Translation for Healthcare

stermi

International Conference on
BIOMATERIALS, REGENERATIVE MEDICINE AND DEVICES
Dec' 14th-18th 2022 | IIT Guwahati, India

Certificate of Participation

This is to certify that

Ms. KALPANA RATHORE

Participated in the conference and presented an Oral talk.

Co-Convener

Convener

Fabrication and characterization of multi-layered coaxial agar-based electrospun biocomposite mat, novel replacement for transdermal patches

Kalpana Rathore [a,b], Indrajeet Singh [a], Kantesh Balani [a], Sandeep Sharma [b,**], Vivek Verma [a,c,d,e,*]

[a] Department of Materials Science and Engineering, Indian Institute of Technology Kanpur, India
[b] Department of Medical Laboratory Sciences, Lovely Professional University, Phagwara, Punjab, India
[c] Centre for Environmental Science & Engineering, Indian Institute of Technology Kanpur, India
[d] Samtel Centre for Display Technologies, Indian Institute of Technology Kanpur, India
[e] National Centre for Flexible Electronics, Indian Institute of Technology Kanpur, India

ARTICLE INFO

ABSTRACT

In the performed study, a novel fabrication of agar-based nanofibers was electrospun in an asymmetric bilayer dressing for biomedical transdermal patches. The optimal parameters for the fabrication of agar-based nanofibers after optimization were a feed rate of 10 μL/min, a 7 cm collector-to-nozzle distance, a 15 kV applied voltage, and a 700-rpm rotating collector speed. Coaxial nanofibers, as a second asymmetric layer, were produced using polyvinyl alcohol (PVA) with cephalexin hydrate, an antibacterial drug, as the core and agar-PCL as the sheath. The morphology of the developed uniaxial and coaxial nanofibrous layers was analysed using a scanning electron microscope and transmission electron microscopy, respectively. For the formation of bilayer asymmetric structures, the agar-PCL uniaxial layer was fabricated over the layer of coaxial PVA and agar-PCL layers for sustained drug release. The agar-based nanofibrous mats exhibited tensile strength of 7 MPa with 40 % elongation failure, 8-fold increased swelling, enhanced wettability (60° contact angle), and a moisture transmission rate of 2174 g/m^2/day. The developed coaxial bilayer mats exhibited antimicrobial activity, hemocompatibility, and cytocompatibility. Overall, this novel agar nanofibrous dressing offers promising potential for advanced biomedical applications, particularly as transdermal patches for efficient drug delivery systems.

1. Introduction

Nanomaterials, such as nanofibers and nanoparticles, exhibit extraordinary efficacy, bioavailability, and versatile capabilities due to their high surface area-to-volume ratio and dimensions of <1000 nm. Owing to their properties, nanomaterials have broad spectrum uses in multiple fields, including biological, pharmaceutical, and textile sectors. Particularly, nanofibers have demonstrated a successful approach for drug delivery, wound healing, and tissue engineering [1].

For drug delivery and wound healing applications, the use of nanofibers enhanced the loading and encapsulation efficiency of bioactive agents, site-specific delivery, controlled drug release, reduced drug side effects [2] and effective absorption of exudates [3]. Although fibre dimensions, drug loading concentration, and polymer properties [3], all affect the release rate from the nanofibers. Most of the time, the initial burst drug release from the uniaxial nanofibers is a major issue that limits its applications. However, this can be modulated with different fabrication methods, including co-axial fibres [4] that would control the release rate of the bioactive agents by reducing burst release and promoting sustained release [5] from the matrix. Additionally, the compatibility of the polymer matrix plays a critical role in initial burst release and low drug loading efficiency in the drug delivery system [6]. Therefore, we can develop new strategies to effectively release and deliver drugs during the wound healing process. Addressing this gap has the potential to significantly enhance the efficacy and efficiency of wound-healing treatments.

For wound healing applications, different polymers have been used for the fabrication of nanofibers, including natural, synthetic, composite, and carbon-based matrix, such as polyvinyl alcohol (PVA), polyacrylamide (PAN) [7] and more, using various processes like

electrospinning, drawing, self-assembly, blow spinning, and jet spinning [1]. Nevertheless, owing to the increasing preference for eco-friendly fabrication methods for nanofibers, natural polymers have predominantly emerged as the sought-after choice. But in natural polymers as well, certain limitations are associated with polymers. For instance, seaweed-based polysaccharides such as alginate have high swelling capabilities yet form free-flowing gels, plant-based polysaccharides like cellulose and guar gum are integral to the food chain; and animal-origin polymers such as gelatin and collagen encounter cultural resistance. Agar, a seaweed-based biopolymer, has shown its potential in wound healing applications with its high swelling properties and low cell adhesion [8–10] without forming free-flowing gels after swelling, which addresses the major concerns of exudate absorption and stickiness, respectively.

Despite agar's high potential in wound healing applications, its properties remain underutilized in the form of nanofibers. Even at lower concentrations, forming agar nanofibers through electrospinning proved challenging, primarily due to its inherent gelling and film-forming capabilities, rendering it a non-spinnable polymer. Moreover, additional studies are necessary to progress in this area due to the limited research available on the fabrication of agar nanofibers. Only a few researchers have examined its spinnability using copolymers such as polyvinyl alcohol (PVA) [11], polyacrylonitrile (PAN) [12], and polyethylene oxide (PEO) [13]. Although the agar concentration used for the electrospinning process was comparatively lower, between 30 % and 10 %, the concentration of the co-polymers, which was >90 %, predominantly resulted in nanofibers primarily composed of the copolymer rather than the agar. Furthermore, utilizing deep eutectic solvents and adding a co-polymer to the matrix polymer can result in the electrospinning of polysaccharides [14]. Different co-polymers, like polycaprolactone (PCL), have been used to assist in the electrospinning of several biopolymers [6,15–17]. The FDA-approved PCL, a hydrophobic polymer, is used in biomedical applications due to its cost-effectiveness, biocompatibility, and outstanding mechanical properties. Unfortunately, its hydrophobicity and lack of functional moieties severely restrict its applications [18].

Introducing PCL into an agar matrix could increase both polymer's potential and utility for biomedical applications. Agar has higher swelling ratios as compared to polycaprolactone. As a result, the blend not only modifies the wettability of agar, but also provides synergistic mechanical characteristics with PCL. Additionally, the presence of hydrophilic and hydrophobic polymers in the same matrix allows for the integration of diverse pharmacological substances, such as hydrophilic and hydrophobic drugs, nanoparticles, and bioactive agents, which improves the bioactivity of the dressing. Blending of polymers with different water affinities results in phase separation, as in the case of agar and PCL, which may hinder the electrospinning process. To overcome such issues, the use of binary solvents was employed. Previously, researchers reported fabrication of agar nanofibers using a variety of solvents, spinnable co-polymers, and other additives [19–21].

In the present work, we initiated a novel approach in this field by electrospinning agar-based nanofibers mixed with polycaprolactone copolymer. We enhanced the miscibility of the two polymers by employing binary solvents, specifically acetic acid and formic acid, aiming to enhance their compatibility. Furthermore, we conducted a thorough assessment of the impact of electrospinning parameters on fibre morphology, specifically voltage, nozzle-to-collector distance, and flow rate. Scanning electron microscopy was used to characterize fibre shape, and surface wettability was assessed using a goniometer. In addition, the material's mechanical, chemical, and permeation characteristics were also analysed. Additionally, we developed uniaxial and coaxial nanofibrous mats that facilitated sustained drug release by combining single and bilayer structures into an asymmetric bilayer dressing. The in vitro antibacterial and biocompatible properties of the developed dressing was evaluated by measuring its zone of inhibition, haemolysis percentage, and cytocompatibility. The sustained release of

the incorporated drug from the developed asymmetric bilayer dressing demonstrated its potential as transdermal patches.

2. Material and methods

Agar, dulbecco's modified eagle medium (DMEM), fetal bovine serum (origin-Brazil) (FBS), penicillin-streptomycin-neomycin solution, and trypsin EDTA solution were procured from Himedia Laboratories Pvt. Ltd., India. Polycaprolactone (PCL), bovine albumin, cephalexin hydrate, and piperine were procured from Sigma Aldrich Pvt. Ltd., India. Potassium bromide (KBr) was purchased from Sisco Research Laboratories (SRL) Pvt. Ltd., India. Formic acid (85 %), dimethyl sulfoxide (DMSO), polyvinyl alcohol (PVA) molecular weight of approx. 1,15,000 with a degree of hydrolysis of 98–99 %, and acetic acid were bought from Loba Chemie Pvt. Ltd., India. Phosphate buffered saline (PBS) formulation constituents including sodium chloride, sodium hydrogen phosphate, potassium chloride, potassium dihydrogen phosphate, sodium hydroxide, hydrochloric acid, calcium chloride dihydrate, and thiazolyl blue tetrazolium bromide (98 %) were procured from Thermo Fisher Scientific India Pvt. Ltd., India.

2.1. Fabrication of agar and PCL solution

Electrospinning was employed to produce nanofibers from the obtained solution. Furthermore, polycaprolactone (PCL) was added to agar in varying proportions to prepare agar-PCL nanofibers. The method consists of solution preparation by dissolving both the polymers, i.e., agar and PCL, in formic acid and acetic acid, respectively. Overnight, on a magnetic stirrer, agar solution was prepared by mixing 20 % agar (w/v) in formic acid at room temperature and was stored at 4 °C for later use to slow down the acid degradation. Similarly, PCL solution was prepared by combining PCL pellets in acetic acid (20 % w/w) and stirred for overnight at 60 °C. A magnetic stirrer was used to mix both the polymer solutions of agar and PCL until a uniform, lump-free solution could be obtained. The solution was kept at room temperature until needed.

2.2. Fabrication of electrospun nanofibers

The concentration of PCL remained constant, while the concentration of agar was altered to yield different proportions. Agar solution was blended with the PCL solution at various concentrations, including 4, 5, 6, and 7 parts per 5 parts of PCL. Briefly, equal volumes of PCL solution were poured into five flasks, and varying portions of the agar solution were added. For example, (3:5) denoted 3 parts agar and 5 parts PCL, while 4:5 represented 4 parts agar and 5 parts PCL. Agar and PCL in the ratios of 4:5, 5:5, 6:5, and 7:5 were taken. Accordingly, agar and PCL solutions were mixed for 30 min at room temperature before electrospinning.

A 2 mL syringe containing the prepared agar:PCL solution was loaded into the programmed injection pump for electrospinning. The distance between the tip of the needle and the collecting drum varied between 5 cm, 7 cm, and 10 cm. Furthermore, the applied potential varied between 10, 15, and 20 kV. Moreover, the flow rate was changed between 10 μL/min and 15 μL/min. The rotational drum speed was also varied between 200 rpm, 500 rpm, 700 rpm, and 1100 rpm. The electrospinning process was performed at 30 °C ambient temperature and ~ 37 % relative humidity (RH). The developed electrospun mats were subjected to vacuum oven drying at 45 °C for 48 h to thoroughly remove any residual solvents. Subsequently, they were stored in a vacuum desiccator for later use.

2.3. Fabrication of co-axial single and bilayer films incorporated with drug

Polyvinyl solution (8 %, 10 %, and 12 %) was prepared in distilled water by heating at 120 °C overnight on a hot plate magnetic stirrer.

PVA solution was electrospun at 15 kV with a flow rate of 10 μL/min, maintaining a distance of 10 cm between the nozzle tip and the collector drum (500 rpm). For co-axial agar:PCL electrospun films, 10 % PVA was used in the core for the incorporation of the drug cephalexin hydrate (CEX) at 20 mg/mL. Moreover, to maintain the efficacy of the drug, the PVA solution incorporated with the drug was stored at 4 °C in the dark. The outer layer of coaxial was formed with the help of an agar:PCL solution. The flow rate was maintained at 10 μL/min using a 2 mL syringe with an internal diameter of 9.12 mm. 15 kV potential was applied with a 7 cm distance between the nozzle and collector sheet. The rotational speed of the drum was maintained at 500 rpm. Films made from co-axial agar:PCL with PVA core were considered single-layer films. Bilayer films, on the other hand, had an additional agar:PCL electrospun layer over the single layer films. The additional layer of fibres in agar:PCL was expected to reduce the release rate of the bioactive agents from the coaxial layer by acting as a barrier layer. The schematic of the fabricated uniaxial and coaxial bilayer film is shown in Fig. 1.

3. Characterization

3.1. Microstructural analysis

For the morphological analysis, samples were mounted on the aluminium stub with the help of double-sided carbon tape. The samples were coated with gold sputter for 180 s using the EMITECH SC 7620 sputter coater. Using FESEM microscopy (FEI NOVA NANO SEM 450 FESEM) with a 10 kV voltage and a 5 mm working distance, micrographs of gold sputter-coated materials were captured. The resulting SEM micrographs were then analysed with ImageJ software to determine the average diameter of about 100 fibres per sample based on the obtained SEM micrographs. The micrographs were taken at 30000 × magnification.

To demonstrate the co-axial structural integrity, transmission electron microscopy was used to examine nanostructural features. We have incorporated silver nitrate (2 mg/mL) into the PVA core to image coaxial morphology. The uniaxial and coaxial fibres were dissected to <1 mm in length and dispersed in methanol. For effective dispersion, the fibres in methanol were sonicated for 20 min at room temperature. A 2 μL droplet

was cast on a carbon-coated grid (PELCO GRIDS 200 CU), followed by vacuum drying. Following the imaging of silver nanoparticles, incorporated samples were performed using an electron transmission microscope (FEI-Tecnai G2 12 Twin 120 KV).

3.2. Chemical characterization

Fourier transform infrared spectroscopy (FTIR) model Perkin Elmer spectrum version 10.03.06 in the range of 400–4000 cm^{-1}, was used to analyze the functional groups on the samples. For analysis, the samples were ground with KBr at a ratio of 1:10, followed by 24 h of conditioning at 45 °C to remove any traces of moisture. The acquired spectrograms were examined for any peak shift, peak absence, or peak formation.

3.3. Mechanical properties analysis

Universal Testing Machine (UTM) INSTRON 3345 was used to study the tensile properties of the prepared samples according to the ASTM D882–12 standard. Using a gauze length of 40 mm for the experiment, samples were cut to 70 mm × 10 mm, leaving 15 mm on both edges as gripping areas. The materials were stressed using a 5 kN load cell with a 10 mm/min crosshead speed. Prior to testing, samples were conditioned for 24 h at 50 % RH and 25 °C. The tensile strength and elongation at break were determined by testing five strips from each sample and then calculating the mean value.

3.4. Wettability

Using a Data Physics goniometer (Model OCA EC15), the contact angle was determined by dropping a 5 μL droplet of deionized (DI) water on the surface of the nanofiber dressing surface, which would be in direct contact with the wound. The angle between the surface and the water droplet was measured, and the average of three drops was used for analysis.
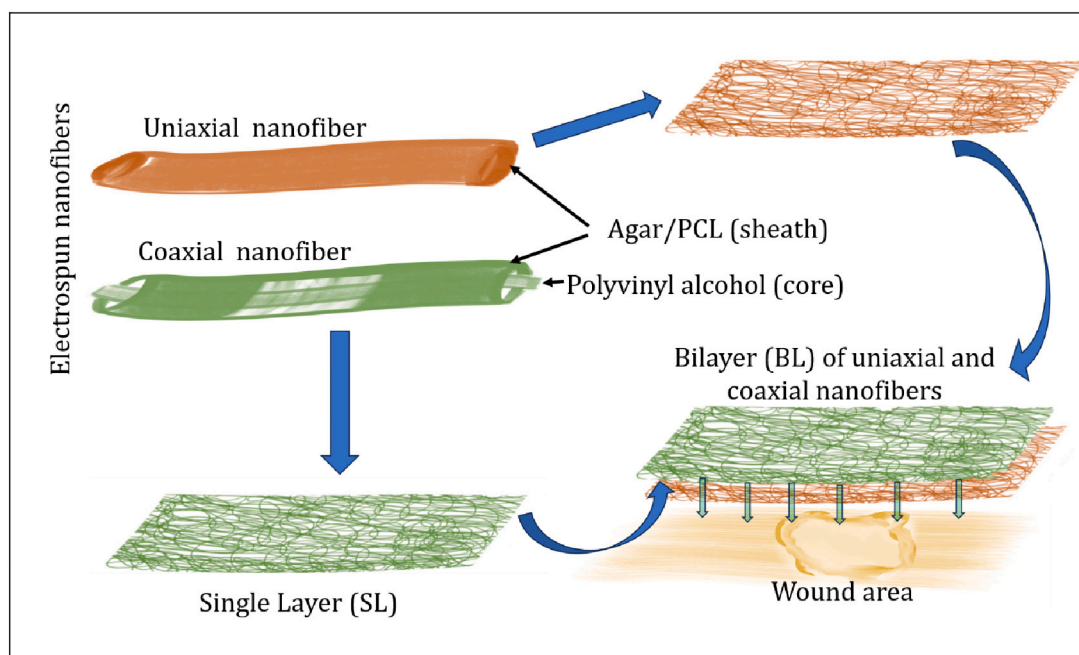

Fig. 1. Schematic diagram for the development of single and bilayer dressing from uniaxial agar:PCL nanofibers and coaxial nanofibers where agar:PCL as sheath polymer and PVA as core.

3.5. Fluid handling properties

3.5.1. Swelling properties

To assess the swelling percentage of the samples, 1 cm × 1 cm squares were cut from the electrospun sample and conditioned at 45 °C in a hot air oven until a consistent weight was achieved. The samples were immersed in DI water for the specified time intervals, followed by the weighing of swollen samples after removing excess surface water with low-linting (Kimwipes®) tissues. The swelling percentage was calculated by using

$$Swelling\ percentage = \frac{Final\ wet\ weight - initial\ dry\ weight}{Initial\ dry\ weight} \times 100$$

After a defined time interval, samples were again dehydrated for 24 h at 45 °C in a hot air oven, followed by measuring the weight of the dehydrated samples to evaluate the degree of dissolution.

3.5.2. Dissolution study

Apart from DI water, the dissolution was performed in various fluids, including phosphate saline (PBS), hydrogen peroxide (H_2O_2), collagenase, and lysozyme enzyme solutions. For the study, samples were cut to dimensions of 1 cm × 1 cm. The samples were soaked in the appropriate solution for a predetermined amount of time. After which, the samples were washed with deionized water, wiped with tissue, and dehydrated at 45 °C in a hot air oven until a steady weight was obtained. The weight loss of the samples after washing represented the degree of weight loss (in percent). Dissolution (%) was calculated using

$$Dissolution\ percentage = \frac{initial\ dry\ weight - Final\ dry\ weight}{Initial\ dry\ weight} \times 100$$

where initial dry weight was the weight before dissolution and final dry weight was the final dried weight of the samples after dissolution.

3.5.3. Absorbency

The fluid handling properties were evaluated based on previously published literature [22,23]. The SMTL test standard BS EN 13726–1:2002, Section 3.2, free swell absorptive capacity, was applied to determine the absorption capacity of electrospun dressing mats. The test was conducted in a solution prepared with sodium chloride (2.298 g/L) and calcium chloride dihydrate (0.368 g/L) dissolved in deionized water. The samples were hydrated with 40 times their own weight for 30 min at 37 °C. The wet weight of the samples was calculated after they were held in forceps for 30 s to drain off any excess solution on the surface of the sample. To calculate the absorption capacity of the samples, the mean of the triplicate samples was determined. Absorbency refers to the capacity of fluid uptake followed by retention, which differs from swelling, wherein the material absorbs fluid and subsequently increases in dimensions. Unlike absorbency, the evaluation of swelling properties involves wiping the surface moisture of the samples to remove excess water.

$$Absorbency = \frac{wet\ weight\ (g) - dry\ weight(g)}{dry\ weight\ (g)}$$

3.5.4. Rate of absorption

The rate of water droplet absorption on the surface of the sample was determined by placing 20 μL of test solution onto the surface. The dispersion time of the fluid was recorded using a digital stopwatch, and the average absorption time of 10 droplets was recorded in seconds (s).

3.5.5. Dehydration

With the use of dehydration measurements, the rate of moisture loss from samples was calculated. The samples were submerged for 30 min in an excess volume of sodium chloride and calcium chloride solution. After suspending samples with forceps to extract excess solution, their moisture content was determined. The samples were subsequently placed in an open petri dish and dehydrated at 37 °C for a specified period. The dehydration rate (g/min) was calculated using

$$Dehydration = \frac{wet\ weight\ (g) - dry\ weight(g)}{time\ duration\ (min)}$$

where wet weight (in g) was the weight of the mats after immersion in the fluid solution, and dried weight (in g) was the weight of the dehydrated sample after the specified time interval (in min).

3.5.6. Water vapor transmission rate

A modified version of the ASTM E96 standard technique was used to calculate the water vapor transmission rate of the developed electrospun membranes [24]. For the water vapor transmission tests, 15 mL of culture bottles were filled with 10 mL of DI water. To place the sample discs on the mouths of the glass containers, 18 mm diameter discs were cut from the samples. Parafilm was utilized to secure the electrospun membrane discs to the openings of the glass bottles, preventing any moisture loss. After mounting the samples, each bottle was carefully weighed every 24 h for seven days at a relative humidity difference between the inner and outer spaces of the bottle of 60 % RH at 30 °C. The WVTR of the permeation area (m²) of the electrospun membranes was determined from the slopes of the linear curves depicting the weight loss (g) with time (24 h) using

$$WVTR = \frac{\Delta weight}{\Delta Time \times Area}$$

3.6. Biocompatibility analysis

3.6.1. Haemolysis

The haemolysis assay was performed according to the literature [25] to assess the hemocompatibility of the developed electrospun mat using RBC suspension. Briefly, fresh goat blood was collected from a butcher and chelated with 0.5 mM EDTA as an anticoagulant. The collected blood was centrifuged at 700 *g* for 10 min. The supernatant was discarded, and the pellet was resuspended in the PBS buffer and was again washed three times with cold PBS (pH 7.4). The RBC pellet was diluted 10 times in cold PBS to obtain erythrocytes or RBC suspension and was used within 24 h of preparation. For the in-vitro haemolysis assay, samples were cut into 8 mm discs and rinsed with cold PBS to prevent erythrocytes from osmotic shock. The PBS-saturated samples were incubated in the prepared RBC suspension for 90 min at 37 °C. After incubation, the samples were centrifuged at 700 *g* for 10 min, and the supernatant was collected. At 540 nm, the absorbance of the collected supernatant was measured using a microplate reader (Medispec BioTek cytation 5 imaging reader). As a positive control, 0.1 % Triton-X was added to a suspension of erythrocytes to induce complete hemolysis, while RBC suspension was used as a negative control. The average result of triplicate samples was recorded, and the haemolysis % was calculated by

$$Haemolysis\% = \frac{Abs\ of\ sample}{Abs\ of\ positive\ control} \times 100$$

where Abs means recorded absorbance at 540 nm.

3.6.2. In-vitro assay

An in vitro cytocompatibility assay was performed using NIH 3 T3 fibroblast cells, which were cultured in Dulbecco's DMEM (also known as complete DMEM) containing 10 % fetal bovine serum (FBS) and 1 % antibiotics (penicillin and streptomycin). Incomplete DMEM was deprived of serum and antibiotics. The cells were incubated at 37 °C with 5 % CO_2 until they reached 70 % confluence, followed by trypsinizing them for a subsequent passage with the addition of trypsin. Meanwhile, the electrospun samples were cut into 1 cm diameter discs using a biopsy cutter, and each side was UV-sterilized for 2 h. The

sterilized samples were pre-washed three times with PBS (pH 7.4), followed by saturating the samples in a complete DMEM medium and testing.

3.6.3. Cytocompatibility -MTT assay

The cell viability was determined using direct and indirect contact assays. For direct assay, cells were cultured in the presence of samples, whereas cell culture insert plates were used for indirect assay, facing the top layer of agar:PCL towards cells. The 3-(4,5 dimethylthiazol-2-yl)-2,5-diphenyl tetrazolium bromide (MTT) assay was conducted to evaluate the cell proliferation and cytocompatibility of the samples. A fresh MTT solution was prepared in an incomplete DMEM medium and kept at 37 °C until use. On the conditioned samples, 70 % confluent fibroblast cells were trypsinized before being seeded at a density of 3×10^4 cells per well. After 2 h of incubation, the samples were incubated for 24 h at 37 °C in a CO_2 incubator with the addition of complete medium. To determine the cell viability, the medium was replaced with 500 μL (0.5 mg/mL) MTT solution for an additional 4 h of incubation. The developed formazan crystals were dissolved by adding 400 μL of DMSO (100 %), followed by 15 min of stirring. At 570 nm, the absorbance of the dissolved formazan crystals was measured using a microplate reader (Medispec BioTek Cytation 5 imaging reader). The wells seeded without any sample in the culture plate served as a positive control for the cytocompatibility assay, and the viability (%) of the cells was determined by calculating the number of viable cells using

$$cell\ viability\% = \frac{sample\ absorbance}{Positive\ control\ absorbance} \times 100$$

3.6.4. Cell adhesion assay

Trypsinized cells were seeded at a density of 3×10^4 cells per well onto conditioned DMEM samples in a 24-well plate. After incubating the samples for 4 h, 400 μL of complete DMEM medium was added to each well. After a specified incubation period, samples were fixed overnight at 4 °C with a 2.5 % glutaraldehyde solution. The fixed cells on the samples were dehydrated using a gradient alcohol treatment for 10 min each in 50 % ethanol, 70 % ethanol, 90 % ethanol, and finally 100 % ethanol. For the morphological studies, the dehydrated samples were freeze-dried and stored at room temperature until SEM examination.

3.6.5. In vitro drug release study

The release study used cephalexin hydrate (CEX) as a model drug to analyze the role of the uniaxial and co-axial electrospun nanofibrous layers. To determine the total concentration of the drug, a 1 cm diameter disc was dispensed in 3 mL of pH 7.4 PBS. To ascertain the amount of the drug released, the solution was heated to 100 °C for 15 min before being cooled to room temperature. The total amount of cephalexin hydrate drug released in the PBS was determined using an Evolution 201 (Thermo Fisher) UV-VIS spectrophotometer at 260 nm. As a control, readings were recorded to quantify PVA, PCL, and agar in PBS to rule out any absorbance owing to the respective polymers. Even though agar exhibited absorbance at 260 nm, drug-free control samples were developed to negate the absorbance of the antibiotic CEX in composite agar at 260 nm. For the release study, circular samples with a diameter of 1 cm were taken from electrospun films. These samples were then mounted on the openings of glass containers filled with 3 mL of PBS buffer (pH 7.4). To ensure that the buffer remained secure (leak-proof), the samples were carefully sealed using parafilm. The mounted samples were inverted for the specified time interval to permit the release of the drug from the desired surface of the mounted samples. The experiments were conducted at 37 °C to simulate the release of antibiotics in wound exudates. The mounted surface in contact with the PBS for drug release was regarded as the permeation area, and precautions were taken to mount the samples to prevent drug leakage from an unintended sample surface during the test. After a pre-defined time interval, the released drug from the affixed surface of the electrospun films was quantified by

measuring the absorbance of the buffer at 260 nm. The released amount of drug was evaluated using a calibration curve at 260 nm. The average value of release% was determined from quadruplicate samples.

$$Release\% = \frac{Released\ amount\ of\ drug}{Total\ amount\ of\ loaded\ drug} \times 100$$

3.6.6. Antibacterial testing

Cephalexin hydrate was evaluated against gram negative (*E. coli, P. vulgaris, and P. aeruginosa*) and gram-positive (*S. aureus*) bacteria to determine its minimum inhibition concentration (MIC) and minimum bactericidal concentration (MBC). The microorganisms were cultured in Muller-Hinton (MH) broth, which was prepared by dissolving 21 g of MH powder in DI water, followed by autoclaving for 15 min at 121 °C. Like the MH broth, 1.5 % agar was added to prepare Muller-Hinton agar (MHA) plates. Following autoclaving, the entire MHA plate preparation procedure was carried out under laminar airflow. To prepare the plates, the autoclaved MHA was cooled slightly. In a laminar hood, 20 mL of the MHA solution was then poured into sterile 90 mm polystyrene plates, and the plates were allowed to cool at room temperature until completely solidified. The prepared MHA plates and MHB were sealed with parafilm and stored at 4 °C for further use. The MIC was calculated using the broth microdilution method according to previous literature [26,27] on a 96-well plate. The MIC of cephalexin hydrate was calculated in a 96-well plate using the broth microdilution procedure. The MIC was quantified against the mentioned bacteria after a half-fold serial dilution starting at 2.5 mg. The wells showing no turbidity were considered to have a minimum inhibitory concentration. For MBC, the lowest concentration of drug with bactericidal activity was determined by subculturing bacterial cultures on MHA plates from MIC 96- wells and incubating them at 37 °C for 24 h. Kanamycin and MHB, without a sample, served as positive and negative controls in the experiment.

MHA plates were inoculated with the mentioned bacteria using an L-shaped spreader. For zone of inhibition (ZOI), a 6 mm diameter sample disc was placed aseptically on the cultured MHA plates. The test samples were incubated at 37 °C for 24 h in an incubator shaker to determine the ZOI diameter for each sample.

4. Results and discussion

4.1. Optimization of agar-based electrospun nanofibers

The current study focused on the fabrication of agar-based nanofibers using a methodology that involved dissolving agar in an acidic solution and subsequently integrating polymeric additives. During the initial phase, the concentrations of both polymers were systematically altered. Subsequently, a tandem methodology was utilized to ascertain the most favourable electrospinning parameters. After establishing the polymer ratio at 5:5, subsequent electrospinning parameters were selected using a tandem approach. All other electrospinning parameters, including applied potential, flow rate, distance between the nozzle tip and collector, and collector rotation speed, were studied.

4.1.1. Effect of solvent

Agar, a polysaccharide derived from seaweed, is mostly composed of alternating D-galactose and 3,6, −anhydropyranose saccharide units [28]. When dissolved in water, agar forms a gel even at extremely low concentrations. Hence, a solvent was necessary to prevent agar from gelling at ambient temperature.

Nanofibers can be generated with the inclusion of another polymer, which can be synthetic or natural. Polycaprolactone (PCL) was chosen as the electrospinnable polymer for the suggested application because of its biodegradability, bioresorbability, and cost-effectiveness. Thus, the hypothesis of the study was to develop a fibrous structure from agar polymer, wherein the addition of spinnable polymer would aid in the production of an electrospun fibrous mat. Moreover, the blending of

polycaprolactone with the agar solution achieved electro-spinnability, biocompatibility, bio-absorbability, and biodegradability. The hydrophobic nature of PCL and the hydrophilic nature of agar made their blending challenging due to the inevitable phase separation, as reported [29]. Considering the miscibility of solvents that can be combined without causing phase separation in polymers, acetic acid and formic acid were chosen as green binary solvents. After dissolving PCL and agar in acetic acid and formic acid, respectively, both polymer solutions were blended for the electrospinning process.

Formic acid can hydrolyse the agar chains at high temperature [30]. Agar was dissolved overnight at room temperature to produce a pale, translucent solution. Yet, even at room temperature, acid hydrolysis cannot be ruled out, and the synthesis of oligosaccharides in agar was expected. Even if the agar oligosaccharides were formed, they would have increased the bioactivity [31] of the dressing material, such as antioxidant, anti-inflammatory, and anti-tumor, among others.

Due to its compatibility with binary solvents, PCL was dissolved in acetic acid. Both formic acid and acetic acid have a high miscibility and are known to promote the electrospinning of nanofibers [32]. As described by Haider et al. [33], the use of acetic acid to dissolve PCL resulted in the creation of beads due to the rapid evaporation of the solvent. Thus, it was anticipated that the final mixture would produce a beaded morphology that could be minimized through the selection of processing parameters.

When adopting a binary solvent for agar:PCL electrospinning, nanofibrous structures were developed that required additional tuning of other electrospinning parameters like applied potential, feed rate, rotational speed of collector, distance between collector and nozzle tip, and many others.

4.1.2. Effect of concentration

Higher concentrations of agar, greater than seven parts, caused solution to sputter from the needle tip during electrospinning and hence were not used. Lower agar concentrations (4:5:: Agar:PCL), on the other hand, resulted in hydrophobic mats because of the higher PCL content. As mentioned previously, the low spinnability of agar and the use of acetic acid as a solvent for PCL resulted in the formation of bead morphology. Hence, only a small window was available to develop a bead-less or low-beaded nanofibrous structure from an agar-PCL blend. In addition, by increasing the agar concentration, the fibre size was reduced and more beads were produced. Comparable morphological outcomes were also reported earlier [34]. Similar morphology was observed for 6:5:: Agar:PCL concentration, with thicker fibres and a larger number of beads compared to 5:5:: Agar:PCL. However, nanofibers developed from 5:5::agar:PCL were thicker compared to those with ratios of 4:5 (Fig. 2a) and 6:5 (Fig. 2c). Despite this, the 5:5:: agar:
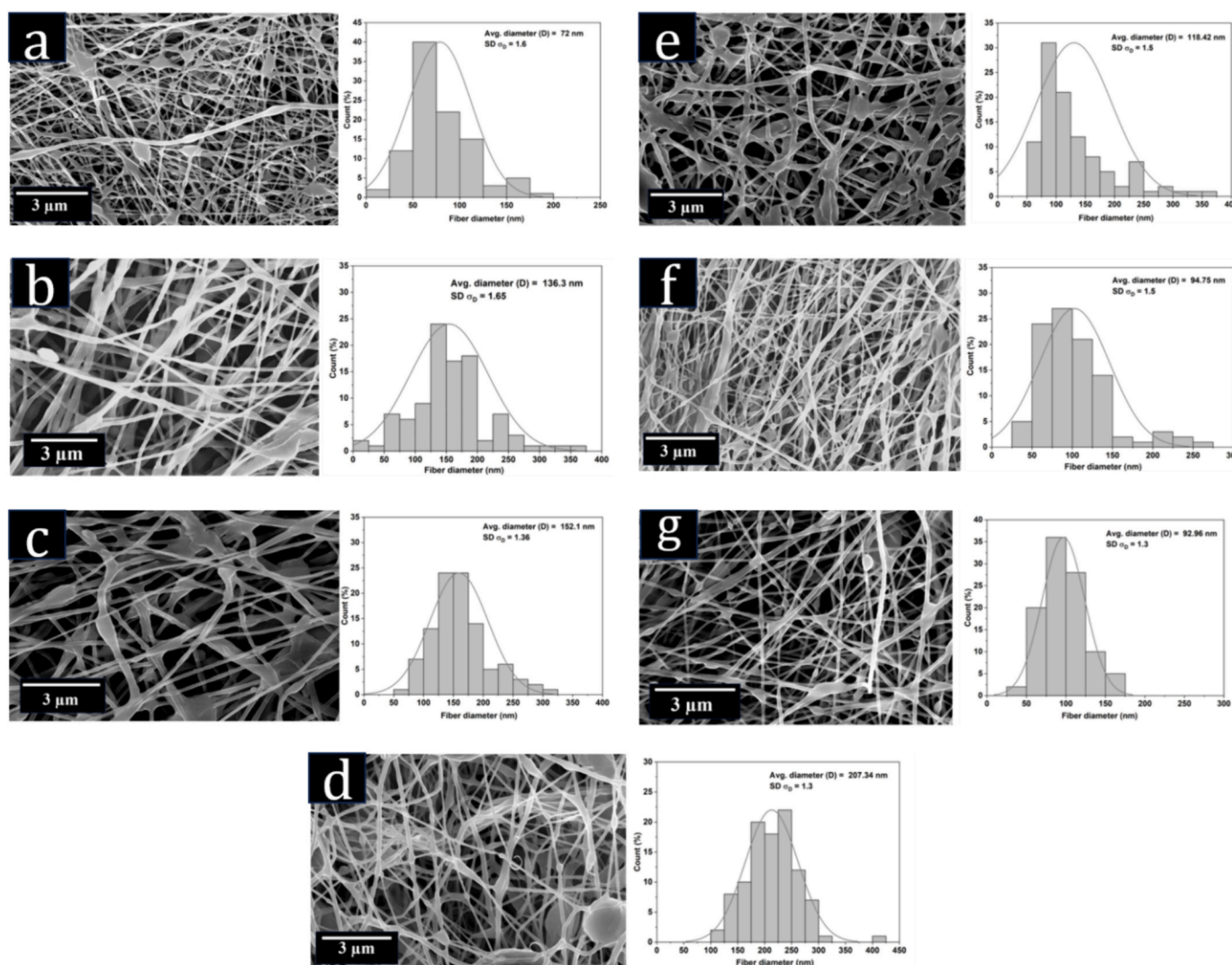

Fig. 2. Nanofibrous morphology of agar:PCL by varying agar:PCL ratios where agar:PCL ratios were 4:5 (a), 5:5 (b), 6:5 (c), 7:5 (d), electrospun from varied distance from 5 cm(e), 7 cm (f), and 10 cm (g).

PCL nanofibers exhibited uniformity with fewer beads. Hence, the optimal nanofibrous microstructures were observed at a 5:5 concentration with low bead formation (Fig. 2b). Electrospun mats with 7:5:: Agar:PCL (Fig. 2d) exhibited large beads. The obtained micrographs displayed beaded morphologies as other electrospinning parameters were further optimized to reduce bead formation in fibre. Hence, a 5:5 concentration was chosen for further studies.

4.1.3. Distance between nozzle tip to collector

The distance between the nozzle tip and collector plays a critical role in defining fibre morphology, diameter, alignment, and uniformity [33]. Notably, the beaded structure was present in each set of agar:PCL mats. Extremely short (< 5 cm) or very long distances (> 10 cm) between the nozzle tip and collector produced collapsed fibres or beaded morphology (Fig. 2e-f), respectively. For the distance between the nozzle tip and the collector ranging from 5 cm to 10 cm, Taylor's cone formed most consistently. At shorter distances (5 cm), the fibres may not have a significant time to solidify, resulting in the formation of a non-uniform morphology with a fibre diameter of 118 nm (Fig. 2e). In contrast, when the distance between the tip-to-collector was increased, the diameter of the fibres was reduced to 92 nm, and the fibre was formed on the collector in a random orientation, resulting in non-aligned nanofibers with smaller beads. Therefore, optimum distance was needed for fibre formation with maximum solvent evaporation [35]. Hence, by considering the fibre formation and diameter distribution through a histogram, 7 cm between the collector and the spinneret was found to be optimal for preparing nanofibrous and was finalized for further studies.

After careful consideration and selection, all other optimized electrospinning parameters (refer to Table 1) were set as follows: 15 kV applied voltage, 700 rpm rotational speed of the collector drum, and a polymer solution flow rate of 10 μL/min. The supplementary data demonstrated in detail that these settings yielded uniform nanofibers with fewer beads.

4.1.4. Fabrication of uniaxial and coaxial agar:PCL electrospun mat

The final selected parameters were agar:PCL::5:5 with a flow rate of 10 μL/min, 15 kV applied potential, 7 cm between nozzle tip and collector, and rotation of the drum collector at 700 rpm. Parchment paper was used as the substrate for the electrospinning process to make it simple to peel the samples off of the collector. A micrograph of the uniaxial agar:PCL mat is shown in Fig. 3a.

The selected electrospinning parameters for agar:PCL were used to develop co-axial electrospun membranes for sustained release of drugs. As coaxial nanofibers are divided into two parts, i.e., sheath and core, agar:PCL (5:5) was used for the sheath and PVA (10 %) was used for the core polymer. The concentration of PVA was selected based on nanofiber formation (shown in supplementary data). Electrospinning parameters used to generate coaxial nanofibers were the same as those used for agar: PCL nanofibers. The electrospun mat developed from coaxial agar:PCL with a PVA core infused with cephalexin hydrate was labelled as a single layer (SL). To further restrict the drug release, a secondary layer of uniaxial agar:PCL nanofibrous layer was applied to the single layer (SL) coaxial PVA- agar:PCL layer, and the two layers were referred to as a

bilayer (BL). Fig. 3b depicts micrographs of the developed single layer of coaxial agar:PCL with PVA in the core without cephalexin hydrate (CEX). Whereas Fig. 3c displays coaxial nanofibers after the incorporation of the drug. Bilayer dressing was developed by layer-by-layer fabrication of a coaxial layer followed by a uniaxial layer, where the uniaxial layer of agar:PCL would be in-contact with the wound site, as displayed in Fig. 1. Similar studies were conducted to fabricate bilayer nanofibrous mats using natural polymers, yielding an average diameter ranging from 175 to 245 nm [36].

Uniaxial and coaxial nanofibers were further demonstrated with the help of TEM micrographs (Fig. 3d & e). Silver nanoparticles were used to increase the contrast between the two polymer layers. The PVA core sheathed agar:PCL shell layer can be easily observed due to the presence of silver nanoparticles.

4.2. Fabrication of electrospun nanofibers mat with other additives

The goal of integrating various additives was to determine the compatibility of polymer fibres with various compounds, such as a hydrophobic medicament (piperine), a model protein (albumin), a bioactive agent (citric acid), etcetera. SEM micrographs illustrate the formation of nanofibers after the addition of piperine, bovine albumin, or citric acid (shown in supplementary data). Nevertheless, the quantity of nanometre-sized beads decreased with the addition of citric acid. With these fabrications in place, we have the potential to explore numerous opportunities for different applications, like drug delivery and wound healing, in the future. Current research has demonstrated that several polar chemicals may be combined with the agar:PCL solution and have the potential for a variety of applications.

4.3. Chemical properties

The FTIR spectra of agar, PCL, and their blend are shown in Fig. 4. The two polymers were blended in a variety of ratios, and the chemical compositions were confirmed using FTIR spectroscopic data. At 3500 cm^{-1}, the vibrational stretching of -OH bonds, which corresponds to the hydroxyl moiety, can be observed. At 2941 cm^{-1} and 2860 cm^{-1}, the asymmetrical and symmetrical stretching of $-CH_2$ and $-CH_3$, respectively, can be observed. For -CH bonds, these stretchings were characteristic of synthetic polymers (PCL) and polysaccharide agar. Another distinctive peak of symmetrical and asymmetrical stretching vibrations of -COOH of carboxylate groups were being found in the spectrogram for polysaccharides [37] in the agar matrix. In polycaprolactone, at 1732 cm^{-1}, the -C=O stretching vibration was present and as reported earlier [38]. The peak of the PCL -C-O ester group was observed at around 1064 cm^{-1}. All the peaks were also observed in the blends of agar with PCL, demonstrating no chemical bond formation between the two polymers in the blend (Fig. 4a). FTIR spectra of coaxial agar:PCL::5:5 with PVA in the core incorporated with and without the drug (CEX) is shown in Fig. 4b. Due to the low concentration of CEX in the electrospun films, a small peak was detected at 1600 cm^{-1} corresponding to N—H bonds. The intensity of the peak was lower in the bilayer as the concentration of the drug decreased due to additional agar and PCL. Moreover, all other characteristic peaks of CEX were reduced in the single and bilayer dressing mats, which also corroborated earlier studies [39].

4.4. Mechanical properties

Stress strain values and plots of agar:PCL::5:5, agar:PCL::5:5 with citric acid (CA), and agar:PCL::5:5 with albumin using uniaxial tensile testing are shown in Fig. 5. For mechanical testing, agar:PCL::5:5 with an average thickness of around 85 μm was used for tensile testing. Agar: PCL samples demonstrated tensile strength of 7 MPa with 40 % elongation at break compared to earlier reported 2 MPa strength of PCL and 300 % elongation at break [40]. Both the polymers (agar and PCL) are incompatible by nature, resulting in poor intermolecular interaction.

Table 1
Electrospinning parameters used for the fabrication of agar: PCL nanofibers.

S. No.	Factors	Parameters	Finalized parameter
1	Polymer concentration ratio (agar: PCL)	4:5, 5:5, 6:5, and 7:5	5:5
2	Distance between tip to collector	5 cm, 7 cm, and 10 cm	7 cm
3	Applied potential	10 kV, 15 kV, and 20 kV	15 kV
4	Rotational collector drum speed	200 rpm, 500 rpm, 700 rpm, and 1100 rpm	700 rpm
5	Flow rate	10 μL/min, and 15 μL/min	10 μL/min
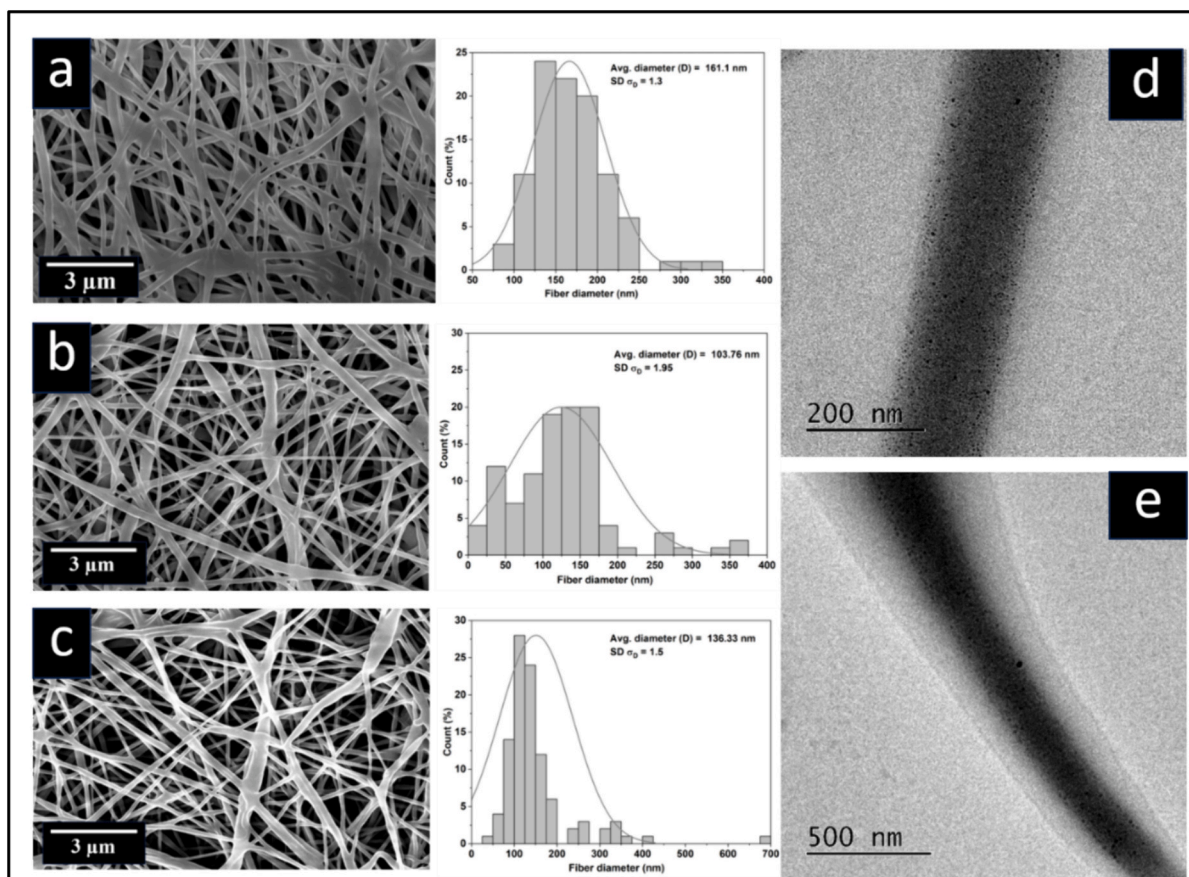
Fig. 3. Micrographs of uniaxial agar:PCL (a), coaxial agar:PCL with PVA as core (b), and coaxial agar:PCL with PVA-CEX (c) nanofibrous mat with their size distribution histograms on right. TEM micrographs of uniaxial nanofiber of PVA infused with silver nanoparticles (d) and coaxial nanofibers of agar:PCL layer encapsulating PVA layer incorporated with silver nanoparticles (e).
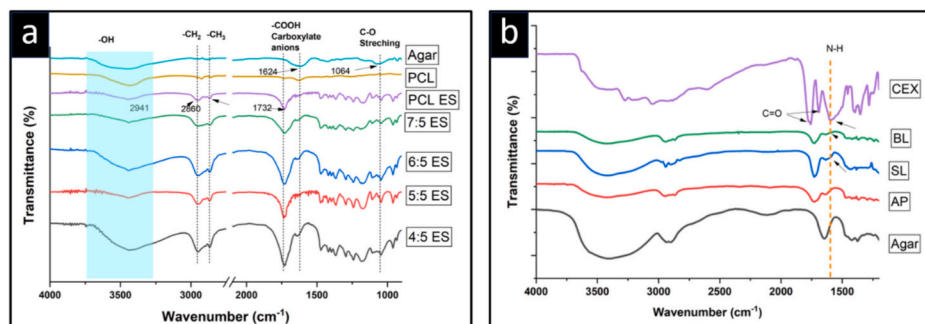
Fig. 4. FTIR spectrogram of all the compositions after blending both the polymers (a) (Top to bottom: Agar, PCL, PCL_ES, agar:PCL::7:5, 6:5, 5:5 (AP), & 4:5 electrospun mats) and (b) after the formation of coaxial single layer (SL) and coaxial bilayer with drug (CEX).

Therefore, there could be chances that agar could restrict the chain mobility of PCL, and hence, a decrease in elongation was observed. In a similar study [41], the addition of chitosan to PCL caused a decline in the elongation at the break value of PCL. Previous studies on bilayer dressing demonstrated that it is strong enough for wound dressing applications [42].

Furthermore, additives can be used to alter the materials mechanical characteristics. In the case of citric acid, the elongation at break increased to 80 %, but the strength was reduced to 5 MPa. Moreover, the addition of albumin reduced the elongation at break to 50 % but improved the strength to 6 MPa. According to Trinca et al. [43], the mechanical strength of human skin ranges from 2 to 16 MPa, and its elongation at break is between 70 and 77 %. The electrospun dressings

prepared from agar:PCL showed the optimum tensile properties, closely matching those of human skin.

4.5. In-vitro fluid handling properties

4.5.1. Wettability

The wettability of the nanofibrous mat is critical for various activities, including cell attachment, protein adsorption, and cellular interaction [44]. Considering PCL being a hydrophobic polymer with limited medical applications [45,46], adding certain hydrophilic polymers to it can make it more biocompatible by decreasing its contact angle and therefore facilitating better cell proliferation. Furthermore, the hydrophilicity of agar reduces cell adhesion, facilitating the separation of the
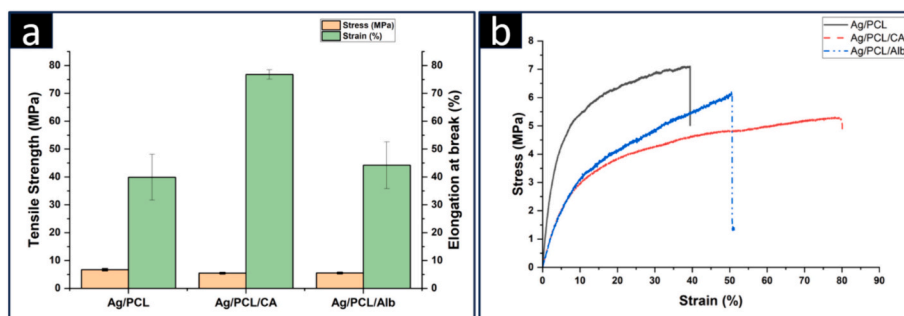
Fig. 5. Tensile properties of electrospun mats prepared from agar:PCL solution (a) with stress-strain graph (b).

wound dressing from the wound site without disrupting the growing cells. Therefore, the agar:PCL::5:5 composition promotes cell proliferation due to its optimum wettability, but due to the agar, the developed mat facilitates lower cell attachment, resulting in painless removal of the dressing mat from the wounds. After blending both polymers, the contact angle of the resulting mat was around 60° (Fig. 6a). Interestingly, the reported optimal contact angle range for cell adhesion is between 55° and 80° [47].

4.5.2. Swelling properties

Agar has higher swelling ratios than polycaprolactone due to its hydrophilic moieties; it was anticipated that blending the polymers in varying proportions would modulate the swelling properties of agar and polycaprolactone. Fig. 6b demonstrates the swelling behaviour of the developed electrospun samples. Due to the hydrophobic nature of PCL,

the nanofibrous mat created from PCL alone exhibited <5 % swelling. Following the combination of agar and PCL in a ratio of 4:5, the swelling percentage observed a significant eight-fold increase, equivalent to 40 %. As the concentration of agar was further increased, for agar:PCL:: 5:5, there was a slight decrease in the swelling percentage, which can be attributed to the higher concentration of agar. As indicated in previous research [48], the degree of swelling was found to decrease with an increase in polymer concentration per unit volume. The limited mobility of polymer chains restricts the swelling process. This could be due to the hydrophilic nature of the protein. The dissolution study displayed that almost 15–20 % of agar was getting dissolved from the developed mats.

4.5.3. Fluid handling capacity

Fig. 6c depicts the fluid absorption and holding capacity of the electrospun mats. Being hydrophobic in nature, the PCL demonstrated
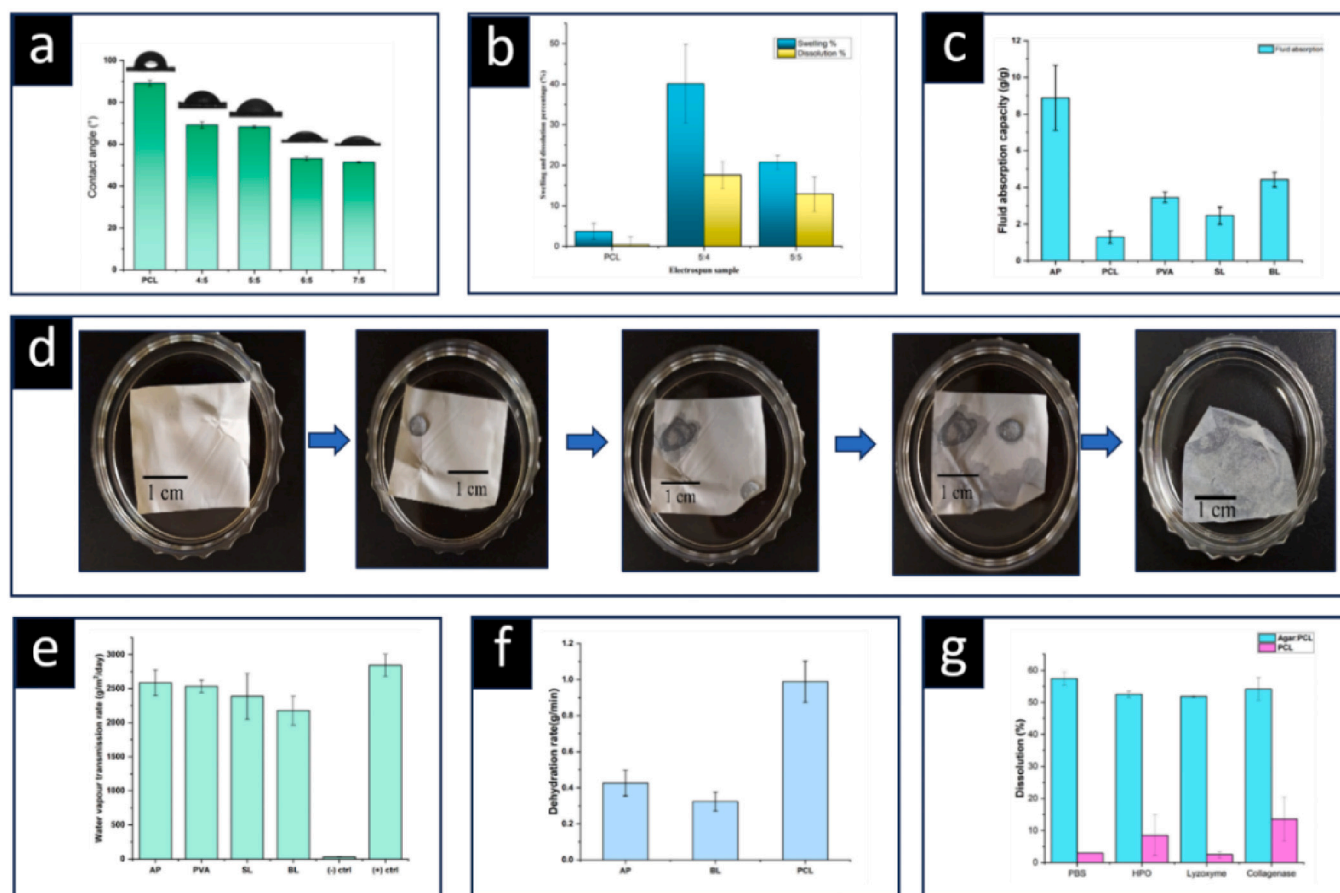
Fig. 6. Fluid handling properties of agar:PCL mats included water contact angle (a), swelling degree (b), fluid absorption capacity (c), fluid absorption behaviour (d), WVTR (e), dehydration rates (f), and dissolution properties (g).

the lowest fluid retention capacity (1.3 g/g) and the maximum dehydration rate of moisture from the PCL (1 g/min) (Fig. 6d). Similarly, the fluid holding capacity of the uniaxial PVA was found to be 3.5 g/g owing to its hydrophilicity. However, the fabrication of agar:PCL electrospun mat with a blend of hydrophilic (agar) and hydrophobic (PCL) polymers resulted in enhanced fluid-holding capacity (8.9 g/g) due to the highly hydrophilic nature of the agar. Although the single layer prepared from co-axial nanofibers containing PVA in the core and agar:PCL as the sheath showed lower fluid holding capacity, this could be due to the lower agar:PCL content as compared to uniaxial agar:PCL. Nevertheless, the bilayer electrospun mats of uniaxial and coaxial structure displayed enhanced fluid holding capacity. This could be due to the additional agar:PCL uniaxial mat, which was fabricated on a single layer of coaxial nanofibrous mat, resulting in an increased agar:PCL content.

In addition to the high absorption capacity of the agar:PCL electrospun mat, the fluid absorption rate was optimal at 134 s, which could be attributed to the unsteady dispersion of fluid but was comparable to work previously reported [22]. As seen in Fig. 6d, the addition of agar made the dispersion region clearly evident, which would not have been the case with a hydrophobic PCL mat.

4.5.4. Water vapor transmission rate

In contrast to cytocompatibility, wettability, and bioactivity, the water vapor transmission rate of wound dressings plays an important role in wound healing. If the dressing has a high rate of moisture transfer from the wound, the wound will get dehydrated, resulting in the dressing sticking to the wound site, causing excruciating discomfort during removal, while delaying the healing process. Nevertheless, if the rate of transmission is too low, the wound exudates can build up and cause back pressure, which will cause the patient discomfort while promoting microbial colonization. Hence, a desired range of moisture permeability is essential for an appropriate healing rate without increasing patient pain. Typically, 240 to 1920 g/m^2/day of moisture loss from the intact skin surface was recorded in the previous studies [49]. The moisture transmission rate of the developed dressing mats could reduce the 4800 g/m^2/day reported WVTR of exposed wounds [49]. As reported earlier, WVTR of 2028 g/m^2/day was found to be the most optimal for a bilayer wound dressing that assists in wound healing [50]. Uniaxial agar:PCL and neat PVA electrospun samples showed much higher moisture transmission rates of 2585 g/m^2/day and 2532 g/m^2/day, respectively, which could be due to the lower thickness of the electrospun layers than bilayer structures. After bilayer formation, the transmission rate of the single coaxial layer was reduced from 2384 g/m^2/day to 2174 g/m^2/day. The transmission rate of the developed agar-based bilayer dressing mats was slightly higher than the necessary range of skin transpiration rate, about 2174 g/m^2/day (Fig. 6e) and hence would be suitable for high exudating wounds. For effective wound healing without dehydration or macerating the wound site, wound dressings with this feature exhibit optimal moisture permeability via water vapor transpiration rate. Furthermore, it was previously reported that maceration can occur in heavenly exudating wounds due to the low WVTR of a bilayer dressing [51].

4.5.5. Dehydration rate

The dehydration rate of moisture from uniaxial agar:PCL and bilayer coaxial (BL) electrospun mats was found to be 0.4 g/min and 0.3 g/min, respectively (Fig. 6f). The dehydration rates were higher than previous reported literature and indicated that the dehydration rate was inversely proportional to the dressing thickness [22], which could be one of the main reasons for the higher dehydration rate of the prepared dressings. It can therefore be used for heavily exudating wounds. Nevertheless, maintaining an optimal hydration balance in an injury is essential for promoting effective healing. As excessive wetness can cause maceration and excessive dryness can cause desiccation, it is important to maintain a balance between the two. Both extremes would hinder the wound recovery process. Moreover, wounds generate varying quantities of

exudates during the healing process. The prepared agar:PCL dressing mats can be used to treat highly exuding wounds that require a high dehydration rate to prevent maceration.

4.5.6. Dissolution study

Various wound dressings are intended to promote proper wound healing by providing the optimal wound healing environment. Some dressings, for instance, produce a moist environment, whereas others absorb excessive wound exudate, resulting in effective healing. Due to exposure to body fluids, enzymes, and mechanical forces, wound dressings suffer incremental breakdown or degradation over time when applied directly to the wound surface. Frequent dressing changes may exacerbate the patient's discomfort and suffering if the dressing material degrades too rapidly, necessitating regular replacements without promoting wound healing. Further, if the dressing does not decompose over time, it will accrue as a pollutant and can burden the environment by persisting in the environment and causing debris to accumulate in landfills. Therefore, biodegradable dressing materials are currently essential for promoting healing without harming the environment. Therefore, the test was performed to evaluate the stability, dissolvability, and degradability of the developed agar:PCL electrospun mat. Lysozyme and H$_2$O$_2$ are abundant in human bodily fluids, especially serum. In addition, an increase in local H$_2$O$_2$ concentration promotes proper healing [52]. In PBS solution, lysozyme and H$_2$O$_2$ degradation aid in simulating an infected wound, whereas collagenase degradation aids in simulating the remodelling phase of skin regeneration and the repair of chronic wounds. The collagenase degradation was performed in a manner analogous to that described previously [53].

The degradation percentage of the developed electrospun dressings is shown in Fig. 6g. There was no significant mass loss observed after 9 days, and the mats remained intact, which was confirmed by visual inspection. Initial dissolution was triggered by agar dissolution from the matrix. As the composition used for the dissolution study was agar:PCL::5:5 for agar and PCL, it was anticipated that the resultant residue in the majority of dissolved samples would be around 50 % due to the dissolution of agar.

4.6. Biocompatibility studies

4.6.1. Hemocompatibility assay

A hemocompatibility assay was used to confirm the blood compatibility of the developed samples for erythrocytes, or red blood cells, for biomedical applications. A biomaterial is categorized as haemolytic (non-hemocompatible) if red blood cells (RBC) get disrupted upon interaction with the biomaterial. If the haemolysis range exceeds >10 %, then it is non-hemocompatible. Material is considered highly hemocompatible if the proportion of total hemolysis is <5 %, whereas if the range varies between 5 and 10 %, then material comes in the hemocompatible range [54]. Fig. 7a illustrates the images of the blood compatibility test. All the observations in our analysis exhibited hemolysis% values <5 %, indicating that the developed nanofibrous mats were highly hemocompatible and ideal for use in biomedical applications.

4.6.2. Cytocompatibility

The MTT test was used to assess the cytocompatibility of agar:PCL nanofiber mats produced by electrospinning. As observed (Fig. 7b and c), the viability percentage on tissue culture plates was >90 %. Considering both polymers are cytocompatible by nature, it was anticipated that the polymer matrix mix would be compatible with cells, which was validated by the MTT assay. Only the viable cells' active mitochondria can reduce the tetrazolium salt with the help of dehydrogenase into a purple formazan crystal that exhibits a maximum absorbance at 570 nm. Considerable cell attachment with adherent morphology was observed on the agar:PCL electrospun dressing mats, after 24 h of incubation. Furthermore, following a period of incubation
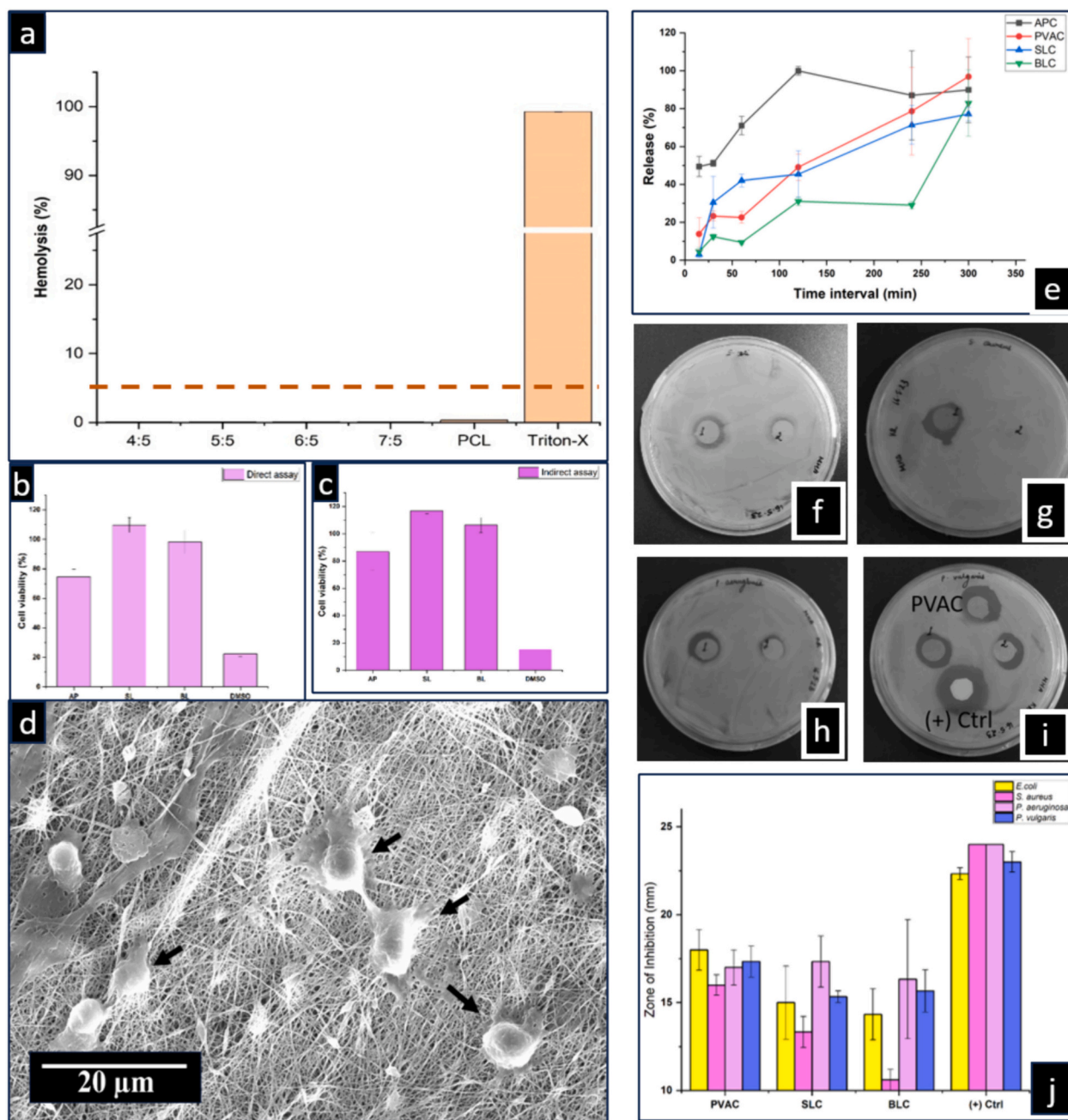
Fig. 7. Hemocompatibility (a) and cytocompatibility of AP, SL, and BL via MTT direct (b) and indirect (c) assay and cell adhesion (d) on dressing mat. Release rate (e) of antibiotic from single layer of AP, PVA, SL and BL. Antibacterial activity of uniaxial (1) (PVAC), coaxial (2) single layer (SLC), and bilayer (BLC) dressing against *E. coli* (f), *S. aureus* (g), *P. aeruginosa* (h), and *P. vulgaris* (i) with ZOI (j) with kanamycin as (+) ctrl.

on the dressing mats, a smaller number of cells were observed to adhere and exhibit cell spreading (Fig. 7d). This observation suggests that cell adherence and the initiation of cell spreading occurred on the mats. Thus, the fabricated agar:PCL dressing mats demonstrated cytocompatibility, which is essential for the healing of wounds since it encourages cell adhesion and proliferation. Furthermore, it was observed that cells had a low affinity for PCL due to limited cell recognition [29], while agar exhibited high hydrophilicity [55]. Additionally, the incorporation of bioactive agents like licorice could influence the cytocompatibility of PVA nanofibers [56]. Nevertheless, the achievement of the most optimum hydrophilicity for cell proliferation was observed when agar and PCL were combined. However, due to the absence of cell recognition sites in the electrospun mat, it was expected to exhibit reduced cell adherence, and therefore, fewer cells adhered. This

characteristic would be beneficial for facilitating the removal of dressings after the recovery phase. As adhesion of dressings to the wound bed can make dressing changes more excruciating and potentially disrupt the cells that have formed during wound healing, it is important to prevent dressings from adhering to the wound bed.

4.6.3. In vitro drug release

Using hydrophilic (agar) and hydrophobic (PCL) polymers in the sheath layer was anticipated to assist in the sustained release of any hydrophilic and hydrophobic drugs from the core matrix. Fig. 7e displays the percentage of drugs released over time from the developed coaxial electrospun films. The uniaxial agar:PCL electrospun mats released 100 % within 2 h, whereas the uniaxial PVA nanofibrous mat released the drug slowly. After developing co-axial nanofibrous mats

with PVA and agar:PCL as the membrane, a single coaxial mat discharged 77 % of the drug within four hours. Adding a second, uniaxial layer of agar:PCL over the coaxial layer did, as expected, lower the released rate from 71 % to 29 % compared to a single coaxial layer. The controlled release of the drug within the defined time interval from the developed electrospun nanofibrous dressing showed potential as a wound dressing material for highly exuding wounds. Certain medical conditions necessitate the sustained release of drugs from the dressing, which can be beneficial for the healing process. The initial burst release of drugs or bioactive agents may induce cellular toxicity instead of healing. Therefore, the incorporation of medicines or antibiotics with sustained release could prevent toxic shock to the cells while controlling microbial infection at the wound site, thereby enhancing the healing outcomes of wound management. Due to the various incorporation methods for introducing drugs, nanofibers develop distinct morphologies that influence drug delivery [57]. Nevertheless, controlled release kinetics may follow a variety of mechanisms, such as a shift in environmental ionic conditions or the degradation or dissolution of a polymer containing a drug [58].

Cephalexin hydrate (CEX) is an effective antibiotic against both gram-positive and gram-negative microorganisms. Previous research [59] was consulted to determine the percentage of antibiotics released in vitro from the nanofibrous PVA core of the coaxial films of agar:PCL. For the release study, 10 mm discs were cut from co-axial and uniaxial electrospun films developed using PVA as the antibiotic matrix in the core and agar:PCL as the exterior polymer mix. Multiple control samples were prepared with and without the incorporation of CEX.

4.6.4. Antibacterial properties

Compared to uniaxial dressings, incorporating cephalexin hydrate into the PVA core of the developed coaxial films delayed the drug release. The release study revealed that the fabrication of bilayer structures further decreased this release. The minimum inhibitory concentration (MIC) of cephalexin hydrate against *E. coli, S. aureus, P. vulgaris*, and *P. aeruginosa* was found to be 312.5 μg, 625 μg, 156 μg, and 78 μg, respectively, in 200 μL of bacterial culture (0.1 OD at 600 nm). The MBC values required to kill the respective bacteria were 625 μg, 1250 μg, 625 μg, and 312.5 μg, respectively. Researchers have developed bilayer PVA-chitosan dressings that contain neem extract to make them more effective at killing gram-positive bacteria [42].

As confirmed by the in vitro release study, the bilayer (BLC) dressings exhibited slower drug release compared to the single layer (SLC), despite containing the same dose of cephalexin. Antibacterial studies yielded consistent results, showing a reduced inhibition zone against all bacterial strains in the BLC dressings compared to the SLC dressings. The additional uniaxial layer in the BLC dressings effectively mitigated the burst release observed in the SLC and PVAC dressings. As the release rate of the antibiotic was affected by the addition of the uniaxial agar:PCL layer, a smaller inhibition zone was observed in bilayer dressings (Fig. 7). This ensured the sustained release of the antibiotic, which will monitor bacterial growth at the site of the wound for an extended period, unlike the burst release of the drug. The trend for the zone of inhibition (ZOI) was observed as uniaxial PVA-CEX (PVAC) > coaxial single layer agar:PCL with PVA-CEX core (SLC) > bilayer uniaxial agar:PCL onto single layer coaxial agar:PCL with PVA-CEX as a core (BLC), as shown in Fig. 7j. This was anticipated due to the swift antibiotic release from the uniaxial mat, followed by the coaxial single and bilayer dressing.

5. Conclusion

In conclusion, the electrospinning technique shows significant possibilities in the development of agar:PCL nanofibers for potential wound dressing applications. Our investigation of the morphology, strength, wettability, and permeability of the mats has provided a broad spectrum for promoting wound healing efficacy. The addition of binary solvents,

including formic acid and acetic acid, has facilitated the fabrication of agar: PCL mats that exhibit enhanced wettability (~60° contact angle), 8.9 g/g fluid retention capacity, and 2174 g/m^2/day permeability, thus supporting their efficacy in promoting wound healing. The introduction of additives allowed the mechanical strength of electrospun agar:PCL mats to be easily modified from 7 MPa to 5 MPa and doubled elongation failure that falls in the range of human skin mechanical strength, thus broadening their potential applications. The synthesis of coaxial mats through the integration of polyvinyl alcohol (PVA) as the core material and agar:PCL as the membrane material has led to the improvement of dressings for controlled drug release that have properties of sustained release. The incorporation of an additional uniaxial layer composed of agar:PCL onto the coaxial mat further limited the burst release rate, resulting in sustained release and enhanced efficacy in wound healing. The agar:PCL mats demonstrated 50 % biodegradability in different conditions due to dissolution, enzymatic, and hydrolytic degradation. Moreover, in the biocompatibility assay, <2 % haemolysis demonstrated excellent hemocompatibility of the developed mats. The results of the direct and indirect MTT assays illustrated their cytocompatibility with enhanced growth and proliferation of the fibroblast. In the antibacterial studies, despite containing the same dose of cephalexin, the bilayer dressing exhibited a reduced inhibition zone, confirming slower release. The incorporation of bilayer morphology effectively modulated drug release from the coaxial layer, leading to sustained release. The developed coaxial bilayer mats demonstrated significant antibacterial activity and excellent biocompatibility properties, which added to their suitability for use in biomedical settings.

However, it is important to mention future advancements that still limit our study. First, we successfully incorporated cephalexin hydrate as a hydrophilic antibacterial drug into the coaxial nanofibers, further research is required to incorporate hydrophilic and hydrophobic drugs for broader therapeutic conditions. Additionally, although we controlled the drug release profile by fabricating an additional uniaxial layer on the coaxial layer, forming a bilayer asymmetric structure, future studies could investigate modulating drug release kinetics by varying the thickness of the layers. Hence, for future objectives, an array of drugs can be incorporated into the nanofibers to provide a sustained drug release profile. All of these efforts show that electrospun agar:PCL mats have great potential to enhance wound care strategies.

CRediT authorship contribution statement

Kalpana Rathore: Visualization, Methodology, Investigation, Formal analysis, Data curation, Conceptualization. **Indrajeet Singh:** Investigation. **Kantesh Balani:** Visualization, Formal analysis. **Sandeep Sharma:** Validation, Supervision, Methodology, Conceptualization. **Vivek Verma:** Visualization, Validation, Supervision, Methodology, Conceptualization.

Declaration of competing interest

The authors declare that they have no known competing financial interests or personal relationships that could have appeared to influence the work reported in this paper.

Appendix A. Supplementary data

Supplementary data to this article can be found online at https://doi.org/10.1016/j.ijbiomac.2024.133712.

References

[1] S. Priya, U. Batra, R.N. Samshritha, S. Sharma, A. Chaurasiya, G. Singhvi, Polysaccharide-based nanofibers for pharmaceutical and biomedical applications: a review, Int. J. Biol. Macromol. 218 (2022) 209–224, https://doi.org/10.1016/j.ijbiomac.2022.07.118.

[2] R. Rasouli, A. Barhoum, M. Bechelany, A. Dufresne, Nanofibers for biomedical and healthcare applications, Macromol. Biosci. 19 (2019) 1–27, https://doi.org/10.1002/mabi.201800256.

[3] R.S. Ambekar, B. Kandasubramanian, Advancements in nanofibers for wound dressing: a review, Eur. Polym. J. 117 (2019) 304–336, https://doi.org/10.1016/j.eurpolymj.2019.05.020.

[4] M.M. Hasan, M.A. Shahid, PVA, licorice, and collagen (PLC) based hybrid bio-nano scaffold for wound healing application, J. Biomater. Sci. Polym. Ed. 34 (2023) 1217–1236, https://doi.org/10.1080/09205063.2022.2163454.

[5] Z. Sultanova, G. Kaleli, G. Kabay, M. Mutlu, Controlled release of a hydrophilic drug from coaxially electrospun polycaprolactone nanofibers, Int. J. Pharm. 505 (2016) 133–138, https://doi.org/10.1016/j.ijpharm.2016.03.032.

[6] H. Yang, P.F. Gao, W.B. Wu, X.X. Yang, Q.L. Zeng, C. Li, C.Z. Huang, Antibacterials loaded electrospun composite nanofibers: release profile and sustained antibacterial efficacy, Polym. Chem. 5 (2014) 1965–1975, https://doi.org/10.1039/C3PY01335A.

[7] M.K. Cho, B.S. Singu, Y.H. Na, K.R. Yoon, Fabrication and characterization of double-network agarose/polyacrylamide nanofibers by electrospinning, J. Appl. Polym. Sci. 133 (2016), https://doi.org/10.1002/APP.42914.

[8] J. Puls, S.A. Wilson, D. Hölter, Degradation of cellulose acetate-based materials: a review, J. Polym. Environ. 19 (2011) 152–165, https://doi.org/10.1007/s10924-010-0258-0.

[9] A. Awadhiya, S. Tyeb, K. Rathore, V. Verma, Agarose bioplastic-based drug delivery system for surgical and wound dressings, Eng. Life Sci. 17 (2017) 204–214, https://doi.org/10.1002/elsc.201500116.

[10] S. Tyeb, N. Kumar, A. Kumar, V. Verma, Agar-iodine transdermal patches for infected diabetic wounds, ACS Appl. Bio Mater. 3 (2020) 7515–7530, https://doi.org/10.1021/acsabm.0c00722.

[11] A.M.M. Sousa, H.K.S. Souza, J. Uknalis, S. Liu, M.P. Gonc, Electrospinning of agar / PVA aqueous solutions and its relation with rheological properties 115, 2015, pp. 348–355, https://doi.org/10.1016/j.carbpol.2014.08.074.

[12] D. Wehlage, R. Böttjer, T. Grothe, A. Ehrmann, Electrospinning water-soluble/insoluble polymer blends, AIMS Mater. Sci. 5 (2018) 190–200, https://doi.org/10.3934/matersci.2018.2.190.

[13] S. Fuchs, J. Hartmann, P. Mazur, V. Reschke, H. Siemens, D. Wehlage, A. Ehrmann, Electrospinning of biopolymers and biopolymer blends, J. Chem. Pharm. Sci. 2017 (2017) 1–3.

[14] A.M.M. Sousa, H.K.S. Souza, J. Uknalis, S. Liu, M.P. Gonc, International Journal of Biological Macromolecules Improving agar electrospinnability with choline-based deep eutectic solvents 80, 2015, pp. 139–148, https://doi.org/10.1016/j.ijbiomac.2015.06.034.

[15] T.P. Armeda, Fabrication of Pcl-collagen nanofiber using chloroform-formic acid solution and its application as wound dressing candidate, Journal of Stem Cell Research and Tissue Engineering 1 (2018), https://doi.org/10.20473/jscrte.v1i1.7567.

[16] N. Raina, R. Pahwa, J.K. Khosla, P.N. Gupta, M. Gupta, Polycaprolactone-based materials in wound healing applications, Polym. Bull. 79 (2022) 7041–7063, https://doi.org/10.1007/s00289-021-03865-w.

[17] K. Ma, Y. Qiu, Y. Fu, Q.Q. Ni, Electrospun sandwich configuration nanofibers as transparent membranes for skin care drug delivery systems, J. Mater. Sci. 53 (2018) 10617–10626, https://doi.org/10.1007/s10853-018-2241-4.

[18] Y.E. Aguirre-Chagala, V. Altuzar, E. León-Sarabia, J.C. Tinoco-Magaña, J.M. Yañez-Limón, C. Mendoza-Barrera, Physicochemical properties of polycaprolactone/collagen/elastin nanofibers fabricated by electrospinning, Materials Science and Engineering C 76 (2017) 897–907, https://doi.org/10.1016/j.msec.2017.03.118.

[19] K. Kanawung, K. Panitchanapan, S.O. Puangmalee, W. Utok, N. Kreua-Ongarjnukool, R. Rangkupan, C. Meechaisue, P. Supaphol, Preparation and characterization of polycaprolactone/ diclofenac sodium and poly(vinyl alcohol)/tetracycline hydrochloride fiber mats and their release of the model drugs, Polym. J. 39 (2007) 369–378, https://doi.org/10.1295/polymj.PJ2006011.

[20] D. Budurova, F. Ublekov, H. Penchev, The use of formic acid as a common solvent for electrospinning of hybrid PHB/soy protein fibers, Mater. Lett. 301 (2021) 130313, https://doi.org/10.1016/j.matlet.2021.130313.

[21] Z. Gounani, S. Pourianejad, M.A. Asadollahi, R.L. Meyer, J.M. Rosenholm, A. Arpanaei, Polycaprolactone-gelatin nanofibers incorporated with dual antibiotic-loaded carboxyl-modified silica nanoparticles, J. Mater. Sci. 55 (2020) 17134–17150, https://doi.org/10.1007/s10853-020-05253-7.

[22] M. Uzun, S.C. Anand, T. Shah, *In vitro* characterisation and evaluation of different types of wound dressing materials, J. Biomed.Eng. Technol. 1 (2013) 1–7, https://doi.org/10.12691/jbet-1-1-1.

[23] Y. Kim, S.J. Doh, G.D. Lee, C. Kim, J.N. Im, Composite nonwovens based on carboxymethyl cellulose for wound dressing materials, Fibers and Polymers 20 (2019) 2048–2056, https://doi.org/10.1007/s12221-019-9261-9.

[24] A.K. Sonker, A.K. Teotia, A. Kumar, R.K. Nagarale, V. Verma, Development of polyvinyl alcohol based high strength biocompatible composite films, Macromol. Chem. Phys. 201700130 (2017) 1–13, https://doi.org/10.1002/macp.201700130.

[25] A.K. Sonker, K. Rathore, A.K. Teotia, A. Kumar, V. Verma, Rapid synthesis of high strength cellulose–poly(vinyl alcohol) (PVA) biocompatible composite films via microwave crosslinking, J. Appl. Polym. Sci. 136 (2019), https://doi.org/10.1002/app.47393.

[26] M. Balouiri, M. Sadiki, S.K. Ibnsouda, Methods for in vitro evaluating antimicrobial activity: a review author's accepted manuscript, J Pharm Anal 6 (2015) 71–79, https://doi.org/10.1016/j.jpha.2015.11.005.

[27] S. Sharma, I.A. Khan, I. Ali, F. Ali, M. Kumar, A. Kumar, R.K. Johri, S.T. Abdullah, S. Bani, A. Pandey, K.A. Suri, B.D. Gupta, N.K. Satti, P. Dutt, G.N. Qazi, Evaluation of the antimicrobial, antioxidant, and anti-inflammatory activities of hydroxychavicol for its potential use as an oral care agent, Antimicrob. Agents Chemother. 53 (2009) 216–222, https://doi.org/10.1128/AAC.00045-08.

[28] L. Wang, J. Rhim, International journal of biological macromolecules preparation and application of agar / alginate / collagen ternary blend functional food packaging films, Int. J. Biol. Macromol. 80 (2015) 460–468, https://doi.org/10.1016/j.ijbiomac.2015.07.007.

[29] J. Zhu, J. Luo, X. Zhao, J. Gao, J. Xiong, Electrospun homogeneous silk fibroin/poly (ε-caprolactone) nanofibrous scaffolds by addition of acetic acid for tissue engineering, J. Biomater. Appl. 31 (2016) 421–437, https://doi.org/10.1177/0885328216659775.

[30] E.J. Yun, H.T. Kim, K.M. Cho, S. Yu, S. Kim, I.G. Choi, K.H. Kim, Pretreatment and saccharification of red macroalgae to produce fermentable sugars, Bioresour. Technol. 199 (2016) 311–318, https://doi.org/10.1016/j.biortech.2015.08.001.

[31] X. Chen, X. Fu, L. Huang, J. Xu, X. Gao, Agar oligosaccharides: A review of preparation , structures , bioactivities and application, Carbohydr. Polym. 265 (2021) 118076, https://doi.org/10.1016/j.carbpol.2021.118076.

[32] L. Van Der Schueren, I. Steyaert, B. De Schoenmaker, K. De Clerck, Polycaprolactone/chitosan blend nanofibres electrospun from an acetic acid/formic acid solvent system, Carbohydr. Polym. 88 (2012) 1221–1226, https://doi.org/10.1016/j.carbpol.2012.01.085.

[33] A. Haider, S. Haider, I. Kang, REVIEW a comprehensive review summarizing the effect of electrospinning parameters and potential applications of nanofibers in biomedical and biotechnology, Arab. J. Chem. 11 (2018) 1165–1188, https://doi.org/10.1016/j.arabjc.2015.11.015.

[34] S. Teng, P. Wang, H. Kim, Blend fibers of chitosan – agarose by electrospinning 63, 2009, pp. 2510–2512, https://doi.org/10.1016/j.matlet.2009.08.051.

[35] S. Mitra, T. Mateti, S. Ramakrishna, A. Laha, A review on curcumin-loaded electrospun nanofibers and their application in modern medicine, Jom 74 (2022) 3392–3407, https://doi.org/10.1007/s11837-022-05180-9.

[36] M.A. Shahid, M.M. Hasan, M.R. Alam, M. Mohebullah, M.A. Chowdhury, Antibacterial multicomponent electrospun nanofibrous mat through the synergistic effect of biopolymers, J. Appl. Biomater. Funct. Mater. 20 (2022), https://doi.org/10.1177/22808000221136061/ASSET/IMAGES/LARGE/10.1177_22808000221136061-FIG 5.JPEG.

[37] J. Liu, Z. Xue, W. Zhang, M. Yan, Y. Xia, Preparation and properties of wet-spun agar fibers, Carbohydr. Polym. 181 (2018) 760–767, https://doi.org/10.1016/j.carbpol.2017.11.081.

[38] M.A. Salami, F. Kaveian, M. Rafienia, S. Saber-Samandari, A. Khandan, M. Naeimi, Electrospun polycaprolactone/lignin-based nanocomposite as a novel tissue scaffold for biomedical applications, J. Med. Signals Sens. 7 (2017) 228–238, https://doi.org/10.4103/jmss.JMSS_11_17.

[39] K. Montiel-Centeno, D. Barrera, F. García-Villén, R. Sánchez-Espejo, A. Borrego-Sánchez, E. Rodríguez-Castellón, G. Sandri, C. Viseras, K. Sapag, Cephalexin loading and controlled release studies on mesoporous silica functionalized with amino groups, J. Drug Deliv. Sci. Technol. 72 (2022), https://doi.org/10.1016/j.jddst.2022.103348.

[40] R. Augustine, H.N. Malik, D.K. Singhal, A. Mukherjee, Electrospun polycaprolactone / ZnO nanocomposite membranes as biomaterials with antibacterial and cell adhesion properties, 2014, https://doi.org/10.1007/s10965-013-0347-6.

[41] T. Prasad, E.A. Shabeena, D. Vinod, T.V. Kumary, P.R.A. Kumar, Characterization and in vitro evaluation of electrospun chitosan / polycaprolactone blend fibrous mat for skin tissue engineering, 2015, https://doi.org/10.1007/s10856-014-5352-8.

[42] A. Ali, M.A. Shahid, M.D. Hossain, M.N. Islam, Antibacterial bi-layered polyvinyl alcohol (PVA)-chitosan blend nanofibrous mat loaded with Azadirachta indica (neem) extract, Int. J. Biol. Macromol. 138 (2019) 13–20, https://doi.org/10.1016/J.IJBIOMAC.2019.07.015.

[43] R.B. Trinca, C.B. Westin, J.A.F. da Silva, Â.M. Moraes, Electrospun multilayer chitosan scaffolds as potential wound dressings for skin lesions, Eur. Polym. J. 88 (2017) 161–170, https://doi.org/10.1016/j.eurpolymj.2017.01.021.

[44] S. Unal, S. Arslan, B. Karademir Yilmaz, D. Kazan, F.N. Oktar, O. Gunduz, Glioblastoma cell adhesion properties through bacterial cellulose nanocrystals in polycaprolactone/gelatin electrospun nanofibers, Carbohydr. Polym. 233 (2020) 115820, https://doi.org/10.1016/j.carbpol.2019.115820.

[45] M. Ranjbar-mohammadi, S. Rabbani, S.H. Bahrami, M.T. Joghataei, F. Moayer, Antibacterial performance and in vivo diabetic wound healing of curcumin loaded gum tragacanth / poly (ε -caprolactone) electrospun nano fi bers, Mater. Sci. Eng. C 69 (2016) 1183–1191, https://doi.org/10.1016/j.msec.2016.08.032.

[46] F. Safdari, M.D. Gholipour, A. Ghadami, M. Saeed, M. Zandi, Multi-antibacterial agent-based electrospun polycaprolactone for active wound dressing, Prog. Biomater. 11 (2022) 27–41, https://doi.org/10.1007/s40204-021-00176-1.

[47] K.L. Menzies, L. Jones, The impact of contact angle on the biocompatibility of biomaterials, Optom. Vis. Sci. 87 (2010) 387–399, https://doi.org/10.1097/OPX.0b013e3181da863e.

[48] T.J. Madera-Santana, Y. Freile-Pelegrín, J.A. Azamar-Barrios, Physicochemical and morphological properties of plasticized poly(vinyl alcohol)–agar biodegradable films, Int. J. Biol. Macromol. 69 (2014) 176–184, https://doi.org/10.1016/j.ijbiomac.2014.05.044.

[49] N.L.B.M. Yusof, A. Wee, L.Y. Lim, E. Khor, Flexible chitin films as potential wound-dressing materials: wound model studies, J. Biomed. Mater. Res. A 66 (2003) 224–232, https://doi.org/10.1002/jbm.a.10545.

[50] M. Wojcik, P. Kazimierczak, A. Benko, K. Palka, V. Vivcharenko, A. Przekora, Superabsorbent curdlan-based foam dressings with typical hydrocolloids properties for highly exuding wound management, Mater. Sci. Eng. C 124 (2021) 112068, https://doi.org/10.1016/j.msec.2021.112068.

[51] H.E. Thu, M.H. Zulfakar, S.F. Ng, Alginate based bilayer hydrocolloid films as potential slow-release modern wound dressing, Int. J. Pharm. 434 (2012) 375–383, https://doi.org/10.1016/j.ijpharm.2012.05.044.

[52] S. Ahtzaz, M. Nasir, L. Shahzadi, F. Iqbal, A.A. Chaudhry, M. Yar, I. Ur Rehman, W. Amir, A. Anjum, R. Arshad, A study on the effect of zinc oxide and zinc peroxide nanoparticles to enhance angiogenesis-pro-angiogenic grafts for tissue regeneration applications, Mater. Des. 132 (2017) 409–418, https://doi.org/10.1016/j.matdes.2017.07.023.

[53] V. Vivcharenko, A. Benko, K. Palka, M. Wojcik, A. Przekora, International journal of biological macromolecules elastic and biodegradable chitosan / agarose fi lm revealing slightly acidic pH for potential applications in regenerative medicine as arti fi cial skin graft, Int. J. Biol. Macromol. 164 (2020) 172–183, https://doi.org/10.1016/j.ijbiomac.2020.07.099.

[54] S. Tripathi, B.N. Singh, S. Divakar, G. Kumar, S.P. Mallick, P. Srivastava, Design and evaluation of ciprofloxacin loaded collagen chitosan oxygenating scaffold for skin tissue engineering, Biomed. Mater. (Bristol) 16 (2021), https://doi.org/10.1088/1748-605X/abd1b8.

[55] B. Chu, A. Zhang, J. Huang, X. Peng, L. You, C. Wu, S. Tang, Preparation and Biological Evaluation of a Novel Agarose-Grafting-Hyaluronan Scaffold for Accelerated Wound Regeneration Preparation and Biological Evaluation of a Novel Agarose-Grafting-Hyaluronan Scaffold for Accelerated Wound Regeneration, 2020.

[56] M.A. Shahid, M.S. Khan, M.M. Hasan, Licorice extract-infused electrospun nanofiber scaffold for wound healing, OpenNano 8 (2022) 100075, https://doi.org/10.1016/J.ONANO.2022.100075.

[57] J. Wang, M. Windbergs, Controlled dual drug release by coaxial electrospun fibers – impact of the core fluid on drug encapsulation and release, Int. J. Pharm. 556 (2019) 363–371, https://doi.org/10.1016/j.ijpharm.2018.12.026.

[58] S. Young, M. Wong, Y. Tabata, A.G. Mikos, Gelatin as a delivery vehicle for the controlled release of bioactive molecules, J. Control. Release 109 (2005) 256–274, https://doi.org/10.1016/j.jconrel.2005.09.023.

[59] M.H. El-Newehy, M.E. El-Naggar, S. Alotaiby, H. El-Hamshary, M. Moydeen, S. Al-Deyab, Preparation of biocompatible system based on electrospun CMC/PVA nanofibers as controlled release carrier of diclofenac sodium, J. Macromol. Sci., Part A: Pure Appl. Chem. 53 (2016) 566–573, https://doi.org/10.1080/10601325.2016.1201752.

Asymmetric Janus Nanofibrous Agar-Based Wound Dressing Infused with Enhanced Antioxidant and Antibacterial Properties

Kalpana Rathore, Dheeraj Upadhyay, Noopur Verma, Ajay Kumar Gupta, Saravanan Matheshwaran, Sandeep Sharma,* and Vivek Verma*

Cite This: https://doi.org/10.1021/acsabm.4c01184

Read Online

ACCESS | Metrics & More | Article Recommendations | Supporting Information

ABSTRACT: In the present study, we have developed an agar-based asymmetric Janus nanofibrous wound dressing comprising a support and an electrospun layer with antibacterial and antioxidant properties, respectively, to facilitate healing effectively. The support layer containing agar and silver nitrate was fabricated by using solvent casting for sustained release, combating the dose-dependent cytotoxicity of silver nanoparticles, where nanoparticles were synthesized using a one-pot reduction method. The electrospun layer, fabricated with a mixture of agar and polycaprolactone infused with gallic acid, was electrospun over the support layer to impart antioxidant properties. Characterizations using UV–vis spectroscopy, transmission electron microscopy, scanning electron microscopy, and Fourier transform infrared spectroscopy validated the synthesis of nanoparticles in 10−20 nm diameter and the asymmetric Janus dressing. The developed Janus nanofibrous structure exhibited 98% porosity, excellent fluid-handling properties, a moisture permeability of 1200 $g/m^2/day$, and a water absorption of ∼250%. Moreover, the time-kill assay confirmed potent bacteriostatic effect against Gram-positive and Gram-negative bacteria, and sustained release of silver nanoparticles followed the Korsmeyer−Peppas model. With over 90% free radical scavenging efficacy, 37% degradation in 7 days, and less than 2% hemolysis, the dressings demonstrated exceptional antioxidant, biodegradable, and hemocompatible properties. The biocompatibility assessment further confirmed its cytocompatible efficacy, with more than 79% wound closure in the wound scratch assay. Most importantly, in vivo studies demonstrated the efficacy of the developed Janus dressing, promoting over 97% healing within 12 days of injury with higher epithelial formation. Overall, the in vitro and in vivo assessment of the developed Janus dressing confirmed its potential to function as a versatile and effective material for wound care applications.

KEYWORDS: agar, PCL, silver nanoparticles, nanofibers, biopolymers, electrospinning, wound healing
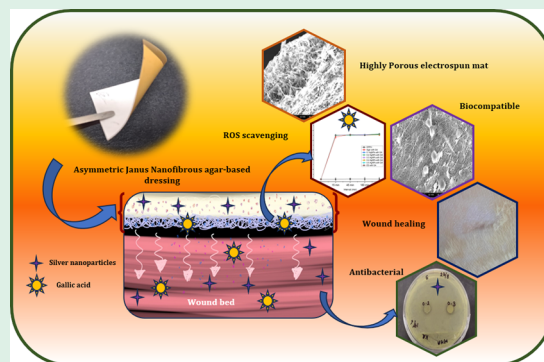
INTRODUCTION

Natural wound healing process consists of four integrated phases that require a multitude of internal and external factors to promote collagen formation, tissue regeneration, and repression of free radical activities. In the first phase of wound healing, hemostasis ensures blood clot formation, followed by formation of exudates, which should be removed to prevent maceration due to excess fluids. Subsequently, during the inflammatory phase, it becomes essential to employ reactive oxygen species (ROS) scavengers to manage the downsides caused by them. Throughout the proliferative phases of healing, antimicrobial measures are required until the wound completely heals. Furthermore, ideal moisture-transfer rates are also necessary to promote optimum exudate evaporation at the wound site without dehydrating or macerating and promote effective healing during the remodeling phase. Furthermore, various factors, including pH, temperature, moisture, infection, etc., can disrupt the natural healing phases, leading to delayed or impaired wound healing.

Depending on the wound care requirements, different functionalities in the wound dressings are required. For instance, dressings with high swelling properties suit exudating wounds, while antibacterial dressings aid in chronic wound healing,[1] and hydrogel dressings accelerate healing in burn wounds.[2] Natural polysaccharide-based dressings developed from hydrophilic matrices like agar, a natural polysaccharide extracted from seaweed, have gained attention in wound dressing applications due to hydration/dehydration properties similar to skin.[3] Moreover, agar hydrogels have a high absorption capacity for fluids without transforming into a free-flowing gel.

Aside from hydrogels,[4] morphologies such as nanofibers are preferable for biomedical dressing,[5] attributed to their high surface area-to-volume ratio and structural resemblance to the extracellular matrix. The morphological asymmetries in the structure and properties of nanofibers, films, and hydrogels could potentially be used and enhanced by integrating different layers to improve the efficacy of the wound dressings.[1] The limited literature,[6] on agar-based nanofibers incorporated with bioactive agents for wound healing, underscores our rationale to pioneer the development of a Janus agar-based dressing. Our approach involves the fabrication of asymmetric layers comprising electrospun agar-based nanofibers of agar-PCL blend atop solvent-cast agar films. Polycaprolactone (PCL), known for its electrospinnability and hydrophobicity, would enhance the spinnability of the agar nanofibers. Notably, by blending agar and PCL for nanofiber formation, we can increase the potential by imparting hydrophilic and hydrophobic phases to the dressing. This dual-phase characteristic of nanofibers would not only enhance the dressing versatility but also broaden the horizons for the incorporation of several hydrophilic and hydrophobic bioactive agents. Despite lacking inherent functional properties, agar is commonly modified with bioactive agents to impart antimicrobial and antioxidant properties.[7]

Several nanoparticles, including silver, gold, and copper nanoparticles, have been incorporated into a polymer matrix[8] to impart antimicrobial properties. Among these, silver nanoparticles (AgNPs) are the most tested nanoparticles due to their strong antimicrobial activity,[9] against a broad spectrum of microbes, including bacteria, fungi, and viruses. New synthesis methods[10] have been evolved to form AgNPs by biological, chemical, and thermal reduction with one-pot synthesis,[11] which are also reported earlier.[12] However, the emergence of reducing-agent-free, one-pot green synthesis of nanoparticles has drawn attention for biocomposite films, considering the dose-dependent toxicity of the nanoparticles.

Furthermore, numerous bioactive agents, such as polyphenols, were integrated into polymers to impart biological functionalities, including antioxidant,[13] anti-inflammatory,[14] antiallergic,[15] and antibacterial[16] properties. Gallic acid, a basic polyphenol,[17] has shown potency in neutralizing oxidative species, which is crucial for the early stage of healing, which involves scavenging ROS. Dressings laden with antioxidant compounds could be designed, particularly electrospun nanofibrous dressings, to release efficiently at the wound site to meet early healing requirements.

Advancements in fabrication techniques, including the electrospinning process, have enabled the formation of nanofibers for advanced structures and functional applications.[18−22] This technique has evolved into more sophisticated techniques serving multiple loadings, such as uniaxial, coaxial, triaxial, and side by side.[23,24] These advancements resulted in the development of various nanostructures, such as core−shell, Janus, and their combos.[25−29]

Our study focuses on developing Janus antibacterial agar dressing coated with an agar/PCL electrospun membrane containing gallic acid as an antioxidant agent. The agar/PCL electrospun membrane functions as the primary layer containing gallic acid and accelerates the healing process with its antioxidant properties. The secondary agar layer was impregnated with AgNPs without the addition of reducing agents. The sustained release of AgNPs provides long-term antibacterial properties while addressing dose-dependent cytotoxicity. Therefore, our research offers a comprehensive approach to meet the diverse needs of the healing process, including antibacterial and antioxidative stress with in vitro and in vivo assessments, thereby facilitating efficient healing.

■ MATERIALS AND METHODS

Agar powder, Dulbecco's modified Eagle's medium (DMEM), trypsin-EDTA solution, penicillin−streptomycin−neomycin solution, and fetal bovine serum (FBS) were procured from Himedia Laboratories Pvt. Limited, India. Dimethyl sulfoxide (DMSO), formic acid, and acetic acid were obtained from Loba Chemie Pvt. Ltd., India. PCL, ethanol, and gallic acid were procured from Merck, Sigma-Aldrich Pvt. Ltd., India. Silver nitrate was obtained from RFCL Limited, India. Potassium bromide (KBr) and 2, 2-diphenyl-1-picrylhydrazyl (DPPH) were purchased from Sisco Research Laboratories Pvt. Ltd., India. Thiazolyl blue tetrazolium bromide (98%) was procured from Thermo Fisher Scientific India Pvt. Ltd., India. *Escherichia coli* (MTCC 443), *Proteus vulgaris* (MTCC 744), *Pseudomonas aeruginosa* (MTCC 3541), and *Staphylococcus aureus* (MTCC 96) were procured from MTCC India.

Preparation of Agar Films Incorporated with Silver Nanoparticles. Silver nitrate solution (50 mg/mL) was prepared, and the stock solution was stored in the dark. To develop agar films, a solvent casting technique was employed. Briefly, 1 g of agar was added to 50 mL of deionized (DI) water with 10% glycerol (with respect to agar) as a plasticizer and varying amounts of silver nitrate (0.1, 0.2, 0.3, 0.4, and 0.5 mM) and labeled 0.1 agar, 0.2 agar, and so on. The flask containing the solutions were wrapped with aluminum foil to prevent photodegradation of silver nitrate and were autoclaved at 121 °C for 15 min to reduce AgNO$_3$ to silver. The autoclaved solutions were poured into 140 mm polystyrene Petri plates and dried overnight at 45 °C in the dark to form films and stored in aluminum foil for future use. The developed agar-silver nanoparticle (agar/AgNPs) films served as a base layer (substrate) for the electrospun agar/PCL (AP) nanofibrous layer, resulting in the formation of a bilayer structure.

Solution Preparation for Electrospinning. Agar and PCL were dissolved in formic acid and acetic acid, respectively, to produce 20% w/v polymer solutions, according to the previous report.[30] Specifically, the agar solution was prepared by dissolving 4 g of agar powder in 20 mL of formic acid at room temperature overnight. Likewise, 20% PCL was dissolved overnight in acetic acid at 60 °C to obtain a homogeneous PCL solution. PCL solution was stored at ambient temperature, while agar solution was kept at 4 °C for subsequent use.

For electrospinning, both solutions (agar and PCL) were mixed in a 1:1 ratio and stirred for 30 min at room temperature with a magnetic stirrer to obtain a homogeneous solution of agar/PCL (AP). To prevent phase separation during the electrospinning procedure, always a fresh agar/PCL blend was prepared, as prolonged storage led to phase separation. The ESPIN ES-3 electrospinning unit was used to fabricate nanofibrous dressings. The AP solution was filled in a 5 mL syringe and was mounted with a multichannel nozzle (4 channel) for electrospinning. The electrospinning parameters were set on a 30 μL/min flow rate applied with 15 kV voltage. The distance between the needles and the rotational drum collector was fixed to 7 cm. The rotational drum collector was wrapped with parchment paper providing a nonadherent surface. The rotational speed of the collector was fixed at 1000 ± 50 rpm. The scan distance of the collector on vertical axis was fixed to 2 cm. All the electrospinning processes were performed at 32 ± 2 °C with 35 ± 4% relative humidity. The obtained nanofibrous dressings were dried in an oven at 30 °C overnight to remove traces of solvent, followed by vacuum drying at 50 °C for 24 h using a vacuum oven.

For the incorporation of gallic acid into the electrospun nanofibrous dressings, a stock solution of gallic acid in methanol was prepared and stored in the dark (amber-colored Eppendorf tubes). The prepared gallic acid solution was added to AP solution at a concentration of 0.5% (w/w) of the AP solution and labeled AP-GA. The prepared AP-GA solution was electrospun on the prepared base layer of agar/AgNPs films in the dark and labeled Agar/AP-GA. The developed Janus dressings were dried at 30 °C in a hot air oven followed by drying in a vacuum oven for 24 h at 50 °C and stored in aluminum foil to avoid
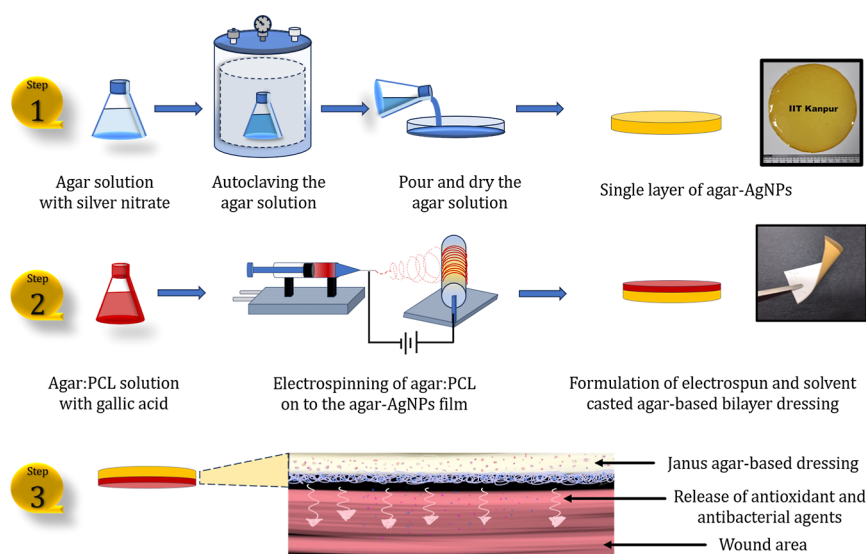
Figure 1. Schematic of fabrication of agar-based bilayer dressing. Step 1 involves the fabrication of single layer of agar incorporated with silver nanoparticles as an antibacterial agent using the solvent casting method. In step 2, the Janus structure was developed using electrospinning of agar/PCL infused with gallic acid as an antioxidant. Step 3 details the sustained release of antioxidant and antibacterial agents at the wound site.

photodegradation of gallic acid for later use. Graphical schematic of the formation of Janus dressing is shown in Figure 1.

Cross-Linking of Electrospun Agar-Based Dressing. The prepared Janus structure of the electrospun AP-GA and agar/AgNPs base layer was cross-linked using vapors of glutaraldehyde (25%). In brief, the prepared films were sealed inside a vacuum desiccator (polypropylene, dia-210 mm) containing 20 mL of glutaraldehyde solution. The desiccator was vacuum-sealed, and the Janus dressings were cross-linked for 5 h in the presence of glutaraldehyde vapors. After the predefined period, the cross-linked bilayer structure was dried in a hot air oven in the dark for 48 h at 30 °C to remove glutaraldehyde, followed by 24 h drying in a vacuum oven at 50 °C. The prepared films were stored for later use in aluminum foil.

Characterization. *Optical Properties.* Using a UV−vis spectrophotometer (Evolution 201, Thermo Fisher), the reduction of $AgNO_3$ to silver nanoparticles was validated. The AgNP-containing agar films (1 cm × 1 cm) were adhered to the cuvette window using a double-sided tape, and absorbance spectra from 300 to 600 nm were recorded.

Morphological Studies. The surface and cross-sectional morphology of the developed bilayers were analyzed using field emission scanning electron microscopy (FEI NOVA NANO SEM 450 FESEM). The samples were mounted on an aluminum stub using carbon tape and gold sputter-coated using an EMITECH SC 7620 sputter coater for 180 s at 40 mA plasma current.

Porosity. The liquid displacement method was employed to determine the microporosity of the electrospun mats, following the previous literature.[31] Briefly, three electrospun samples, each measuring 1.5 cm × 1.5 cm, were preweighed and then soaked in absolute ethanol for 1 h. After a defined time interval, the wet samples were weighed again to evaluate the porosity of the electrospun mats using

$$\text{Porosity \%} = \frac{\text{wet weight} - \text{dry weight}}{\text{density of ethanol} \times \text{volume of mat}} \times 100$$

where the wet and dry weight refers to the weights of the electrospun mats after and before ethanol submersion, respectively. The density of ethanol was accounted for based on the ambient conditions.

Nanostructure Analysis. Using an electron transmission microscope (FEI-Tecnai G2 12 Twin 120 kV), we observed the nanoparticles of AgNPs. Carbon-coated PELCO GRIDS 200 CU were utilized for sample mounting. The samples (AgNPs incorporated agar films) were immersed in DI water overnight to release nanoparticles into the medium; then, 2 μL of solution was spread on a copper grid and dried in a vacuum desiccator. The grid with nanoparticles was observed by TEM using selected area electron diffraction.

Chemical Analysis. The FTIR spectrum was investigated using Fourier transform infrared spectrometer model PerkinElmer spectrum version 10.03.06 in the range of 400−4000 cm^{-1} to analyze the presence of functional groups. Briefly, 20 mg of finely chopped electrospun sample was mixed with 80 mg of potassium bromide (KBr) powder and ground into fine powder using a mortar and pestle followed by drying it overnight at 45 °C in a hot air oven to remove moisture from the samples.

Mechanical Testing. The tensile properties of the developed samples were evaluated according to ASTM standard D 88212 using a 5 kN load cell on an Instron universal testing machine. Rectangular strips of 70 × 10 mm, grip separation 40 mm, were cut from the prepared agar samples. The thickness of the film was measured at 3 different points using a digital micrometer (Mitutoyo). The samples were stretched with a 10 mm min^{-1} cross-head speed. The average of five samples was tested for tensile strength and percentage elongation at break.

Fluid Handling Properties. The samples were tested in a solution containing 229 mg of sodium chloride and 36.8 mg of calcium chloride in 100 mL of DI water. Briefly, 1 cm × 1 cm square samples of bilayer agar films with an electrospun layer were cut and preweighed prior to submersion in 5 mL of solution for varying amounts of time. After specific time intervals, the soaked bilayer dressings were suspended from one corner using forceps to allow the solution to drip from the surface of the sample, and then the samples were weighed. The recorded increased weight relative to the initial dry weight of the samples was used to calculate the fluid retention degree by dividing the increase in weight by the initial dry weight.

$$\text{Swelling degree} = \frac{(\text{wet weight} - \text{dry weight})}{\text{dry weight}}$$

To calculate the dehydration rate, the samples were immersed overnight in the aforementioned solution and were dehydrated in an incubator at 37 °C with 42% RH for a predetermined time interval. The dehydration rate (g/min) was calculated by dividing the weight difference (g) by the dehydration time (min).

In a similar manner, the absorption rate of the prepared solution was determined by dropping a 20 μL droplet of the solution on the surface of the sample and timing the droplet absorption using a digital stopwatch. The durations of 10 drops were recorded in order to determine the average absorption rate. The protocols were in accordance with the SMTL test standard BS EN 13726-1:2002 Section 3.2—free swell absorptive capacity.[32]

C

Wettability. To achieve a uniform surface, electrospun samples were adhered to coverslips by using a double-sided tape. Using a micropipette (Tarson), 5 μL of DI water was dropped gingerly on the sample. To determine the wettability of the developed samples, the Goniometer DSA 25 (Drop shape analyzer) was used to measure the average of three water contact angles.

Water Vapor Transmission Rate. The water vapor transmission rate was determined by using the ASTM standard E-96 with a slight modification. Briefly, 15 mL of DI water was added to 20 mL culture bottles, leaving a uniform headspace between the sample and water interface. The 19 mm-diameter sample films were mounted with care on the mouths of the filled vessels, and then the rims were sealed using parafilm. As positive and negative controls, an open container and a polyester sheet-capped culture bottle were designated. After mounting the samples, the initial weight (in grams) was determined, followed by weight measurements at regular intervals every 24 h for 7 days. Using the graph, the slope of weight loss vs time was determined. The WVTR ($g/m^2/24$ h) for the samples was then calculated by dividing the slope by the area of moisture transmission (A, in m^2).

$$\text{WVTR} = \frac{\Delta W}{A \times \Delta t}$$

In Vitro Degradation Studies. Biodegradation of the bilayer dressing was performed using an in vitro degradation study, as previously described.[33] 1 cm × 1 cm samples were incubated in 5 mL of phosphate-buffered saline (PBS), pH 7.4, containing lysozyme (1 mg/mL) and H_2O_2 (2.58 μM) at 37 °C for defined time intervals (1, 3, and 7 days). The degradation percentage of the samples is calculated as follows

$$\text{Degradation \%} = \frac{W_0 - W_t}{W_0} \times 100$$

where W_0 is the initial weight and W_t is the dried weight of the sample at time t.

Antioxidant Properties—DPPH Assay. To quantify free-radical scavenging properties of the gallic acid-incorporated electrospun top layer on silver NPs containing an agar-based bilayer dressing, the 2,2-diphenyl-1-picrylhydrazyl (DPPH) spectroscopic method was employed. Dressings of 1 cm (diameter) were taken off from the asymmetric Janus dressing using a 1 cm (diameter) biopsy cutter. After 15 min of soaking in 200 μL of DI water, 500 μL of DPPH methanolic solution (500 μM) was added to the circular discs and were incubated at 37 °C for varying amounts of time. The absorption of reduced DPPH radicals from the hydrogen donor gallic acid was measured using a microplate reader at 517 nm after a predetermined time interval. As a control, a DPPH solution was taken. The test was conducted in triplicate with the mean value and standard error reported.

$$\text{Inhibition \%} = \frac{(\text{absorbance of control} - \text{absorbance of sample})}{\text{absorbance of control}} \times 100$$

ICP-MS Analysis of Released Silver Concentration. Silver release from the developed Janus nanofibrous dressing was assessed using an ICP-MS from Agilent Technologies (model no: 7900 ICP-MS). For the ICP-MS analysis, Milli-Q ultrapure deionized (DI) water was utilized for all dilutions and standard preparations. A high-purity ICP multielement calibration standard 2A solution from Agilent Technologies was employed for the standard calibration curve. The linearity of the samples in relation to the reference solution curve was considered acceptable with a standard deviation less than 5% (coefficient of linear correlation, >0.999).

For the release assay, 1 cm^2 circular discs (triplicates) of the developed dressing were incubated in Milli-Q ultrapure water for the required time intervals. After defined incubation intervals, aliquots from each sample were collected and replaced with the same volume of Milli-Q ultrapure water. To evaluate the total amount of silver content, sample discs were dissolved in the required Milli-Q ultrapure water at 90 °C and diluted accordingly. All of the solutions were filtered using a 0.22 μm syringe filter (PVDF hydrophilic membrane, Himedia).

The release kinetics were evaluated with the assistance of different release models, including zero-order, first-order, Higuchi, and Korsmeyer–Peppas models. The models that best fitted with the data with an R^2 value of 0.99 were considered the best release model for the developed dressing. The model equations[34] are mentioned as follows

$$\text{Zero} - \text{order model: } Q = kt + Q_0$$

$$\text{First} - \text{order model: } Q = Q_0(1 - e^{-kt})$$

$$\text{Higuchi model: } Q = kt^{1/2}$$

$$\text{Korsmeyer} - \text{Peppas model: } Q = kt^n$$

where Q represents silver release at any time, Q_0 defines total drug concentration, the rate constant is specified as k, and n is a release exponent. The power law model[35] includes different mechanisms, including Fickian diffusion and release mechanism due to relaxation and swelling of the polymer matrix, depending on the n value. When $n = 0.5$, it represents Fickian diffusion, $n = 1$ represents zero-order release, and $n > 0.5$ indicates non-Fickian release due to relaxation or swelling of the polymer matrix.

Antibacterial Properties. *Agar Disc Diffusion Assay.* The antibacterial activity of the developed Janus nanofibrous dressing was tested using a disk diffusion assay. Overnight growth cultures for *E. coli*, *P. vulgaris*, *P. aeruginosa*, and *S. aureus* were prepared, and the optical density (OD) was measured at 600 nm using a UV spectrophotometer (Thermo Scientific Evolution 201). The cell suspensions were further diluted to a final inoculum of 10^6 cells/mL and were seeded in Mueller Hinton agar media (MHA) plates. To prepare MHA plates, Muller–Hinton broth (MHB) 21 g was dissolved in 1 L with 1.5% agar, followed by autoclaving at 121 °C for 15 min. Sample discs were placed carefully on the inoculated plates and were kept 37 °C. After 24 h of incubation, the zone of inhibition (ZOI) against the aforementioned microorganisms was measured (in mm) for each sample in triplicates.

Time-Kill Assay—Log Reduction. Time-kill assay was performed to analyze the antibacterial properties of silver nanoparticle-incorporated agar films in accordance with the method described by Sharma et al.[36] Briefly, overnight grown culture of *E. coli*, *P. vulgaris*, *P. aeruginosa*, and *Staphylococcus* was cultured using a single colony of the respective bacteria in MH Broth (MHB). The overnight bacterial cultures were diluted to 0.1 OD (600 nm) for the log reduction assay using MHB. In a 48-well plate, samples of agar/AP-GA, 0.1 agar/AP-GA, 0.2 agar/AP-GA, and 0.3 agar/AP-GA were incubated in the mentioned bacterial solution at 37 °C for varied duration. After every 2 h intervals, samples of the bacterial suspension were collected, followed by serial dilution in sterile normal saline solution, plating on MHA plates, and incubation at 37 °C overnight. The bacterial colonies were enumerated from the overnight incubated plates, and the number of colony-forming units per unit volume (CFU/mL) was evaluated. The results were presented in log CFU count of bacterial growth.

Hemocompatibility—Hemolysis Assay. The hemocompatibility of the prepared samples was evaluated using a freshly prepared suspension of ruminant (goat) red blood cells (RBCs). To produce the RBC suspension, fresh goat blood chelated with 0.5 mM EDTA (500 μL) was collected from a local butcher shop in a sterile polystyrene tube (Tarsons). Blood was centrifuged at 700g for 10 min to separate RBCs from blood. Plasma and other blood components contained in the supernatant were discarded, while the RBCs were preserved for the preparation of the RBC suspension. The RBC pellet was then rinsed three times with a cold PBS (pH 7.4) solution by dispersing it in PBS and centrifuging it at 700g for 10 min. Finally, the obtained RBC pellet was then subsequently dispersed in PBS with a 10-fold dilution and used as an RBC suspension. In the meantime, 6 mm (diameter) sample discs were cut from the developed Janus nanofibrous dressings including agar/AP-GA, 0.1 agar/AP-GA, 0.2 agar/AP-GA, 0.3 agar/AP-GA, 0.4 agar/AP-GA, and 0.5 agar/AP-GA films. The samples were rinsed three times with PBS to impede osmotic shock to RBCs, followed by incubation in RBC suspension for 120 min at 37 °C. Triton-X (0.01%) and RBC suspension were regarded as positive and

negative controls, respectively. After a predetermined period of incubation, the samples were centrifuged again at 700g to acquire the supernatant. At 540 nm, the absorbance of the sample supernatants was measured using a plate reader (BioTek microplate reader). The hemolysis percentage was computed by

$$\text{Haemolysis}\% = \frac{(\text{abs of sample} - \text{abs of negative control})}{(\text{abs of positive control} - \text{abs of negative control})} \times 100$$

where Abs stands for absorbance recorded at 540 nm.

Platelet Adhesion. With the help of a platelet aggregation assay, the hemocompatibility of the Janus nanofibrous dressing was determined. Platelet-rich plasma (PRP) was extracted from fresh goat blood by centrifuging at 700g for 10 min. The supernatant PRP was again centrifuged at 2000g for 20 min at 4 °C using a tabletop centrifuge (Thermo Scientific SORVALL ST 16R) to obtain platelet poor plasma (PPP). Platelets were enumerated with a hemocytometer and adjusted to 1×10^7 platelets with platelet-poor plasma (PPP). The bilayer dressing (1 cm in diameter) was rinsed twice with PBS, infused with 200 μL of PRP, and incubated at 37 °C for 1 h. After the incubation period, samples were delicately rinsed three times with PBS and dehydrated using a gradient ethanol treatment (50%, 60%, 70%, 80%, 90%, and 100% ethanol) for 10 min in each concentration. The alcohol was removed from the dehydrated samples using freeze-drying, followed by gold coating for SEM visualization (as mentioned above).

Cytocompatibility—MTT Assay. The cytocompatibility of the developed Janus nanofibrous dressing against NIH 3T3 fibroblast cells was evaluated. The fibroblast cells were cultured in complete DMEM containing 10% FBS, 1% antibiotic (penicillin and streptomycin) solution, along with 5% CO_2 in a humidified environment at 37 °C. According to Jiji et al.[37] and Ying et al.,[38] direct and indirect assays were performed, respectively. Briefly, bilayer scaffolds measuring 10 mm in diameter were UV-sterilized for 2 h on each side. Three $\times 10^4$ cells were inoculated in 24-well tissue culture plates (TCP) for a defined period, with samples in direct contact and using insert plates for indirect contact. The culture plates were incubated for 24 h in the presence of samples. To evaluate cell viability, the complete medium was substituted with a 0.5 mg/mL MTT solution prepared in incomplete DMEM (complete DMEM without FBS). After 4 h of incubation with the MTT solution, the percentage of viable cells was determined based on the formation of formazan crystals within the cells. The formed formazan crystals were dissolved in 200 μL of DMSO, and then their absorption at 570 nm was measured. The wells inoculated with cells without any sample or sample extract were regarded as positive control.

$$\text{Cell viability}\% = \frac{\text{sample absorbance}}{\text{control absorbance}} \times 100$$

Cytocompatibility—Wound Scratch Assay. The wound scratch assay was conducted in accordance with a previously cited literature.[39] In short, fibroblast cells were cultured in a 24-well plate with a cell density of 4×10^5 cells/well and incubated for 48 h at 37 °C with 5% CO_2 in a humidified environment until 90% confluency was achieved. To simulate a wound scratch, a monolayer of fibroblast cells was scratched with a 10 μL pipet tip. The 5 mm × 5 mm samples were UV-sterilized for 2 h, washed with PBS (pH 7.4), and then saturated with complete DMEM. The cells were then treated with saturated samples comprising Janus nanofibrous agar films devoid of silver nanoparticles (A), 0.1 mM bilayer agar films (B), 0.2 mM bilayer agar films (C), and an electrospun primary layer with gallic acid (D) loaded in insert plates. As a positive control, cells cultured on TCP without any sample were considered, whereas DMSO-infused cultured cells were used as the negative control. After 24 h of cell culture, digital images were acquired using a Leica inverted DMi8 microscope at 20× magnification, and the wound scratches were monitored for cell migration and proliferation by captured images. Wound closure area was measured with the help of ImageJ software[40] by using the equation

$$\text{Wound closure area (\%)} = \frac{(\text{initial scratched area} - \text{final scratched area})}{\text{initial scratched area}} \times 100$$

In Vivo Wound Healing Studies. The wound healing ability of the developed Janus nanofibrous dressing was evaluated using in vivo studies with full-thickness excisional wound healing on a rat model approved by the Institutional Animal Ethics Committee (approval number: IAEC/UIP/AUG.2023/029). The adult male SD rats weighing 200−250 g were kept separately in plastic cages and acclimatized at 23 ± 2 °C and humidity 50−60%. They were fed pelleted food and tap water ad libitum during an experimental period of 18 days. The animals were anesthetized with two interperitoneal injections of ketamine and diazepam with doses of 50 and 5 mg/kg of rat, respectively. The sedation was followed by shaving the surgical area on the dorsal skin of the rats using a manual razor. Prior to the experiment, the rats were divided into six groups ($n = 3$ per group). Group I was a 0.2 mM silver nanoparticle solution (AgNPs), group II was treated with neat agar film, group III was an agar-based electrospun Janus nanofibrous dressing, group IV was an antibacterial silver-based commercial dressing (Sterizone), group V was treated with povidone-iodine, and group VI was the untreated control group. Six excision wounds of 6 mm diameter were created on the dorsal skin, three on each side of the median line, using a punch-biopsy needle. Then, the wounds were treated with a 1 cm^2 circular disk of developed dressings and other controls (groups II and IV). While groups I and V were treated with 200 μL of AgNPs and povidone solution, respectively, followed by the measurement of the contraction area of each wound after every consecutive 3 days for each group of animals until completely healed. For the wound contraction, the healing was examined visually, and the wound area was measured using ImageJ software.

$$\text{Wound contraction}\% = \frac{\text{wound area on day 0} - \text{wound area (day 3, 6, 9, \&12)}}{\text{wound area on day 0}} \times 100$$

For histopathological studies, the healed 1 cm^2 circular wound area was excised using a punch-biopsy and fixed in a 10% formalin (v/v) solution at 4 °C. The excised tissue sections were dehydrated using gradient alcohol from 50 to 100% (v/v). The tissue blocks were cleared in xylene, followed by xylene and paraffin wax (1:1) solution, followed by embedding in paraffin wax and sliced into 10 μm-thick sections, followed by placing on glass microscopic slides coated with polylysine solution. The sliced sections were stained with hematoxylin and eosin (H&E) stains for microscopic imaging. The stained samples were dehydrated and imaged with the help of a light microscope Leica inverted DMi8 microscope at 4× magnification.

Statistical Ananlysis. The results were expressed as mean ($n = 3$) ± standard error for all analysis. For the test groups, one-way analysis of variance was performed; p-value ≤ 0.05 was considered significant. In the figures, p-value was represented as star "*", where one stars "*" equated to ≤0.05 significance level, two stars "**" equated to ≤0.01, and three stars "***" equated to ≤0.001.

■ RESULTS AND DISCUSSION

Preparation of a Silver-Incorporated Agar Film. In the present study, one-pot in situ reduction of silver nanoparticles was performed using a hydrothermal method in the presence of agar, which includes a standard autoclave procedure. To the best of our knowledge, this process has not been previously reported with agar. Earlier, similar studies were performed in the presence of starch and gum ghatti.[41] After standard autoclaving, the agar solution containing the resultant silver nanoparticle solution changed from transparent to light yellow, indicating the formation of Ag^0 from Ag$^+$ ions. The reduction of silver ions to silver atoms could occur by reducing groups, mainly
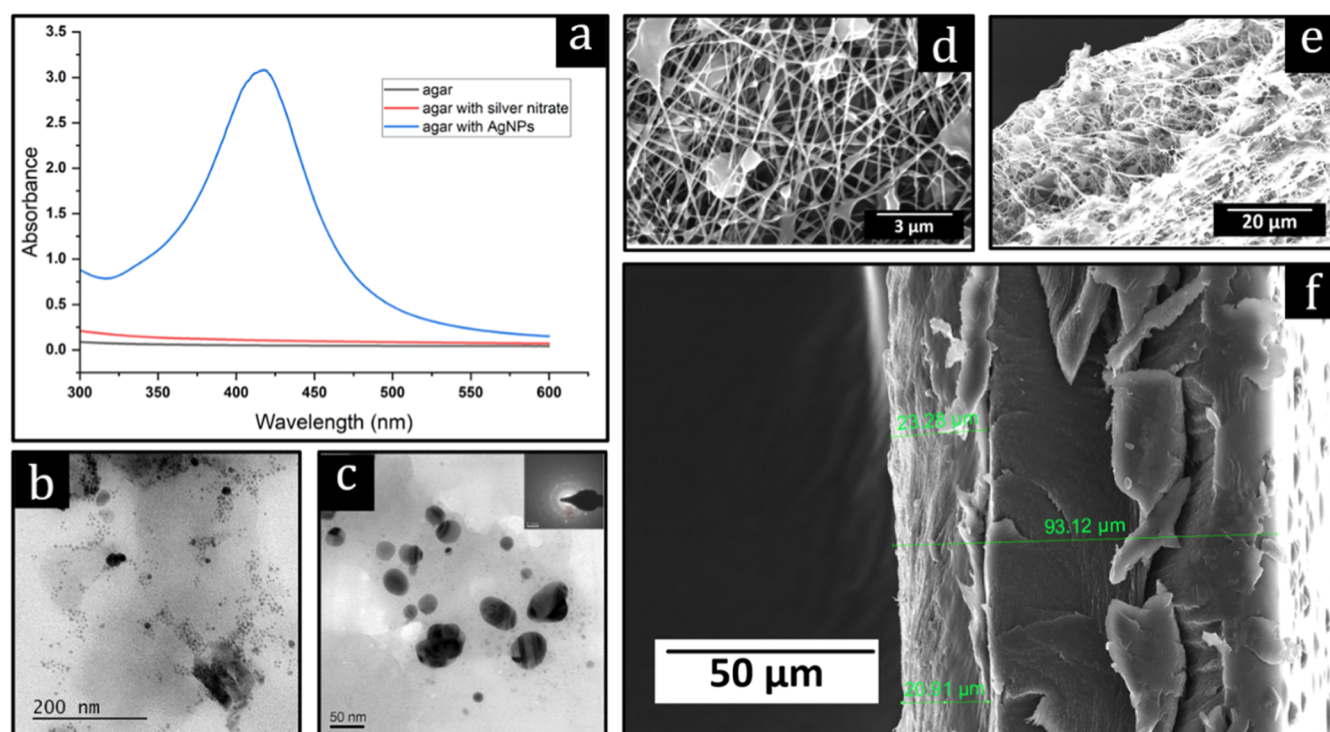
Figure 2. (a)Absorption spectra of agar solution, agar with silver nitrate solution (before autoclaving), and agar with silver nanoparticles (after autoclaving). TEM micrograph (b,c) of AgNPs synthesized using an autoclave with ED patterns in the inset view (c). Micrograph of surface (d) and cross-sectional morphology (e) of agar/PCL-gallic acid (AP-GA) electrospun mat and bilayer morphology (f) of the developed agar-based dressing (agar/AP-GA) where the electrospun layer (left side) was coated on a solvent-casted agar layer (right side).

aldehydes and alcoholic groups of saccharides,[42] and further catalyzed by thermal activity using autoclaving. The developed nanoparticles were characterized by using various techniques, including UV−vis spectroscopy and transmission electron microscopy.

Characterization of Silver Nanoparticles. *Optical Properties.* Due to autoclaving, silver nitrate was reduced to silver nanoparticles (AgNPs) that exhibited a characteristic absorption peak at 417 nm (Figure 2a) due to surface plasmon resonance. Furthermore, the solution changed from colorless to light pale, indicating the formation of silver nanoparticles (AgNPs), during the autoclaving process. After solvent-casting of the autoclaved agar solution, the resultant dried films also exhibited same pale color.

Figure 2b,c shows the transmission electron micrographs of AgNPs with wide size distribution ranging from 10 to 100 nm. Electron diffraction patterns (Figure 2c—inset image) of AgNPs are consistent with the family of the reflection of (111), (200), (220), (311), and (222) planes that are reported in the literature.[43]

Fabrication of Janus Nanofibrous Dressing Mats. With the development of Janus nanofibrous wound dressings, it was anticipated that the primary layer, in contact with the wound, would release bioactive agents rapidly, while the secondary layer would exhibit sustained release of antibacterial agents over an extended period. By using bilayer or multilayer dressings laden with multiple bioactive agents, chronic wound management can be enhanced throughout various phases of the healing process. The nanofibrous layer in contact with a lesion would display high loading efficacy due to a high surface area-to-volume ratio and enhance vapor permeability. Furthermore, the second layer of agar would form a hydrogel after absorbing the requisite

volume of wound exudates, which would further assist in the release of infused silver nanoparticles. Moreover, exhibiting antibacterial efficacy would enhance wound care management.

Morphological Analysis. Using SEM imaging, the surface and cross-sectional morphology of the electrospun nanofibrous dressings were evaluated (Figure 2d,e). The developed nanofibrous mats exhibited a studded structure. As solvents such as glacial acetic acid evaporate rapidly, beaded structures form in the electrospun membranes.[44]

The micrographs of cross sections of the developed Janus nanofibrous dressing revealed both electrospun (∼20 μm) and solvent-casted (∼90 μm) layers (Figure 2f). The cross-sectional image of the electrospun layer revealed a porous structure that would allow for the consistent release of antibacterial silver nanoparticles to the wound. Albeit, the primary layer enhances the free radical scavenging behavior with the release of gallic acid. Moreover, the porous structure will allow absorption of wound exudates, thereby preventing maceration, in addition to protecting against external injury and infection.

Porosity. The porosity of the developed electrospun porous layer was assessed by using the liquid displacement method. The electrospun agar/PCL-gallic acid electrospun mat exhibited a porosity of over 98.9% (±2.2). The nanofibrous morphology of the electrospun layer facilitates the exchange of nutrients, gases, and fluids while effectively retaining exudates, owing to its high surface area. According to the Figueira et al., a porosity of over 90% is beneficial for wound healing.[31]

Compositional Analysis. Figure 3a and b depicts the FTIR spectrograms of the electrospun and solvent-cast films' chemical compositions. Except for peak intensity, the chemical compositional peaks of agar with and without $AgNO_3$ were exactly the same (Figure 3a). The absorption band between 3600 and 3100
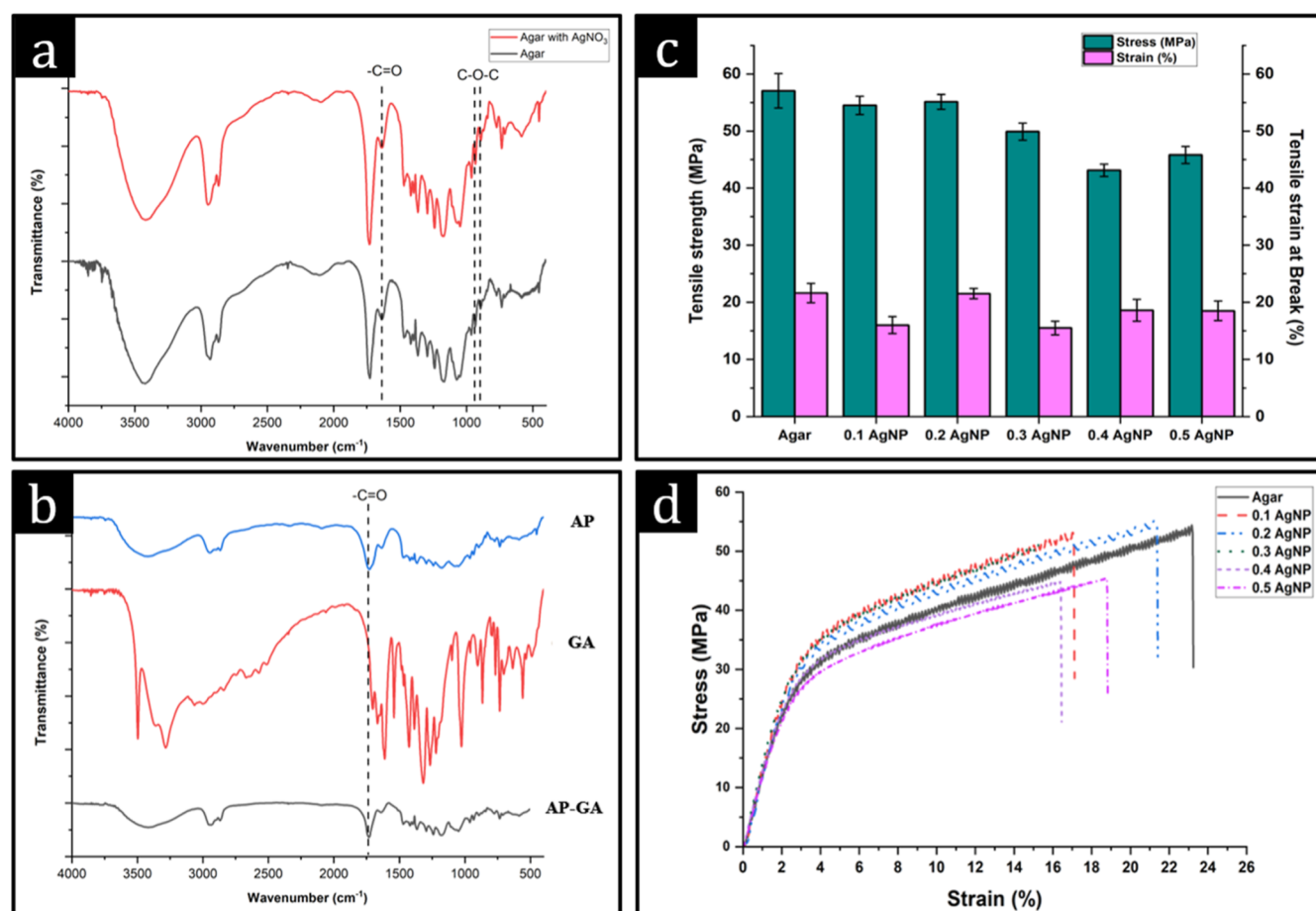
Figure 3. FTIR spectrogram of both the layers after blending agents with the polymers: (a) agar film with and without silver nitrate and (b) agar/PCL electrospun (AP) layer without gallic acid and with gallic acid (AP-GA), where GA indicates gallic acid. Tensile properties (c) of the developed agar-based silver nanoparticle films with their characteristic stress−strain graphs (d).

cm^{-1} was allocated for O−H stretching, which accounted for the hydrophilic properties of the polymer. The carbonyl group (C= O) was associated with the distinct band at 1639 cm^{-1}. At 1364 cm^{-1}, an extra intense peak of ester sulfate was observed. In addition, the C−O−C vibration bands of anhydrogalactose and galactose of agar at 934 and 890 cm^{-1}, respectively, were observed. The spectrograms of agar with AgNO$_3$ are similar to the earlier reported literature.[45,46]

After the two polymers (agar and PCL) were combined in equal proportions, FTIR spectroscopy was used to verify the chemical compositions of the electrospun layers. The vibrational elongation of −OH bonds, which corresponds to the hydroxy group, can be observed between 3600 and 3200 cm^{-1}. At 2931 and 2868 cm^{-1}, the asymmetrical and symmetrical elongation of −CH$_2$ and −CH$_3$, respectively, can be observed. At approximately 1068 cm^{-1}, the synthetic polymer PCL −C−O stretch of the ester group has attained its maximum. These stretchings are typical of −CH bonds in PCL and agar. In polymer agar, another characteristic peak of symmetrical and asymmetrical stretching vibrations of −COOH of carboxylate ions can be identified in the spectrogram for polysaccharides.[47] For synthetic polymers, the −C=O stretching vibration of the carbonyl functional group can be observed at 1727 cm^{-1}.[48] All of the previously mentioned peaks were also observed in the composites of polymers with synthetic polymers, indicating that the addition of polymer or silver nitrate had no effect on the chemical

composition of the polymer matrix. The outcomes are depicted in Figure 3b.

Mechanical Properties. Wound dressings necessitate both strength and flexibility to conform to the body's natural movements without causing disruption or tearing. The tensile properties of the silver-impregnated agar films were evaluated by using a uniaxial tensile test. Agar demonstrated a strength of 54.88 MPa with 20% elongation at break. The tensile strength and strain of the developed silver impregnated agar film are depicted in Figure 3c,d. The tensile strengths of 0.1 and 0.2 AgNPs agar films remained the same as that of agar films. However, when the concentration of silver nitrate exceeded 0.3 mM, there was a slight decrease in the strength. The reduction of silver nitrate led to the formation of well-dispersed silver nanoparticles, which acted as hard phases within the matrix. Higher concentrations of silver nanoparticles may result in nonuniform agglomeration of NPs, leading to decreased strength in the resulting films.[49] Since the material was developed for wound dressing application and a very high amount of silver was not required for such applications, the role of even higher silver content on the mechanical properties was not studied. Moreover, due to the inclusion of glycerol, the films exhibited moderate strain values.

Fluid Handling Properties. The test measured the fluid absorption capacity, dehydration rate, and absorption rate to evaluate the fluid-handling capabilities of the Janus nanofibrous films. Fluid handling properties play a crucial role in wound
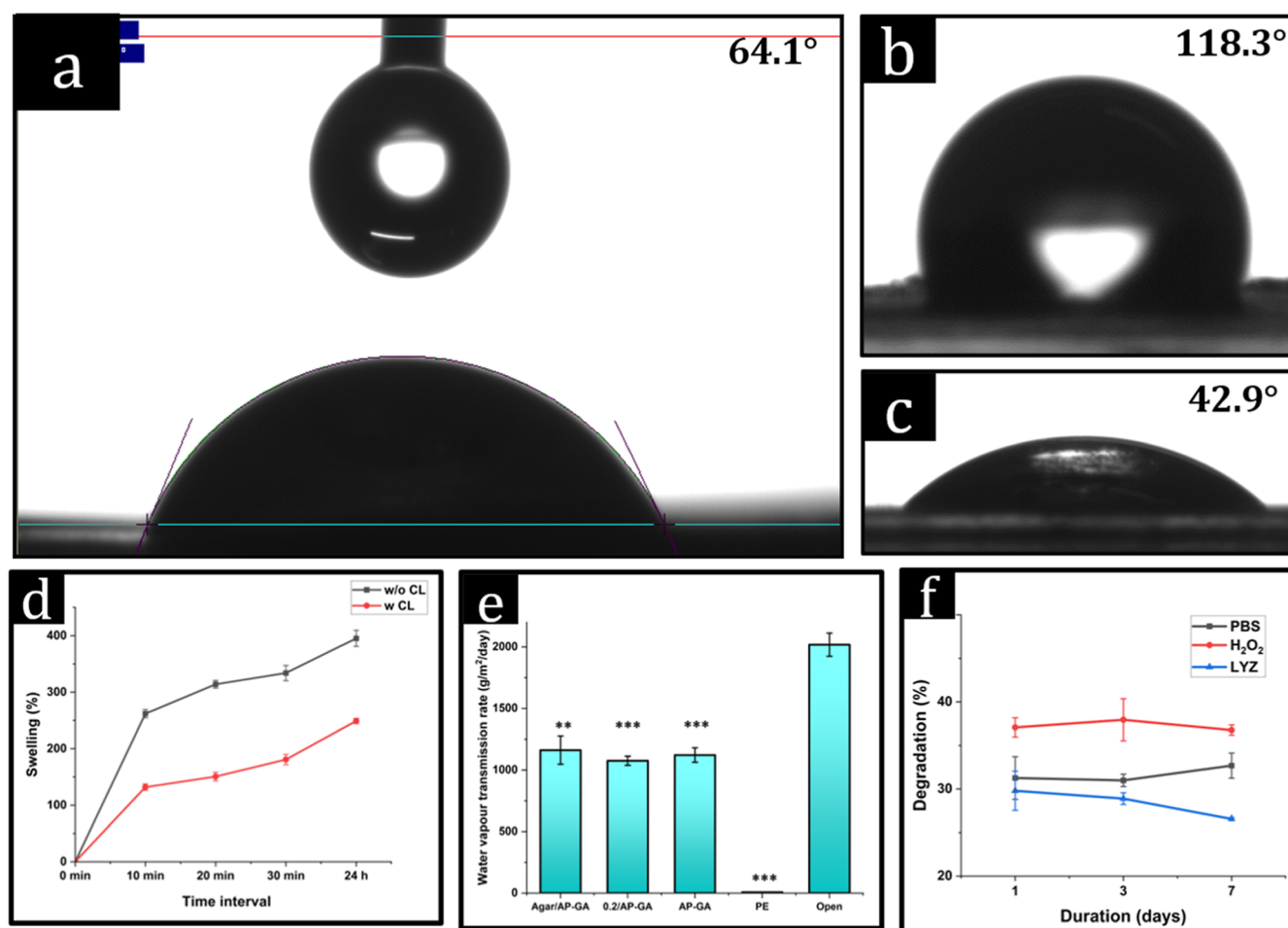
Figure 4. Contact angle of electrospun agar/PCL with gallic acid (a) dressings as an antioxidant agent (AP-GA). The contact angle of control film PCL (b) and agar (c) also displayed their wettability. (d) Swelling behavior of the developed Janus nanofibrous dressings before and after glutaraldehyde cross-linking. (e) Water vapor transmission rate of the developed bilayer dressings agar/AP-GA, 0.2 agar/AP-GA, AP-GA, and polyester (PE) film. (f) Degradation percentage of 0.2 agar/AP-GA films in PBS solutions.

management and healing processes. Wound exudates are composed of numerous solutes, nutrients, growth factors, and cellular agents (inflammatory agents and enzymes). The presence of wound exudates promotes wound healing but in the optimum range to avoid both maceration and desiccation of wounds. The fluid handling properties of a dressing are demonstrated by their surface wetting behavior, moisture absorption capacity, moisture permeability, and rate of dehydration from the dressing surface.

Wettability of Electrospun Agar Films. Since the electrospun layer would serve as the interface between the wound dressing and the wound, its hydrophilicity was evaluated. Apart from fluid handling properties, the surface hydrophilicity of a wound dressing is also a crucial property. In several processes, including cell adhesion, protein adsorption, cellular contact, and other processes, the wettability of the nanofibrous mat is crucial. Given that synthetic polymer PCL is a hydrophobic polymer with a few biomedical applications, some hydrophilic polymers can improve PCL biocompatibility, as PCL (Figure 4b) contact angle ($115.7° ± 1.4$) was too high to be effective for cell adhesion. Moreover, the surface wettability of agar films was found to be $42.1° ± 1.5$ (Figure 4c), which falls within the hydrophilic range and could also limit the cell adhesion. The wettability was increased after mixing agar with PCL, and the resultant electrospun AP dressing contact angle was found to be

$61.2° ± 2.4$ (Figure 4a). Additionally, the ideal contact angle range for cell attachment should be between 55 and $80°$.[50]

Swelling Behavior. The adsorption of wound exudates is an important requirement for a dressing, especially when it is employed on chronic wounds. Fluid absorption capacity of the wound dressing depends on the composition of matrix polymer, the pH of the media, and the temperature. The swelling percentage of the neat PCL electrospun mat was observed as 6%. After the blend of agar and PCL for the fabrication of the AP electrospun mat, the swelling percentage was increased to 20%, whereas the swelling percentage of solvent-cast agar was higher due to the hydrophilic nature of the agar matrix. Nevertheless, because of the distinct swelling properties of the two layers (electrospun and solvent-cast), the fabricated layers became detachable over time in a wet environment, a problem that was resolved by glutaraldehyde cross-linking (Supporting Information, Figure S1). After cross-linking both layers with glutaraldehyde vapors, the developed Janus nanofibers of electrospun and solvent cast dressing, the swelling percentage dropped from 400% to 250% (Figure 4d).

The fluid handling capacity of the bilayer agar film (2.11 g/g ± 0.1) was slightly lower than that of 0.2 mM agar films (2.15 g/g ± 0.05), which could be due to the presence of silver in the modified films. Moreover, the dehydration rate of the developed Janus nanofibrous agar films (0.0015 g/min) was also like the 0.2

mM agar films (0.002 g/min) as the base layer was the same, which was agar. Moreover, as displayed earlier in swelling percentage after cross-linking, the developed films were getting slowly saturated with the surrounding fluid within 10 min of absorption. Hence, the dressing would absorb the excess wound exudate efficiently, impeding leakage of exudate in the surrounding tissue.

Water Vapor Transmission Rate. The permeability of the dressing materials is highly crucial to the healing process. Low wound dressing permeability causes maceration, whereas high permeability promotes desiccation. To stay moist without retaining exudates, the wound dressing must have optimal water vapor permeability (~2000 g/m^2/day).[51] Our electrospun and bilayer dressings transferred 1200 g/m^2/day of water (Figure 4e), a comparable amount of intact skin transpiration rate.[52] Therefore, these Janus nanofibrous dressings could be used for low to moderate exudating wounds.

In Vitro Biodegradation Studies. Figure 4f depicts an analysis of in vitro biodegradation, wherein the agar-based Janus nanofibrous dressing was subjected to various physiological environments. PBS solution enriched with lysozyme and hydrogen peroxide assisted in the breakdown of polymer chains within the matrix via hydrolytic and enzymatic degradation. Maximum degradation, approximately 37%, was observed in H$_2$O$_2$ PBS solution, attributed to hydrogen abstraction,[53] resulting in the digestion of glycosidic bonds.[33]

Antioxidant Properties. The antioxidant properties of a wound dressing are crucial for proper healing because they significantly reduce oxidative stress caused by ROS creation. Although ROS is required for signaling and tissue repair, excessive ROS in the lesion area may result in protein, DNA, and tissue damage. To manage this, our body's enzymatic defense systems, including superoxide dismutase (SOD), catalase (CAT), and glutathione-dependent antioxidant enzymes (GPx, GRx, and GST), regulate these free radicals. Incorporating antioxidant agents into dressings can scavenge free radicals and reduce ROS at the wound site through hydrogen atom transfer or single electron transfer.[54] This approach promotes wound healing by regulating inflammation,[55] enhancing collagen synthesis,[56] and stimulating angiogenesis.[13] Additionally, it disrupts microbial membrane,[57] preventing infection and supporting tissue regeneration for appropriate healing throughout the different phases.

In the DPPH assay, the percent reduction of free radicals was quantified by measuring absorption drop from dark purple color to pale-yellow color. The developed Janus nanofibrous dressing displayed free radical scavenging properties within minutes of sample interaction with the DPPH methanolic solution. In 15 min, the material attained 90% of antioxidant properties (Figure 5). Even after 360 min, the scavenging capabilities were at their peak due to the incorporation of gallic acid. Gallic acid possesses anti-inflammatory, antibacterial, antioxidant, antilipid peroxidation, and tissue regeneration properties, among others.[58]

Release Kinetics of Silver Nanoparticles. The efficacy of the developed antibacterial dressing incorporated with nanoparticles relies on the release kinetics of the nanoparticles. An instantaneous burst release could lead to cytotoxicity, highlighting the requirement for a controlled release to ensure efficient antibacterial properties throughout the healing phase. The release of silver nanoparticles from 0.2 agar/AP-GA was quantified by using ICP-MS. A release of silver nanoparticles (8%) was observed within 24 h, gradually increasing to a release percentage of 73% over 14 days from the samples (Figure 6).
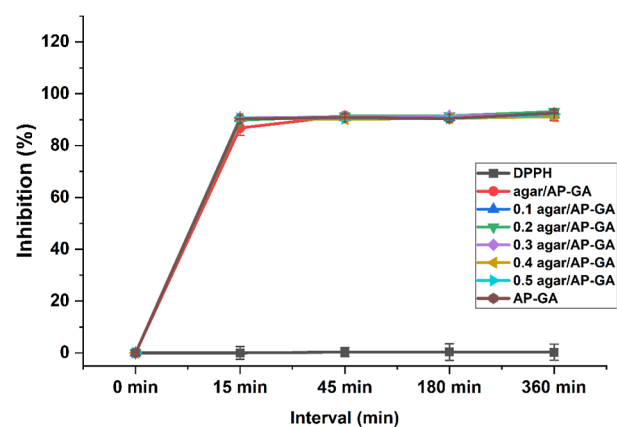

Figure 5. Antioxidant properties of the developed Janus nanofibrous dressing.
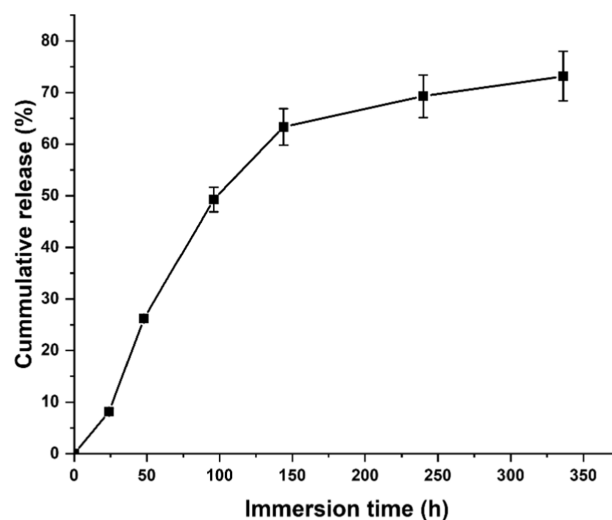

Figure 6. Silver nanoparticles' cumulative release calculated through ICP-MS.

The release kinetics were elucidated using different release kinetics models, including zero-order, first-order, Higuchi, and Korsmeyer–Peppas model. The initial 60% of the release curves were used for the model fitting,[59] and analysis was based on a statistically higher R^2 value. After fitting the zero-order model, the R^2 value indicated a high level of correlation, suggesting a consistent release rate of silver nanoparticles over time, independent of the concentration of the silver. However, Korsmeyer–Peppas found strong fits based on statistically higher R^2 (Table 1). Since these models involve release kinetics from polymeric entities, typically exhibiting non-Fickian diffusional characteristics, where both diffusion and polymer relaxation contribute to the release, the release mechanism indicated that the release of silver nanoparticles was more dependent on the relaxational release of the polymeric chains. This release behavior would mitigate the dose-dependent cytotoxicity associated with instant release and demonstrated antibacterial efficacy throughout the wound healing.

Antibacterial Testing. Antibacterial mechanism of silver (Ag^0 or Ag$^+$) for a potent bactericidal effect is investigated in earlier studies.[60] Multiple factors such as nanoparticle (NP) size, NP shape, and their uniform dispersion may influence the antibacterial properties. It could also be affected by the type of bacteria, the thickness of its lipopolysaccharide layer, the

Table 1. Release Kinetics Parameters Obtained after Applying Different Kinetic Models for the Release of Silver from the Dressing

kinetic models		sample
zero order	R^2	0.98995
	k	0.4663
first order	R^2	0.90835
	k	0.015612
Higuchi model	R^2	0.963142
	k	4.368571
Korsmeyer–Peppas model	R^2	0.99216
	n	0.898786
	k	0.753433

structural distinctions between the outer and inner membranes, and the efflux pump.

ZOI test was performed on the samples with AgNPs to evaluate their antibacterial properties. In *E. coli,* the ZOI after 24 h incubation was increased by 36%, 44.4%, and 22% for 0.1 agar/AP-GA, 0.2 agar/AP-GA, and 0.3 agar/AP-GA bilayer samples, respectively. For 0.2 agar/AP-GA test samples, the 44.4% and 39% increased inhibition zone was observed for *S. aureus* and *P. aeruginosa*, respectively. Compared to *E. coli*, *S. aureus,* and *P. aeruginosa*, the ZOI value of *P. vulgaris* plates were significantly higher, indicating greater antibacterial activity of NPs against Gram-negative bacteria. Thus, AgNPs demonstrated distinct antibacterial efficacy against both Gram-positive and Gram-negative bacteria. Similar antibacterial properties of silver have been observed in previous studies.[61] 0.2 agar/AP-GA films demonstrated good antibacterial activity (Figure 7a) without sacrificing their biocompatibility (Figure 7b), as higher concentrations of these particles result in cytotoxicity. In addition, increased silver nanoparticle concentrations result in agglomeration, which delays the nanoparticle dissolution from the solvent-cast films.

Time-Kill Assay. Using the time-kill assay, antibacterial properties against Gram-positive and Gram-negative microorganisms were evaluated as log reduction in CFU count (Figure 7c–f). The growth curve of control cells increased with time, whereas the growth curve of cells in contact with silver NP agar Janus nanofibrous films remained stationary, indicating bacteriostatic behavior of the Janus nanofibrous structure. In addition, 0.2 mM agar/AP-GA bilayer films exhibited the most potent antibacterial effect against Gram-negative bacteria such as *P. aeruginosa* and *P. vulgaris*, reducing bacterial growth by 92% and 81%, respectively. Reduced antimicrobial properties were observed for 0.1 mM and 0.3 mM samples, which could be due to low concentration and nanoparticle agglomeration, respectively.

Hemocompatibility Assay. The functionality of the developed samples for erythrocytes, or RBC, was examined using a hemocompatibility assay to validate their blood compatibility for wound dressing application. Hemolysis or nonhemocompatibility is demonstrated if the developed material disrupts RBC within the allotted period when interacting with the biomaterial. Hemolysis of all samples was less than 5% (Figure 8a), depicting a highly hemocompatible nature of the developed material.[62]

Platelet Adhesion. Additionally, the samples were incubated with PRP to further explore the effect on the platelets. As illustrated in Figure 8b, the agar/AP-GA Janus nanofibrous dressing exhibited platelet adhesion and aggregation, as indicated by the presence of spiny pseudopodia, thus confirming platelet activation. The activation of platelets observed in this study can be attributed to the inclusion of gallic acid, which resulted in increased platelet aggregation and activation, which was absent in the PCL nanofibrous mat (Figure 8c). Previous studies have demonstrated that gallic acid exhibits a comparable impact on platelet adhesion.[63]

The results indicate that the developed agar/AP-GA Janus nanofibrous dressing plays a significant role in promoting platelet adhesion and activation, making it a promising option for improving wound healing and related applications.

In Vitro Cytocompatibility Test. Direct and indirect contact assay using inset plates; the cytocompatibility of the prepared dressing material was evaluated using the MTT assay. The adverse effects resulting from direct contact or by nanoparticle release on the cells were assessed using direct and indirect assays of the developed dressings, respectively. Cellular attachment and proliferation were found to be more prominent in the PCL electrospun mat (Figure 8d), as compared to AP nanofibrous dressings (Figure 8e). The cellular attachment and proliferation on the electrospun mats could be attributed to the surface morphologies, providing molecular physical cues for proliferation and attachment.[64] Therefore, the beaded structure of the electrospun layer could influence the reduced cell adherence. After incubating in the presence of cells, the electrospun mats exhibited the characteristic cell attachment. Since silver nanoparticles are toxic at high concentrations, cytocompatibility testing was used to determine the optimal concentration. The percentage of viable fibroblast cells decreased as the concentration of silver nanoparticles in the direct contact assay increased (Figure 8g). Up to a concentration of 0.2 mM, more than 60% of cells were viable in silver nitrate-incorporated agar films with agar/AP-GA Janus nanofibrous dressings, but as the concentration was increased, the mats began to exhibit cytotoxicity due to contact-killing phenomenon.[65] Therefore. 0.2 mM silver nitrate was the optimal concentration of silver nanoparticles for the mats. In the indirect contact experiment, all the produced films exhibited greater than 95% cell viability (Figure 8f).

Wound Scratch Assay. After 24 h of incubation in the presence of samples, the cells migrated and multiplied in the scratched area (Figure 9a–f). Although films containing silver nanoparticles exhibited a small amount of cytotoxicity, the base material agar had a positive effect on cell migration and proliferation. Consequently, the developed dressing materials exhibited optimal cytocompatibility and cell proliferation.

Scratch analysis depicts the percentage of wound closure that signifies scratch healing (Figure 9g). The healing of the scratch in the presence of samples was compared with the control samples. Janus nanofibrous agar films displayed good cell migration, which could be due to agar. Wound closure of a 0.2 agar/AP-GA film (79.2%) was lower than that observed in a 0.1 agar/AP-GA film (86.8%), which could be due to release of silver NPs. Although there was a slight decrease in cell migration within the scratched area compared to the control cells, the developed dressings demonstrated a promotion of cell proliferation and growth, albeit at a slower rate in the cell migration process. Nonetheless, the developed Janus nanofibrous dressing exhibited cell proliferation and growth, making it a viable candidate for biomedical application.

In Vivo Studies. Despite the slower rate of cell migration observed in the scratch assay with 0.2 agar/AgNPs, the sample was selected for in vivo studies due to its significant antibacterial
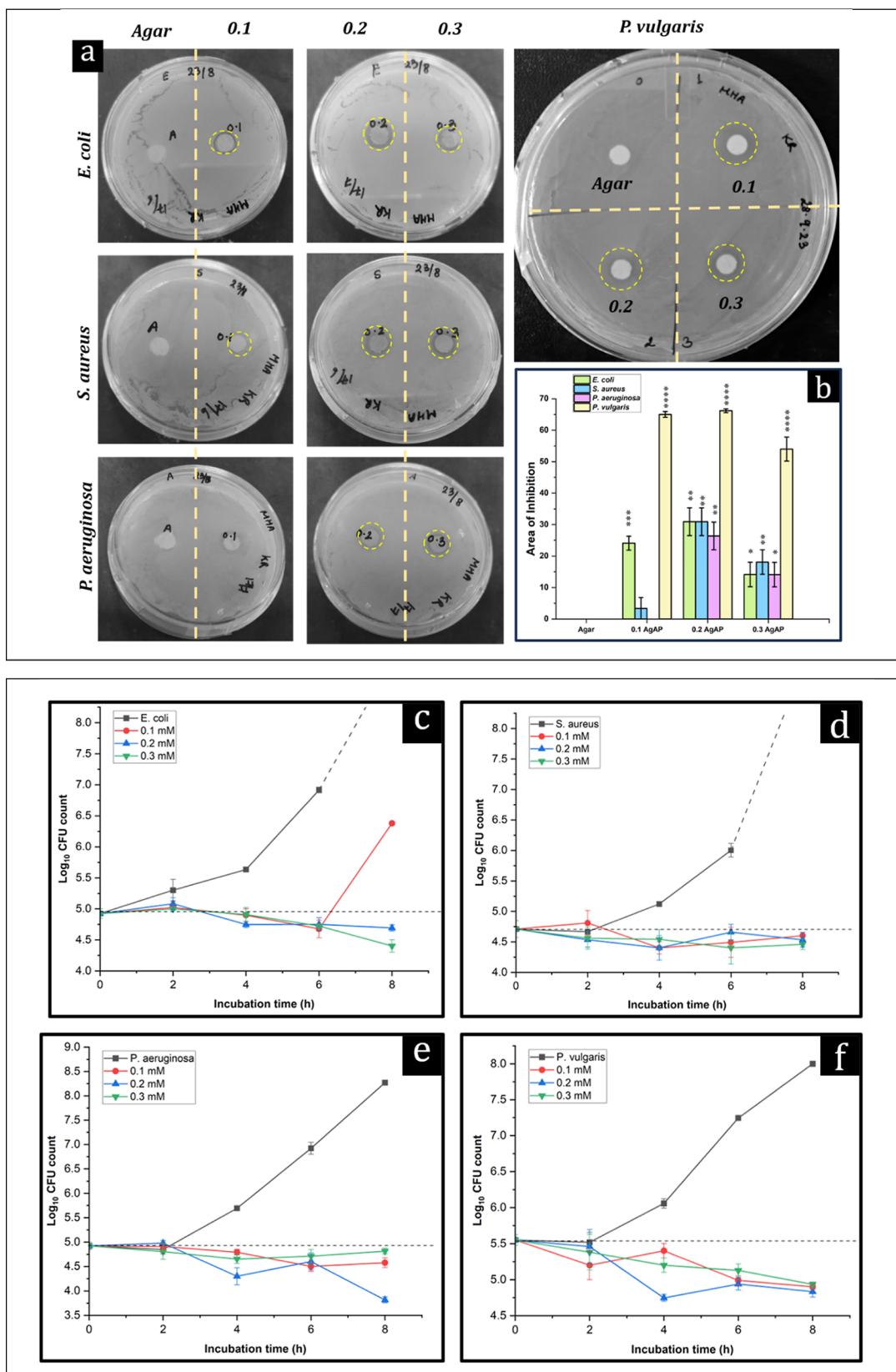
Figure 7. (a) ZOI of silver nanoparticles impregnated in agar/AP-GA bilayer dressings (left to right: Ag, 0.1 mM, 0.2 mM, and 0.3 mM; top to bottom: *E. coli*, *S. aureus,* and *P. aeruginosa*; and upper right: *P. vulgaris)*. (b) ZOI of silver nanoparticles impregnated in solvent-cast agar with agar/PCL containing gallic acid as Janus nanofibrous dressings (left to right: Ag, 0.1 mM, 0.2 mM, and 0.3 mM). Antibacterial activity of 0.1 mM, 0.2 mM, and 0.3 mM agar-based bilayer films in time-kill assay against *E. coli* (c), *S. aureus* (d), *P. aeruginosa*(e), and *P. vulgaris*. (f) Dotted line indicates that the growth was more than log 9.
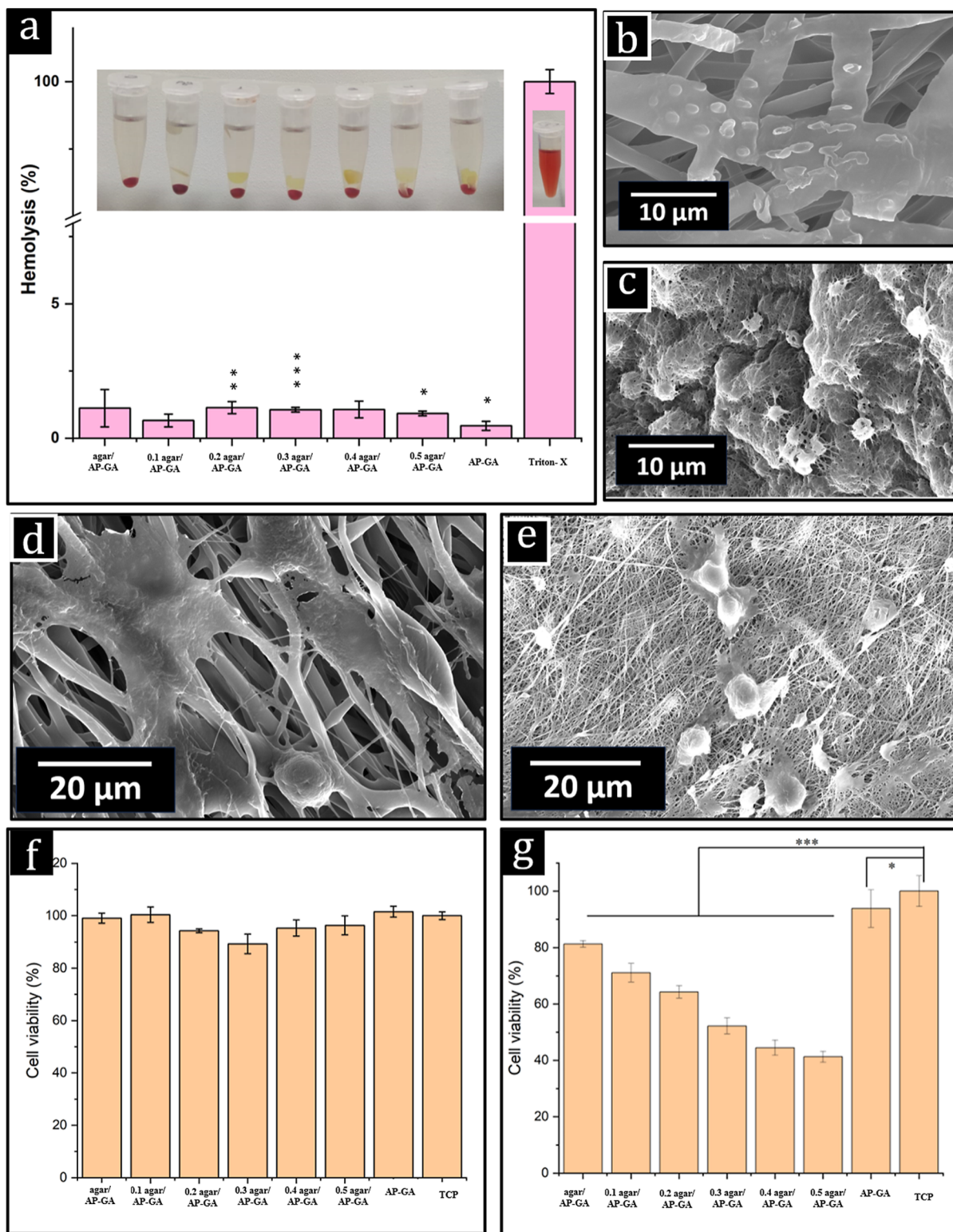
Figure 8. (a) Digital images (a) of hemolysis assay of the developed Janus nanofibrous dressing are presented in the inset image. Hemolysis percentage of the developed Janus nanofibrous dressing where GA was the electrospun layer of AP with gallic acid and Triton-X-treated RBC solution as (+) control. Micrographs of the platelet adhesion on the developed PCL nanofibrous mat (b) and AP-GA mats (c). Cellular attachment and proliferation on the PCL electrospun mat (d) and AP (e) electrospun layer. Indirect (f) and direct (g) contact assay of the developed agar/AP-GA bilayer dressings containing AgNPs at varied concentration from 0 mM to 0.5 mM.

efficacy while demonstrating more than 60% cell viability in the MTT assay. Figure 9h−l summarizes the healing progress of the wound for all of the groups at varying time intervals. The bioactivity of the Janus nanofibrous wound dressing displayed

the best healing action according to the wound area measurement (group III). Moreover, on the third day, all the wounds showed inflammation and redness around the wound, except for the test sample, which had the least inflammation and redness.
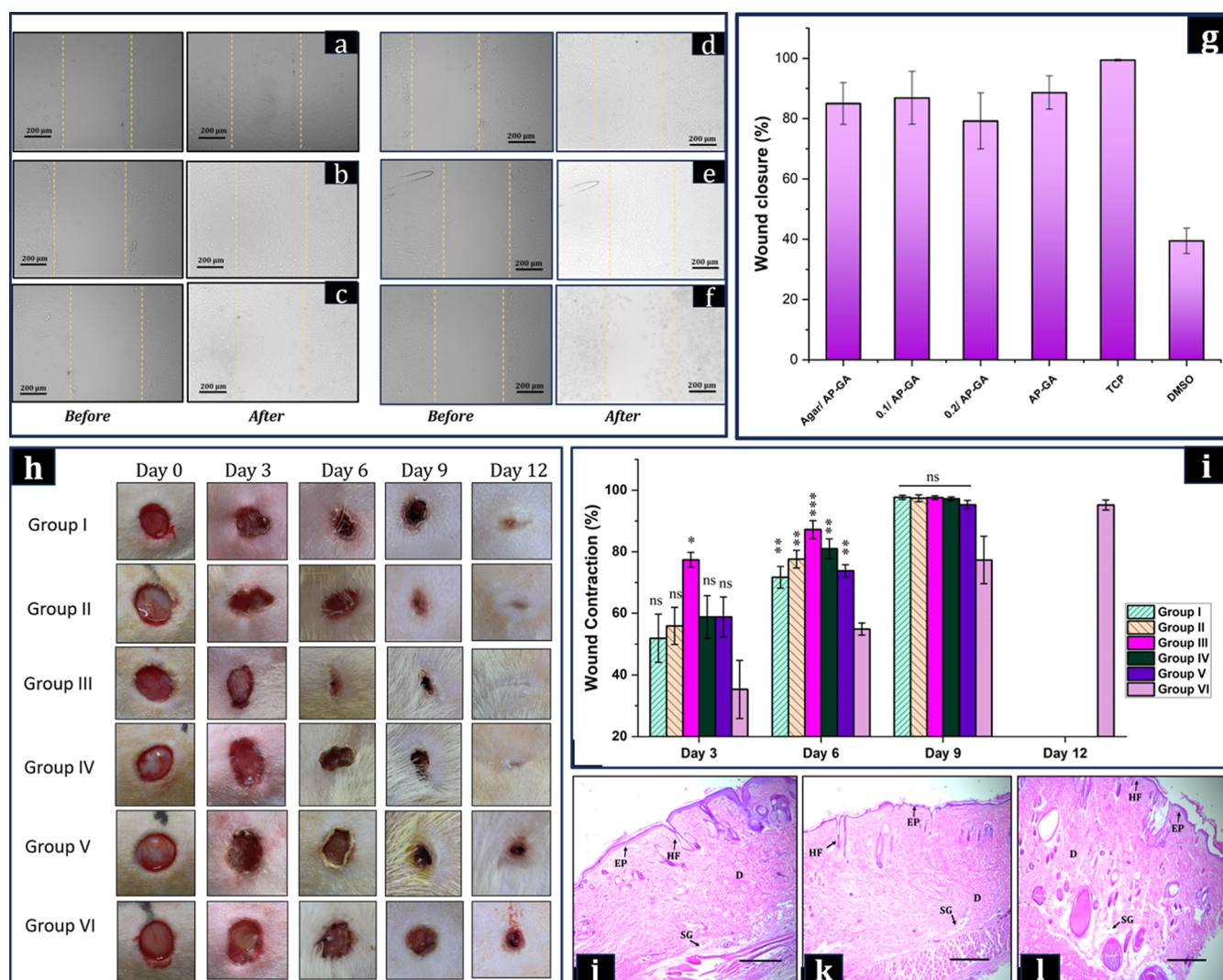
L

Figure 9. Wound scratch assay: micrographs of agar/AP-GA (a), 0.1 agar/AP-GA (b), 0.2 agar/AP-GA (c), AP-GA (d), positive control (e), and negative control with DMSO (f) where the left panel shows before sample incubation and the right panel displayed after 24 h sample incubation, and the scale bar is equal to 200 μm. Graphical representation illustrating the percent wound closure, in 24 h. (g) In vivo wound healing. (h) Digital photographs of the wound for various treated groups of different time intervals. Wound contraction rate (i) on days 3, 6, 9, and 12 of the study. Photomicrographs of the H&E-stained healed wound sections treated with Janus nanofibrous dressing (j), normal skin (k), and untreated wound (l), where EP—epidermal cells, D—dermal cells, HF—hair follicles, and SG—sebaceous glands, and the scale bar is equal to 500 μm.

The visual inspection was performed during dressing changes until the wounds were completely healed.

The wound contraction was highest for group III Janus nanofibrous dressing, around 77.4% on the third day, followed by 87% by the sixth day. Group IV (treated with a commercially available Sterizone dressing) also demonstrated 81% healing on the sixth day. However, group III (treated with Janus nanofibrous dressing) and group IV (treated with Sterizone dressing) healed by day 12, and the scar formation in the wound treated with Janus nanofibrous dressing was significantly less compared to the other groups. Group V wounds treated with povidone healed in 15 days, whereas group VI untreated wounds took 21 days to complete the natural healing process. Additionally, the Janus nanofibrous dressing samples showed the highest rate of wound contraction. By the end of day 12, groups II, III, and IV were completely healed. This demonstrates that agar itself has healing capabilities, enhancing antioxidant and antibacterial properties in the agar matrix, thereby broadening the spectrum for advanced solutions. This confirms

that the developed Janus nanofibrous agar-based wound dressing promotes healing by more than 97.5% within 12 days of injury. Histopathological results (Figure 9 j–l) demonstrated excellent epithelial tissue formation in the treated group compared to the untreated group, which showed incomplete epithelial tissue formation. The epithelial layer was significantly thicker in wounds that were treated with Janus nanofibrous dressing (47.9 ± 2.6 μm) than in the untreated group (33.1 ± 10.6 μm), while normal skin exhibited the thinnest epithelial layer (13.9 ± 4 μm). Wounds treated with silver nanoparticle solution and commercial dressing also demonstrated good epithelial formation (Supporting Information, Figure S2). The superior absorption properties of the agar in the developed agar-based Janus nanofibrous dressing facilitated exudate absorption and maintained a moist wound bed that resulted in accelerated wound healing due to enhanced fibroblast proliferation.[66,67] Furthermore, the synergistic effect of antioxidant, anti-inflammatory, and antibacterial properties of agar/PCL incorporated with gallic acid and silver nanoparticles could

account for this. The incorporation of antioxidant agents can scavenge free radicals, resulting in accelerating wound healing.

CONCLUSIONS

In conclusion, we have successfully developed a Janus nanofibrous agar-based wound dressing consisting of a solvent-cast support layer and a primary electrospun layer with antibacterial and antioxidant properties, respectively. The developed asymmetric Janus nanofibrous dressing would promote healing by scavenging free radicals at the wound site, a crucial requirement of early wound healing, and provide antibacterial properties throughout the different stages of wound healing, providing sustained release of antibacterial silver nanoparticles throughout the wound healing process. Previously performed research on bilayer dressings by Zhang et al.[68] and Eskandarinia et al.[1] overlooked the significance of moisture transmission rate and biodegradation in the developed bilayer wound dressing, respectively. The present study demonstrated that a sustained release of nanoparticles due to diffusion and relaxation of polymeric chains aids in creating a barrier to microbial infection and protects the wound during the healing process without affecting cell migration and proliferation. Various characterization techniques demonstrated the successful fabrication of a Janus nanofibrous dressing incorporated with 10−20 nm silver nanoparticles. Moderate strength (∼50 MPa) and water handling properties, including 1200 g/(m²·day) of water vapor transmission rate of the dressing, demonstrated dressing abilities that fall within the moisture transmission range of human skin. In addition to 98% porosity in the nanofibrous layer, strong antioxidant properties (over 90%) and efficient bacteriostatic behavior were recorded in the time-kill assay. The stability of the Janus nanofibrous dressing was demonstrated by its degradation behavior in PBS solutions. Additionally, hemocompatibility, cytocompatibility, and wound scratch assays confirmed the biocompatibility and clinical safety, demonstrating its efficacy in chronic wound healing. Moreover, in vivo experiments demonstrated the efficacy of the developed Janus nanofibrous dressing by efficiently combating bacterial invasion, scavenging free radicals, and promoting wound healing up to 54.4% and higher epithelial thickness compared to untreated wounds. We believe that the developed Janus nanofibrous dressings are promising candidates for addressing diverse requirements of wound healing.

ASSOCIATED CONTENT

Ⓢ Supporting Information

The Supporting Information is available free of charge at https://pubs.acs.org/doi/10.1021/acsabm.4c01184.

Delamination of asymmetric Janus nanofibrous dressings and pictomicrographs of the H&E-stained samples (PDF)

AUTHOR INFORMATION

Corresponding Authors

Sandeep Sharma − *Department of Medical Laboratory Sciences, Lovely Professional University, Phagwara 144401 Punjab, India*; Phone: +91-9682605898; Email: sandeep.23995@lpu.co.in

Vivek Verma − *Department of Materials Science & Engineering, Indian Institute of Technology Kanpur, Kanpur 208018 Uttar Pradesh, India; Centre for Environmental Science & Engineering, Samtel Centre for Display Technologies, and National Centre for Flexible Electronics, Indian Institute of Technology Kanpur, Kanpur 208018 Uttar Pradesh, India;* ⓞ orcid.org/0000-0003-4701-3397; Phone: +91-0512-2596527; Email: vverma@iitk.ac.in

Authors

Kalpana Rathore − *Department of Materials Science & Engineering, Indian Institute of Technology Kanpur, Kanpur 208018 Uttar Pradesh, India; Department of Medical Laboratory Sciences, Lovely Professional University, Phagwara 144401 Punjab, India*

Dheeraj Upadhyay − *School of Pharmaceutical Sciences (Formerly University of Pharmacy), Chhatrapati Shahu Ji Maharaj University, Kanpur 208024 Uttar Pradesh, India*

Noopur Verma − *School of Pharmaceutical Sciences (Formerly University of Pharmacy), Chhatrapati Shahu Ji Maharaj University, Kanpur 208024 Uttar Pradesh, India*

Ajay Kumar Gupta − *School of Pharmaceutical Sciences (Formerly University of Pharmacy), Chhatrapati Shahu Ji Maharaj University, Kanpur 208024 Uttar Pradesh, India*

Saravanan Matheshwaran − *Biological Sciences & Bioengineering, Indian Institute of Technology Kanpur, Kanpur 208018 Uttar Pradesh, India;* ⓞ orcid.org/0000-0001-6762-9928

Complete contact information is available at:
https://pubs.acs.org/10.1021/acsabm.4c01184

Notes

The authors declare no competing financial interest.

ACKNOWLEDGMENTS

REFERENCES

(1) Eskandarinia, A.; Kefayat, A.; Agheb, M.; Rafienia, M.; Amini Baghbadorani, M.; Navid, S.; Ebrahimpour, K.; Khodabakhshi, D.; Ghahremani, F. A Novel Bilayer Wound Dressing Composed of a Dense Polyurethane/Propolis Membrane and a Biodegradable Polycaprolactone/Gelatin Nanofibrous Scaffold. *Sci. Rep.* **2020**, *10* (1), 3063.

(2) Alvandi, H.; Jaymand, M.; Eskandari, M.; Aghaz, F.; Hosseinzadeh, L.; Heydari, M.; Arkan, E. A Sandwich Electrospun Nanofibers/Tragacanth Hydrogel Composite Containing Aloe Vera Extract and Silver Sulfadiazine as a Wound Dressing. *Polym. Bull.* **2022**, *80*, 11235−11248.

(3) Roy, N.; Saha, N.; Kitano, T.; Saha, P. Development and Characterization of Novel Medicated Hydrogels for Wound Dressing. *Soft Mater.* **2010**, *8* (2), 130−148.

(4) Janipour, Z.; Najafi, H.; Abolmaali, S. S.; Heidari, R.; Azarpira, N.; Özyılmaz, E. D.; Tamaddon, A. M. Simvastatin-Releasing Nanofibrous Peptide Hydrogels for Accelerated Healing of Diabetic Wounds. *ACS Appl. Bio Mater.* **2023**, *6* (11), 4620−4628.

(5) Yadav, B. K.; Solanki, N.; Patel, G. Electrospun Nanofibers as Advanced Wound Dressing Materials: Comparative Analysis of Single-Layered and Multilayered Nanofibers Containing Polycaprolactone, Methylcellulose, and Polyvinyl Alcohol. *J. Biomater. Sci., Polym. Ed.* **2024**, *35*, 869−879.

(6) Kashani, M. Z.; Bagher, Z.; Asgari, H. R.; Koruji, M.; Mehraein, F. Differentiation of Neonate Mouse Spermatogonial Stem Cells on Three-Dimensional Agar/Polyvinyl Alcohol Nanofiber Scaffold. *Syst. Biol. Reprod. Med.* **2020**, *66* (3), 202−215.

(7) Shakya, K. R.; Nigam, K.; Sharma, A.; Jahan, K.; Tyagi, A. K.; Verma, V. Preparation and Assessment of Agar/TEMPO-Oxidized Bacterial Cellulose Cryogels for Hemostatic Applications. *J. Mater. Chem. B* **2024**, *12* (14), 3453−3468.

(8) Li, L.; Wang, Y.; Liu, K.; Yang, L.; Zhang, B.; Luo, Q.; Luo, R.; Wang, Y. Nanoparticles-Stacked Superhydrophilic Coating Supported

Synergistic Antimicrobial Ability for Enhanced Wound Healing. *Mater. Sci. Eng.,C* **2022**, *132*, 112535.

(9) Bruna, T.; Maldonado-Bravo, F.; Jara, P.; Caro, N. Silver Nanoparticles and Their Antibacterial Applications. *Int. J. Mol. Sci.* **2021**, *22* (13), 7202.

(10) Dawadi, S.; Katuwal, S.; Gupta, A.; Lamichhane, U.; Thapa, R.; Jaisi, S.; Lamichhane, G.; Bhattarai, D. P.; Parajuli, N. Current Research on Silver Nanoparticles: Synthesis, Characterization, and Applications. *J. Nanomater.* **2021**, *2021*, 6687290.

(11) Rhim, J. W.; Wang, L. F.; Hong, S. I. Preparation and characterization of agar/silver nanoparticles composite films with antimicrobial activity. *Food Hydrocolloids* **2013**, *33* (2), 327−335.

(12) Pryshchepa, O.; Pomastowski, P.; Buszewski, B. Silver Nanoparticles: Synthesis, Investigation Techniques, and Properties. *Adv. Colloid Interface Sci.* **2020**, *284*, 102246.

(13) Comino-Sanz, I. M.; López-Franco, M. D.; Castro, B.; Pancorbo-Hidalgo, P. L. The Role of Antioxidants on Wound Healing: A Review of the Current Evidence. *J. Clin. Med.* **2021**, *10* (16), 3558.

(14) Ninan, N.; Forget, A.; Shastri, V. P.; Voelcker, N. H.; Blencowe, A. Antibacterial and Anti-Inflammatory PH-Responsive Tannic Acid-Carboxylated Agarose Composite Hydrogels for Wound Healing. *ACS Appl. Mater. Interfaces* **2016**, *8* (42), 28511−28521.

(15) Mlcek, J.; Jurikova, T.; Skrovankova, S.; Sochor, J. Quercetin and Its Anti-Allergic Immune Response. *Molecules* **2016**, *21* (5), 623.

(16) El-Samad, L. M.; Hassan, M. A.; Basha, A. A.; El-Ashram, S.; Radwan, E. H.; Abdul Aziz, K. K.; Tamer, T. M.; Augustyniak, M.; El Wakil, A. Carboxymethyl Cellulose/Sericin-Based Hydrogels with Intrinsic Antibacterial, Antioxidant, and Anti-Inflammatory Properties Promote Re-Epithelization of Diabetic Wounds in Rats. *Int. J. Pharm.* **2022**, *629* (October), 122328.

(17) Das, A.; Ahmad, P.; Kumar, A. A Coaxially Structured Trilayered Gallic Acid-Based Antioxidant Vascular Graft for Treating Coronary Artery Disease. *Eur. Polym. J.* **2021**, *143*, 110203.

(18) Li, J.; Du, Q.; Wan, J.; Yu, D.-G.; Tan, F.; Yang, X. Improved Synergistic Anticancer Action of Quercetin and Tamoxifen Citrate Supported by an Electrospun Complex Nanostructure. *Mater. Des.* **2024**, *238*, 112657.

(19) Gong, W.; Yang, W.; Zhou, J.; Zhang, S.; Yu, D. G.; Liu, P. Engineered Beads-on-a-String Nanocomposites for an Improved Drug Fast-Sustained Bi-Stage Release. *Nanocomposites* **2024**, *10* (1), 240−253.

(20) Chen, S.; Zhou, J.; Fang, B.; Ying, Y.; Yu, D. G.; He, H. Three EHDA Processes from a Detachable Spinneret for Fabricating Drug Fast Dissolution Composites. *Macromol. Mater. Eng.* **2024**, *309* (4), 2300361.

(21) Sun, L.; Zhou, J.; Chen, Y.; Yu, D. G.; Liu, P. A Combined Electrohydrodynamic Atomization Method for Preparing Nanofiber/Microparticle Hybrid Medicines. *Front. bioeng. biotechnol.* **2023**, *11*, 1308004.

(22) Liu, Y.; Chen, X.; Lin, X.; Yan, J.; Yu, D. G.; Liu, P.; Yang, H. Electrospun Multi-Chamber Core-Shell Nanofibers and Their Controlled Release Behaviors: A Review. *Wiley Interdiscip. Rev.: Nanomed. Nanobiotechnol.* **2024**, *16* (2), No. e1954.

(23) Zhang, Z.; Liu, H.; Yu, D.-G.; Bligh, S. W. A. Alginate-Based Electrospun Nanofibers and the Enabled Drug Controlled Release Profiles: A Review. *Biomolecules* **2024**, *14*, 789.

(24) Zhao, P.; Zhou, K.; Xia, Y.; Qian, C.; Yu, D. G.; Xie, Y.; Liao, Y. Electrospun Trilayer Eccentric Janus Nanofibers for a Combined Treatment of Periodontitis. *Adv. Fiber Mater.* **2024**, *6* (4), 1053−1073.

(25) Liu, J.; Zou, Q.; Wang, C.; Lin, M.; Li, Y.; Zhang, R.; Li, Y. Electrospinning and 3D Printed Hybrid Bi-Layer Scaffold for Guided Bone Regeneration. *Mater. Des.* **2021**, *210*, 110047.

(26) Lu, H. H.; Zheng, K.; Boccaccini, A. R.; Liverani, L. Electrospinning of Cotton-like Fibers Based on Cerium-Doped Sol−Gel Bioactive Glass. *Mater. Lett.* **2023**, *334*, 133712.

(27) Yu, D. G.; Gong, W.; Zhou, J.; Liu, Y.; Zhu, Y.; Lu, X. Engineered Shapes Using Electrohydrodynamic Atomization for an Improved Drug Delivery. *Wiley Interdiscip. Rev.: Nanomed. Nanobiotechnol.* **2024**, *16* (3), No. e1964.

(28) Xu, L.; Li, Q.; Wang, H.; Liu, H.; Yu, D. G.; Bligh, S. W. A.; Lu, X. Electrospun Multi-Functional Medicated Tri-Section Janus Nanofibers for an Improved Anti-Adhesion Tendon Repair. *Chem. Eng. J.* **2024**, *492*, 152359.

(29) Sun, Y.; Zhou, J.; Zhang, Z.; Yu, D. G.; Bligh, S. W. A. Integrated Janus Nanofibers Enabled by a Co-Shell Solvent for Enhancing Icariin Delivery Efficiency. *Int. J. Pharm.* **2024**, *658*, 124180.

(30) Rathore, K.; Singh, I.; Balani, K.; Sharma, S.; Verma, V. Fabrication and Characterization of Multi-Layered Coaxial Agar-Based Electrospun Biocomposite Mat, Novel Replacement for Transdermal Patches. *Int. J. Biol. Macromol.* **2024**, *275* (P2), 133712.

(31) Figueira, D. R.; Miguel, S. P.; de Sá, K. D.; Correia, I. J. Production and Characterization of Polycaprolactone- Hyaluronic Acid/Chitosan- Zein Electrospun Bilayer Nanofibrous Membrane for Tissue Regeneration. *Int. J. Biol. Macromol.* **2016**, *93*, 1100−1110.

(32) Kim, Y.; Doh, S. J.; Lee, G. D.; Kim, C.; Im, J. N. Composite Nonwovens Based on Carboxymethyl Cellulose for Wound Dressing Materials. *Fibers Polym.* **2019**, *20* (10), 2048−2056.

(33) Ahtzaz, S.; Nasir, M.; Shahzadi, L.; Amir, W.; Anjum, A.; Arshad, R.; Iqbal, F.; Chaudhry, A. A.; Yar, M.; ur Rehman, I.; Arshad, R. A Study on the Effect of Zinc Oxide and Zinc Peroxide Nanoparticles to Enhance Angiogenesis-pro-Angiogenic Grafts for Tissue Regeneration Applications. *Mater. Des.* **2017**, *132*, 409−418.

(34) Chalitangkoon, J.; Wongkittisin, M.; Monvisade, P. Silver Loaded Hydroxyethylacryl Chitosan/Sodium Alginate Hydrogel Films for Controlled Drug Release Wound Dressings. *Int. J. Biol. Macromol.* **2020**, *159*, 194−203.

(35) Mathematical Models of Drug Release. *Strategies to Modify the Drug Release from Pharmaceutical Systems*; Bruschi, M. L., Ed.; Woodhead Publishing, 2015; pp 63−86..

(36) Sharma, S.; Khan, I. A.; Ali, I.; Ali, F.; Kumar, M.; Kumar, A.; Johri, R. K.; Abdullah, S. T.; Bani, S.; Pandey, A.; Suri, K. A.; Gupta, B. D.; Satti, N. K.; Dutt, P.; Qazi, G. N. Evaluation of the Antimicrobial, Antioxidant, and Anti-Inflammatory Activities of Hydroxychavicol for Its Potential Use as an Oral Care Agent. *Antimicrob. Agents Chemother.* **2009**, *53* (1), 216−222.

(37) Jiji, S.; Udhayakumar, S.; Rose, C.; Muralidharan, C.; Kadirvelu, K. Thymol enriched bacterial cellulose hydrogel as effective material for third degree burn wound repair. *Int. J. Biol. Macromol.* **2019**, *122*, 452−460.

(38) Ying, R.; Huang, W. C.; Mao, X. Synthesis of Agarose-Based Multistimuli-Responsive Hydrogel Dressing for Accelerated Wound Healing. *ACS Biomater. Sci. Eng.* **2022**, *8* (1), 293−302.

(39) Vivcharenko, V.; Wojcik, M.; Przekora, A. Cellular Response to Vitamin C-Enriched Chitosan/Agarose Film with Potential Application as Artificial Skin Substitute for Chronic Wound Treatment. *Cells* **2020**, *9* (5), 1185.

(40) Suarez-Arnedo, A.; Figueroa, F. T.; Clavijo, C.; Arbeláez, P.; Cruz, J. C.; Muñoz-Camargo, C. An Image J Plugin for the High Throughput Image Analysis of in Vitro Scratch Wound Healing Assays. *PLoS One* **2020**, *15* (7 July), No. e0232565.

(41) Kora, A.; Beedu, S.; Jayaraman, A. Size-Controlled Green Synthesis of Silver Nanoparticles Mediated by Gum Ghatti (Anogeissus Latifolia) and Its Biological Activity. *Org. Med. Chem. Lett.* **2012**, *2* (1), 17.

(42) Emam, H. E.; Saleh, N. H.; Nagy, K. S.; Zahran, M. K. Functionalization of Medical Cotton by Direct Incorporation of Silver Nanoparticles. *Int. J. Biol. Macromol.* **2015**, *78*, 249−256.

(43) Tankhiwale, R.; Bajpai, S. K. Graft Copolymerization onto Cellulose-Based Filter Paper and Its Further Development as Silver Nanoparticles Loaded Antibacterial Food-Packaging Material. *Colloids Surf., B* **2009**, *69* (2), 164−168.

(44) Haider, A.; Haider, S.; Kang, I. A comprehensive review summarizing the effect of electrospinning parameters and potential applications of nanofibers in biomedical and biotechnology. *Arabian J. Chem.* **2018**, *11* (8), 1165−1188.

(45) Madera-Santana, T. J.; Freile-Pelegrín, Y.; Azamar-Barrios, J. A. Physicochemical and Morphological Properties of Plasticized Poly-

(Vinyl Alcohol)-Agar Biodegradable Films. *Int. J. Biol. Macromol.* **2014**, *69* (May), 176−184.

(46) Belay, M.; Tyeb, S.; Rathore, K.; Kumar, M.; Verma, V. Synergistic effect of bacterial cellulose reinforcement and succinic acid crosslinking on the properties of agar. *Int. J. Biol. Macromol.* **2020**, *165*, 3115−3122.

(47) Liu, J.; Xue, Z.; Zhang, W.; Yan, M.; Xia, Y. Preparation and Properties of Wet-Spun Agar Fibers. *Carbohydr. Polym.* **2018**, *181* (March 2017), 760−767.

(48) Rafienia, M.; Salami, M.; Kaveian, F.; Saber-Samandari, S.; Khandan, A.; Naeimi, M. Electrospun Polycaprolactone/Lignin-Based Nanocomposite as a Novel Tissue Scaffold for Biomedical Applications. *J. Med. Signals Sens* **2017**, *7* (4), 228−238.

(49) Alipour, R.; Khorshidi, A.; Fallah, A.; Mashayekhi, F. Skin Wound Healing Acceleration by Ag Nanoparticles Embedded in PVA/PVP/Pectin/Mafenide Acetate Composite Nanofibers. *Polym. Test.* **2019**, *79* (August), 106022.

(50) Menzies, K. L.; Jones, L. The Impact of Contact Angle on the Biocompatibility of Biomaterials. *Optom. Vis. Sci.* **2010**, *87* (6), 387−399.

(51) Barros, N. R.; Ahadian, S.; Tebon, P.; Rudge, M. V. C.; Barbosa, A. M. P.; Herculano, R. D. Highly Absorptive Dressing Composed of Natural Latex Loaded with Alginate for Exudate Control and Healing of Diabetic Wounds. *Mater. Sci. Eng.* **2021**, *119* (April 2020), 111589.

(52) Yusof, N. L. B. M.; Wee, A.; Lim, L. Y.; Khor, E. Flexible Chitin Films as Potential Wound-Dressing Materials: Wound Model Studies. *J. Biomed. Mater. Res., Part A* **2003**, *66A* (2), 224−232.

(53) Chen, X.; Sun-Waterhouse, D.; Yao, W.; Li, X.; Zhao, M.; You, L. Free Radical-Mediated Degradation of Polysaccharides: Mechanism of Free Radical Formation and Degradation, Influence Factors and Product Properties. *Food Chem.* **2021**, *365* (June), 130524.

(54) Badhani, B.; Sharma, N.; Kakkar, R. Gallic Acid: A Versatile Antioxidant with Promising Therapeutic and Industrial Applications. *RSC Adv.* **2015**, *5* (35), 27540−27557.

(55) Gong, W.; Wang, R.; Huang, H.; Hou, Y.; Wang, X.; He, W.; Gong, X.; Hu, J. Construction of Double Network Hydrogels Using Agarose and Gallic Acid with Antibacterial and Anti-Inflammatory Properties for Wound Healing. *Int. J. Biol. Macromol.* **2023**, *227*, 698−710.

(56) Patole, V.; Bhosale, P.; Ingavle, G.; Behere, I.; Vyawahare, N.; Ottoor, D.; Sanap, A.; Bhonde, R.; Kheur, S. In Vitro and in Vivo Assessment of Gallic Acid-Chitosan/Polycaprolactone Conjugate Electrospun Nanofibers for Wound Healing. *J. Drug Delivery Sci. Technol.* **2024**, *95*, 105569.

(57) Keyvani-Ghamsari, S.; Rahimi, M.; Khorsandi, K. An Update on the Potential Mechanism of Gallic Acid as an Antibacterial and Anticancer Agent. *Food Sci. Nutr.* **2023**, *11* (10), 5856−5872.

(58) Lang, S.; Chen, C.; Xiang, J.; Liu, Y.; Li, K.; Hu, Q.; Liu, G. Facile and Robust Antibacterial Functionalization of Medical Cotton Gauze with Gallic Acids to Accelerate Wound Healing. *Ind. Eng. Chem. Res.* **2021**, *60* (28), 10225−10234.

(59) Elmas, A.; Akyüz, G.; Bergal, A.; Andaç, M.; Andaç, O.∴. Mathematical Modelling of Drug Release. *Res. Eng. Struct. Mater.* **2020**, *6* (4), 327−350.

(60) Bie, X.; Khan, M. Q.; Ullah, A.; Ullah, S.; Kharaghani, D.; Phan, D. N.; Tamada, Y.; Kim, I. S. Fabrication and Characterization of Wound Dressings Containing Gentamicin/Silver for Wounds in Diabetes Mellitus Patients. *Mater. Res. Express* **2020**, *7* (4), 045004.

(61) Sarviya, N.; Mahanta, U.; Dart, A.; Giri, J.; Deshpande, A. S.; Khandelwal, M.; Bhave, M.; Kingshott, P. Biocompatible and Antimicrobial Multilayer Fibrous Polymeric Wound Dressing with Optimally Embedded Silver Nanoparticles. *Appl. Surf. Sci.* **2023**, *612*, 155799.

(62) Tripathi, S.; Singh, B. N.; Divakar, S.; Kumar, G.; Mallick, S. P.; Srivastava, P. Design and Evaluation of Ciprofloxacin Loaded Collagen Chitosan Oxygenating Scaffold for Skin Tissue Engineering. *Biomed. Mater.* **2021**, *16* (2), 025021.

(63) Sanandiya, N. D.; Lee, S.; Rho, S.; Lee, H.; Kim, I. S.; Hwang, D. S. Tunichrome-Inspired Pyrogallol Functionalized Chitosan for Tissue

Adhesion and Hemostasis. *Carbohydr. Polym.* **2019**, *208* (September 2018), 77−85.

(64) Bharadwaz, A.; Jayasuriya, A. C. Recent Trends in the Application of Widely Used Natural and Synthetic Polymer Nanocomposites in Bone Tissue Regeneration. *Mater. Sci. Eng.* **2020**, *110* (May 2019), 110698.

(65) Lallukka, M.; Houaoui, A.; Miola, M.; Miettinen, S.; Massera, J.; Verné, E. In Vitro Cytocompatibility of Antibacterial Silver and Copper-Doped Bioactive Glasses. *Ceram. Int.* **2023**, *49* (22), 36044−36055.

(66) Jaiswal, L.; Shankar, S.; Rhim, J. Carrageenan-Based Functional Hydrogel Fi Lm Reinforced with Sulfur Nanoparticles and Grapefruit Seed Extract for Wound Healing Application. *Carbohydr Polym* **2019**, *224* (August), 115191.

(67) Kamoun, E. A.; Kenawy, E. R. S.; Chen, X. A Review on Polymeric Hydrogel Membranes for Wound Dressing Applications: PVA-Based Hydrogel Dressings. *J. Adv. Res.* **2017**, *8* (3), 217−233.

(68) Zhang, T.; Xu, H.; Zhang, Y.; Zhang, S.; Yang, X.; Wei, Y.; Huang, D.; Lian, X. Fabrication and Characterization of Double-Layer Asymmetric Dressing through Electrostatic Spinning and 3D Printing for Skin Wound Repair. *Mater. Des.* **2022**, *218*, 110711.